

Electronic Thesis and Dissertation Repository

---

6-11-2020 1:00 PM

## Investigating pathways associated with intervertebral disc degeneration and back pain.

Geoffrey J. Kerr, *The University of Western Ontario*

Supervisor: Seguin, Cheryle A., *The University of Western Ontario*

A thesis submitted in partial fulfillment of the requirements for the Doctor of Philosophy degree in Physiology and Pharmacology

© Geoffrey J. Kerr 2020

Follow this and additional works at: <https://ir.lib.uwo.ca/etd>



Part of the [Musculoskeletal, Neural, and Ocular Physiology Commons](#), and the [Physiological Processes Commons](#)

---

### Recommended Citation

Kerr, Geoffrey J., "Investigating pathways associated with intervertebral disc degeneration and back pain." (2020). *Electronic Thesis and Dissertation Repository*. 7044.  
<https://ir.lib.uwo.ca/etd/7044>

This Dissertation/Thesis is brought to you for free and open access by Scholarship@Western. It has been accepted for inclusion in Electronic Thesis and Dissertation Repository by an authorized administrator of Scholarship@Western. For more information, please contact [wlsadmin@uwo.ca](mailto:wlsadmin@uwo.ca).

## Abstract

Lower back pain (LBP) is one of the most common conditions worldwide, yet, current therapeutics are limited to symptomatic relief and do not directly treat the underlying cause of pain. This is largely due to an incomplete understanding of the biological pathways and tissues involved in LBP. While many tissues appear to be involved, intervertebral disc (IVD) degeneration is believed to be a major contributor.

The main aim of this thesis was to characterize the role of two environmental risk factors, mechanical loading and obesity, in the initiation of IVD degeneration and associated pain using the mouse as a preclinical model. We first investigated the effects of mechanical loading, specifically whole-body vibration (WBV), on joint health. In contrast to previous findings in CD-1 mice, we show that WBV delivered using parameters that model those used clinically does not affect joint health in C57BL/6 mice. These findings suggest that the response of joint tissues to WBV may vary in a strain-specific manner.

We next evaluated the impact of diet-induced obesity on IVD degeneration and associated pain. Ten-week-old male C57BL/6N mice were fed either a control, high-fat, or western diet for 12, 24 or 40 weeks. At endpoint, mice were assessed for behavioral indicators of pain and histological and molecular analyses were carried out on joint and neural tissues. We demonstrated that diet-induced obesity accelerates IVD degeneration; however, pain-related behaviors precede histological joint damage.

Finally, we examined the role of peroxisome proliferator-activated receptor delta (PPAR $\delta$ ) as a potential mediator of IVD degeneration. We confirmed that PPAR $\delta$  was expressed and functionally active in the IVD and used male and female, cartilage-specific *Ppard* knockout

(*Ppard* KO) mouse to assess age- and obesity-associated IVD degeneration. Loss of PPAR $\delta$  appeared to be protected against age-associated IVD degeneration; however, this protective effect was not observed with obesity-induced IVD degeneration or knee osteoarthritis.

Overall, this data highlights the complex interactions between modifiable and non-modifiable risk factors as drivers of IVD degeneration and associated back pain. Furthermore, these studies highlight the importance of including sex as a biological variable and assessing pain and IVD degeneration, as they do not always correlate.

**Keywords:** Intervertebral disc degeneration; Back pain; Whole-body vibration; Obesity; Peroxisome proliferator activated receptor delta (PPAR $\delta$ ); Mouse models.

## Summary for Lay Audience

Lower back pain (LBP) is one of the most common causes of disability worldwide, yet current treatments are limited to pain relief and do not directly treat the underlying cause of pain. This is largely due to an incomplete understanding of what tissues contribute to LBP and why pain occurs. Large-scale association studies in humans have identified several risk factors for the development of LBP including age, genetics, mechanical loading and obesity; however, how and why they cause the pain is largely unknown.

While many tissues appear to be involved in LBP, intervertebral disc (IVD) degeneration is believed to be a major contributor in many cases. IVDs are specialized joints located between the vertebrae in the spine that act as shock absorbers, helping to dissipate mechanical loading. Degeneration is a progressive biological process that results in the functional failure of the tissue and can result in pain. This research was designed to investigate the impact of mechanical loading, specifically whole-body vibration (WBV), and obesity on IVD degeneration and associated pain using the mouse as a model system. Furthermore, we investigate a potential biological mediator to explain how obesity impacts IVD degeneration and associated pain.

In our first study we demonstrate that the response of joint tissues to WBV vary based on genetic background of the animals. In our second study we demonstrated that diet-induced obesity does accelerate IVD degeneration and pain-related behavior in a mouse model; however, pain related behaviors precede structural IVD damage. Lastly, we assessed a potential biological mediator of IVD degeneration - peroxisome proliferator activated receptor delta (PPAR $\delta$ ) – in aging and obesity. Using mice that had the PPAR $\delta$  gene deleted in joint tissues, we showed that loss of PPAR $\delta$  protected against age-associated IVD

degeneration; however, this protective effect was not observed with obesity-induced IVD degeneration.

Taken together, this thesis highlights the complex interactions between mechanical loading and obesity as drivers of IVD degeneration and associated back pain. Furthermore, these studies highlight the importance of including sex as a biological variable and assessing pain and IVD degeneration, as they do not always correlate.

## Co-Authorship Statement

Comprehensive co-authorship statements are included at the beginning of each chapter.

## Acknowledgments

The last 5 years have been a journey that I will never forget, and my progress to this point would not have been possible without amazing mentors, collaborators, and friends that were with me every step of the way. It was an honor to work alongside such hard-working and talented people in the Department of Physiology & Pharmacology and the Bone & Joint Institute, and I want to say thank you to everyone that has helped me along my journey.

First and foremost, I want to thank my supervisor, Dr. Cheryle Séguin. Cheryle, without your guidance my grad school experience would not have been as positive as it was. From starting in your lab with no basic science experience, you taught me to think like a scientist. You instilled in me a love for research and allowed me to recognize my potential. All the awards I have won, skills I have developed, and manuscripts I have published are thanks to your guidance. Whenever I ran into an obstacle, I could always count on you to meet with me, and you give me confidence to carry on, so thank you. I would also like to convey my thanks to my advisory committee, Drs. Frank Beier, Jeff Dixon, John DiGuglielmo, and Nica Borradaile for providing valuable feedback which strengthened this thesis. I would also like to thank other faculty members in the Department of Physiology and Pharmacology. Thank you, Tom Stavrakys and Dr. Anita Woods for giving me the opportunity to teach undergraduate courses and explore my love of teaching.

I am also extremely grateful for Diana Quinonez and Courtney Brooks, two laboratory technicians who are the backbone of the Séguin lab. Diana, it has been an absolute pleasure working with you and I will miss the days we were stuck over in Robarts doing experiments. Thank you for all the help in the lab, especially keeping me out of the mouse

house. None of this project would be possible without your help. Courtney, thank you for all your help training me in cell culture and keeping the lab in line. Joking around with you made the days fly by and always put a smile on my face. Thank you both for helping keep the lab run smoothly over the last 5 years.

To my fellow graduate students in the Séguin lab, I feel honored to have met such fun and talented group of people. You have become like a family to me and I wish the best for everyone. Veras, we started our grad school journey together and I could not have asked for a better person to experience it with. From the start you have pushed me to be a better scientist and the last 5 years have flown by thanks to you. We travelled the world together to talk about our research and had a great time along the way. While Canada is losing one of its talents, I am sure you will do great work down in San Francisco. Mark, you must be one of the best science illustrators I have ever come across. We have had great times together and I cannot believe that it is coming to an end. Dale, you are one of the hardest workers I have ever met, and I can always count on you for advice on anything. To Meg, Nadia, McCann, Marco, Jeff, Matt L., Mayu, I cannot thank you enough for all your guidance, encouragement and most importantly your friendship. To the Beier lab, I have had a great time with all of you over the past 5 years. A special thanks Anusha for helping me start up on the PPAR $\delta$  project. Mike, you helped show me the ropes early on and for that I am grateful. Finally, Bethia, thank you for all the work you did on the diet studies, I could not have done them without you. I also need to thank all the undergraduate thesis students for the help that they have given in the lab over the years. A special thank you to Ian White and Denis Margalik who helped with aspects of this thesis.



The greatest takeaway from this graduate school experience is the friendships that I have made over the years. I have had so many great times socializing with graduate students in the department and have made memories that will last a lifetime. There are too many people to name however, the following people have made a lasting impact and really changed my graduate school experience: Adam Raffoul, Andrew Kucey, Jake Bedore, Anusha Ratneswaran, Katherine Lee, Laura Russell, Joshua Dierdorf, Melissa Fenech, Victoria Deveau, Phyo Win, Elizabeth Greco, Alexandra Pearce and Carol Ma just to name a few. To my two roommates over the years, Anish Engineer and Brandon Baer, I could not have asked for better group of guys to live with. We have had a great time together and I will miss all our adventures. Best of luck in medical school Anish, and with the rest of your Ph.D. Brandon.

Finally, I want to thank my wonderful family for supporting me through my education. You always believed in me and that unending love and support helped me along every step of the way. Mom and Dad, you have always been there for me and encouraged me to follow my dreams. You two are the best role models a son could ask for and I appreciate everything that you have sacrificed to allow me to get to this point.

# Table of Contents

Abstract.....	ii
Summary for Lay Audience .....	iv
Co-Authorship Statement.....	vi
Acknowledgments .....	vii
Table of Contents.....	x
List of Tables .....	xvi
List of Figures.....	xvii
List of Appendices .....	xix
Chapter 1 .....	1
1 Introduction .....	1
1.1 What is pain? .....	1
1.1.1 Biological mechanisms of pain .....	1
1.1.2 Acute vs. Chronic pain .....	2
1.2 Back pain is a problem .....	4
1.3 The Spine .....	5
1.3.1 Vertebral bone.....	5
1.3.2 The Intervertebral Disc.....	7
1.3.3 Muscle and connective tissue .....	10
1.3.4 Innervation & Vascularization .....	10
1.4 Intervertebral Disc Degeneration.....	11
1.4.1 Risk factors for IVD degeneration .....	11
1.4.2 Pathogenesis of IVD degeneration.....	13
1.4.3 The link between IVD degeneration and pain .....	17

1.4.4	Treatment for IVD degeneration .....	18
1.5	Similarities between IVD degeneration and osteoarthritis.....	18
1.6	Mechanobiology of the IVD .....	19
1.6.1	Mechanical loads seen by the IVD .....	20
1.6.2	Mechanotransduction.....	20
1.6.3	IVD tissue response to aberrant mechanical loads.....	21
1.7	Metabolism of the IVD.....	23
1.8	Animal models of IVD degeneration and back pain.....	24
1.9	Obesity.....	26
1.9.1	Metabolic syndrome.....	26
1.9.2	Musculoskeletal health.....	27
1.9.3	Pain.....	29
1.10	..... Nuclear Receptors .....	31
1.10.1	Structure.....	31
1.10.2	Peroxisome Proliferator Activated Receptors (PPARs) .....	32
1.11	..... Overall objectives and hypothesis.....	34
1.11.1	Objective #1.....	34
1.11.2	Objective #2.....	35
1.11.3	Objective # 3 .....	36
1.12	.....References	38
Chapter 2	.....	60
2	C57BL/6 mice are resistant to joint degeneration induced by whole-body vibration.	61
2.1	Co-authorship Statement.....	61

2.2 Chapter Summary.....	62
2.3 Introduction.....	63
2.4 Methods.....	64
2.4.1 Whole body vibration .....	64
2.4.2 Gene expression analysis .....	65
2.4.3 Histological analysis .....	65
2.4.4 Statistical analysis.....	66
2.5 Results .....	66
2.6 Discussion .....	70
2.7 Acknowledgments.....	72
2.8 References .....	73
Chapter 3.....	75
3 Diet-induced obesity leads to behavioral indicators of pain preceding structural joint degeneration in wild-type mice. ....	76
3.1 Co-authorship Statement.....	76
3.2 Chapter Summary.....	77
3.3 Introduction.....	78
3.4 Methods.....	80
3.4.1 Mice and Diets .....	80
3.4.2 Characterization of pain-associated behavior .....	81
3.4.3 Micro-computed tomography (Micro-CT) .....	83
3.4.4 Histological analysis .....	84
3.4.5 Gene expression analysis .....	85
3.4.6 Immunohistochemistry.....	85
3.4.7 Serum analysis by Multiplex Assay .....	87

3.4.8	Statistical Analysis .....	87
3.5	Results .....	88
3.5.1	Weights and adiposity.....	88
3.5.2	Behavioral indicators of axial discomfort.....	90
3.5.3	Behavioral indicators of mechanical and cold sensitivity .....	90
3.5.4	Spontaneous locomotion.....	92
3.5.5	Assessment of IVD degeneration .....	92
3.5.6	Assessment of degenerative changes in the knee .....	94
3.5.7	Analysis of sensory neuroplasticity within the lumbar spinal cord.....	97
3.5.8	Circulating inflammatory factors .....	100
3.5.9	Linear regression analysis .....	100
3.6	Discussion .....	104
3.7	Supplementary Figures .....	113
3.8	References .....	119
Chapter 4	.....	126
4	Role of PPAR $\delta$ in the regulation of joint degeneration: context-specific roles in obesity and aging .....	127
4.1	Co-authorship Statement.....	127
4.2	Chapter Summary.....	128
4.3	Introduction.....	129
4.4	Methods.....	132
4.4.1	Mice and Ex Vivo organ culture.....	132
4.4.2	Dimethylmethylene blue assay .....	134
4.4.3	Histological analysis .....	134
4.4.4	Gene expression analysis .....	135

4.4.5	Micro-computed tomography (Micro-CT) .....	136
4.4.6	Behavioral measures of pain.....	137
4.4.7	Pharmacological manipulation of pain .....	138
4.4.8	Statistical analysis.....	139
4.5	Results .....	140
4.5.1	IVD cells express PPAR $\delta$ and respond to pharmacological activation...	140
4.5.2	Effect of PPAR $\delta$ activation on proteoglycan levels in the IVD .....	142
4.5.3	Deletion of PPAR $\delta$ may protect against age associated IVD degeneration.....	142
4.5.4	Wild-type and <i>Ppard</i> KO mice gain weight on the western diet .....	143
4.5.5	Deletion of PPAR $\delta$ does not protect against obesity related IVD degeneration.....	146
4.5.6	Deletion of PPAR $\delta$ does not protect against obesity-related knee OA ...	148
4.5.7	Behavioral indicators of stretch-induced axial discomfort .....	151
4.5.8	Behavioral indicators of cold and mechanical sensitivity .....	153
4.5.9	Behavioral indicators of physical function and spontaneous locomotion .....	153
4.5.10	Statistical modeling .....	156
4.6	Discussion .....	158
4.7	Supplementary Figures .....	166
4.8	References .....	173
Chapter 5	.....	180
5	General Discussion.....	180
5.1	Overview.....	180
5.2	Contributions and significance of findings .....	183
5.3	Limitations of research .....	187

5.4 Future Directions .....	191
5.5 References .....	195
Appendices .....	200
CURRICULUM VITAE .....	202

## List of Tables

Table 3.1: Multiplex analysis of cytokines, chemokines and growth factors in serum. .	103
Table 3.2: Impact of diet-induced obesity and age on behavioral, molecular, and histological changes.....	105
Table 3.3, Supplementary Table 1: Experimental diet compositions.....	115
Table 3.4, Supplementary Table 2: Real-time qPCR primer sequences. ....	116
Table 3.5, Supplementary Table 3: Multiplex analysis of cytokines, chemokines and growth factors in serum (continued). ....	117
Table 3.6, Supplementary Table 4: Association between behavioral indicators of pain and histological joint damage. ....	118
Table 4.1: Impact of sex, genotype, and diet on behavioral, molecular and histological changes. ....	157
Table 4.2, Supplementary Table 1: Realtime qPCR primer sequences .....	171
Table 4.3, Supplementary Table 2. Association between behavioral indicators of pain and histological joint damage. ....	172



## List of Figures

Figure 1.1: Schematic depiction of the major components of the spine.....	6
Figure 1.2: Proposed feed forward model of intervertebral disc degeneration with contributing risk factors.....	16
Figure 1.3: Proposed mechanism underlying the association between obesity/ metabolic syndrome, IVD degeneration, and pain. ....	30
Figure 2.1: Effect of repeated exposure to WBV on IVD health. ....	68
Figure 2.2: Effect of repeated exposure to WBV on knee health.....	69
Figure 3.1: Chronic consumption of high-fat and western diets increases adiposity and bone mineral density in C57BL/6N mice.....	89
Figure 3.2: Obesity induced by the high-fat and western diets reduces grip strength but does not alter behavior in tail suspension.....	91
Figure 3.3: Obesity induced by a high-fat and western diet increases sensitivity to mechanical stimulation and alters spontaneous locomotion. ....	93
Figure 3.4: Effect of diet-induced obesity on the intervertebral disc. ....	96
Figure 3.5: Effect of diet-induced obesity on the knee joint.....	99
Figure 3.6: Effect if diet-induced obesity on neuroplastic changes within the lumbar spinal cord. ....	102
Figure 3.7, Supplementary Figure 1: Spontaneous locomotion (Continued).....	113
Figure 3.8, Supplementary Figure 2: SYBR-based qPCR of thoracic IVDs (continued). .....	114
Figure 4.1: PPAR $\delta$ is expressed in the IVD and responds to pharmacological agonism. .....	141

Figure 4.2: Loss of Ppard alters age associated IVD degeneration. ....	144
Figure 4.3: Weight and adiposity.....	145
Figure 4.4: Effect of diet-induced obesity and PPAR $\delta$ deletion on IVD health. ....	147
Figure 4.5: Effect of diet-induced obesity and PPAR $\delta$ KO on IVD gene expression. ....	149
Figure 4.6: Effect of diet-induced obesity and PPAR $\delta$ deletion on knee joint health. ....	150
Figure 4.7: Diet-induced obesity reduces grip strength in female mice. ....	152
Figure 4.8: Diet-induced obesity increases sensitivity to mechanical stimuli in wild-type mice. ....	154
Figure 4.9: Diet-induced obesity affects physical function and locomotion.....	155
Figure 4.10, Supplementary Figure 1: Schematic overview of PPAR $\delta$ diet study design. ....	166
Figure 4.11, Supplementary Figure 2: Effect of PPAR $\delta$ activation on metabolic gene expression in IVD explant cultures. ....	167
Figure 4.12, Supplementary Figure 3: Effect of PPAR $\delta$ agonism on extracellular matrix in IVD explant cultures.....	168
Figure 4.13, Supplementary Figure 4: Tail Flick assay. ....	169
Figure 4.14, Supplementary Figure 5: Tramadol induced a slight sedative effect in male mice. ....	170
Figure 5.1: Schematic illustrating the proposed contributions of mechanical loading and obesity to IVD degeneration and associated pain. ....	186
Figure 5.2: Schematic overview of proposed context-dependent role of PPAR $\delta$ in the IVD. ....	188

## List of Appendices

APPENDIX A: PERMISSION TO REUSE MATERIAL .....	200
APPENDIX B: ANIMAL PROTOCOL NOTICE OF APPROVAL.....	201

## List of Abbreviations

<b>Abbreviation</b>	<b>Full Name</b>
Abca1	ATP binding cassette subfamily A member 1
Acan	Aggrecan
ADAMTS	A disintegrin and metalloproteinase with thrombospondin motifs
AF	Annulus Fibrosus
AF-1	Activating function-1
AF-2	Activating function-2
AGE	Advanced glycation end product
Angptl4	Angiopoietin-like 4
ATF3	Activating transcription factor 3
ATP	Adenosine triphosphate
BDNF	Brain-derived neurotrophic factor
BMD	Bone mineral density
BMI	Body mass index
CCN2	Cellular communication network factor 2
CEP	Cartilage endplate
CGRP	Calcitonin gene-related peptide
Cpt1a	Carnitine palmitoyltransferase 1A
CRP	C-reactive protein
CT	Computed tomography
DMMB	Dimethylmethylene blue
DNA	Deoxyribonucleic acid

DRG	Dorsal root ganglia
ECM	Extracellular matrix
FFA	Free fatty acid
FXR	Farnesoid X receptor
GAG	Glycosaminoglycan
Gdf5	Growth differentiation factor 5
GFAP	Glial Fibrillary acidic protein
Gsta4	Glutathione S-transferase A4
HU	Hounsfield unit
IBA-1	Ionized calcium binding adaptor molecule 1
IL	Interleukin
Insig1	Insulin induced gene 1
IP	Intraperitoneal
ISO	International organization of standardization
IVD	Intervertebral disc
KO	Knockout
LBP	Lower back pain
LFC	Lateral femoral condyle
LTP	Lateral tibial plateau
LXR	Liver X receptor
MCP-1	Monocyte chemoattractant protein-1
MFC	Medial femoral condyle
MHO	Metabolically healthy obese

MMP	Matrix metalloproteinase
MSK	Musculoskeletal
MTP	Medial tibial plateau
NGF	Nerve growth factor
Noto	Notochord homeobox
NP	Nucleus pulposus
OA	Osteoarthritis
OARSI	Osteoarthritis research society international
Pdk4	Pyruvate dehydrogenase kinase 4
PPAR	Peroxisome proliferator-activated receptor
Ptgs2	Prostaglandin-endoperoxide synthase 2
RAGE	Receptor for advanced glycation end products
ROS	Reactive oxygen species
Rps29	Ribosomal protein S29
RXR	Retinoid X receptor
Scx	Scleraxis BHLH transcription factor
SPARC	Secreted protein acidic and cysteine rich
TNF	Tumor necrosis factor
TrkA	Tropomyosin-related kinase A receptor
TRPV	Transient receptor potential vanilloid
Txnip	Thioredoxin interacting protein
VDR	Vitamin D receptor
VEGF	Vascular endothelial growth factor

WBV	Whole-body vibration
WT	Wild type

## Chapter 1

### 1 Introduction

#### 1.1 What is pain?

The International Association for the Study of Pain defines pain as “an unpleasant sensory and emotional experience associated with actual or potential tissue damage or described in terms of such damage”<sup>1</sup>. The ability to detect noxious and potentially dangerous stimuli is essential to avoid tissue injury and facilitate healing. While pain is unpleasant, it is essential for overall survival and wellbeing<sup>2</sup>. This is highlighted in individuals that have congenital insensitivity to pain. These individuals cannot feel broken bones, heat from a fire or being cut. As a result, they are not aware of potentially life-threatening injuries and do not know when to take appropriate protective behaviors<sup>3</sup>.

##### 1.1.1 Biological mechanisms of pain

Pain is a multidimensional, dynamic interaction between biological, psychological, and social factors that influence one another and can contribute to how a person interprets noxious stimuli signaling tissue injury<sup>4</sup>. At the biological level, nociception is the process by which information about actual or potential tissue damage is relayed to the brain<sup>5</sup>. These signals are initiated at specialized receptors called nociceptors, which are attached to thin myelinated A $\delta$  fibers and unmyelinated C-fibers that transmit the signal to the brain<sup>6</sup>. At the site of injury these nociceptors become activated by chemical activation or mechanical and thermal stimuli<sup>2</sup>, leading to the opening of voltage-gated sodium and potassium



channels<sup>2</sup>. The opening of these channels forms an action potential, which is then propagated to the dorsal horn of the spinal cord and ultimately the brain<sup>2</sup>.

### 1.1.2 Acute vs. Chronic pain

While acute pain plays a physiological role in response to tissue damage, chronic pain is defined as “pain that persists past the normal time of healing”, which, in the context of back pain, is typically over 3 months in duration<sup>7</sup>. Chronic pain conditions are one of the most common reasons people seek medical care, and have been linked with decreased quality of life, decreased mobility, and the development of psychiatric conditions such as depression and anxiety<sup>8-11</sup>. Chronic pain conditions have a large socioeconomic effect, affecting up to 40% of Canadians<sup>12</sup>. Chronic pain costs the Canadian taxpayer more than cancer and heart disease combined, with direct healthcare costs at \$6 billion a year<sup>13,14</sup> and indirect costs estimated at \$37 billion a year<sup>13</sup>. Uncontrolled pain is the most common cause of disability amongst working-age adults in Canada, and up to 60% of people living with chronic pain lose their jobs<sup>14,15</sup>.

While the precise mechanisms associated with the transition from acute to chronic pain are largely unknown, several potential mediators have been implicated including peripheral and central sensitization. Peripheral sensitization involves increased excitability of the primary afferent nociceptors, resulting in a decreased threshold for action potential generation or the generation of spontaneous action potentials without the presence of a noxious stimuli<sup>16,17</sup>. While many biological mechanisms can contribute to peripheral sensitization, inflammatory mediators secreted at the site of injury can change the properties of nociceptors<sup>5,18</sup>. Nerve growth factor (NGF) appears to be one key mediator

driving peripheral sensitization through both direct actions on the nociceptors and indirect actions on surrounding tissues. NGF is a neurotrophin released by many cell types, including inflammatory cells, at the site of tissue injury<sup>19,20</sup>. NGF exerts its actions through binding with its receptor, Tropomyosin-related kinase A receptor (TrkA), activating a series of downstream signaling pathways. NGF-TrkA activation on nociceptors leads to rapid sensitization of the neuron through intracellular signaling cascades that results in increased expression and phosphorylation of channels and receptors involved in pain transduction<sup>21,22</sup>. NGF-TrkA activation also leads to a prolonged increase in the expression of neuropeptides, receptors and ion channels involved in pain transmission<sup>23</sup>.

Central sensitization can also contribute to chronic pain. Central sensitization is caused by increased excitability of second order neurons within the spinal cord that transmit the nociceptive signals from the primary afferent neurons to the brain<sup>17,24</sup>. This increased excitability within the central nervous system can contribute to the lack of a direct correlation between nociceptor activation and painful experience<sup>17</sup>. Several mechanisms contribute to central sensitization including increased neuronal membrane excitability, facilitated synaptic transmission, and disinhibition of second order neurons<sup>25</sup>. While neuropeptides released from nociceptive neurons contribute to central sensitization, glial cells (astrocytes and microglia) within the spinal cord also play an important role in this process<sup>26</sup>. Astrocytes are the most abundant cell type within the brain and perform a variety of different functions including, but not limited to, regulating synaptic transmission and providing metabolic support to neurons<sup>27,28</sup>. However, in cases of chronic pain and neuroinflammation, these cells undergo a phenotypic switch to a so called “state of activation” marked by increased production of the astrocyte-specific marker glial fibrillary

acidic protein (GFAP), and an enlargement of the astrocyte processes<sup>26</sup>. Activated astrocytes have decreased glutamate reuptake and release neuromodulators that can alter synaptic transmission within the spinal cord<sup>26</sup>. Microglia, which are the resident macrophages in the spinal cord, are also activated in chronic pain conditions and contribute to central sensitization<sup>26</sup>. Activated microglia release pro-inflammatory cytokines that further modulate synaptic activity by altering the activity and expression of ion channels and receptors<sup>26</sup>. While both peripheral and central sensitization are potential mediators of chronic pain, it should be noted that pain is a biopsychosocial experience that has sensory, affective, and cognitive components that contribute to the interpretation of nociceptive signals, and whether the signals coming into the brain are perceived as pain<sup>5</sup>.

## 1.2 Back pain is a problem

The most recent *Global Burden of Disease* study reported back pain as the single most common cause of disability worldwide, with a lifetime prevalence of over 84% in developed countries<sup>29</sup>. While 90% of people recover from acute episodes of lower back pain (LBP) within a few months, some will not recover and instead develop chronic LBP<sup>30,31</sup>. Chronic LBP is debilitating physically as well as socially. People suffering from LBP report feeling hopelessness, loss of identity and social isolation, which can lead to depression and suicide ideation<sup>32,33</sup>. Like other chronic pain conditions, chronic LBP has a large impact at the societal level as well. In the United States, LBP costs the economy an estimated \$100 billion a year in both direct (primary care, pharmaceuticals, etc.) and indirect costs (lost wages, reduced productivity)<sup>34</sup>. Several tissues appear to be involved in chronic LBP, including muscles, ligaments, facet joints, nerve roots, vertebral bones, and

the intervertebral discs (IVDs)<sup>35</sup>. Of these, pain arising from IVD degeneration – termed discogenic back pain - is believed to be the major contributor to pain in an estimated 40% of cases<sup>36,37</sup>. Current therapeutic interventions focus on providing symptomatic relief, but do not address the underlying cause of the pain<sup>38</sup>, or restore the mechanical function of the tissue<sup>39</sup>. Altered mechanical function of the tissue can accelerate IVD degeneration in adjacent spinal levels, which can further contribute to pain and disability<sup>40,41</sup>. Our ability to treat IVD degeneration is limited due to an incomplete understanding of molecular processes that regulate IVD homeostasis and disease.

## 1.3 The Spine

In humans, the spine has 3 main functions: protect the spinal cord and nerve roots, provide structural support to maintain balance and upright posture, and enable flexible motion<sup>42</sup>. Anatomically, the spine consists of an osseous vertebral column surrounded by musculature and connective tissues that aid in the overall function of the structure (**Figure 1.1**). The basic functional unit of the spine is called a motion segment, consisting of a single intervertebral disc, the inferior and superior vertebrae and associated connective tissue<sup>43</sup>.

### 1.3.1 Vertebral bone

In humans, the vertebral column is composed of 24 presacral vertebrae separated by 23 intervertebral discs (IVDs), subdivided into three anatomical regions: cervical (7 vertebrae, 6 IVDs), thoracic (12 vertebrae, 12 IVDs) and the lumbar region (5 vertebrae, 5 IVDs)<sup>44</sup>. In mice, the vertebral column is composed of 7 cervical, 13 thoracic, 6 lumbar,

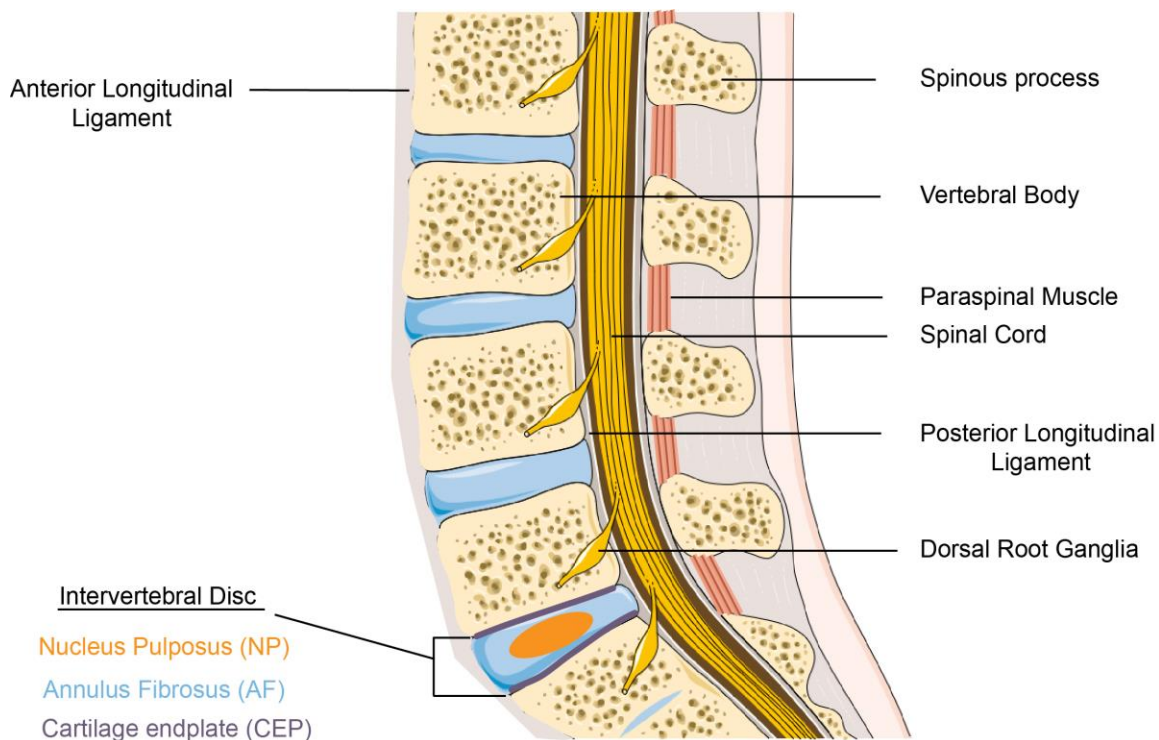


**Figure 1.1: Schematic depiction of the major components of the spine.**

The spine is composed of several different tissues that are essential for its overall function. These include osseous vertebrae, fibrocartilaginous intervertebral discs, muscles, and ligaments. The spine also serves structurally to surround the spinal cord. The spinal cord is a component of the central nervous system that transmits motor and sensory information between the brain and the peripheral nervous systems.

4 sacral, and 28 caudal (tail) vertebrae<sup>45</sup>. While the osseous features of each vertebrae are generally preserved in the different anatomical areas, their morphology differs slightly and contribute to the biomechanical stability and flexibility of the vertebral column<sup>44</sup>.

### 1.3.2 The Intervertebral Disc

The intervertebral disc (IVD) is a fibrocartilaginous joint that links vertebral bodies along the spine and allows for spine flexibility and stability under axial compression<sup>46</sup>. Anatomically, the IVD is a heterogeneous structure composed of three distinct, yet interdependent tissues. At the core of the IVD lies the gelatinous nucleus pulposus (NP), surrounded by the fibrocartilaginous annulus fibrosus (AF), and cartilage endplates that anchor the IVD to adjacent vertebrae (**Figure 1.1**). Each tissue is structurally and mechanically unique, but closely coupled with one another to contribute synergistically to the function of the IVD<sup>47</sup>.

#### 1.3.2.1 Nucleus Pulposus

At the center of the IVD lies the nucleus pulposus (NP), a gelatinous tissue composed of proteoglycans and water held together by an irregular network of type II collagen<sup>48</sup>.

Although the NP contains several different types of proteoglycans such as decorin, versican, and biglycan, the major proteoglycan in the NP is aggrecan<sup>48,49</sup>. These proteoglycan core proteins are covalently bound by glycosaminoglycans (GAGs), such as chondroitin sulfate and keratin sulfate, that act to draw water into the NP thereby contributing to its osmotic properties and ability to dissipate compressive loads<sup>48,50,51</sup>. Aggrecan also has the ability to form proteoglycan aggregates, in which many aggrecan molecules interact with hyaluronan via link protein, which limits their diffusion through

the tissue, allowing for an even distribution of load across the NP<sup>51,52</sup>. Within the NP there are two different cell types that contribute to extracellular matrix (ECM) production: notochord cells and cartilage-like NP cells. During development, notochord cells are the major cell type in the NP and produce a proteoglycan rich ECM<sup>53,54</sup>. In humans, the number of notochord cells within the NP steadily decrease with age, and the NP is populated instead by cartilage-like NP cells<sup>55</sup> that secrete an altered ECM<sup>53</sup>. Functionally, the role of the NP is to dissipate compressive loading between adjacent vertebral segments of the spine. This is facilitated through the osmotic pressure created by the anionic side chains attached to proteoglycan, which act to draw in water to this tissue<sup>46,47</sup>. The NP's ability to dissipate compressive loading is dependent on the radial forces of the surrounding annulus fibrosus<sup>56</sup>.

### 1.3.2.2 Annulus Fibrosus

The fibrocartilaginous annulus fibrosus (AF) encapsulates the gelatinous NP. The major component of the AF ECM is collagen, with lower levels of proteoglycans compared to the NP<sup>57</sup>. In the AF, the collagen fibers run in parallel to one another within distinct lamella. In humans, the AF is arranged in 15-25 concentric lamellae, where collagen fibers of adjacent lamellae travel in opposite directions at oblique angles, to form an angle-ply structure providing tensile strength<sup>56,58,59</sup>. The AF is typically divided into the outer AF and the inner AF, which have different ECM components. The outer AF is composed largely of type I collagen and elastic fibers, helping the tissue to dissipate tensile load<sup>56,60</sup>. This is in contrast to the inner AF, which serves as a transition between the fibrocartilaginous outer AF and the NP, and has a higher type II collagen and proteoglycan

content within the interlamellar matrix than the outer AF; a feature that provides resistance to compressive loading<sup>56,61</sup>. Similar to the ECM composition, the cellular morphology and biochemical profiles of the cells are different based on anatomical location within the AF<sup>62</sup>. Cells in the inner AF have more of a rounded, chondrocyte-like morphology compared to the spindle-shaped, fibroblast-like cells of the outer AF<sup>62</sup>. The difference in cellular profiles across this tissue are thought to arise from variations in mechanical loading seen across the tissue, where cells of the inner AF are exposed to compression and tension and the cells of the outer AF are exposed to predominantly tension<sup>63,64</sup>. Functionally, the role of the AF is to support the radial forces exerted by the NP<sup>63</sup>, which requires the tissue to be able to resist tensile loading and depends on the microarchitecture of the collagen network<sup>47</sup>.

### 1.3.2.3 Cartilage endplates

The cartilage endplates (CEP) are thin layers of hyaline cartilage at the superior and inferior ends of the IVD<sup>57</sup>. Similar to articular cartilage, the CEP is composed mostly of water, followed by type II collagen and proteoglycans<sup>57,65</sup>. The collagen fibrils within the CEP are arranged differentially based on location within the CEP, but merge with collagen fibers of the AF at the margins of the IVD<sup>56</sup>. The cells of the CEP are very similar in morphology and density to articular chondrocytes, yet, no zonal arrangement is seen within the CEP<sup>66</sup>. The main role of the CEP is to act as a semi-permeable barrier. While the outer lamellae of the AF is vascularized, the NP is completely avascular and depends on diffusion through the CEP for nutrient supply<sup>67</sup>. The vertebral bone underlying the CEP is highly vascularized, allowing for the diffusion of small molecules such as oxygen and glucose



into the IVD<sup>67</sup>. With age, the CEP can become calcified, thereby impairing the diffusion of solutes into the IVD; a process thought to drive IVD degeneration<sup>67,68</sup>.

### 1.3.3 Muscle and connective tissue

Muscle and connective tissues (i.e. ligaments and tendons) connect to the vertebral bodies at a number of anatomical landmarks and play a major role in movement as well as supporting the axial skeleton in an upright posture<sup>69,70</sup>. Muscle specifically plays a very important role in supporting the spine against forces seen in everyday life<sup>71</sup>. Muscular dysfunction, whether due to muscle weakness or impaired neurological coordination, contributes to decreased stability of spinal structures, leading to gradual degeneration of joints and soft tissue over time, potentially contributing to LBP<sup>71,72</sup>. Clinically, atrophy of paraspinal muscles (e.g. multifidus muscle) has been associated with chronic LBP<sup>73</sup>, however, it is difficult to determine whether this is a cause or consequence of pain.

### 1.3.4 Innervation & Vascularization

In the lumbar spine, the vertebral bodies, muscles and ligaments are innervated by several different nerves including the sinuvertebral nerves, ventral rami, dorsal rami, and gray rami<sup>74,75</sup>. While lumbar IVDs receive innervation from some of the same neural sources (sinuvertebral nerve, dorsal rami)<sup>76</sup>, the presence of nerves is restricted to the outermost layers of the AF in healthy tissues<sup>77,78</sup>. The lumbar spine receives its blood supply from several sources, including the lumbar, middle sacral, and branches of the iliolumbar arteries<sup>79</sup>. While the tissues surrounding the IVD are well vascularized, only the outermost layers of the AF receive direct vascular supply<sup>80</sup>.

## 1.4 Intervertebral Disc Degeneration

IVD degeneration has been defined as an aberrant, cell-mediated response leading to progressive structural failure<sup>81</sup>. It involves a progressive cascade of events, beginning with changes to the IVD microenvironment and eventually resulting in structural breakdown and functional impairment of the tissue<sup>39</sup>. Disc degeneration is characterized by increased ECM breakdown and abnormal (fibrotic) matrix synthesis leading to reduced hydration, loss of disc height, and decreased ability to absorb load<sup>50,82</sup>. As mentioned previously, IVD degeneration is believed to be the primary contributor to chronic LBP in an estimated 40% of cases<sup>36</sup>. IVD degeneration is distinguished from disc herniation, which is associated with a tear of the AF (often associated with acute injury), leading to extrusion of the NP into the space surrounding the IVD also resulting in pain<sup>83</sup>.

### 1.4.1 Risk factors for IVD degeneration

Risk factors for IVD degeneration include non-modifiable risk factors such as genetics, age and sex, as well as modifiable/environmental risk factors such as obesity, mechanical loading, and smoking. It should be noted that these risk factors are not mutually exclusive, and individuals can have multiple risk factors contributing to disease progression. Moreover, IVD degeneration is likely a group of diseases with distinct etiologies yet a common radiographic presentation.

#### 1.4.1.1 Non-modifiable risk factors

Genetic predisposition is the largest risk factor for IVD degeneration, followed by age<sup>50,84,85</sup>. With the advance in genetic technologies, genome-wide association studies

have highlighted several gene variants as risk factors for the development of IVD degeneration. Many of these genes encode for proteins involved in ECM homeostasis including collagen I, collagen IX, aggrecan, matrix metalloproteinase-3 (MMP-3) amongst many others<sup>86,87</sup>. Polymorphisms in the coding region of these matrix components may lead to altered protein products, functional impairment, and ultimately accelerated IVD degeneration. For example, polymorphisms within aggrecans coding region are believed to decrease the number of GAG binding sites, impairing the hydrophilic nature of the molecule. This is thought to contribute to IVD degeneration through decreased hydration of the IVD, reducing its ability to dissipate compressive load<sup>88</sup>. While polymorphisms within intronic and exonic regions of single genes have been associated with IVD degeneration, it is believed that IVD degeneration is likely polygenic, where minor variations within several genes work synergistically to contribute to disease progression<sup>89-92</sup>. In addition to genetic predisposition, age and sex are also established risk factors for IVD degeneration<sup>93,94</sup>. In humans, IVD degeneration accelerates linearly during the fifth decade of life<sup>94</sup>, with potential causes being loss of nutrition caused by CEP calcification, cellular senescence, and accumulation of degraded ECM<sup>50,67,93</sup>. In addition, females show an increased risk of developing IVD degeneration (Odds Ratio [OR], 1.69 when adjusted for age) compared to males, although biological mechanisms underlying this association are currently unknown<sup>95</sup>.

#### 1.4.1.2 Modifiable risk factors

Life-style related risk factors have been shown to have a large impact on IVD health. These risk factors include mechanical loading, obesity, shift work and smoking<sup>81,96,97</sup>. Mechanical

loading plays a major role in IVD cell function<sup>47</sup>, and mechanical overloading can promote processes associated with IVD degeneration including induction of catabolic gene expression and cell death<sup>98</sup>. In humans, increased loading is associated with IVD degeneration, through occupational hazards<sup>99</sup> or recreational sports such as weightlifting<sup>100</sup>. Increased mechanical loading on the IVD is also seen in obesity, which is a risk factor for both structural IVD degeneration and LBP<sup>101,102</sup>. However, this link between obesity, IVD degeneration, and LBP is likely multifactorial, involving both mechanical and metabolic components<sup>103</sup>. The exact mechanisms by which these modifiable risk factors contribute to IVD degeneration are still being explored, but their impact can be reduced through life-style modifications and education.

#### 1.4.2 Pathogenesis of IVD degeneration

Cells of the IVD are necessary to produce, maintain and repair the extensive ECM needed for the IVD to be functional. With IVD degeneration, cells undergo substantial biological changes including altered cellular phenotype, senescence, and apoptosis, that may contribute to disease progression<sup>53</sup>. Cellular senescence – the irreversible arrest of cell proliferation<sup>104</sup> – is increased in IVD degeneration<sup>105</sup>. Alongside reduced proliferative capacity of these cells, there are also alterations in cellular function and phenotype. In human IVD cells, markers of senescence positively correlate with increased expression of matrix degrading enzymes such as MMP13 and ADAMTS5, which mediate matrix degradation in IVD degeneration<sup>106</sup>. While senescence naturally occurs during aging through telomere shortening, it can be accelerated by stress signals such as the pro-inflammatory cytokine interleukin 1 (IL-1), which is also associated with IVD

degeneration<sup>107,108</sup>. However, it is unlikely that all phenotypic differences associated with IVD degeneration are due to cellular senescence, as reversible changes can be caused by environmental signals such as mechanical loading<sup>53</sup>. During IVD degeneration, cells produce increased levels of inflammatory and catabolic factors, decrease synthesis of normal ECM components (type II collagen, aggrecan), increase synthesis of fibrotic matrix components (type I collagen), and alter secretion of growth factors that can potentiate the degenerative process<sup>53</sup>. In addition to alterations in the phenotype of remaining IVD cells, IVD degeneration is also associated with increased levels of cell apoptosis<sup>109</sup>. Together these factors decrease the number of properly functioning cells needed to maintain and repair the ECM, potentially accelerating IVD degeneration.

Alterations in cellular function associated with IVD degeneration is marked by increased production of factors that accelerate ECM degradation, including matrix metalloproteinases (MMPs) and ‘a disintegrin and metalloproteinase with thrombospondin motifs’ (ADAMTS)<sup>110</sup>. MMP-1,-2,-3,-7,-12,-13 are upregulated in human IVD degeneration<sup>110-112</sup>, and degrade a number of ECM components, including collagens type I and II, as well as non-collagenous proteins such as aggrecan<sup>113</sup>. ADAMTS-4, and -5 are also upregulated in IVD degeneration<sup>113,114</sup>. Unlike the MMPs, ADAMTS enzymes demonstrate a narrow substrate specificity; ADAMTS-4, and -5 primarily cleave aggrecan, and their increased activity leads to the accumulation of fragmented proteoglycans within the IVD<sup>114</sup>. While not directly investigated in the IVD, these proteoglycan fragments potentiate inflammatory processes in articular cartilage through activation of toll-like receptors, and may therefore likewise accelerate IVD degeneration<sup>115</sup>. In addition to matrix degrading enzymes, IVD cells intrinsically produce and secrete inflammatory cytokines

and neurotrophins such as IL-1 $\beta$ , IL-6, Tumor Necrosis Factor alpha (TNF  $\alpha$ ), NGF, which are all elevated with IVD degeneration<sup>78,108,116</sup>. Aside from their pro-nociceptive roles on nerve roots<sup>93,117</sup>, these inflammatory cytokines can potentiate pathways leading to increased expression of many of the catabolic enzymes mentioned above including MMP-1,-3,-13 and ADAMTS-4,-5<sup>108</sup>. As a result of ECM breakdown and an altered secretion of matrix components, the biomechanical properties of the IVD are impaired<sup>50,118</sup>. As the NP becomes less hydrated and more fibrous, it is no longer able to dissipate compressive loads effectively, resulting in increased transfer of load to the AF<sup>118</sup>. Increased AF mechanical loading in turn leads to structural degeneration of the AF<sup>119</sup>.

Lastly, IVD degeneration is associated with vascular and neural ingrowth into the normally avascular and aneural tissue<sup>120,121</sup>. It has been suggested that this neural ingrowth is an important contributor to discogenic pain, which is pain originating from the IVD<sup>120,122</sup>. While the mechanisms responsible for nerve ingrowth into the IVD are largely unknown, ECM breakdown and neurotrophins are believed to play an important role<sup>78</sup>. In healthy IVDs, aggrecan has been shown to inhibit nerve ingrowth, however, when IVDs degenerate, loss of intact aggrecan may result in nerve ingrowth<sup>78,123</sup>. This appears to be coupled with increased expression of proinflammatory cytokines such as IL-1 $\beta$ , TNF $\alpha$  and IL-4 inducing the expression of the NGF, which can directly stimulate nociceptive afferents and cause further ingrowth of nociceptive nerve fibers into the IVD<sup>78</sup>.

Once the process of IVD degeneration has started, it is difficult to stop. A recent review describes IVD degeneration as a vicious circle, where abnormal interactions between biomechanics, cellular processes, and ECM components result in a positive feedback loop resulting in accelerated IVD degeneration (**Figure 1.2**)<sup>119</sup>. An alteration in any of these

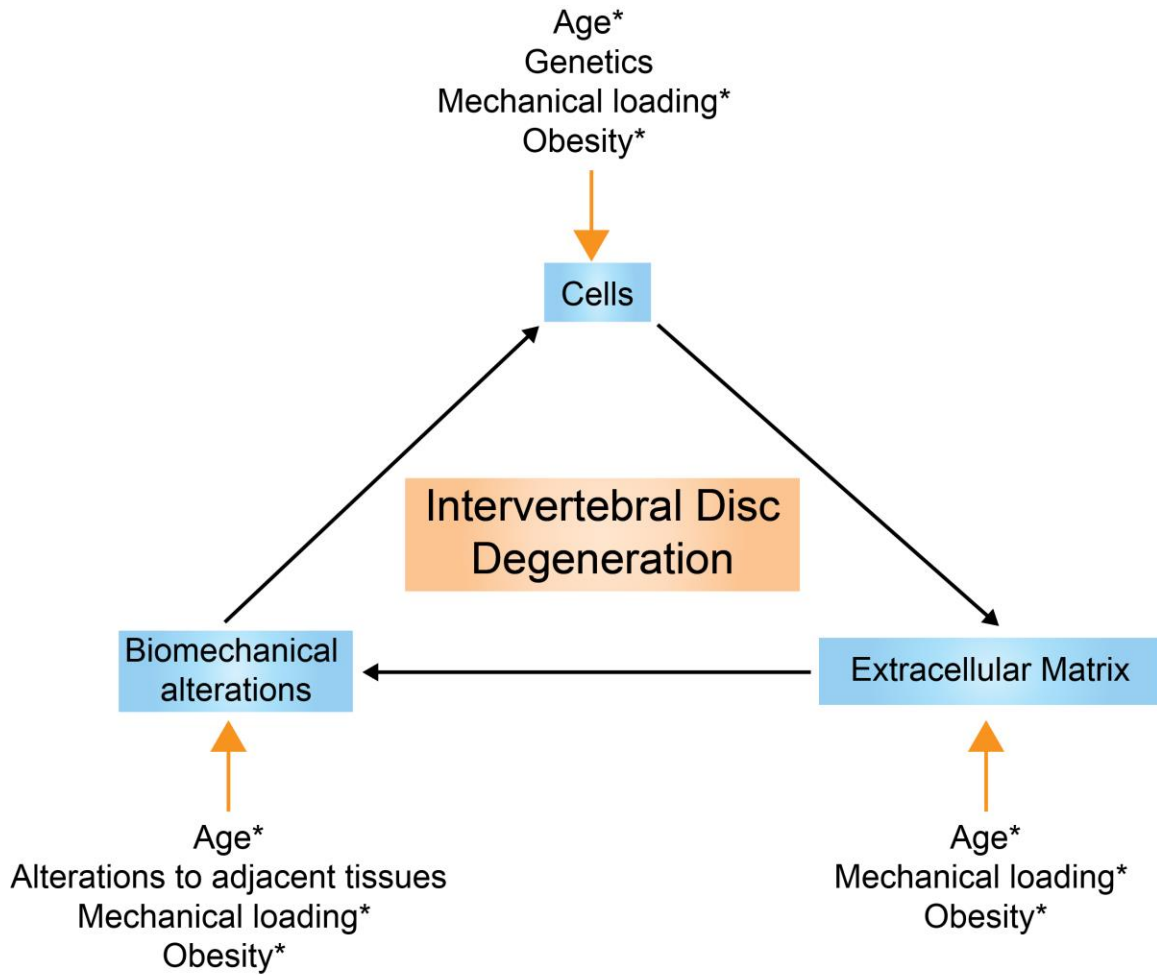


**Figure 1.2: Proposed feed forward model of intervertebral disc degeneration with contributing risk factors.**

Intervertebral disc homeostasis is dependent on interactions between cells, extracellular matrix, and biomechanics of the spine. Alterations in any of these factors alter the others and can initiate the degenerative cycle. For an example, upregulation of catabolic genes (i.e. *Mmp3*, *Mmp13*, *Adamts4*, *Adamts5*) from the cells of the IVD – perhaps caused by aberrant mechanical loading or obesity - would lead to the degradation of the extracellular matrix, thereby altering the biomechanical properties of the IVD. Alterations in tissue mechanics would then alter the mechanical loads experienced by cells, causing further alterations to cellular function. Figure modified from<sup>118</sup>; Asterix indicate risk factors assessed in the current thesis.

elements may initiate IVD degeneration, ultimately leading to structural and functional failure of the tissue<sup>118</sup>.

### 1.4.3 The link between IVD degeneration and pain

Despite the clinical association between radiographic IVD degeneration and LBP, this link remains poorly understood. In fact, patients presenting with back pain often lack radiographic signs of IVD degeneration, and many individuals with radiographic IVD degeneration are completely asymptomatic<sup>124,125</sup>. While the difference between symptomatic and asymptomatic IVD degeneration is not well understood, it has been suggested that nerve in-growth may cause discogenic back pain<sup>126-128</sup>. During IVD degeneration, both NP and AF cells release pro-nociceptive factors including IL-1, IL-6, TNF $\alpha$ , and NGF<sup>108,129,130</sup>, which can act as nociceptive triggers. In addition to nerve ingrowth to the disc and direct activation of nociceptors, it is believed that IVD degeneration contributes to LBP in indirect mechanisms as well<sup>128</sup>. With IVD degeneration there are structural and function changes within the IVD that impact adjacent tissues and may provoke pain indirectly<sup>128</sup>. For example, in advanced IVD degeneration the significant loss of IVD height can cause foraminal or central stenosis leading to compression of the nerve roots or spinal cord<sup>128</sup>. Functional failure of the IVD may also lead to motion segment instability<sup>43</sup> leading to compensation from surrounding tissues<sup>128</sup>. This functional compensation can lead to muscle strain/spasm, or degeneration of other tissues in the spine such as the facet joint, which may also contribute to pain directly<sup>128,131</sup>.



#### 1.4.4 Treatment for IVD degeneration

There are no treatments to modify or prevent the progression of IVD degeneration. Current therapeutic options address the primary clinical concern with IVD degeneration – back pain - using lifestyle, pharmacological, and surgical interventions<sup>132</sup>. Recent clinical guidelines suggest non-pharmacological therapies such as exercise and cognitive behavioral therapy as first-line treatments, with limited pharmacological and surgical interventions<sup>132</sup>. Despite these recommendations, surgical interventions (i.e. spinal fusions) for chronic LBP is on the rise despite a lack of evidence of effectiveness<sup>132,133</sup>. The current lack of disease-modifying treatments for IVD degeneration and associated LBP is largely due to an incomplete understanding of the pathophysiology of the disease, and the interplay between the tissues involved.

### 1.5 Similarities between IVD degeneration and osteoarthritis

The IVD shares several similarities with articular cartilage, and many of the pathways associated with disc degeneration (detailed above) have also been implicated in the pathogenesis of osteoarthritis (OA)<sup>134</sup>. OA is a heterogeneous disease that can affect multiple joints – most commonly the knee - resulting in pain and loss of function in patients<sup>135,136</sup>. It is characterized by a progressive loss of articular cartilage, subchondral bone sclerosis and synovial hyperplasia<sup>137</sup>. Clinically, OA is typically diagnosed based on radiographic evidence of joint space narrowing, osteophyte formation, and sclerosis<sup>138</sup>. Interestingly, these OA features are also detected in IVD degeneration<sup>139</sup>, which has driven speculation about a potential link between the two pathologies. At the cellular level, NP cells resemble articular chondrocytes and produce a similar ECM rich in type II

collagen and aggrecan, while AF cells resemble those of the fibrous connective tissue comprising of the articular joint capsule<sup>134</sup>. Similarities exist between the degenerative processes in IVD degeneration and OA including alterations to the ECM, biomechanics, genetic factors, inflammation, symptoms and risk factors, as recently reviewed<sup>134</sup>.

Despite these similarities, it should not be supposed that OA and IVD degeneration are identical. There are differences in both the developmental origins and biomechanical properties of each tissue. The IVD is formed by two different structures during development, the notochord and sclerotome<sup>140,141</sup>. The notochord serves as the embryonic precursor to the NP<sup>141</sup>, while the sclerotome contributes to the AF and adjacent vertebral bones<sup>140</sup>. In contrast, the articular joints of the appendicular skeleton are formed later in development, through the condensation of mesenchymal precursor cells<sup>142</sup>. While there are key similarities between these two disease states, each involves distinct tissue types and may differ in potential pathogenic pathways.

## 1.6 Mechanobiology of the IVD

In order for humans to remain upright, muscles of the posterior trunk contract and exert high levels of mechanical load, especially in the lumbar spine<sup>143</sup>. As the “shock absorber” of the spine, cells within the IVD are exposed to a variety of different loading modalities such as compressive and tensile load<sup>143</sup>. Mechanical loading is a key regulator of IVD homeostasis; multiple studies have highlighted the complexity of the cellular and molecular events that it triggers in IVD cells (as reviewed in<sup>143</sup>). The effects of mechanical loading on IVD cell physiology are dependent on both cell type and the loading parameters applied (including load type, magnitude, frequency and duration). Several reviews have recently

described the biological response of NP and AF cells to various mechanical loads<sup>47,98,143,144</sup>. This body of work describes the physiological zone in which loading promotes matrix synthesis and growth factor secretion to maintain disc health<sup>98</sup>. Outside of this zone – either underloading or overloading - the cellular response shifts towards catabolism, marked by the induction of matrix-degrading enzymes, inflammatory cytokines, and cell apoptosis<sup>98</sup>.

### 1.6.1 Mechanical loads seen by the IVD

Different compartments of the IVD experience different parameters of mechanical load and respond to these loads through different mechanisms. Due to overall anatomy of the spine and surrounding musculature and ligaments, IVDs are never completely unloaded. Instead, IVDs experience a constant level of mechanical stimulation known as preload<sup>59</sup>. In addition to this preload, daily activity such as walking or lifting exerts additional mechanical forces on the spine that are dissipated by the IVD<sup>143</sup>. In response to mechanical loading, the osmotic properties of the NP enable to absorb compressive loads on the spine. The consequent intradiscal pressure exerted by the NP is then dissipated by the tension that develops between the lamellae of the AF<sup>81</sup>.

### 1.6.2 Mechanotransduction

The process by which cells sense mechanical stress and convert it into downstream biological activity is known as mechanotransduction. Mechanotransduction occurs in three coupled, yet distinct, steps: first, the mechanical stimulus is sensed by mechanoreceptors; second, these receptors activate signal transduction pathways; and third, these pathways

induce a cellular response<sup>145</sup>. While mechanotransduction pathways are not fully defined in the IVD, several targets including integrins, purinergic receptors, and transient receptor potential vanilloid 4 (TRPV4) ion channels have been implicated in the response of NP and AF cells to mechanical loading<sup>146</sup>.

### 1.6.3 IVD tissue response to aberrant mechanical loads

While mechanical loading is essential for IVD health, overloading or underloading can lead to catabolic processes associated with IVD degeneration<sup>98</sup>. Underloading of the spine is experienced during prolonged immobilization or in zero gravity and has been shown to accelerate IVD degeneration<sup>147,148</sup>. On the opposite end of the spectrum is overloading, experienced for example during weightlifting or whole-body vibration, which likewise has been shown to induce IVD degeneration<sup>147</sup>. *In vitro*, exposure to aberrant mechanical loading induces the expression of matrix-degrading enzymes, inflammatory cytokines, and cell apoptosis in both NP and AF cells<sup>98</sup>.

#### 1.6.3.1 Whole-body vibration

Occupational exposure to high-amplitude, low-frequency whole-body vibration - typically created by the operation of heavy equipment – has been shown to contribute to the development of IVD degeneration and back pain<sup>149</sup>. Despite this, whole-body vibration (WBV) platforms designed to deliver low-amplitude, high frequency mechanical vibration are being used clinically based on their reported ability to increase bone density<sup>150</sup> and muscle strength<sup>151</sup>. Within the last decade, WBV has been integrated into physical therapy regimens for a variety of musculoskeletal (MSK) disorders, including osteoporosis<sup>150</sup>, back

pain<sup>152</sup>, and OA<sup>153</sup>. In addition to their clinical use, WBV platforms are marketed by the health and wellness industry as “no-workouts” to replace traditional resistance training. However, a dichotomy exists surrounding the safety of WBV: WBV is being promoted as a safe and effective treatment for MSK conditions, yet epidemiological studies have established a strong association between workplace exposure to WBV and the development of MSK conditions<sup>149</sup>. Recognizing the potential of WBV to cause tissue damage, the International Organization for Standardization (ISO) implemented guidelines indicating the maximum daily limit workers can be exposed to WBV without being at risk for injury<sup>154</sup>. However, there are no regulation associated with use of commercially available WBV platforms, which are typically able to deliver vibration far greater than what ISO-2631 guidelines deem as acceptable<sup>155</sup>.

Raising further concern, clinical trials have shown conflicting reports regarding the ability of WBV to slow bone loss, and its effectiveness in reducing back and OA-associated pain. In young women (15-20 years old) with low bone mineral density (BMD) daily WBV therapy increased cortical BMD in the femoral mid-shaft<sup>156</sup>; however, the same researchers subsequently reported that older males and females (mean age = 82) showed no significant differences in BMD following exposure to WBV<sup>157</sup>. Clinical trials investigating the effectiveness of WBV to treat back pain reported improvements in patient self-reported pain<sup>158,159</sup>; however, these studies did not directly assess joint health. Based on the lack of rigorous research-based evidence, a recent analysis cautioned against the use of WBV to treat back pain<sup>152</sup>. Clinical trials evaluating the effectiveness of WBV for the treatment of joint pain in knee OA have also shown conflicting results. A number of studies reported that WBV reduced pain intensity<sup>153,160</sup>, while other studies report no significant

improvement in pain intensity in knee OA patients following WBV<sup>161</sup>. The lack of rigorous evidence-based research surrounding the efficacy and safety of WBV is concerning given their prevalent use in physiotherapy clinics and gyms.

Given this conflicting evidence, our group carried out several studies using the mouse as a preclinical model to directly assess the effects of WBV on skeletal health. These studies demonstrated that exposure of mice to WBV using vibrational parameters used clinically induces significant IVD degeneration and OA-like damage to the knee in as little as 4-weeks<sup>162–164</sup>. In addition to gross histological damage, WBV induced inflammation within the IVD marked by upregulation of *Il-1 $\beta$*  followed by upregulation of matrix degrading enzymes associated with IVD degeneration including *Mmp-3,-13* and *Adamts5*<sup>165</sup>. These findings highlight the need for more comprehensive studies investigating the effects of WBV on joint health.

## 1.7 Metabolism of the IVD

As the largest avascular tissue in the human body, the IVD has a unique metabolic profile compared to other tissues. Aside from the outermost lamellae of the AF, the majority of the nutrients are supplied to the IVD through diffusion from the CEPs<sup>67</sup>. As such, several factors including blood supply to the adjacent tissues, loading and matrix composition affect nutrient supply to the IVD<sup>67</sup>. The IVD has low cellularity and an extensive ECM that impacts nutrient transport. The major components of this matrix are collagen fibers and negatively charged proteoglycans that act as semi-permeable barrier to molecules entering the disc. While small molecules such as oxygen and glucose are able to diffuse through, the ECM limits the movement of large molecules such as growth factors and

cytokines<sup>67,166</sup>. As a result of cellular metabolism and limits of diffusion, large concentration gradients of oxygen, glucose and lactic acid are observed within the IVD<sup>67</sup>. The center of the NP is an oxygen and glucose poor environment, with high levels of lactic acid<sup>67,167</sup>. The main source of ATP for AF and NP cells is through anerobic glycolysis<sup>168,169</sup>, allowing NP cells to survive up to 13 days in the absence of oxygen<sup>170,171</sup>. While the role of glucose and glycolytic production of ATP has been well characterized in the IVD, the role of lipid metabolism in IVD homeostasis is unknown. Of note, mediators of lipid metabolism impact articular cartilage health both negatively and positively, and have been shown to alter the progression of OA<sup>172,173</sup>.

## 1.8 Animal models of IVD degeneration and back pain

As with many other MSK diseases, animal models are often used to understand the pathophysiology of IVD degeneration and associated back pain<sup>174</sup>. A range of animal models are used to study IVD degeneration, from large animals (e.g. sheep, goats) to small rodents, that each have unique strengths and weaknesses. A common criticism of basic spine research is the use of quadrupedal animals. It is often assumed that humans experience higher mechanical loading on their IVDs due to upright posture. However, muscular contraction is the major contributor to axial compression along the spine and quadrupedal animals in fact experience higher relative compressive loading on their spines compared to bipedal animals<sup>174-176</sup>. Spinal tissues from large animal models such as sheep, and goats have a similar size, anatomy, mechanical loading and cellularity to those from humans<sup>175</sup>, and have been used extensively for models of surgically-induced IVD degeneration<sup>175</sup>. Despite these advantages, cost and associated limitations to sample size

in experiments is a major deterrent for research involving large animals<sup>177</sup>. Most basic research investigating IVD degeneration use small animal models. Rodents are most frequently used based on their ease of use, low cost and the ability to manipulate their genome<sup>174</sup>. Despite the size difference between human and mouse IVDs, both species have similar geometry, biomechanics and extracellular matrix composition<sup>178–180</sup>. Aside from their low housing costs and short generational times, one of the largest advantages of mouse models is the relative ease of genetic manipulation. Use of the *Cre/LoxP* recombinase system allows for modification of the murine genome in either a global or tissue specific manner<sup>181–183</sup>. A number of studies using genetically modified mice have highlighted the importance of matricellular and ECM components including CCN2, SPARC, and collagen type IX in IVD degeneration and back pain<sup>184–186</sup>.

In addition to genetic manipulation, mouse models have been used extensively for pain research<sup>187</sup>. Given the discordance between IVD degeneration and back pain, it is important to simultaneously assess both in preclinical models of disease<sup>188</sup>. While pain is a complex phenomenon, and limitations of mouse models should be acknowledged, their use has provided a number of promising therapeutic targets for the treatment of chronic pain<sup>189</sup>. To assess pain, several behavioral metrics have been developed for various modalities of pain<sup>187,188</sup>. Generally, these tests assess for behavioral indicators of evoked or spontaneous pain and are used extensively in the pain field<sup>187</sup>. In addition to behavioral metrics, mouse models also allow for the assessment of biological indicators associated with pain, such as neuroinflammation<sup>190</sup>. The use of animal models has provided researchers with valuable knowledge about potential mechanisms contributing to IVD degeneration and LBP and may potentially yield future therapeutic targets.



## 1.9 Obesity

Obesity – traditionally defined as a body mass index over 30 – is a worldwide epidemic. Obesity substantially increases the risk of developing metabolic, cardiovascular, neurological and MSK diseases<sup>191</sup>. With the prevalence of obesity nearly tripling over the last 30 years<sup>191</sup>, it poses a large public health concern. In the US, it is estimated that 21% of the total healthcare expenditure is used to directly treat obesity and obesity-related comorbidities<sup>192</sup>. At the individual level, obesity not only decreases life expectancy<sup>193</sup> but also decreases quality of life and leads to disability, mental illness and unemployment<sup>191,194</sup>.

### 1.9.1 Metabolic syndrome

Although several factors contribute to obesity including hormonal, nutritional, psychological and metabolic factors, obesity is fundamentally caused by an imbalance in energy input and expenditure<sup>191,195</sup> resulting in an accumulation of adipose tissue. Evolutionarily, the ability to store energy for long periods of time was essential for survival. However, in today's industrial world where food is abundant and lifestyles are sedentary, fat accumulation has negative health implications. As mentioned previously, obesity – or more specifically the accumulation of abdominal fat – is related to the development of several metabolic diseases, together termed metabolic syndrome<sup>196</sup>. Components of metabolic syndrome include abdominal obesity/large waist circumference, type II diabetes mellitus, hypertension, and dyslipidemia<sup>191,196,197</sup>. Together, these conditions have a tremendous impact on overall systemic health, and increase the risk of developing cardiovascular<sup>198</sup>, renal<sup>199</sup> and MSK<sup>200</sup> pathologies. Although the pathogenesis

of metabolic syndrome is complex, abdominal obesity appears to be a key causative factor<sup>201</sup>. Adipose tissue not only stores and releases fatty acids, but is also is a major endocrine organ that synthesizes and secretes proteins and hormones termed adipokines (e.g. leptin, adiponectin, visfatin, resistin) and inflammatory cytokines (e.g. TNF- $\alpha$ , IL-6)<sup>202,203</sup>. Increased release of these molecules is associated with the development of many aspects of metabolic syndrome including insulin sensitivity, hypertension and dyslipidemia independently<sup>204,205</sup>. However, this link between obesity and metabolic syndrome appears to be multifactorial, as increased adiposity is also associated with increase plasma levels of free fatty acids (FFAs), which can independently contribute to insulin sensitivity, hypertension and dyslipidemia<sup>206</sup>.

### 1.9.2 Musculoskeletal health

Obesity impacts several MSK tissues, including muscle, bone, and cartilage. Clinically, obesity is associated with an increased risk of sarcopenia, osteoporosis, OA, LBP and IVD degeneration<sup>207,208</sup>. While the mechanisms underlying these associations are not fully elucidated, obesity and obesity-associated diseases likely contribute through direct actions on the tissue of interest, as well as indirectly through effects on supporting tissues. A recent review by Zhuo *et al*<sup>200</sup> highlighted the differential impact of each component of metabolic syndrome in the context of OA. A common indirect mechanism believed to impact joint health is cardiovascular complications – postulated to lead to subchondral bone ischemia and impaired nutrition of the joint. Hypertension<sup>162</sup>, dyslipidemia<sup>79,209</sup> and type II diabetes<sup>210,211</sup> can lead to microvascular narrowing, atherosclerosis and endothelial dysfunction<sup>79,209,210</sup>, potentially resulting in subchondral bone ischemia. Lack of blood

supply could compromise nutrient exchange ultimately leading to cartilage degeneration<sup>200,212</sup>. In humans, hypertension, dyslipidemia, and type II diabetes are also independently associated with increased risk of IVD degeneration<sup>213-215</sup>. While the exact mechanisms have not been determined, impaired nutrient exchange has been implicated as a mediator of IVD degeneration<sup>67</sup>, and may be caused by these conditions. Aside from these indirect effects, components of metabolic syndrome may impact joint health directly through abnormalities in lipid/glucose metabolism and release of systemic factors<sup>200,216</sup>. Dyslipidemia may contribute to IVD degeneration through alterations in the lipid metabolism pathway. In chondrocytes, lipid metabolism regulates viability, matrix synthesis and inflammation<sup>217</sup>. While the role of lipid metabolism in the IVD is not well characterized, dysregulation of metabolic pathways in hypertriglyceridemia is associated with IVD degeneration, caused by IVD cell apoptosis and matrix catabolism<sup>214</sup>. Hyperglycemia resulting from type II diabetes is thought to contribute to IVD degeneration through increased production of reactive oxygen species (ROS) and advanced glycation end products (AGEs)<sup>200</sup>. *In vitro*, hyperglycemic conditions induce ROS production in both articular chondrocytes<sup>218</sup> and NP cells<sup>219</sup>, leading to matrix degeneration and apoptosis in both tissues<sup>219,220</sup>. AGEs are products of non-enzymatic glycation of proteins that accumulate with uncontrolled hyperglycemia<sup>221</sup>. In humans, AGEs accumulate in IVDs of people with type II diabetes<sup>222</sup>, which is thought to contribute to IVD degeneration through increased protein crosslinking, causing increased mechanical stiffness of the IVD<sup>223</sup>. Supporting this, dietary consumption of AGEs in mice was associated with increased IVD degeneration and altered biomechanics of spinal motion segments<sup>224</sup>. While biomechanical changes may play a role in AGE-induced IVD degeneration, AGEs may also activate the

receptor for advanced glycation end products (RAGE), which has been found to activate pro-inflammatory and catabolic processes in chondrocytic cells<sup>225,226</sup>.

Studies investigating the role of adipokines have also highlighted the importance of secreted factors in obesity-associated pathologies. For example, leptin-deficient mice become obese, yet they do not develop knee OA, suggesting leptin may play a key role in obesity-induced OA<sup>227</sup>. In the IVD, exposure of NP cells to adipokines, such as leptin and resistin, promotes catabolic metabolism associated with increased expression of matrix remodeling enzymes such as MMP and ADAMTS genes<sup>228,229</sup>.

### 1.9.3 Pain

In addition to the induction of degenerative joint diseases, obesity is also associated with chronic pain conditions, such as fibromyalgia, headaches and abdominal pain<sup>230</sup>. While the underlying mechanisms linking obesity and chronic pain remains unknown, it has been suggested that systemic immune and endocrine alterations play a role in the altered pain response<sup>231</sup>. Obesity is considered a low-grade chronic systemic inflammatory state with elevated levels of IL-6 and C-reactive protein (CRP) that may contribute to pain<sup>231,232</sup>. Pain is a biopsychosocial phenomenon<sup>4</sup>, so, in addition to these biological factors, obesity is also associated with depression<sup>233</sup> and poor sleep quality<sup>234</sup>. These conditions are both known to contribute to pain through various mechanisms<sup>235,236</sup>. A summary of the proposed mechanisms linking obesity with IVD degeneration and associated pain can be seen in **Figure 1.3**.

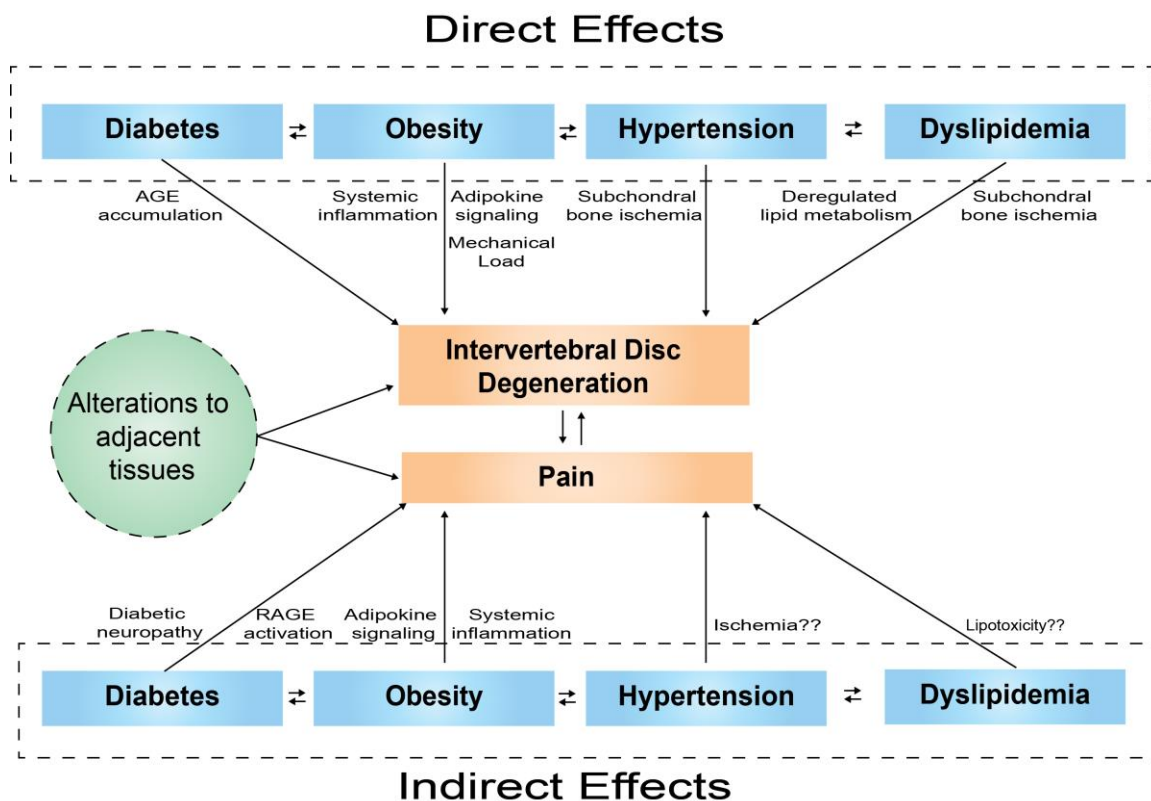


**Figure 1.3: Proposed mechanism underlying the association between obesity/metabolic syndrome, IVD degeneration, and pain.**

The link between obesity, IVD degeneration and back pain is multifactorial, involving both direct effects on the IVD and indirect effects on the nervous system and other tissues. Obesity may directly contribute to structural IVD degeneration through increased mechanical loading, systemic inflammation and adipokine signaling. Metabolic dysregulation associated with obesity leading to diabetes, hypertension and dyslipidemia may compound these direct effects and potentiate further degeneration. Indirectly, obesity and obesity-related pathologies may also alter pain-processing pathways contributing to back pain. Furthermore, damage/dysfunction of adjacent tissues (i.e. vasculature, muscle, vertebral bone, facet joints) caused by obesity may lead to both structural IVD degeneration and back pain. Figure based on content provided in<sup>199</sup>.

## 1.10 Nuclear Receptors

### 1.10.1 Structure

Nuclear receptors are a large family of ligand-regulated transcription factors activated by binding of steroid hormones, such as estrogen and progesterone, and lipid-soluble signals, including retinoic acid, oxysterols, and thyroid hormone, to alter transcription of downstream target genes<sup>237</sup>. Although nuclear receptors have different, and often opposing actions, they share a common structure. All nuclear receptors contain 4 domains, including the N-terminal domain that is of variable size and sequence, a conserved DNA binding domain, a variable hinge domain, and a ligand binding domain<sup>237</sup>. Some nuclear receptors contain an activation function-1 (AF-1) domain at the N-terminal domain, which is a ligand-independent domain that assists in the recruitment of coactivators<sup>238</sup>. The centrally located DNA binding domain is the most conserved segment of nuclear receptors; it contains two zinc fingers that binds to hormone response elements on the promoter of downstream target genes<sup>239</sup>. The hinge domain connects the DNA binding domain to the ligand-binding domain, which is a 12 helixed structure containing a ligand-dependent activation-function 2 (AF-2) domain<sup>237</sup>. A major characteristic of the ligand binding domain is a hydrophobic cavity that allows lipophilic ligands to be shielded from the hydrophilic environment<sup>237</sup>. These pockets allow selectivity for specific ligands through variations in size and amino-acid composition<sup>240</sup>. Binding of the ligand stabilizes the surface elements of the ligand binding domain and allows for coactivator/corepressor binding, altering downstream gene transcription<sup>237,241,242</sup>.

Nuclear receptors are divided into 4 main classes. Class I nuclear receptors are normally located in the cytoplasm bound to chaperone proteins, but through ligand activation are translocated to the nucleus where they can bind DNA and affect gene transcription<sup>243</sup>. Class I nuclear receptor ligands are steroid hormones such as estrogen, testosterone and corticoids<sup>244</sup>. Class II nuclear receptors on the other hand, remain in the nucleus regardless of ligand-activation<sup>243</sup>. Class II nuclear receptors are commonly found as heterodimers with retinoid X receptor (RXR), and include Peroxisome Proliferator Activated Receptors (PPARs), Liver X receptor (LXR), Farnesoid X receptor (FXR) and Vitamin D receptor (VDR)<sup>245</sup>. Class III nuclear receptors are similar to class II, however they typically exist as homodimers on their response elements<sup>243</sup>. Class IV nuclear receptors also have a similar mechanism of action to class II nuclear receptors, but typically are found as monomers on DNA<sup>243</sup>.

Many class II receptors respond to dietary lipids such as fatty acids (PPARs), sterols (LXR), bile acid (FXR), serving as “lipid sensors”<sup>246</sup>. Activation of these receptors occurs at physiological lipid concentrations influenced by dietary intake and leads to changes in transcription of genes involved in lipid metabolism, storage, transport and elimination<sup>246</sup>. While ligand binding is the major activator of nuclear receptors, their activity can also be modulated by posttranslational modifications, including phosphorylation, ubiquitination, and SUMOylation<sup>239</sup>.

### 1.10.2 Peroxisome Proliferator Activated Receptors (PPARs)

The PPARs are a subfamily of nuclear receptors whose ligands include fatty acids and their metabolites, which are of interest as they are dysregulated in obesity<sup>200,247</sup>. As a type II

nuclear receptor, PPARs form heterodimers with RXR, and when bound to their ligands they recruit co-activators or co-repressors to either activate or repress downstream gene expression depending on specific gene and cellular context<sup>243,248</sup>. There are three PPAR isoforms (alpha, delta, gamma) that play distinct roles in energy balance and metabolism<sup>249</sup>. The two most studied isoforms, PPAR $\alpha$  and PPAR $\gamma$ , are highly expressed in the liver and adipose, respectively. Agonists of these receptors are currently being used clinically for the treatment of a variety of obesity-associated conditions including dyslipidemia and type II diabetes mellitus<sup>250,251</sup>. Studies examining the role of PPAR $\gamma$  in murine cartilaginous tissues have shown that a cartilage-specific knockout of PPAR $\gamma$  leads to spontaneous OA development<sup>252</sup>. In contrast to the tissue-specific expression of other PPARs, PPAR $\delta$  has broad expression patterns and affects glucose and lipid metabolism, cell differentiation, proliferation, apoptosis and immune regulation<sup>253</sup>. Recent studies in mice have shown PPAR $\delta$  agonism improves insulin resistance, fat burning, and muscle endurance<sup>247,254,255</sup>; however, PPAR $\delta$  agonism has also been shown to induce catabolic processes within articular cartilage<sup>172,256</sup>. In a murine organ culture model, activation of PPAR $\delta$  lead to proteoglycan degradation in articular cartilage through increased expression of proteases including *Mmp-3* and *Adamts-5*<sup>172,256</sup>. Moreover, mice with cartilage-specific deletion of PPAR $\delta$  are protected from cartilage damage in a post-traumatic model of OA<sup>172</sup>. While the biological mechanisms behind the role of PPAR $\delta$  in articular cartilage are not fully understood, it appears to contribute to the regulation of lipid metabolism and the cellular response to oxidative stress<sup>256</sup>. Although the role of PPARs in the IVD have not been directly investigated, PPAR expression is detected in both the NP and AF<sup>257</sup>. The



similarities between articular cartilage and IVD biology and pathophysiology suggest that PPARs may be intriguing candidates as potential regulators of IVD degeneration.

## 1.11 Overall objectives and hypothesis

Using the mouse as a preclinical model, this thesis focuses predominantly on examining the role of two important environmental risk factors in the initiation and progression of IVD degeneration and associated pain: mechanical loading and obesity.

### 1.11.1 Objective #1

Investigate whether the detrimental effects of WBV on joint health are altered by genetic background in mouse models.

#### 1.11.1.1 Rationale #1

Previous research by our group demonstrated that exposure of mice to protocols of WBV that model those used clinically (30 minutes/day, 5 days/week; 45 Hz, 0.3 g) induced damage to the IVD and knee joint within two weeks, that progressed in severity with continued daily exposure to WBV (i.e. 4, 8 weeks)<sup>162,164,165</sup>. These studies were however limited to skeletally mature (10-week old) male mice of a single outbred stock (CD1). Due to the diverse human population using WBV platforms we aimed to determine whether the response of joint tissues to WBV was consistent between mice of different genetic backgrounds.

### 1.11.1.2 Hypothesis # 1

The effects of whole-body vibration on joint health will differ based on genetic background.

### 1.11.2 Objective #2

Determine whether chronic exposure of mice to a high-fat or high-fat/high-sugar western diet will accelerate age-related IVD degeneration and/or back pain.

#### 1.11.2.1 Rationale #2

Throughout the world, the prevalence of obesity is on the rise. In 2014 over 25% of Canadians were obese, resulting in an enormous toll on our health care system of over \$4 billion spent annually on direct costs alone, let alone costs associated with obesity-associated co-morbidities<sup>258</sup>. In addition to being a major risk factor for the development of type II diabetes, cardiovascular disease and metabolic syndrome<sup>259</sup>, obesity also increases the risk of IVD degeneration and lower back pain<sup>260,261</sup>. Despite this association there is very little known about the pathogenesis of obesity induced IVD degeneration. Previous research demonstrated that obesity induced by a high-fat diet accelerates OA in mouse and rat models<sup>262-266</sup>. In addition to structural changes in the joint, the high-fat diet also induces symptomatic characteristic of OA, such as hyperalgesia<sup>263</sup>. To date, the effect of diet-induced obesity on IVD degeneration and back pain has not been directly studied.

### 1.11.2.2 Hypothesis # 2

Chronic consumption of a high-fat or high-fat/high-sugar western diet will accelerate IVD degeneration and/or behavioral indicators of back pain in the mouse model.

### 1.11.3 Objective # 3

Determine the role of PPAR $\delta$  in age- and obesity-associated IVD degeneration and investigate sex as a variable in the mouse model system.

#### 1.11.3.1 Rationale # 3

Based on previous research demonstrating that loss of PPAR $\delta$  in articular cartilage protects from surgically-induced and age-associated OA<sup>172,267</sup>, we sought to determine the role of PPAR $\delta$  in the IVD and its contribution to both age- and obesity-associated IVD degeneration and pain. Previous studies by our lab using genome-wide transcriptome analysis demonstrated that many nuclear receptor pathways are activated in age-associated IVD degeneration, including the PPAR signaling pathway<sup>257</sup>, highlighting the potential importance of PPAR in age-associated IVD degeneration. Given that its endogenous ligands are dysregulated in obesity<sup>247</sup>, and the detrimental role of PPAR $\delta$  activation in articular cartilage<sup>172</sup>, we aimed to determine whether similar findings would be seen between the different models of IVD degeneration.

This study also sought to address potential sex-related differences in IVD degeneration and back pain in our model of diet-induced disc degeneration. Numerous pre-clinical and clinical studies have shown that IVD degeneration and back pain are sexually dimorphic,

where females are disproportionately more affected by spinal pathologies and back pain than males<sup>95,268</sup>.

### 1.11.3.2 Hypothesis # 3

Loss of PPAR $\delta$  in IVD cells will delay the progression of age- and obesity-related IVD degeneration and back pain.

## 1.12 References

1. Pain terms: a list with definitions and notes on usage. Recommended by the IASP Subcommittee on Taxonomy. *Pain*. 1979.
2. Basbaum AI, Bautista DM, Scherrer G, Julius D. Cellular and molecular mechanisms of pain. *Cell*. 2009;139(2):267-284. doi:10.1016/j.cell.2009.09.028
3. Nagasako EM, Oaklander AL, Dworkin RH. Congenital insensitivity to pain: An update. *Pain*. 2003. doi:10.1016/S0304-3959(02)00482-7
4. Edwards RR, Dworkin RH, Sullivan MD, Turk DC, Wasan AD. The Role of Psychosocial Processes in the Development and Maintenance of Chronic Pain. *J Pain*. 2016. doi:10.1016/j.jpain.2016.01.001
5. Garland EL. Pain processing in the human nervous system: a selective review of nociceptive and biobehavioral pathways. *Prim Care*. 2012;39(3):561-571. doi:10.1016/j.pop.2012.06.013
6. Bishop GH, Landau WM, Jones MH. Evidence for a double peripheral pathway for pain. *Science (80- )*. 1958;128(3326):712-714. doi:10.1126/science.128.3326.713
7. Treede RD, Rief W, Barke A, et al. A classification of chronic pain for ICD-11. *Pain*. 2015;156(6):1003-1007. doi:10.1097/j.pain.000000000000160
8. Schappert SM, Burt CW. Ambulatory care visits to physician offices, hospital outpatient departments, and emergency departments: United States, 2001-02. *Vital Health Stat 13*. 2006.
9. Gureje O, Von Korff M, Simon GE, Gater R. Persistent pain and well-being: A World Health Organization study in primary care. *J Am Med Assoc*. 1998. doi:10.1001/jama.280.2.147
10. Smith BH, Elliott AM, Alastair Chambers W, Smith WC, Hannaford PC, Penny K. The impact of chronic pain in the community. *Fam Pract*. 2001. doi:10.1093/fampra/18.3.292
11. Mills SEE, Nicolson KP, Smith BH. Chronic pain: a review of its epidemiology and associated factors in population-based studies. *Br J Anaesth*. 2019. doi:10.1016/j.bja.2019.03.023
12. Birse TM, Lander J. Prevalence of chronic pain. *Can J Public Heal*. 1998. doi:10.1007/bf03404405
13. Choinière M, Dion D, Peng P, et al. The Canadian STOP-PAIN project - Part 1: Who are the patients on the waitlists of multidisciplinary pain treatment facilities? *Can J Anesth*. 2010. doi:10.1007/s12630-010-9305-5

14. Lynch ME. The need for a Canadian pain strategy. *Pain Res Manag.* 2011. doi:10.1155/2011/654651
15. Statistics Canada. A Profile of Disability in Canada , 2001. *Report.* 2002.
16. Miller RJ, Jung H, Bhangoo SK, White FA. Cytokine and chemokine regulation of sensory neuron function. *Handb Exp Pharmacol.* 2009;(194):417-449. doi:10.1007/978-3-540-79090-7\_12
17. Malfait AM, Schnitzer TJ. Towards a mechanism-based approach to pain management in osteoarthritis. *Nat Rev Rheumatol.* 2013;9(11):654-664. doi:10.1038/nrrheum.2013.138
18. Loeser JD, Melzack R. Pain: an overview. *Lancet.* 1999;353(9164):1607-1609. doi:10.1016/S0140-6736(99)01311-2
19. Mendell LM, Albers KM, Davis BM. Neurotrophins, nociceptors, and pain. *Microsc Res Tech.* 1999;45(4-5):252-261. doi:10.1002/(SICI)1097-0029(19990515/01)45:4/5<252::AID-JEMT9>3.0.CO;2-N
20. Mantyh PW, Koltzenburg M, Mendell LM, Tive L, Shelton DL. Antagonism of nerve growth factor-TrkA signaling and the relief of pain. *Anesthesiology.* 2011;115(1):189-204. doi:10.1097/ALN.0b013e31821b1ac5
21. Shu X, Mendell LM. Nerve growth factor acutely sensitizes the response of adult rat sensory neurons to capsaicin. *Neurosci Lett.* 1999;274(3):159-162. <http://www.ncbi.nlm.nih.gov/pubmed/10548414>.
22. Lewin GR, Ritter AM, Mendell LM. Nerve growth factor-induced hyperalgesia in the neonatal and adult rat. *J Neurosci.* 1993;13(5):2136-2148. doi:https://doi.org/10.1523/JNEUROSCI.13-05-02136.1993
23. Gangadharan V, Kuner R. Pain hypersensitivity mechanisms at a glance. *Dis Model Mech.* 2013;6(4):889-895. doi:10.1242/dmm.011502
24. Woolf CJ. Central sensitization: implications for the diagnosis and treatment of pain. *Pain.* 2011;152(3 Suppl):S2-15. doi:10.1016/j.pain.2010.09.030
25. Latremoliere A, Woolf CJ. Central sensitization: a generator of pain hypersensitivity by central neural plasticity. *J Pain.* 2009;10(9):895-926. doi:10.1016/j.jpain.2009.06.012
26. Gosselin RD, Suter MR, Ji RR, Decosterd I. Glial cells and chronic pain. *Neuroscientist.* 2010;16(5):519-531. doi:10.1177/1073858409360822
27. Haydon PG. GLIA: listening and talking to the synapse. *Nat Rev Neurosci.* 2001;2(3):185-193. doi:10.1038/35058528

28. Ben Haim L, Rowitch DH. Functional diversity of astrocytes in neural circuit regulation. *Nat Rev Neurosci*. 2016. doi:10.1038/nrn.2016.159
29. Global Burden of Disease Study C. Global, regional, and national incidence, prevalence, and years lived with disability for 301 acute and chronic diseases and injuries in 188 countries, 1990-2013: a systematic analysis for the Global Burden of Disease Study 2013. *Lancet*. 2015;386(9995):743-800. doi:10.1016/S0140-6736(15)60692-4
30. Carey TS, Garrett J, Jackman A, McLaughlin C, Fryer J, Smucker DR. The outcomes and costs of care for acute low back pain among patients seen by primary care practitioners, chiropractors, and orthopedic surgeons. *N Engl J Med*. 1995. doi:10.1056/NEJM199510053331406
31. Freburger JK, Holmes GM, Agans RP, et al. The rising prevalence of chronic low back pain. *Arch Intern Med*. 2009. doi:10.1001/archinternmed.2008.543
32. Snelgrove S, Lioffi C. An interpretative phenomenological analysis of living with chronic low back pain. *Br J Health Psychol*. 2009. doi:10.1348/135910709X402612
33. MacNeela P, Doyle C, O’Gorman D, Ruane N, McGuire BE. Experiences of chronic low back pain: a meta-ethnography of qualitative research. *Health Psychol Rev*. 2015. doi:10.1080/17437199.2013.840951
34. Katz JN. Lumbar disc disorders and low-back pain: Socioeconomic factors and consequences. In: *Journal of Bone and Joint Surgery - Series A*. ; 2006. doi:10.2106/JBJS.E.01273
35. Deyo RA, Weinstein JN. Low back pain. *N Engl J Med*. 2001. doi:10.1056/NEJM200102013440508
36. DePalma MJ, Ketchum JM, Saullo T. What is the source of chronic low back pain and does age play a role? *Pain Med*. 2011;12(2):224-233. doi:10.1111/j.1526-4637.2010.01045.x
37. Fujii K, Yamazaki M, Kang JD, et al. Discogenic Back Pain: Literature Review of Definition, Diagnosis, and Treatment. *JBMR Plus*. 2019. doi:10.1002/jbm4.10180
38. Mafi JN, McCarthy EP, Davis RB, Landon BE. Worsening trends in the management and treatment of back pain. *JAMA Intern Med*. 2013;173(17):1573-1581. doi:10.1001/jamainternmed.2013.8992
39. Smith LJ, Nerurkar NL, Choi KS, Harfe BD, Elliott DM. Degeneration and regeneration of the intervertebral disc: Lessons from development. *DMM Dis Model Mech*. 2011. doi:10.1242/dmm.006403
40. Urban JPG, Roberts S. Degeneration of the intervertebral disc. *Arthritis Res Ther*.

2003. doi:10.1186/ar629
41. Ghiselli G, Wang JC, Bhatia NN, Hsu WK, Dawson EG. Adjacent segment degeneration in the lumbar spine. *J Bone Jt Surg - Ser A*. 2004. doi:10.2106/00004623-200407000-00020
  42. Rawls A, Fisher RE. Developmental and functional anatomy of the spine. In: *The Genetics and Development of Scoliosis: Second Edition*. ; 2018. doi:10.1007/978-3-319-90149-7\_1
  43. Rohlmann A, Zander T, Schmidt H, Wilke HJ, Bergmann G. Analysis of the influence of disc degeneration on the mechanical behaviour of a lumbar motion segment using the finite element method. *J Biomech*. 2006. doi:10.1016/j.jbiomech.2005.07.026
  44. Hansen JT NFB. In: Netter's Clinical Anatomy. In: *Netter's Clinical Anatomy*. Third. Philadelphia, PA: Saunders/Elsevier; :49–86.
  45. Harrison M, O'Brien A, Adams L, et al. Vertebral landmarks for the identification of spinal cord segments in the mouse. *Neuroimage*. 2013. doi:10.1016/j.neuroimage.2012.11.048
  46. Setton LA, Chen J. Cell mechanics and mechanobiology in the intervertebral disc. *Spine (Phila Pa 1976)*. 2004. doi:10.1097/01.brs.0000146050.57722.2a
  47. Setton LA, Chen J. Mechanobiology of the intervertebral disc and relevance to disc degeneration. *J Bone Jt Surg Am*. 2006;88 Suppl 2:52-57. doi:10.2106/JBJS.F.00001
  48. Watanabe H, Yamada Y, Kimata K. Roles of aggrecan, a large chondroitin sulfate proteoglycan, in cartilage structure and function. *J Biochem*. 1998;124(4):687-693. doi:10.1093/oxfordjournals.jbchem.a022166
  49. Singh K, Masuda K, Thonar EJMA, An HS, Cs-Szabo G. Age-related changes in the extracellular matrix of nucleus pulposus and annulus fibrosus of human intervertebral disc. *Spine (Phila Pa 1976)*. 2009. doi:10.1097/BRS.0b013e31818e5ddd
  50. Buckwalter JA. Spine update: Aging and degeneration of the human intervertebral disc. *Spine (Phila Pa 1976)*. 1995;20(11):1307-1314. doi:10.1097/00007632-199506000-00022
  51. Sivan SS, Wachtel E, Roughley P. Structure, function, aging and turnover of aggrecan in the intervertebral disc. *Biochim Biophys Acta - Gen Subj*. 2014. doi:10.1016/j.bbagen.2014.07.013
  52. Roughley PJ, Geng Y, Mort JS. The non-aggregated aggrecan in the human intervertebral disc can arise by a non-proteolytic mechanism. *Eur Cells Mater*.



2014. doi:10.22203/eCM.v028a10
53. Zhao CQ, Wang LM, Jiang LS, Dai LY. The cell biology of intervertebral disc aging and degeneration. *Ageing Res Rev.* 2007;6(3):247-261. doi:10.1016/j.arr.2007.08.001
  54. McCann MR, Seguin CA. Notochord Cells in Intervertebral Disc Development and Degeneration. *J Dev Biol.* 2016;4(1):1-18. doi:10.3390/jdb4010003
  55. Lee CR, Sakai D, Nakai T, et al. A phenotypic comparison of intervertebral disc and articular cartilage cells in the rat. *Eur Spine J.* 2007;16(12):2174-2185. doi:10.1007/s00586-007-0475-y
  56. Humzah MD, Soames RW. Human intervertebral disc: Structure and function. *Anat Rec.* 1988. doi:10.1002/ar.1092200402
  57. Pattappa G, Li Z, Peroglio M, Wismer N, Alini M, Grad S. Diversity of intervertebral disc cells: Phenotype and function. *J Anat.* 2012. doi:10.1111/j.1469-7580.2012.01521.x
  58. Marchand F, Ahmed AM. Investigation of the laminate structure of lumbar disc anulus fibrosus. *Spine (Phila Pa 1976).* 1990. doi:10.1097/00007632-199005000-00011
  59. Jensen GM. Biomechanics of the lumbar intervertebral disk: A review. *Phys Ther.* 1980. doi:10.1093/ptj/60.6.765
  60. Smith LJ, Fazzalari NL. The elastic fibre network of the human lumbar anulus fibrosus: Architecture, mechanical function and potential role in the progression of intervertebral disc degeneration. *Eur Spine J.* 2009. doi:10.1007/s00586-009-0918-8
  61. Roughley PJ, Melching LI, Heathfield TF, Pearce RH, Mort JS. The structure and degradation of aggrecan in human intervertebral disc. *Eur Spine J.* 2006. doi:10.1007/s00586-006-0127-7
  62. Li J, Liu C, Guo Q, Yang H, Li B. Regional variations in the cellular, biochemical, and biomechanical characteristics of rabbit annulus fibrosus. *PLoS One.* 2014. doi:10.1371/journal.pone.0091799
  63. Iu J, Santerre JP, Kandel RA. Inner and outer annulus fibrosus cells exhibit differentiated phenotypes and yield changes in extracellular matrix protein composition in vitro on a polycarbonate urethane scaffold. *Tissue Eng - Part A.* 2014. doi:10.1089/ten.tea.2013.0777
  64. Hutkins DWL, Meakin JR. Relationship Between Structure and Mechanical Function of the Tissues of the Intervertebral Joint. *Am Zool.* 2015;40(1):42-52. doi:https://doi.org/10.1093/icb/40.1.42

65. Mwale F, Roughley P, Antoniou J, et al. Distinction between the extracellular matrix of the nucleus pulposus and hyaline cartilage: A requisite for tissue engineering of intervertebral disc. *Eur Cells Mater*. 2004. doi:10.22203/eCM.v008a06
66. Moore RJ. The vertebral end-plate: What do we know? *Eur Spine J*. 2000. doi:10.1007/s005860050217
67. Urban JP, Smith S, Fairbank JC. Nutrition of the intervertebral disc. *Spine (Phila Pa 1976)*. 2004;29(23):2700-2709. <http://www.ncbi.nlm.nih.gov/pubmed/15564919>.
68. Roberts S, Urban JPG, Evans H, Eisenstein SM. Transport properties of the human cartilage endplate in relation to its composition and calcification. *Spine (Phila Pa 1976)*. 1996. doi:10.1097/00007632-199602150-00003
69. Cholewicki J, Panjabi MM, Khachatryan A. Stabilizing function of trunk flexor-extensor muscles around a neutral spine posture. *Spine (Phila Pa 1976)*. 1997. doi:10.1097/00007632-199710010-00003
70. Thorstensson A, Carlson H, Zomlefer MR, Nilsson J. Lumbar back muscle activity in relation to trunk movements during locomotion in man. *Acta Physiol Scand*. 1982. doi:10.1111/j.1748-1716.1982.tb10593.x
71. Barr KP, Griggs M, Cadby T. Lumbar stabilization: Core concepts and current literature, part 1. *Am J Phys Med Rehabil*. 2005. doi:10.1097/01.phm.0000163709.70471.42
72. Farfan HF. Muscular mechanism of the lumbar spine and the position of power and efficiency. *Orthop Clin North Am*. 1975.
73. Wallwork TL, Stanton WR, Freke M, Hides JA. The effect of chronic low back pain on size and contraction of the lumbar multifidus muscle. *Man Ther*. 2009. doi:10.1016/j.math.2008.09.006
74. Buonocore M, Aloisi AM, Barbieri M, Gatti AM, Bonezzi C. Vertebral body innervation: Implications for pain. *J Cell Physiol*. 2010. doi:10.1002/jcp.21996
75. Bogduk N. The innervation of the lumbar spine. *Spine (Phila Pa 1976)*. 1983. doi:10.1097/00007632-198304000-00009
76. Bogduk N, Tynan W, Wilson AS. The nerve supply to the human lumbar intervertebral discs. *J Anat*. 1981.
77. Edgar MA. The nerve supply of the lumbar intervertebral disc. *J Bone Jt Surg - Ser B*. 2007. doi:10.1302/0301-620X.89B9.18939
78. García-Cosamalón J, del Valle ME, Calavia MG, et al. Intervertebral disc, sensory

- nerves and neurotrophins: who is who in discogenic pain? *J Anat.* 2010. doi:10.1111/j.1469-7580.2010.01227.x
79. Kauppila LI, Tallroth K. Postmortem angiographic findings for arteries supplying the lumbar spine: Their relationship to low-back symptoms. *J Spinal Disord Tech.* 1993. doi:10.1097/00002517-199304000-00005
  80. Nerlich AG, Schaaf R, Wälchli B, Boos N. Temporo-spatial distribution of blood vessels in human lumbar intervertebral discs. *Eur Spine J.* 2007. doi:10.1007/s00586-006-0213-x
  81. Adams M, Roughley PJ. What is intervertebral disc degeneration, and what causes it? *Spine (Phila Pa 1976).* 2006. doi:10.1097/01.brs.0000231761.73859.2c
  82. Costi JJ, Stokes IA, Gardner-Morse MG, Iatridis JC. Frequency-dependent behavior of the intervertebral disc in response to each of six degree of freedom dynamic loading - Solid phase and fluid phase contributions. *Spine (Phila Pa 1976).* 2008;33(16):1731-1738. doi:DOI 10.1097/BRS.0b013e31817bb116
  83. Ma X long, Tian P, Wang T, Ma J xiong. A study of the relationship between type of lumbar disc herniation, straight leg raising test and peripheral T lymphocytes. *Orthop Surg.* 2010. doi:10.1111/j.1757-7861.2009.00065.x
  84. Battie MC, Videman T, Gibbons LE, Fisher LD, Manninen H, Gill K. 1995 volvo award in clinical sciences determinants of lumbar disc degeneration -a study relating lifetime exposures and magnetic resonance imaging findings in identical twins. *Spine (Phila Pa 1976).* 1995. doi:10.1097/00007632-199512150-00001
  85. Battie MC, Videman T, Parent E. Lumbar disc degeneration: epidemiology and genetic influences. *Spine (Phila Pa 1976).* 2004;29(23):2679-2690. <http://www.ncbi.nlm.nih.gov/pubmed/15564917>.
  86. Munir S, Rade M, Määttä JH, Freidin MB, Williams FMK. Intervertebral Disc Biology: Genetic Basis of Disc Degeneration. *Curr Mol Biol Reports.* 2018. doi:10.1007/s40610-018-0101-2
  87. Rigal J, Léglise A, Barnette T, Cogniet A, Aunoble S, Le Huec JC. Meta-analysis of the effects of genetic polymorphisms on intervertebral disc degeneration. *Eur Spine J.* 2017. doi:10.1007/s00586-017-5146-z
  88. Solovieva S, Nojonen N, Männikkö M, et al. Association between the aggrecan gene variable number of tandem repeats polymorphism and intervertebral disc degeneration. *Spine (Phila Pa 1976).* 2007. doi:10.1097/BRS.0b013e3180b9ed51
  89. Battié MC, Videman T, Kaprio J, et al. The Twin Spine Study: Contributions to a changing view of disc degeneration†. *Spine J.* 2009. doi:10.1016/j.spinee.2008.11.011

90. Toktaş ZO, Ekşi MŞ, Yılmaz B, et al. Association of collagen I, IX and vitamin D receptor gene polymorphisms with radiological severity of intervertebral disc degeneration in Southern European Ancestor. *Eur Spine J.* 2015. doi:10.1007/s00586-015-4206-5
91. Mayer JE, Iatridis JC, Chan D, Qureshi SA, Gottesman O, Hecht AC. Genetic polymorphisms associated with intervertebral disc degeneration. *Spine J.* 2013. doi:10.1016/j.spinee.2013.01.041
92. Zhou X, Cheung CL, Karasugi T, et al. Trans-ethnic polygenic analysis supports genetic overlaps of lumbar disc degeneration with height, body mass index, and bone mineral density. *Front Genet.* 2018. doi:10.3389/fgene.2018.00267
93. Kepler CK, Ponnappan RK, Tannoury CA, Risbud M V, Anderson DG. The molecular basis of intervertebral disc degeneration. *Spine J.* 2013;13(3):318-330. doi:10.1016/j.spinee.2012.12.003
94. Siemionow K, An H, Masuda K, Andersson G, Cs-Szabo G. The effects of age, sex, ethnicity, and spinal level on the rate of intervertebral disc degeneration: A review of 1712 intervertebral discs. *Spine (Phila Pa 1976).* 2011. doi:10.1097/BRS.0b013e3181f2a177
95. Teraguchi M, Yoshimura N, Hashizume H, et al. Progression, incidence, and risk factors for intervertebral disc degeneration in a longitudinal population-based cohort: the Wakayama Spine Study. *Osteoarthr Cartil.* 2017. doi:10.1016/j.joca.2017.01.001
96. Jakoi AM, Pannu G, D'Oro A, et al. The Clinical Correlations between Diabetes, Cigarette Smoking and Obesity on Intervertebral Degenerative Disc Disease of the Lumbar Spine. *Asian Spine J.* 2017;11(3):337-347. doi:10.4184/asj.2017.11.3.337
97. Elfering A, Semmer N, Birkhofer D, Zanetti M, Hodler J, Boos N. Young investigator award 2001 winner: Risk factors for lumbar disc degeneration: A 5-year prospective MRI study in asymptomatic individuals. *Spine (Phila Pa 1976).* 2002. doi:10.1097/00007632-200201150-00002
98. Chan SC, Ferguson SJ, Gantenbein-Ritter B. The effects of dynamic loading on the intervertebral disc. *Eur Spine J.* 2011;20(11):1796-1812. doi:10.1007/s00586-011-1827-1
99. Anderson JAD, Otun EO, Sweetman BJ. Occupational hazards and low back pain. *Rev Environ Health.* 1987. doi:10.1515/REVEH.1987.7.1-2.121
100. Videman T, Sarna S, Battie MC, et al. The long-term effects of physical loading and exercise lifestyles on back-related symptoms, disability, and spinal pathology among men. *Spine (Phila Pa 1976).* 1995;20(6):699-709.
101. Xu X Wu W LX. Association Between Overweight or Obesity and Lumbar Disk

- Diseases: A Meta-Analysis. *J Spinal Disord Tech.* 2015;10:370-376.  
doi:10.1097/BSD.0000000000000235
102. Samartzis D, Karppinen J, Cheung JP, Lotz J. Disk degeneration and low back pain: are they fat-related conditions? *Glob Spine J.* 2013;3(3):133-144.  
doi:10.1055/s-0033-1350054
  103. Ruiz-Fernández C, Francisco V, Pino J, et al. Molecular relationships among obesity, inflammation and intervertebral disc degeneration: Are adipokines the common link? *Int J Mol Sci.* 2019. doi:10.3390/ijms20082030
  104. Campisi J, Kim S ho, Lim CS, Rubio M. Cellular senescence, cancer and aging: The telomere connection. *Exp Gerontol.* 2001. doi:10.1016/S0531-5565(01)00160-7
  105. Gruber HE, Ingram JA, Norton HJ, Hanley EN. Senescence in Cells of the Aging and Degenerating Intervertebral Disc. *Spine (Phila Pa 1976).* 2007.  
doi:10.1097/01.brs.0000253960.57051.de
  106. Le Maitre CL, Freemont AJ, Hoyland JA. Accelerated cellular senescence in degenerate intervertebral discs: A possible role in the pathogenesis of intervertebral disc degeneration. *Arthritis Res Ther.* 2007. doi:10.1186/ar2198
  107. Toussaint O, Medrano EE, Von Zglinicki T. Cellular and molecular mechanisms of stress-induced premature senescence (SIPS) of human diploid fibroblasts and melanocytes. *Exp Gerontol.* 2000. doi:10.1016/S0531-5565(00)00180-7
  108. Le Maitre CL, Freemont AJ, Hoyland JA. The role of interleukin-1 in the pathogenesis of human intervertebral disc degeneration. *Arthritis Res Ther.* 2005;7(4):R732-45. doi:10.1186/ar1732
  109. Zhao CQ, Jiang LS, Dai LY. Programmed cell death in intervertebral disc degeneration. *Apoptosis.* 2006. doi:10.1007/s10495-006-0290-7
  110. Le Maitre CL, Pockert A, Buttle DJ, Freemont AJ, Hoyland JA. Matrix synthesis and degradation in human intervertebral disc degeneration. In: *Biochemical Society Transactions.* ; 2007. doi:10.1042/BST0350652
  111. Vo N V., Hartman RA, Yurube T, Jacobs LJ, Sowa GA, Kang JD. Expression and regulation of metalloproteinases and their inhibitors in intervertebral disc aging and degeneration. *Spine J.* 2013. doi:10.1016/j.spinee.2012.02.027
  112. Lv FJ, Peng Y, Lim FL, et al. Matrix metalloproteinase 12 is an indicator of intervertebral disc degeneration co-expressed with fibrotic markers. *Osteoarthr Cartil.* 2016. doi:10.1016/j.joca.2016.05.012
  113. Le Maitre CL, Freemont AJ, Hoyland JA. Localization of degradative enzymes and their inhibitors in the degenerate human intervertebral disc. *J Pathol.* 2004.

doi:10.1002/path.1608

114. Pockert AJ, Richardson SM, Le Maitre CL, et al. Modified expression of the ADAMTS enzymes and tissue inhibitor of metalloproteinases 3 during human intervertebral disc degeneration. *Arthritis Rheum.* 2009;60(2):482-491. doi:10.1002/art.24291
115. Lees S, Golub SB, Last K, et al. Bioactivity in an aggrecan 32-mer fragment is mediated via toll-like receptor 2. *Arthritis Rheumatol.* 2015. doi:10.1002/art.39063
116. Weiler C, Nerlich AG, Bachmeier BE, Boos N. Expression and distribution of tumor necrosis factor alpha in human lumbar intervertebral discs: A study in surgical specimen and autopsy controls. *Spine (Phila Pa 1976).* 2005. doi:10.1097/01.brs.0000149186.63457.20
117. Kepler CK, Anderson DG, Tannoury C, Ponnappan RK. Intervertebral disk degeneration and emerging biologic treatments. *J Am Acad Orthop Surg.* 2011. doi:10.5435/00124635-201109000-00005
118. Adams MA, McNally DS, Dolan P. "Stress" distributions inside intervertebral discs. The effects of age and degeneration. *J Bone Joint Surg Br.* 1996;78(6):965-972. <http://www.ncbi.nlm.nih.gov/pubmed/8951017>. Accessed June 13, 2018.
119. Vergroesen PP, Kingma I, Emanuel KS, et al. Mechanics and biology in intervertebral disc degeneration: a vicious circle. *Osteoarthr Cartil.* 2015;23(7):1057-1070. doi:10.1016/j.joca.2015.03.028
120. Freemont AJ, Peacock TE, Goupille P, Hoyland JA, O'Brien J, Jayson MI. Nerve ingrowth into diseased intervertebral disc in chronic back pain. *Lancet.* 1997;350(9072):178-181. <http://www.ncbi.nlm.nih.gov/pubmed/9250186>.
121. Rätsep T, Minajeva A, Asser T. Relationship between neovascularization and degenerative changes in herniated lumbar intervertebral discs. *Eur Spine J.* 2013. doi:10.1007/s00586-013-2842-1
122. Freemont AJ, Watkins A, Le Maitre C, et al. Nerve growth factor expression and innervation of the painful intervertebral disc. *J Pathol.* 2002. doi:10.1002/path.1108
123. Johnson WEB, Caterson B, Eisenstein SM, Hynds DL, Snow DM, Roberts S. Human intervertebral disc aggrecan inhibits nerve growth in vitro. *Arthritis Rheum.* 2002. doi:10.1002/art.10585
124. Modic MT, Ross JS. Lumbar degenerative disk disease. *Radiology.* 2007;245(1):43-61. doi:10.1148/radiol.2451051706
125. Jensen MC, Brant-Zawadzki MN, Obuchowski N, Modic MT, Malkasian D, Ross JS. Magnetic resonance imaging of the lumbar spine in people without back pain.

- N Engl J Med.* 1994;331(2):69-73. doi:10.1056/NEJM199407143310201
126. Takahashi K, Aoki Y, Ohtori S. Resolving discogenic pain. *Eur Spine J.* 2008;17 Suppl 4:428-431. doi:10.1007/s00586-008-0752-4
  127. Millecamps M, Czerminski JT, Mathieu AP, Stone LS. Behavioral signs of axial low back pain and motor impairment correlate with the severity of intervertebral disc degeneration in a mouse model. *Spine J.* 2015;15(12):2524-2537. doi:10.1016/j.spinee.2015.08.055
  128. Ito K, Creemers L. Mechanisms of intervertebral disk degeneration/injury and pain: a review. *Glob Spine J.* 2013;3(3):145-152. doi:10.1055/s-0033-1347300
  129. Abe Y, Akeda K, An HS, et al. Proinflammatory cytokines stimulate the expression of nerve growth factor by human intervertebral disc cells. *Spine (Phila Pa 1976).* 2007. doi:10.1097/01.brs.0000257556.90850.53
  130. Le Maitre CL, Hoyland JA, Freemont AJ. Catabolic cytokine expression in degenerate and herniated human intervertebral discs: IL-1 $\beta$  and TNF $\alpha$  expression profile. *Arthritis Res Ther.* 2007. doi:10.1186/ar2275
  131. Gries NC, Berlemann U, Moore RJ, Vernon-Roberts B. Early histologic changes in lower lumbar discs and facet joints and their correlation. *Eur Spine J.* 2000. doi:10.1007/s005860050004
  132. Foster NE, Anema JR, Cherkin D, et al. Prevention and treatment of low back pain: evidence, challenges, and promising directions. *Lancet.* 2018. doi:10.1016/S0140-6736(18)30489-6
  133. Dhillon KS. Spinal fusion for chronic low back pain: A 'Magic Bullet' or wishful thinking? *Malaysian Orthop J.* 2016.
  134. Rustenburg CME, Emanuel KS, Peeters M, Lems WF, Vergroesen P-PA, Smit TH. Osteoarthritis and intervertebral disc degeneration: Quite different, quite similar. *JOR Spine.* 2018. doi:10.1002/jsp2.1033
  135. Lories RJ, Luyten FP. The bone-cartilage unit in osteoarthritis. *Nat Rev Rheumatol.* 2011. doi:10.1038/nrrheum.2010.197
  136. Lorenz H, Richter W. Osteoarthritis: Cellular and molecular changes in degenerating cartilage. *Prog Histochem Cytochem.* 2006. doi:10.1016/j.proghi.2006.02.003
  137. Hunter DJ, Bierma-Zeinstra S. Osteoarthritis. *Lancet.* 2019. doi:10.1016/S0140-6736(19)30417-9
  138. Gupta KB, Duryea J, Weissman BN. Radiographic evaluation of osteoarthritis. *Radiol Clin North Am.* 2004. doi:10.1016/S0033-8389(03)00169-6

139. Pye SR, Reid DM, Lunt M, Adams JE, Silman AJ, O'Neill TW. Lumbar disc degeneration: Association between osteophytes, end-plate sclerosis and disc space narrowing. *Ann Rheum Dis*. 2007. doi:10.1136/ard.2006.052522
140. V S, Lufkin T. Bridging the Gap: Understanding Embryonic Intervertebral Disc Development. *Cell Dev Biol*. 2012. doi:10.4172/2168-9296.1000103
141. McCann MR, Tamplin OJ, Rossant J, Seguin CA. Tracing notochord-derived cells using a Noto-cre mouse: implications for intervertebral disc development. *Dis Model Mech*. 2012;5(1):73-82. doi:10.1242/dmm.008128
142. Longobardi L, Li T, Tagliafierro L, et al. Synovial Joints: from Development to Homeostasis. *Curr Osteoporos Rep*. 2015. doi:10.1007/s11914-014-0247-7
143. Neidlinger-Wilke C, Galbusera F, Pratsinis H, et al. Mechanical loading of the intervertebral disc: from the macroscopic to the cellular level. *Eur Spine J*. 2014;23 Suppl 3:S333-43. doi:10.1007/s00586-013-2855-9
144. Hsieh AH, Twomey JD. Cellular mechanobiology of the intervertebral disc: new directions and approaches. *J Biomech*. 2010;43(1):137-145. doi:10.1016/j.jbiomech.2009.09.019
145. Papachroni KK, Karatzas DN, Papavassiliou KA, Basdra EK, Papavassiliou AG. Mechanotransduction in osteoblast regulation and bone disease. *Trends Mol Med*. 2009;15(5):208-216. doi:10.1016/j.molmed.2009.03.001
146. Kerr GJ, Veras MA, Kim MK, Seguin CA. Decoding the intervertebral disc: Unravelling the complexities of cell phenotypes and pathways associated with degeneration and mechanotransduction. *Semin Cell Dev Biol*. 2017;62:94-103. doi:10.1016/j.semcdb.2016.05.008
147. Stokes IA, Iatridis JC. Mechanical Conditions That Accelerate Intervertebral Disc Degeneration: Overload Versus Immobilization. *Spine (Phila Pa 1976)*. 2004;29(23):2724-2732.
148. Hutton WC, Yoon ST, Elmer WA, et al. Effect of tail suspension (or simulated weightlessness) on the lumbar intervertebral disc study of proteoglycans and collagen. *Spine (Phila Pa 1976)*. 2002. doi:10.1097/00007632-200206150-00008
149. Bovenzi M. Low back pain disorders and exposure to whole-body vibration in the workplace. *Semin Perinatol*. 1996;20(1):38-53. doi:10.1136/oem.2007.035147
150. Rubin C, Recker R, Cullen D, Ryaby J, McCabe J, McLeod K. Prevention of postmenopausal bone loss by a low-magnitude, high-frequency mechanical stimuli: a clinical trial assessing compliance, efficacy, and safety. *J Bone Min Res*. 2004;19(3):343-351. doi:10.1359/JBMR.0301251
151. Delecluse C, Roelants M, Diels R, Koninckx E, Verschueren S. Effects of whole



- body vibration training on muscle strength and sprint performance in sprint-trained athletes. *Int J Sport Med*. 2005;26(8):662-668. doi:10.1055/s-2004-830381
152. Perraton L, Machotka Z, Kumar S. Whole-body vibration to treat low back pain: fact or fad? *Physiother Can*. 2011;63(1):88-93. doi:10.3138/ptc.2009.44
  153. Park YG, Kwon BS, Park JW, et al. Therapeutic effect of whole body vibration on chronic knee osteoarthritis. *Ann Rehabil Med*. 2013;37(4):505-515. doi:10.5535/arm.2013.37.4.505
  154. Standardization IO for. ISO 2631-1:1997, Mechanical Vibration and Shock - Evaluation of Human Exposure to Whole-Body Vibration, Part 1, General Requirements. 1997.
  155. Muir J, Kiel DP, Rubin CT. Safety and severity of accelerations delivered from whole body vibration exercise devices to standing adults. *J Sci Med Sport*. 2013;16(6):526-531. doi:10.1016/j.jsams.2013.01.004
  156. Gilsanz V, Wren TA, Sanchez M, Dorey F, Judex S, Rubin C. Low-level, high-frequency mechanical signals enhance musculoskeletal development of young women with low BMD. *J Bone Min Res*. 2006;21(9):1464-1474. doi:10.1359/jbmr.060612
  157. Kiel DP, Hannan MT, Barton BA, et al. Low-Magnitude Mechanical Stimulation to Improve Bone Density in Persons of Advanced Age: A Randomized, Placebo-Controlled Trial. *J Bone Min Res*. 2015;30(7):1319-1328. doi:10.1002/jbmr.2448
  158. Iwamoto J, Takeda T, Sato Y, Uzawa M. Effect of whole-body vibration exercise on lumbar bone mineral density, bone turnover, and chronic back pain in postmenopausal osteoporotic women treated with alendronate. *Aging Clin Exp Res*. 2005;17(2):157-163. doi:10.1007/s40520-019-01373-6.
  159. Rittweger J, Just K, Kautzsch K, Reeg P, Felsenberg D. Treatment of chronic lower back pain with lumbar extension and whole-body vibration exercise: a randomized controlled trial. *Spine (Phila Pa 1976)*. 2002;27(17):1829-1834. <http://www.ncbi.nlm.nih.gov/pubmed/12221343>.
  160. Tsuji T, Yoon J, Aiba T, Kanamori A, Okura T, Tanaka K. Effects of whole-body vibration exercise on muscular strength and power, functional mobility and self-reported knee function in middle-aged and older Japanese women with knee pain. *Knee*. 2014;21(6):1088-1095. doi:10.1016/j.knee.2014.07.015
  161. Li X, Wang XQ, Chen BL, Huang LY, Liu Y. Whole-Body Vibration Exercise for Knee Osteoarthritis: A Systematic Review and Meta-Analysis. *Evid Based Complement Altern Med*. 2015;2015:758147. doi:10.1155/2015/758147
  162. McCann MR, Patel P, Pest MA, et al. Repeated exposure to high-frequency low-amplitude vibration induces degeneration of murine intervertebral discs and knee

- joints. *Arthritis Rheumatol.* 2015;67(8):2164-2175. doi:10.1002/art.39154
163. McCann MR, Veras MA, Yeung C, et al. Whole-body vibration of mice induces progressive degeneration of intervertebral discs associated with increased expression of Il-1 $\beta$  and multiple matrix degrading enzymes. *Osteoarthr Cartil.* 2017. doi:10.1016/j.joca.2017.01.004
  164. McCann MR, Yeung C, Pest MA, et al. Whole-body vibration of mice induces articular cartilage degeneration with minimal changes in subchondral bone. *Osteoarthr Cartil.* 2017;25(5):770-778. doi:10.1016/j.joca.2016.11.001
  165. McCann MR, Veras MA, Yeung C, et al. Whole-body vibration of mice induces progressive degeneration of intervertebral discs associated with increased expression of Il-1beta and multiple matrix degrading enzymes. *Osteoarthr Cartil.* 2017;25(5):779-789. doi:10.1016/j.joca.2017.01.004
  166. Urban JPG, Maroudas A. The measurement of fixed charged density in the intervertebral disc. *BBA - Gen Subj.* 1979. doi:10.1016/0304-4165(79)90415-X
  167. Grunhagen T, Wilde G, Soukane DM, Shirazi-Adl SA, Urban JPG. Nutrient supply and intervertebral disc metabolism. *J Bone Jt Surg - Ser A.* 2006. doi:10.2106/00004623-200604002-00007
  168. Holm S, Maroudas A, Urban JPG, Selstam G, Nachemson A. Nutrition of the intervertebral disc: Solute transport and metabolism. *Connect Tissue Res.* 1981. doi:10.3109/03008208109152130
  169. Salvatierra JC, Yuan TY, Fernando H, et al. Difference in energy metabolism of annulus fibrosus and nucleus pulposus cells of the intervertebral disc. *Cell Mol Bioeng.* 2011. doi:10.1007/s12195-011-0164-0
  170. Bibby SRS, Jones DA, Ripley RM, Urban JPG. Metabolism of the intervertebral disc: Effects of low levels of oxygen, glucose, and pH on rates of energy metabolism of bovine nucleus pulposus cells. *Spine (Phila Pa 1976).* 2005. doi:10.1097/01.brs.0000154619.38122.47
  171. Horner HA, Urban JPG. 2001 Volvo award winner in basic science studies: Effect of nutrient supply on the viability of cells from the nucleus pulposus of the intervertebral disc. *Spine (Phila Pa 1976).* 2001. doi:10.1097/00007632-200112010-00006
  172. Ratneswaran A, LeBlanc EA, Walser E, et al. Peroxisome proliferator-activated receptor delta promotes the progression of posttraumatic osteoarthritis in a mouse model. *Arthritis Rheumatol.* 2015;67(2):454-464. doi:10.1002/art.38915
  173. Vasheghani F, Zhang Y, Li YH, et al. PPAR $\gamma$  deficiency results in severe, accelerated osteoarthritis associated with aberrant mTOR signalling in the articular cartilage. *Ann Rheum Dis.* 2015. doi:10.1136/annrheumdis-2014-205743

174. Alini M, Eisenstein SM, Ito K, et al. Are animal models useful for studying human disc disorders/degeneration? *Eur Spine J*. 2008;17(1):2-19. doi:10.1007/s00586-007-0414-y
175. Daly C, Ghosh P, Jenkin G, Oehme D, Goldschlager T. A Review of Animal Models of Intervertebral Disc Degeneration: Pathophysiology, Regeneration, and Translation to the Clinic. *Biomed Res Int*. 2016. doi:10.1155/2016/5952165
176. Smit TH. The use of a quadruped as an in vivo model for the study of the spine - Biomechanical considerations. *Eur Spine J*. 2002. doi:10.1007/s005860100346
177. Ziegler A, Gonzalez L, Blikslager A. Large Animal Models: The Key to Translational Discovery in Digestive Disease Research. *CMGH*. 2016. doi:10.1016/j.jcmgh.2016.09.003
178. Beckstein JC, Sen S, Schaer TP, Vresilovic EJ, Elliott DM. Comparison of animal discs used in disc research to human lumbar disc: Axial compression mechanics and glycosaminoglycan content. *Spine (Phila Pa 1976)*. 2008. doi:10.1097/BRS.0b013e318166e001
179. Showalter BL, Beckstein JC, Martin JT, et al. Comparison of animal discs used in disc research to human lumbar disc: Torsion mechanics and collagen content. *Spine (Phila Pa 1976)*. 2012. doi:10.1097/BRS.0b013e31824d911c
180. O'Connell GD, Vresilovic EJ, Elliott DM. Comparison of animals used in disc research to human lumbar disc geometry. *Spine (Phila Pa 1976)*. 2007. doi:10.1097/01.brs.0000253961.40910.c1
181. Schwenk F, Baron U, Rajewsky K. A cre-transgenic mouse strain for the ubiquitous deletion of loxP-flanked gene segments including deletion in germ cells. *Nucleic Acids Res*. 1995. doi:10.1093/nar/23.24.5080
182. Lewandoski M. Conditional control of gene expression in the mouse. *Nat Rev Genet*. 2001. doi:10.1038/35093537
183. Nagy A. Cre recombinase: The universal reagent for genome tailoring. *Genesis*. 2000. doi:10.1002/(SICI)1526-968X(200002)26:2<99::AID-GENE1>3.0.CO;2-B
184. Millemcamps M, Tajerian M, Naso L, Sage EH, Stone LS. Lumbar intervertebral disc degeneration associated with axial and radiating low back pain in ageing SPARC-null mice. *Pain*. 2012;153(6):1167-1179. doi:10.1016/j.pain.2012.01.027
185. Bedore J, Sha W, McCann MR, Liu S, Leask A, Seguin CA. Impaired intervertebral disc development and premature disc degeneration in mice with notochord-specific deletion of CCN2. *Arthritis Rheum*. 2013;65(10):2634-2644. doi:10.1002/art.38075
186. Boyd LM, Richardson WJ, Allen KD, et al. Early-onset degeneration of the

- intervertebral disc and vertebral end plate in mice deficient in type IX collagen. *Arthritis Rheum.* 2008. doi:10.1002/art.23231
187. Gregory NS, Harris AL, Robinson CR, Dougherty PM, Fuchs PN, Sluka KA. An overview of animal models of pain: Disease models and outcome measures. *J Pain.* 2013. doi:10.1016/j.jpain.2013.06.008
  188. Mosley GE, Evashwick-Rogler TW, Lai A, Iatridis JC. Looking beyond the intervertebral disc: The need for behavioral assays in models of discogenic pain. *Ann N Y Acad Sci.* 2017. doi:10.1111/nyas.13429
  189. Burma NE, Leduc-Pessah H, Fan CY, Trang T. Animal models of chronic pain: Advances and challenges for clinical translation. *J Neurosci Res.* 2017. doi:10.1002/jnr.23768
  190. Ji RR, Nackley A, Huh Y, Terrando N, Maixner W. Neuroinflammation and central sensitization in chronic and widespread pain. *Anesthesiology.* 2018. doi:10.1097/ALN.0000000000002130
  191. Blüher M. Obesity: global epidemiology and pathogenesis. *Nat Rev Endocrinol.* 2019. doi:10.1038/s41574-019-0176-8
  192. Cawley J, Meyerhoefer C. The medical care costs of obesity: An instrumental variables approach. *J Health Econ.* 2012. doi:10.1016/j.jhealeco.2011.10.003
  193. De Gonzalez AB, Hartge P, Cerhan JR, et al. Body-mass index and mortality among 1.46 million white adults. *N Engl J Med.* 2010. doi:10.1056/NEJMoa1000367
  194. Taylor VH, Forhan M, Vigod SN, McIntyre RS, Morrison KM. The impact of obesity on quality of life. *Best Pract Res Clin Endocrinol Metab.* 2013. doi:10.1016/j.beem.2013.04.004
  195. Hebebrand J, Holm JC, Woodward E, et al. A Proposal of the European Association for the Study of Obesity to Improve the ICD-11 Diagnostic Criteria for Obesity Based on the Three Dimensions Etiology, Degree of Adiposity and Health Risk. *Obes Facts.* 2017. doi:10.1159/000479208
  196. Han TS, Lean ME. A clinical perspective of obesity, metabolic syndrome and cardiovascular disease. *JRSM Cardiovasc Dis.* 2016. doi:10.1177/2048004016633371
  197. Miranda PJ, DeFronzo RA, Califf RM, Guyton JR. Metabolic syndrome: Definition, pathophysiology, and mechanisms. *Am Heart J.* 2005. doi:10.1016/j.ahj.2004.07.013
  198. Alshehri AM. Review Article Metabolic syndrome and cardiovascular risk. *J Fam Community Med.* 2010.

199. Prasad GR. Metabolic syndrome and chronic kidney disease: Current status and future directions. *World J Nephrol.* 2014. doi:10.5527/wjn.v3.i4.210
200. Zhuo Q, Yang W, Chen J, Wang Y. Metabolic syndrome meets osteoarthritis. *Nat Rev Rheumatol.* 2012;8(12):729-737. doi:10.1038/nrrheum.2012.135
201. Aganović I, Dušek T. Pathophysiology of Metabolic Syndrome. *EJIFCC.* 2007;18(1):3-6. doi:10.1016/j.mcna.2007.06.005.
202. Das UN. Is obesity an inflammatory condition? *Nutrition.* 2001;17(11-12):953-966. doi:10.1016/s0899-9007(01)00672-4
203. Kershaw EE, Flier JS. Adipose tissue as an endocrine organ. In: *Journal of Clinical Endocrinology and Metabolism.* ; 2004. doi:10.1210/jc.2004-0395
204. Ellulu MS, Patimah I, Khaza'ai H, Rahmat A, Abed Y. Obesity & inflammation: The linking mechanism & the complications. *Arch Med Sci.* 2017. doi:10.5114/aoms.2016.58928
205. Jung UJ, Choi MS. Obesity and its metabolic complications: The role of adipokines and the relationship between obesity, inflammation, insulin resistance, dyslipidemia and nonalcoholic fatty liver disease. *Int J Mol Sci.* 2014. doi:10.3390/ijms15046184
206. Boden G. Obesity and Free Fatty Acids. *Endocrinol Metab Clin North Am.* 2008. doi:10.1016/j.ecl.2008.06.007
207. Anandacoomarasamy A, Caterson I, Sambrook P, Fransen M, March L. The impact of obesity on the musculoskeletal system. *Int J Obes.* 2008. doi:10.1038/sj.ijo.0803715
208. Batsis JA, Villareal DT. Sarcopenic obesity in older adults: aetiology, epidemiology and treatment strategies. *Nat Rev Endocrinol.* 2018. doi:10.1038/s41574-018-0062-9
209. Keser N, Celikoglu E, İs M, et al. Is there a relationship between blood lipids and lumbar disc herniation in young Turkish adults? *Arch Med Sci - Atheroscler Dis.* 2017. doi:10.5114/amsad.2017.68651
210. Cade WT. Diabetes-Related Microvascular and Macrovascular Diseases in the Physical Therapy Setting. *Phys Ther.* 2008. doi:10.2522/ptj.20080008
211. Chen S, Liao M, Li J, Peng H, Xiong M. The correlation between microvessel pathological changes of the endplate and degeneration of the intervertebral disc in diabetic rats. *Exp Ther Med.* 2013. doi:10.3892/etm.2012.868
212. Imhof H, Sulzbacher I, Grampp S, Czerny C, Youssefzadeh S, Kainberger F. Subchondral bone and cartilage disease: A rediscovered functional unit. *Invest*

*Radiol.* 2000. doi:10.1097/00004424-200010000-00004

213. Samartzis D, Bow C, Karppinen J, Luk KDK, Cheung BMY, Cheung KMC. Hypertension is Independently Associated with Lumbar Disc Degeneration: A Large-Scale Population-Based Study. *Glob Spine J.* 2014. doi:10.1055/s-0034-1376579
214. Zhang X, Chen J, Huang B, et al. Obesity Mediates Apoptosis and Extracellular Matrix Metabolic Imbalances via MAPK Pathway Activation in Intervertebral Disk Degeneration. *Front Physiol.* 2019. doi:10.3389/fphys.2019.01284
215. Cannata F, Vadalà G, Ambrosio L, et al. Intervertebral disc degeneration: A focus on obesity and type 2 diabetes. *Diabetes Metab Res Rev.* 2020. doi:10.1002/dmrr.3224
216. Sellam J, Berenbaum F. Is osteoarthritis a metabolic disease? *Jt Bone Spine.* 2013;80(6):568-573. doi:10.1016/j.jbspin.2013.09.007
217. Villalvilla A, Gómez R, Largo R, Herrero-Beaumont G. Lipid transport and metabolism in healthy and osteoarthritic cartilage. *Int J Mol Sci.* 2013. doi:10.3390/ijms141020793
218. Rosa SC, Gonçalves J, Judas F, Mobasheri A, Lopes C, Mendes AF. Impaired glucose transporter-1 degradation and increased glucose transport and oxidative stress in response to high glucose in chondrocytes from osteoarthritic versus normal human cartilage. *Arthritis Res Ther.* 2009. doi:10.1186/ar2713
219. Cheng X, Ni B, Zhang F, Hu Y, Zhao J. High Glucose-Induced Oxidative Stress Mediates Apoptosis and Extracellular Matrix Metabolic Imbalances Possibly via p38 MAPK Activation in Rat Nucleus Pulposus Cells. *J Diabetes Res.* 2016. doi:10.1155/2016/3765173
220. Henrotin YE, Bruckner P, Pujol JPL. The role of reactive oxygen species in homeostasis and degradation of cartilage. *Osteoarthr Cartil.* 2003. doi:10.1016/S1063-4584(03)00150-X
221. Saremi A, Howell S, Schwenke DC, Bahn G, Beisswenger PJ, Reaven PD. Advanced glycation end products, oxidation products, and the extent of atherosclerosis during the VA diabetes trial and follow-up study. In: *Diabetes Care.* ; 2017. doi:10.2337/dc16-1875
222. Tsai TT, Ho NYJ, Lin YT, et al. Advanced glycation end products in degenerative nucleus pulposus with diabetes. *J Orthop Res.* 2014. doi:10.1002/jor.22508
223. Wagner DR, Reiser KM, Lotz JC. Glycation increases human annulus fibrosus stiffness in both experimental measurements and theoretical predictions. *J Biomech.* 2006;39(6):1021-1029. doi:10.1016/j.jbiomech.2005.02.013

224. Krishnamoorthy D, Hoy RC, Natelson DM, et al. Dietary advanced glycation end-product consumption leads to mechanical stiffening of murine intervertebral discs. *DMM Dis Model Mech*. 2018. doi:10.1242/dmm.036012
225. Loeser RF, Yammani RR, Carlson CS, et al. Articular chondrocytes express the receptor for advanced glycation end products: Potential role in osteoarthritis. *Arthritis Rheum*. 2005. doi:10.1002/art.21199
226. Steenvoorden MMC, Huizinga TWJ, Verzijl N, et al. Activation of receptor for advanced glycation end products in osteoarthritis leads to increased stimulation of chondrocytes and synoviocytes. *Arthritis Rheum*. 2006. doi:10.1002/art.21523
227. Griffin TM, Huebner JL, Kraus VB, Guilak F. Extreme obesity due to impaired leptin signaling in mice does not cause knee osteoarthritis. *Arthritis Rheum*. 2009;60(10):2935-2944. doi:10.1002/art.24854
228. Miao D, Zhang L. Leptin modulates the expression of catabolic genes in rat nucleus pulposus cells through the mitogen-activated protein kinase and Janus kinase 2/signal transducer and activator of transcription 3 pathways. *Mol Med Rep*. 2015;12(2):1761-1768. doi:10.3892/mmr.2015.3646
229. Liu C, Yang H, Gao F, et al. Resistin Promotes Intervertebral Disc Degeneration by Upregulation of ADAMTS-5 Through p38 MAPK Signaling Pathway. *Spine (Phila Pa 1976)*. 2016;41(18):1414-1420. doi:10.1097/BRS.0000000000001556
230. Wright LJ, Schur E, Noonan C, Ahumada S, Buchwald D, Afari N. Chronic pain, overweight, and obesity: findings from a community-based twin registry. *J Pain*. 2010;11(7):628-635. doi:10.1016/j.jpain.2009.10.004
231. Okifuji A, Hare BD. The association between chronic pain and obesity. *J Pain Res*. 2015;8:399-408. doi:10.2147/JPR.S55598
232. Blüher M, Fasshauer M, Tönjes A, Kratzsch J, Schön MR, Paschke R. Association of interleukin-6, C-reactive protein, interleukin-10 and adiponectin plasma concentrations with measures of obesity, insulin sensitivity and glucose metabolism. *Exp Clin Endocrinol Diabetes*. 2005. doi:10.1055/s-2005-872851
233. Pratt LA, Brody DJ. Depression and obesity in the U.S. adult household population, 2005-2010. *NCHS Data Brief*. 2014.
234. Beccuti G, Pannain S. Sleep and obesity. *Curr Opin Clin Nutr Metab Care*. 2011. doi:10.1097/MCO.0b013e3283479109
235. Dworkin RH, Gitlin MJ. Clinical aspects of depression in chronic pain patients. *Clin J Pain*. 1991. doi:10.1097/00002508-199106000-00004
236. Kundermann B, Krieg JC, Schreiber W, Lautenbacher S. The effect of sleep deprivation on pain. *Pain Res Manag*. 2004. doi:10.1155/2004/949187

237. Rastinejad F, Huang P, Chandra V, Khorasanizadeh S. Understanding nuclear receptor form and function using structural biology. *J Mol Endocrinol*. 2013. doi:10.1530/JME-13-0173
238. He B, Kempainen JA, Wilson EM. FXXLF and WXXLF sequences mediate the NH2-terminal interaction with the ligand binding domain of the androgen receptor. *J Biol Chem*. 2000. doi:10.1074/jbc.M002807200
239. Sever R, Glass CK. Signaling by nuclear receptors. *Cold Spring Harb Perspect Biol*. 2013. doi:10.1101/cshperspect.a016709
240. Li Y, Lambert MH, Xu HE. Activation of nuclear receptors: A perspective from structural genomics. *Structure*. 2003. doi:10.1016/S0969-2126(03)00133-3
241. Wang Z, Benoit G, Liu J, et al. Structure and function of Nurr1 identifies a class of ligand-independent nuclear receptors. *Nature*. 2003. doi:10.1038/nature01645
242. Hua G, Ganti KP, Chambon P. Glucocorticoid-induced tethered transrepression requires SUMOylation of GR and formation of a SUMO-SMRT/NCoR1-HDAC3 repressing complex. *Proc Natl Acad Sci U S A*. 2016. doi:10.1073/pnas.1522826113
243. Weikum ER, Liu X, Ortlund EA. The nuclear receptor superfamily: A structural perspective. *Protein Sci*. 2018. doi:10.1002/pro.3496
244. Fuller PJ. The steroid receptor superfamily: mechanisms of diversity. *FASEB J*. 1991. doi:10.1096/fasebj.5.15.1743440
245. Olefsky JM. Nuclear Receptor Minireview Series. *J Biol Chem*. 2001. doi:10.1074/jbc.R100047200
246. Chawta A, Repa JJ, Evans RM, Mangelsdorf DJ. Nuclear receptors and lipid physiology: Opening the x-files. *Science (80- )*. 2001. doi:10.1126/science.294.5548.1866
247. Evans RM, Barish GD, Wang YX. PPARs and the complex journey to obesity. *Nat Med*. 2004. doi:10.1038/nm1025
248. Germain P, Chambon P, Eichele G, et al. International Union of Pharmacology. LX. Retinoic acid receptors. *Pharmacol Rev*. 2006;58(4):712-725. doi:10.1124/pr.58.4.4
249. Tyagi S, Gupta P, Saini A, Kaushal C, Sharma S. The peroxisome proliferator-activated receptor: A family of nuclear receptors role in various diseases. *J Adv Pharm Technol Res*. 2011. doi:10.4103/2231-4040.90879
250. Steiner G, Hamsten A, Hosking J, et al. Effect of fenofibrate on progression of coronary-artery disease in type 2 diabetes: The Diabetes Atherosclerosis



- Intervention Study, a randomised study. *Lancet*. 2001. doi:10.1016/S0140-6736(00)04209-4
251. Mooradian AD, Chehade J, Thurman JE. The role of thiazolidinediones in the treatment of patients with type 2 diabetes mellitus. *Treat Endocrinol*. 2002. doi:10.2165/00024677-200201010-00002
  252. Vasheghani F, Monemdjou R, Fahmi H, et al. Adult cartilage-specific peroxisome proliferator-activated receptor gamma knockout mice exhibit the spontaneous osteoarthritis phenotype. *Am J Pathol*. 2013. doi:10.1016/j.ajpath.2012.12.012
  253. Narkar VA, Downes M, Yu RT, et al. AMPK and PPARdelta agonists are exercise mimetics. *Cell*. 2008;134(3):405-415. doi:10.1016/j.cell.2008.06.051
  254. Fan W, Waizenegger W, Lin CS, et al. PPAR $\delta$  Promotes Running Endurance by Preserving Glucose. *Cell Metab*. 2017. doi:10.1016/j.cmet.2017.04.006
  255. Lee CH, Olson P, Hevener A, et al. PPAR $\delta$  regulates glucose metabolism and insulin sensitivity. *Proc Natl Acad Sci U S A*. 2006. doi:10.1073/pnas.0511253103
  256. Ratneswaran A, Sun MM, Dupuis H, Sawyez C, Borradaile N, Beier F. Nuclear receptors regulate lipid metabolism and oxidative stress markers in chondrocytes. *J Mol Med*. 2017;95(4):431-444. doi:10.1007/s00109-016-1501-5
  257. Veras MA, McCann MR, Tenn NA, Séguin CA. Transcriptional profiling of the murine intervertebral disc and age-associated changes in the nucleus pulposus. *Connect Tissue Res*. 2020. doi:10.1080/03008207.2019.1665034
  258. Janssen I. The public health burden of obesity in Canada. *Can J Diabetes*. 2013;37(2):90-96. doi:10.1016/j.jcjd.2013.02.059
  259. Balistreri CR, Caruso C, Candore G. The role of adipose tissue and adipokines in obesity-related inflammatory diseases. *Mediat Inflamm*. 2010;2010:802078. doi:10.1155/2010/802078
  260. Samartzis D, Karppinen J, Cheung JPY, Lotz JC. Disk Degeneration and Low Back Pain: Are They Fat-Related Conditions? *Glob Spine J*. 2013;3:133-144. doi:10.1055/s-0033-1350054
  261. Shiri R, Karppinen J, Leino-Arjas P, Solovieva S, Viikari-Juntura E. The association between obesity and low back pain: a meta-analysis. *Am J Epidemiol*. 2010;171(2):135-154. doi:10.1093/aje/kwp356
  262. Datta P, Zhang Y, Parousis A, et al. High-fat diet-induced acceleration of osteoarthritis is associated with a distinct and sustained plasma metabolite signature. *Sci Rep*. 2017;7(1):8205. doi:10.1038/s41598-017-07963-6
  263. Griffin TM, Fermor B, Huebner JL, et al. Diet-induced obesity differentially

regulates behavioral, biomechanical, and molecular risk factors for osteoarthritis in mice. *Arthritis Res Ther*. 2010;12(4):R130. doi:10.1186/ar3068

264. Griffin TM, Huebner JL, Kraus VB, Yan Z, Guilak F. Induction of osteoarthritis and metabolic inflammation by a very high-fat diet in mice: effects of short-term exercise. *Arthritis Rheum*. 2012;64(2):443-453. doi:10.1002/art.33332
265. Collins KH, Paul HA, Reimer RA, Seerattan RA, Hart DA, Herzog W. Relationship between inflammation, the gut microbiota, and metabolic osteoarthritis development: studies in a rat model. *Osteoarthr Cartil*. 2015;23(11):1989-1998. doi:10.1016/j.joca.2015.03.014
266. Collins KH, Hart DA, Reimer RA, Seerattan RA, Herzog W. Response to diet-induced obesity produces time-dependent induction and progression of metabolic osteoarthritis in rat knees. *J Orthop Res*. 2016;34(6):1010-1018. doi:10.1002/jor.23103
267. Ratneswaran A, To B, Kerr G., Benipal S, Beier F. PPARdelta inactivation protects against joint damage in age associated osteoarthritis. *Prep*.
268. Rosen S, Ham B, Mogil JS. Sex differences in neuroimmunity and pain. *J Neurosci Res*. 2017. doi:10.1002/jnr.23831

## Chapter 2

### **C57BL/6 mice are resistant to joint degeneration induced by whole-body vibration.**

Chapter 2 is adapted from Kerr, G.J., McCann M.R., Branch, J.K, Ratneswaran, A., Pest, M.A., Holdsworth, D.W., Beier, F., Dixon, S.J, Séguin, C.A, (2017). C57BL/6 mice are resistant to joint degeneration induced by whole-body vibration. *Osteoarthritis Cartilage*. Mar;25(3):421-425. doi: 10.1016/j.joca.2016.09.020.

Permission to reuse material is not required (**Appendix A**).

## 2 C57BL/6 mice are resistant to joint degeneration induced by whole-body vibration.

### 2.1 Co-authorship Statement

G.J. Kerr performed most of the experiments, contributed to study design and wrote the manuscript. J.K. Branch assisted with the *in vivo* vibration and sectioning of the lumbar spines (**Figure 2.1**). M.R. McCann assisted with histopathological scoring for IVD degeneration (**Figure 2.1**). A. Ratneswaran, and M.A. Pest conducted histopathological scoring on the knee joints (**Figure 2.2**). Drs. D.W. Holdsworth, F. Beier, S.J. Dixon and C.A. Séguin contributed to the study design and editing of the manuscript. All authors read and approved the submitted version of the manuscript.

## 2.2 Chapter Summary

**Objective:** Whole-body vibration (WBV) platforms are commercially available devices that are used clinically to treat numerous musculoskeletal conditions based on their reported ability to increase bone mineral density and muscle strength. Despite widespread use, there is an alarming lack of understanding of the direct effects of WBV on joint health. Previous work by our lab demonstrated that repeated exposure to WBV using protocols that model those used clinically, induces intervertebral disc (IVD) degeneration and osteoarthritis-like damage in the knee of skeletally mature, male mice of a single outbred strain (CD-1). The present study examined whether exposure to WBV induces similar deleterious effects in a genetically different strain of mouse (C57BL/6).

**Design:** Male 10-week-old C57BL/6 mice were exposed to vertical sinusoidal WBV for 30 min/day, 5 days/ week, for 4 or 8 weeks using previously reported protocols (45 Hz, 0.3 g peak acceleration). Following WBV, joint tissues were examined using histological analysis and gene expression was quantified using real-time PCR (qPCR).

**Results:** Our analyses show a lack of WBV-induced degeneration in either the knee or IVDs of C57BL/6 mice exposed to WBV for 4 or 8 weeks, in direct contrast to the WBV-induced damage previously reported by our lab in CD-1 mice.

**Conclusions:** Together with previous studies from our group, the present study demonstrates that the effects of WBV on joint tissues vary in a strain-specific manner. These findings highlight the need to examine genetic or physiological differences that may underlie susceptibility to the deleterious effects of WBV on joint tissues.

## 2.3 Introduction

Platforms that deliver whole-body vibration (WBV) are currently used in the clinical setting based on their reported ability to increase bone density<sup>1</sup> and muscle strength<sup>2</sup>. Within the last decade, WBV has been integrated into physical therapy regimens for a variety of musculoskeletal disorders, including osteoporosis<sup>1</sup>, back pain<sup>3</sup>, and osteoarthritis<sup>4</sup>. In addition to their clinical use, WBV platforms are promoted in the health and wellness industries as “no-work workouts” equivalent to traditional resistance training. The proposed use of WBV as a treatment for musculoskeletal conditions appears contradictory to epidemiological studies establishing an association between workplace exposure to WBV and the development of several conditions, including back pain<sup>5</sup>. Recognizing the potential of WBV to induce tissue damage, the International Organization for Standardization (ISO) implemented guidelines defining the maximum daily limit of WBV that workers can be exposed to without risk for injury<sup>6</sup>. Conversely, commercially available WBV platforms are currently unregulated, with some able to deliver accelerations that exceed current ISO-2631 recommended guidelines<sup>7</sup>.

Raising further concern regarding the use of WBV, clinical trials show conflicting reports regarding the ability of WBV to increase bone mineral density<sup>1,8</sup>. Similarly, clinical trials investigating the effectiveness of WBV for knee or back pain have failed to show conclusive evidence, with only a small proportion of trials showing benefits based on assessments of patient self-reported pain<sup>3,9</sup>. A cause for concern is that the widespread use of WBV has not been validated with rigorous research-based evidence addressing the broad range of parameters used and potential harmful effects.

Investigating the effects of WBV on joint tissues, our research has demonstrated that exposure of mice to protocols of low-amplitude, high-frequency WBV that model those used clinically induced intervertebral disc (IVD) degeneration and osteoarthritis-like damage in the knee of skeletally mature, male mice, of a single outbred strain (CD-1)<sup>10-12</sup>. Given these strikingly deleterious effects of WBV, the present study aimed to determine if the response of joint tissues to WBV was consistent in age- and sex-matched C57BL/6 mice representing a distinct genetic background.

## 2.4 Methods

### 2.4.1 Whole body vibration

Based on WBV parameters used in clinical protocols and our previous studies<sup>10-12</sup>, 10-week-old male C57BL/6 mice (Charles River) were subjected to vertical sinusoidal vibration (45Hz, peak-to-peak amplitude 74  $\mu$ m, peak acceleration 0.3 g) 30 minutes/day, 5 days/week for 4 or 8 weeks. Age- and sex-matched controls were housed in identical chambers on a non-vibrating sham platform to replicate handling and environmental conditions. Following WBV, mice were returned to conventional housing and monitored daily. No differences in total body mass were detected between groups. Mice were euthanized with sodium pentobarbital 24 hours after final exposure to WBV. The Council on Animal Care at Western University approved all procedures, in accordance with the Canadian Council on Animal Care and the ARRIVE guidelines.

### 2.4.2 Gene expression analysis

Thoracic IVDs (T10-T15) were isolated from mice exposed to 8 weeks WBV and sham controls, placed in TRIzol (Life Technologies) and homogenized using a PRO250 tissue homogenizer (PRO Scientific). RNA was extracted according to manufacturer's instructions, quantified using a NanoDrop 2000 spectrophotometer (Thermo Scientific), and 0.5  $\mu$ g was reverse transcribed into complementary DNA (cDNA) (iScript; Bio-Rad). Gene expression was assessed by real-time PCR (qPCR) using the Bio-Rad CFX384. PCR analyses were run in triplicate using 120 ng of cDNA per reaction and 310 nM forward and reverse primers with 2x SsoFast EvaGreen Supermix (Bio-Rad) using previously optimized PCR parameters and primers<sup>11</sup>. Transcript levels were calculated using  $\Delta\Delta$ Ct, with data normalized for input based on Ribosomal protein S29 (*Rps29*) and expressed relative to non-vibrated sham controls.

### 2.4.3 Histological analysis

Intact lumbar spine segments (L1-L5) and knees were isolated, fixed and paraffin embedded as previously described<sup>11</sup>. Spines were sectioned sagittally and knees were sectioned coronally, at a thickness of 5  $\mu$ m using a microtome (Leica Microsystems). Spines sections were stained using 0.1% Safranin-O/0.05% fast green, and knee sections were stained with 0.04% Toluidine Blue. Sections were imaged on a Leica DM1000 microscope, with Leica Application Suite (Leica Microsystems). To evaluate IVD degeneration, mid-sagittal sections were scored using the modified Thompson grading scheme to assess IVD health based on criteria specific to each tissue compartment (scores 1-4, where a lower score corresponds to a more healthy tissue), as previously reported<sup>10,11</sup>.



Knee joint health was assessed using the murine Osteoarthritis Research Society International (OARSI) histopathological scale<sup>13</sup>. For each mouse, the four quadrants of the knee joint were evaluated in 10 serial sections taken 75  $\mu\text{m}$  apart to include most of the weight-bearing area of the femorotibial joint. For each quadrant of each section individual scores were averaged between three independent blinded observers and summed across the 10 sections for each mouse. The whole joint score was calculated as the sum of the quadrant scores for each mouse.

#### 2.4.4 Statistical analysis

Data are from experiments conducted with  $n = 5-6$  mice per group at each time point. For qPCR analyses, data from mice exposed to WBV were compared to non-vibrated sham controls using a parametric Welch's t-test. At each time point, histopathological scores from the IVD or knee joint were compared using a non-parametric Mann-Whitney U-test. Differences were accepted as statistically significant at  $P < 0.05$ .

## 2.5 Results

To examine the effects of repeated exposure to WBV on joint health, 10-week-old C57BL/6 mice were exposed to WBV for 30 min/day, 5 days/week for either 4 or 8 weeks, using parameters that model clinical use in humans (45 Hz, 0.3 g)<sup>11</sup>. Importantly, these parameters were previously found to induce degeneration of both the IVD and knee joint in age- and sex-matched CD-1 mice, marked by histological hallmarks of tissue damage including annulus fibrosus degeneration in the IVD as well as meniscal damage and focal defects in the articular surface of the knee<sup>10-12</sup>. In the C57BL/6 mice, we first assessed

IVD health. No discernable differences were detected in the histological appearance of lumbar IVDs in mice exposed to 4 or 8 weeks of WBV compared to their respective sham controls (**Figure 2.1A**). Accordingly, evaluation of IVD structure using the modified Thompson score showed no significant differences in degeneration grade between mice exposed to 4 or 8 weeks of WBV and their respective sham controls (**Figure 2.1B**). As a more sensitive measure of early degenerative changes in IVD tissues, we evaluated the cellular response to WBV using real-time PCR. Similar to histological evaluation, this analysis revealed no change in the expression of anabolic (*Acan*, *Col1a1*, *Col2a1*, *Sox9*) or catabolic (*Mmp3*, *Mmp13*, *Adamts4*, *Adamts5*) factors between mice exposed to 8 weeks of WBV and non-vibrated sham controls (**Figure 2-1C**).

We then assessed if exposure of C57BL/6 mice to WBV induced changes to knee joint tissues. Consistent with findings in the IVD, no discernable differences were detected in the knee joint of C57BL/6 mice exposed to 4 or 8 weeks of WBV compared to their respective sham controls (**Figure 2-2A**). In contrast to our previous studies in CD-1 mice<sup>10</sup>, exposure of C57BL/6 mice to WBV did not induce any observable meniscal damage, articular cartilage erosion or osteophyte formation. Evaluation of cartilage degeneration using the OARSI histopathological score supported these observations; no significant differences were found in the summed OARSI score between mice exposed to WBV and sham controls (**Figure 2-2B**).

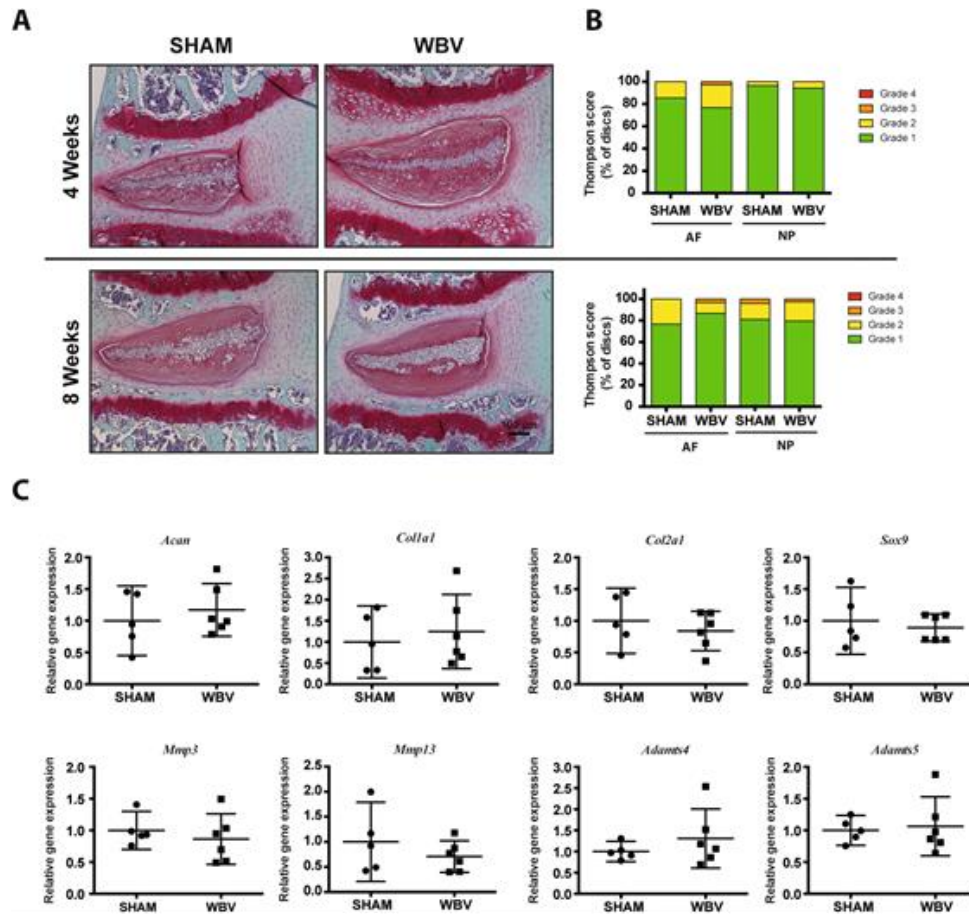


**Figure 2.1: Effect of repeated exposure to WBV on IVD health.**

A. Representative sagittal sections of the lumbar spine stained with safranin-O/fast green from mice exposed to WBV (for 4 or 8 weeks, 30 minutes per day, 5 days per week, at 45 Hz and 0.3 g) and non-vibrated sham controls. Images are oriented with rostral portion of the lumbar spine on top and dorsal portion on the left. B. Histopathological scores generated using the modified Thompson grading scale demonstrated no significant differences in degeneration score corresponding to the annulus fibrosus (AF) or nucleus pulposus (NP) from mice exposed to either 4 or 8 weeks WBV compared to their respective non-vibrated sham controls. C. Real-time PCR analysis of IVD gene expression in mice exposed to 8 weeks WBV and sham controls. Expression of extracellular matrix genes (*Acan*, *Col1a1*, *Col2a1*), the transcription *Sox9*, and matrix remodeling enzymes (*Mmp3*, *Mmp13*, *Adamts4*, *Adamts5*) were determined relative to the expression of the housekeeping gene *Rps29* and normalized to that of non-vibrated sham controls. Data are presented as mean  $\pm$  95% CI (n = 5-6 mice per group).

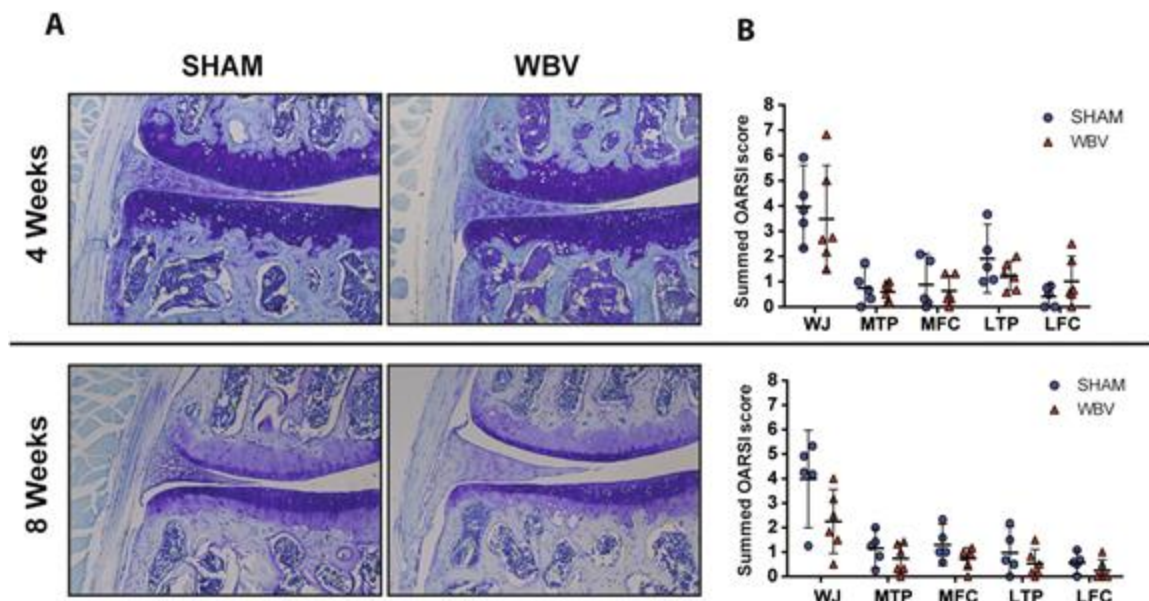


**Figure 2.2: Effect of repeated exposure to WBV on knee health.**

A. Representative coronal sections of the medial knee compartment stained with toluidine blue from mice exposed to WBV (30 minutes per day, 5 days per week, for 4 or 8 weeks at 45 Hz and 0.3 g) and non-vibrated sham control mice. Images are oriented with the medial femoral condyle located superiorly, and the medial tibial plateau inferiorly. B. Histopathological grading of the knee joints using the murine Osteoarthritis Research Society International (OARSI) scale. Joints from each mouse were evaluated using 10 serial sections (taken 75  $\mu\text{m}$  apart) and the summed OARSI scores are presented corresponding to the medial femoral condyle (MFC), medial tibial plateau (MTP), lateral femoral condyle (LFC) and lateral tibial plateau (LTP), which were then combined to generate the summed score for the whole joint (WJ). No significant differences in degeneration scores were detected between mice exposed to WBV and sham controls in any of the compartments investigated. Data are presented as mean  $\pm$ 95% CI (n = 5-6 mice per group).

## 2.6 Discussion

Despite the widespread clinical and recreational use of WBV platforms, there is an alarming lack of understanding of the effects of WBV on overall joint health as well as the effects elicited in specific joint tissues. Previous studies from our group demonstrated the ability of WBV to induce IVD degeneration and osteoarthritis-like damage in the knee of skeletally mature male outbred CD-1 mice<sup>11</sup>. After 4 weeks of repeated exposure to WBV, CD-1 mice showed degeneration in the annulus fibrosus of the IVD, marked by disruption of collagen organization, enhanced MMP-mediated collagen and aggrecan degradation, and increased cell death. Similarly, 4 of 5 CD-1 mice exposed to WBV for 4 weeks showed meniscal damage, and 2 of 5 showed focal damage to the articular cartilage associated with increased MMP-mediated matrix degradation<sup>11</sup>. Subsequent studies from our group showed that WBV-induced damage to both the IVD and knee joint increased in severity when CD-1 mice were exposed to 8 weeks WBV<sup>10,12</sup>. In direct contrast, the current study demonstrates that exposure of C57BL/6 mice to those same parameters of WBV did not induce degeneration-associated changes in either the knee or IVD after 4 or 8 weeks of exposure. Thus, the effects of WBV on joint tissues differ between different strains of mice, highlighting the need to examine factors that may determine susceptibility to the deleterious effects of mechanical loading on joint health.

Previous work has reported strain-specific differences in the attenuation of vibration loading in rodent models, as well as its downstream consequences on bone parameters<sup>14,15</sup>. Studies investigating vibration frequency thresholds in rodents reported that the resonant frequency range differs between strains of mice<sup>14</sup>. At the resonant frequency, it is assumed

that there is maximal displacement and consequently strain experienced by skeletal structures, whereas frequencies outside of this range of vibration are attenuated by the body<sup>14</sup>. When anesthetized mice were exposed to vibration frequencies ranging from 0-600 Hz (at a constant magnitude of 0.3 m/s<sup>2</sup>), C57BL/6 mice showed the least amount of attenuation between 41-50 Hz, whereas CD-1 mice showed the least amount of attenuation between 51-60 Hz, suggesting difference in their resonant frequency ranges<sup>14</sup>. While the biological factors underlying these differences were not explored, it has been suggested that differences in baseline bone parameters between mouse strains may alter the mechanical forces experienced at the tissue level<sup>15</sup>. Studies investigating the response of trabecular bone to whole-body vibration (45 Hz, 0.25 g; 10 min/day, 3 weeks) demonstrated that low bone mineral density C57BL/6 mice showed significantly higher bone formation rates induced by WBV compared to mid-density BALB/cByJ mice<sup>15</sup>. Moreover, C3H/HeJ mice which showed the highest bone mineral density, showed no changes in bone formation rates following exposure to the same parameters of WBV<sup>15</sup>.

Clinical trials in humans report that women with lower body mass showed a greater inhibition of bone loss when exposed to WBV compared to women with higher body mass; since bone mineral density is positively correlated with body mass the authors suggested that women with low bone mineral density may be most responsive to mechanical loading to prevent bone loss<sup>1</sup>. Attenuation of vibration may depend on bone density and other physiological factors including activity levels, body mass or joint structure, may alter the mechanical loading experienced at the tissue or cellular level, and potentially contribute to the differential response of joint tissues to WBV that we have shown between the CD-1 and C57BL/6 strains. Of note, the C57BL/6 mice used in the current study had an average

mass of 26 g at 18 weeks of age, compared to the CD-1 mice used in the previous study which had an average mass of 41 g at 18 weeks of age. Further studies are required to assess the relative contribution of biological mediators that might underlie the differences in the effects of WBV on joint tissues in different strains of mice, allowing for potential extrapolation to the clinical setting.

In summary, this study showed that repeated exposure of skeletally mature male C57BL/6 mice to WBV for 4 or 8 weeks did not alter overall health of the IVD and knee joints; in direct contrast to the WBV-induced joint degeneration we previously reported in CD-1 mice of the same age and sex. Although the results of the current study suggest that C57BL/6 mice are resistant to WBV-induced damage, it should be noted that different frequencies and accelerations may lead to differential responses. Previous studies in musculoskeletal tissues established that mechanical loading can induce both catabolic and anabolic responses, dependent on the load type, frequency, amplitude and exposure time<sup>16</sup>. Previous research by our group has shown the potential of WBV to induce anabolic effects in the IVD after acute exposure<sup>17</sup>. Together, these findings highlight the need for more rigorous investigations to examine the efficacy and safety of WBV in the diverse human populations currently using them, with emphasis on quantifying potential beneficial or detrimental effects on musculoskeletal tissues.

## 2.7 Acknowledgments

We thank Cynthia Yeung and Jake Bedore for their assistance in animal handling and histopathological scoring, respectively.

## 2.8 References

1. Rubin C, Recker R, Cullen D, Ryaby J, McCabe J, McLeod K. Prevention of postmenopausal bone loss by a low-magnitude, high-frequency mechanical stimuli: a clinical trial assessing compliance, efficacy, and safety. *J Bone Min Res.* 2004;19(3):343-351. doi:10.1359/JBMR.0301251
2. Delecluse C, Roelants M, Diels R, Koninckx E, Verschueren S. Effects of whole body vibration training on muscle strength and sprint performance in sprint-trained athletes. *Int J Sport Med.* 2005;26(8):662-668. doi:10.1055/s-2004-830381
3. Perraton L, Machotka Z, Kumar S. Whole-body vibration to treat low back pain: fact or fad? *Physiother Can.* 2011;63(1):88-93. doi:10.3138/ptc.2009.44
4. Park YG, Kwon BS, Park JW, et al. Therapeutic effect of whole body vibration on chronic knee osteoarthritis. *Ann Rehabil Med.* 2013;37(4):505-515. doi:10.5535/arm.2013.37.4.505
5. Bovenzi M. Low back pain disorders and exposure to whole-body vibration in the workplace. *Semin Perinatol.* 1996;20(1):38-53. <http://www.ncbi.nlm.nih.gov/pubmed/8899913>.
6. Standardization IO for. ISO 2631-1:1997, Mechanical Vibration and Shock - Evaluation of Human Exposure to Whole-Body Vibration, Part 1, General Requirements. 1997.
7. Muir J, Kiel DP, Rubin CT. Safety and severity of accelerations delivered from whole body vibration exercise devices to standing adults. *J Sci Med Sport.* 2013;16(6):526-531. doi:10.1016/j.jsams.2013.01.004
8. Slatkovska L, Alibhai SM, Beyene J, Hu H, Demaras A, Cheung AM. Effect of 12 months of whole-body vibration therapy on bone density and structure in postmenopausal women: a randomized trial. *Ann Intern Med.* 2011;155(10):668-679, W205. doi:10.7326/0003-4819-155-10-201111150-00005
9. Li X, Wang XQ, Chen BL, Huang LY, Liu Y. Whole-Body Vibration Exercise for Knee Osteoarthritis: A Systematic Review and Meta-Analysis. *Evid Based Complement Altern Med.* 2015;2015:758147. doi:10.1155/2015/758147
10. McCann MR, Veras MA, Yeung C, et al. Whole-body vibration of mice induces progressive degeneration of intervertebral discs associated with increased



- expression of Il-1beta and multiple matrix degrading enzymes. *Osteoarthr Cartil.* 2017;25(5):779-789. doi:10.1016/j.joca.2017.01.004
11. McCann MR, Patel P, Pest MA, et al. Repeated exposure to high-frequency low-amplitude vibration induces degeneration of murine intervertebral discs and knee joints. *Arthritis Rheumatol.* 2015;67(8):2164-2175. doi:10.1002/art.39154
  12. McCann MR, Yeung C, Pest MA, et al. Whole-body vibration of mice induces articular cartilage degeneration with minimal changes in subchondral bone. *Osteoarthr Cartil.* 2017. doi:10.1016/j.joca.2016.11.001
  13. Glasson SS, Chambers MG, Van Den Berg WB, Little CB. The OARSI histopathology initiative - recommendations for histological assessments of osteoarthritis in the mouse. *Osteoarthr Cartil.* 2010;18 Suppl 3:S17-23. doi:10.1016/j.joca.2010.05.025
  14. Rabey KN, Li Y, Norton JN, Reynolds RP, Schmitt D. Vibrating Frequency Thresholds in Mice and Rats: Implications for the Effects of Vibrations on Animal Health. *Ann Biomed Eng.* 2015;43(8):1957-1964. doi:10.1007/s10439-014-1226-y
  15. Judex S, Donahue LR, Rubin C. Genetic predisposition to low bone mass is paralleled by an enhanced sensitivity to signals anabolic to the skeleton. *FASEB J.* 2002;16(10):1280-1282. doi:10.1096/fj.01-0913fje
  16. Neidlinger-Wilke C, Galbusera F, Pratsinis H, et al. Mechanical loading of the intervertebral disc: from the macroscopic to the cellular level. *Eur Spine J.* 2014;23 Suppl 3:S333-43. doi:10.1007/s00586-013-2855-9
  17. McCann MR, Patel P, Beaucage KL, et al. Acute vibration induces transient expression of anabolic genes in the murine intervertebral disc. *Arthritis Rheum.* 2013;65(7):1853-1864. doi:10.1002/art.37979

## Chapter 3

**Diet-induced obesity leads to behavioral indicators of pain preceding structural joint degeneration in wild-type mice.**

Chapter 3 is authored by Kerr, G.J, To, B., White, I., Millecamps, M., Beier, F., Stone, L.S., and Séguin, C.A. and is entitled “Diet-induced obesity leads to behavioral indicators of pain preceding structural joint damage in wild-type mice”. This study is in preparation for submission.

### 3 Diet-induced obesity leads to behavioral indicators of pain preceding structural joint degeneration in wild-type mice.

#### 3.1 Co-authorship Statement

G.J. Kerr performed most of the experiments, contributed to study design and wrote the manuscript. I. White assisted with scoring the tail suspension (**Figure 3.2**) and cold sensitivity assay (**Figure 3.3**). B. To conducted all histological and histomorphometry analysis on the knee joints and G. J. Kerr assisted with histopathological scoring. (**Figure 3.5**). I. White assisted with sectioning, staining and analysis of spinal cord sections (**Figure 3.6**). Manuscript was written by G.J. Kerr with suggestions from Dr. C.A. Séguin.

## 3.2 Chapter Summary

**Introduction:** Obesity is one of the largest modifiable risk factors for the development of musculoskeletal diseases, including intervertebral disc (IVD) degeneration and back pain. Despite the clinical association, no studies have directly assessed whether diet-induced obesity accelerates IVD degeneration, back pain, or investigated the biological mediators underlying this association. In this study we examine the effects of chronic consumption of a high-fat or high-fat/high-sugar (western) diet on the IVD and pain-associated outcomes.

**Methods:** Male C57BL/6N mice were randomized into one of three diet groups (chow control; high-fat; high-fat, high-sugar western diet) at 10-weeks of age and remained on the diet for 12, 24 or 40 weeks. At endpoint, animals were assessed for behavioral indicators of pain, joint tissues were collected for histological and molecular analysis, and IBA-1, GFAP and CGRP were measured in spinal cords by immunohistochemistry .

**Results:** Animals fed obesogenic (high-fat or western) diets showed behavioral indicators of pain beginning at 12 weeks and persisting up to 40 weeks of diet consumption. Histological indicators of joint degeneration were not detected in the IVD or knee until 40 weeks on the experimental diets. Mice fed the obesogenic diets showed increased intradiscal expression of inflammatory cytokines and circulating levels of MCP-1 compared to control. Linear regression modeling demonstrated that age and diet were both significant predictors of most pain-related behavioral outcomes, but not histopathological joint degeneration.

**Conclusion:** Diet-induced obesity accelerates IVD degeneration and knee OA in mice; however, pain-related behaviors precede and are independent of histopathological structural damage. These findings contribute to understanding the source of obesity-related back pain and the contribution of structural IVD degeneration.

### 3.3 Introduction

Obesity – traditionally defined as a body mass index over 30 – is a worldwide epidemic. Obesity substantially increases the risk of developing metabolic, cardiovascular, neurological and musculoskeletal diseases<sup>1</sup>, and with the prevalence nearly tripling over the last 30 years<sup>1</sup>, it poses a large public health concern. Obesity decreases both life expectancy<sup>2</sup> and quality of life, and is associated with increased disability, mental illness and unemployment<sup>1,3</sup>. A significant contributor to obesity-induced disability is low back pain (LBP)<sup>4,5</sup>, which is the single most common cause of long-term pain and disability worldwide<sup>6</sup>. Despite efforts to improve the clinical management of LBP, treatments are limited to symptomatic relief, often without treating the underlying cause of the pain<sup>7</sup>. This is largely due to an incomplete understanding of the tissues and pathways involved in the initiation and progression of LBP. While several tissues appear to be involved in LBP, including the paraspinal muscles, ligaments, and facet joints<sup>8-10</sup>, degeneration of the fibrocartilaginous intervertebral disc (IVD) is believed to be the major contributor to pain in an approximately 40% of cases<sup>8</sup>.

Despite the clinical associations between LBP, IVD degeneration, and obesity, the underlying mechanisms and biological pathways responsible remain unknown. One contributing factor appears to be increased mechanical loading. Excess weight alters the

mechanical load experienced by the IVD<sup>11</sup>, a known regulator of IVD cellular function<sup>12,13</sup>. Increased body weight is associated with indices of lumbar disc degeneration including disc space narrowing and decreased lumbar disc signal intensity detected by MRI<sup>14,15</sup>. In articular cartilage, excess weight and altered mechanical loading has also been suggested to contribute to osteoarthritis (OA)<sup>16</sup>, a degenerative musculoskeletal disease with many similarities to IVD degeneration<sup>17</sup>. Of note, increased mechanical load alone does not account for the association between obesity and OA, as obese individuals also present more frequently with OA in non-weight bearing joints, such as the hand<sup>18</sup>.

In addition to increased mechanical load, metabolic abnormalities associated with obesity impact musculoskeletal health<sup>19,20</sup>. Obesity is associated with chronic metabolic disorders including hypertension, diabetes mellitus and dyslipidemia, collectively known as metabolic syndrome<sup>21</sup>. In the context of OA, it is postulated that each component of metabolic syndrome may independently contribute to disease progression, as comprehensively reviewed by Zhuo et al.<sup>22</sup> Specifically, alterations in the release of systemic factors (inflammatory cytokines, adipokines), nutrient exchange, advanced glycation end-products (AGEs) levels and glucose/lipid metabolism are believed to be major contributors to OA progression<sup>19,22</sup>. Studies from multiple groups have demonstrated using mouse models that obesity induced by a high-fat diet accelerates the progression of both age- and surgically-induced knee OA<sup>23-27</sup>, accompanied by behavioral indicators of pain<sup>23</sup>. Aside from its role in energy storage, adipose tissue is also a major endocrine organ and has been shown to secrete hormones termed adipokines (e.g. leptin, adiponectin, visfatin, resistin) and inflammatory cytokines (e.g. TNF- $\alpha$ , IL-6, TGF- $\beta$ )<sup>28</sup>. Studies investigating the role of adipokines have highlighted their importance in obesity-associated

pathologies. For example, leptin-deficient mice become obese yet they do not develop knee OA, suggesting leptin may play a key role in obesity-induced OA<sup>29</sup>. In the IVD, exposure of NP cells to adipokines, such as leptin and resistin, promotes catabolic metabolism associated with increased expression of matrix remodeling enzymes such as MMP and ADAMTS genes<sup>30,31</sup>. Adipokines also appear to play a role systemically as modulators of pain sensitivity<sup>32</sup>. In addition to back pain, obese individuals are more likely to develop chronic pain conditions such as fibromyalgia, headaches and abdominal pain<sup>33</sup>. While the underlying mechanisms linking obesity and chronic pain remains unknown, it has been suggested that systemic immune and endocrine alterations play a role in the altered pain response<sup>34</sup>. This systemic modulation of pain may contribute to LBP in addition to structural alterations and local inflammation within the IVD itself.

While there is extensive clinical evidence supporting the association between obesity, LBP and IVD degeneration<sup>35,36</sup>, no studies have directly assessed whether diet-induced obesity accelerates IVD degeneration, back pain, or investigated biological mediators underlying this association. The current study was designed to investigate whether chronic consumption of a high-fat or high-fat, high-sugar western diet alters the progression of age-related IVD degeneration or back pain using the mouse as a model.

## 3.4 Methods

### 3.4.1 Mice and Diets

Wild-type, male, C57BL/6N (Charles River: Wilmington, MA, USA) mice were used. Mice were fed standard chow (Envigo 2018) after weaning and randomized at 10-weeks of age into one of three diet groups (n=9-16 mice/group; **Table 3.3, Supplementary Table**

1) based on previous reports of obesity and metabolic derangement in mice<sup>26,37</sup>: high-fat diet (60% kcal fat, 21% kcal carbohydrate; Envigo TD.06414), western diet (45% kcal fat, 41% kcal carbohydrate; Envigo TD.10885), or standard chow (18% kcal fat, 58% kcal carbohydrate). Mice remained on the experimental diets until sacrifice at 5, 8 or 11.5 months-of-age (12-, 24-, 40-weeks on diet, respectively). Mice were housed in standard cages and maintained on a 12 hr light/dark cycle, with food and water consumed *ad libitum*; food consumption and body weight were measured weekly. All aspects of this study were conducted in accordance with the policies and guidelines set forth by the Canadian Council on Animal Care and were approved by the Animal Use Subcommittee of the University of Western Ontario (protocol 2017-154; **Appendix B**).

### 3.4.2 Characterization of pain-associated behavior

Behavioral analysis was conducted on mice following 12-, 24-, or 40-weeks on experimental or control diets. Behavioral studies were preceded by a two-week habituation to the neurobehavioral testing facility, and mice were habituated to all tests one week prior to data collection. On data collection days, animals were habituated to the testing room for 1 h before test start. To avoid confounding variables associated with the diurnal cycle, all behavioral assessments were conducted between 8 and 11 AM.

#### 3.4.2.1 Stretch induced axial discomfort

Stretch-induced axial discomfort was measured using the tail suspension test and grip force during axial stretch, as described previously<sup>38-40</sup>. For the tail suspension test, spontaneous reaction to gravity-induced stretch was assessed in mice suspended by the base of their tails



for 180 s. Two observers blinded to the experimental groups independently scored the duration of time spent by mice in immobility, full extension, rearing, or self-supporting using ANY-maze software (Stoelting Co.: Wood Dale, IL). Voluntary activity was quantified for 5 min immediately before (pre) and after (post) tail suspension using open field activity monitors (AccuScan Instruments, Omnitech Electronic: Columbus, OH), to quantify movement-evoked discomfort. The difference in total distance between the two open-field sessions (post - pre) was calculated for each mouse.

For the grip force assay, mice were positioned to grab onto a metal bar attached to a grip force meter (Stoelting Co.: Wood Dale, IL), and then gently pulled back by their tails to exert axial stretch. Tolerance was assessed by measuring the grip strength, in grams, for each mouse at the point of release averaged over 3 trials.

#### 3.4.2.2 Hind limb sensitivity to mechanical and cold stimuli

Mechanical sensitivity was measured through application of calibrated Von Frey filaments (Stoelting Co.: Wood Dale, IL) to the plantar surface of the hind paw for 3 s or withdrawal. 50% withdrawal threshold was calculated using the Chaplan up-down method<sup>41</sup>. The stimulus intensity ranged from 0.07-6.0 g, beginning with a stimulus intensity of 1.4 g. Cold sensitivity was assessed by measuring the total time spent by mice in behavior evoked by evaporative cooling of acetone (flicking, stamping or licking of ventral surface of the paw) during the first 40 s following application of 50  $\mu$ L acetone to the ventral surface of the hind paw. The test was carried out twice for each paw, with at least 5 min recovery between each test. Times were then averaged between paws.

### 3.4.2.3 Spontaneous activity

Voluntary locomotor activity was assessed using open field activity monitors (AccuScan Instruments, Omnitech Electronic: Columbus, OH). Mice were placed into individual boxes and their activity was monitored over 2 h. This was repeated for 3 consecutive days and values were averaged for each mouse.

### 3.4.3 Micro-computed tomography (Micro-CT)

Forty-eight hours before sacrifice,  $\mu$ CT imaging was performed using a cone-beam imaging system (eXplore SpeCZT scanner, GE Healthcare Biosciences: London, CAN). For imaging, mice were anesthetized using 2-3% inhaled isoflurane (CA2L9100, Baxter: Mississauga, CAN) infused with oxygen at a flow rate of 1.0 mL/min. To maintain sedation, a nose cone apparatus was used to administer 1.75% inhaled isoflurane for 20 min while scanning was performed. During a single 5 min rotation of the gantry, 900 X-ray projections were acquired (peak voltage of 90 kVp, peak tube current of 40 mA, and integration time of 16 ms). A calibrating phantom composed of air, water, and cortical bone-mimicking epoxy (SB3; Gammex, Middleton WI, USA) was included in each scan. Data were reconstructed into 3D volumes with an isotropic voxel spacing of 50  $\mu$ m and scaled into Hounsfield units (HU). Using MicroView software (GE Healthcare Biosciences) three signal-intensity thresholds (-200, -30, and 190 HU) were used to classify each voxel as adipose, lean, or skeletal tissue, respectively. Custom software was used to calculate tissue masses from assumed densities of 0.95 (adipose), 1.05 (lean), and 1.92 (skeletal) g/cm<sup>3</sup>, as previously reported <sup>42</sup>.

### 3.4.4 Histological analysis

Intact lumbar spine segments (L1-S1) and knees were isolated, fixed, decalcified and paraffin embedded, as previously described<sup>43</sup>. Spines were sectioned sagittally, and knees were sectioned coronally at a thickness of 5  $\mu\text{m}$  using a microtome (Leica Microsystems: Wetzlar, DEU). Lumbar spines were stained using a 0.1% Safranin-O/0.05% Fast Green. Knees were stained with either 0.1% Safranin-O/0.05% Fast Green or 0.04% Toluidine Blue. Sections were imaged on a Leica DM1000 microscope, with Leica Application Suite (Leica Microsystems: Wetzlar, DEU).

To evaluate IVD degeneration, spine sections were scored by 2 independent scorers using the modified Boos system<sup>44</sup>. Knee joint health was assessed using the murine Osteoarthritis Research Society International (OARSI) histopathological scale<sup>45</sup>. Articular surfaces of the medial femoral condyle (MFC), medial tibial plateau (MTP), lateral femoral condyle (LFC) and lateral tibial plateau (LTP), were scored by two blinded observers and averaged. For each knee joint surface, scores from 10 serial sections spanning 500  $\mu\text{m}$  of the joint were summed to represent OARSI score for each quadrant. Total scores from each of the four quadrants were then added together to generate whole joint OARSI score. Thickness of articular cartilage of the MTP and LTP was quantified using the OsteoMeasure7 Program (v.4.2.0.1, OsteoMetrics Inc., Decatur, GA, USA). Articular cartilage thickness within each quadrant was averaged using three serial sections spanning 150  $\mu\text{m}$  of the weight-bearing region of the knee. Using the same histomorphometry system, trabecular bone area was calculated by measuring the total surface area of the bone between the articular cartilage

and growth plate and subtracting the area of bone marrow. Measurements were taken for both medial and lateral compartments of the joint and averaged from 3 serial sections.

### 3.4.5 Gene expression analysis

Thoracic IVDs (4-5 per mouse; 5-8 mice per diet/per timepoint) were isolated by microdissection, placed in TRIzol reagent (Thermo Fisher Canada: Mississauga, ON, CAN) and homogenized using a PRO250 tissue homogenizer (PRO Scientific: Oxford, CT, USA). RNA was extracted according to manufacturer's instructions, quantified using a NanoDrop 2000 spectrophotometer (Thermo Fisher Canada: Mississauga, ON, CAN), and 0.5 µg was reverse transcribed into complementary DNA (cDNA) (iScript; Bio-Rad Laboratories (Canada): Mississauga, ON, CAN). Gene expression was assessed by real-time PCR using a Bio-Rad CFX384 instrument. PCR analyses were run in triplicate using 120 ng of cDNA per reaction and 310 nM forward and reverse primers with 2x SsoFast EvaGreen Supermix (Bio-Rad Laboratories (Canada): Mississauga, ON, CAN) using optimized PCR parameters and primers (**Table 3.4, Supplementary Table 2**). Primers were designed and validated to have efficiency values between 90 and 120%. Transcript levels were calculated relative to a 6-point standard curve made from pooled cDNA generated from murine IVD explants treated with lipopolysaccharide for 4 days (50 mg/mL; Thermo Fisher Canada: Mississauga, ON, CAN).

### 3.4.6 Immunohistochemistry

The intact spinal cord was removed, dissected to separate the upper (L1-L2) and lower (L3-L6) segments of the lumbar enlargement, and fixed in 4% paraformaldehyde (PFA) for 24

h at 4°. Tissues were cryoprotected for 4 days in 10% sucrose and embedded in optimal cutting temperature compound (Tissue-Tek O.C.T; Sakura Finetek US: Torrance, CA, USA) and stored at -20°C. Tissues were sectioned on a cryostat (Leica Microsystems: Wetzlar, DEU) in the transverse plane at a thickness of 14 µm, thaw mounted onto gelatin-coated slides, and stored at -80°C.

Slides were brought to room temperature, washed twice in PBS and blocked using 5% donkey serum, 0.1% Triton X-100 in PBS for 2h at room temperature. Sections were incubated overnight in a humidified chamber at 4°C in 5% donkey serum in PBS (with 0.1% Triton-X) containing primary antibodies directed against glial fibrillary acidic protein (GFAP) (1:500; G3893, Sigma-Aldrich: St. Louis, MO, USA), ionized calcium binding adaptor molecule 1 (IBA-1) (1:1000; AB-10341, Abcam: Cambridge, UK), or calcitonin gene-related peptide (CGRP) (1:750; BML-CA1137, Enzo Biochem: New York, NY, USA). Slides were rinsed 3 x 10 min in PBS-T (PBS + 0.01% Triton X-100) and then incubated for 45 min at room temperature with secondary antibodies diluted 1:500 in PBS: Alexa Fluor 488 conjugated donkey anti-mouse IgG for GFAP (A-21202, Thermofisher: Waltham, MA, USA); Alexa Fluor 594 conjugated donkey anti-rabbit IgG for Iba-1 (A-21207, Thermofisher: Waltham, MA, USA); or Alexa Fluor 488 donkey anti-sheep IgG for CGRP (A-11015, Thermofisher: Waltham, MA, USA). Slides were rinsed 3 x 10 min in PBS, dipped in deionized water, and cover slips mounted using Fluoroshield Mounting Medium with 4',6-diamidino-2-phenylindole to visualize nuclei (ab104139, Abcam: Cambridge, UK). Tissue sections were imaged using a Leica Microsystems DMI6000B fluorescence microscope and DFC360FX camera with Leica Advanced Application Suite software (Version 2.7.0-9329, Leica Microsystems: Wetzlar, DEU). A region of interest

(ROI) was manually defined to contain lamellae 1-4 of the spinal cord dorsal horn using ImageJ software. The dorsal horn was differentiated from surrounding white matter based on brightfield images. Integrated density of fluorescence within the ROI was used to quantify astrocyte/microglia density, and CGRP-immunoreactivity.

### 3.4.7 Serum analysis by Multiplex Assay

At euthanasia, blood was obtained by cardiac puncture, coagulated for 30 min at room temperature, and centrifuged at 3 000 rpm for 10 min at 4°C to collect serum. Serum (n=5-6 mice per diet/per timepoint) was diluted 2-fold in DPBS and analyzed using the Luminex™ 200 system (Luminex, Austin, TX, USA) by Eve Technologies Corp. (Calgary, Alberta). Thirty-two markers were simultaneously measured in each serum sample using the MILLIPLEX Mouse Cytokine/Chemokine 32-plex kit (Millipore, St. Charles, MO, USA) according to the manufacturer's protocol. The multiplex assay quantified Eotaxin, G-CSF, GM-CSF, IFN $\gamma$ , IL-1 $\alpha$ , IL-1 $\beta$ , IL-2, IL-3, IL-4, IL-5, IL-6, IL-7, IL-9, IL-10, IL-12 (p40), IL-12 (p70), IL-13, IL-15, IL-17, IP-10, KC, LIF, LIX, MCP-1, M-CSF, MIG, MIP-1 $\alpha$ , MIP-1 $\beta$ , MIP-2, RANTES, TNF $\alpha$ , and VEGF. The assay sensitivities range from 0.3 – 30.6 pg/mL for the 32-plex.

### 3.4.8 Statistical Analysis

For all assays except histopathological scoring of the joints, outcome measures for mice within each time point were compared between the different diet groups by one-way ANOVA with Tukey's multiple comparisons test. For histopathological analysis, within each timepoint scores for mice were compared between the different diet groups by non-

parametric Kruskal-Wallis test with Dunn's multiple comparison test.  $P < 0.05$  was considered significant. Statistical analysis was conducted using GraphPad Prism 8 (Graphpad Software: San Diego, CA, USA).

To assess the effect of diet, adiposity, knee OA and IVD degeneration on behavioral, molecular, and histological changes assessed, bivariate and multivariate linear regression models were used to identify which variables remained independently associated with the other outcomes. Bivariate and multivariate modelling was conducted using STATA 16 (StataCorp LLC: College Station, TX, USA).

## 3.5 Results

### 3.5.1 Weights and adiposity

As expected, following 12, 24- and 40-weeks mice fed the high-fat and western diets showed a significant increase in body mass and weight gain compared to age-matched chow fed controls (**Figure 3.1A**). Analysis of body composition by micro-CT (**Figure 3.1B**) demonstrated that the increase in adiposity in mice fed the experimental diets was accompanied by a significant decrease in the percentage of both lean and skeletal tissues at all time points (**Figure 3.1C**). This analysis also showed a significant increase in overall bone mineral density (BMD) in mice fed the high-fat diet at all timepoints, and at the 24- and 40-week timepoints for mice fed the western diet, compared to age-matched chow fed controls (**Figure 3.1C**).

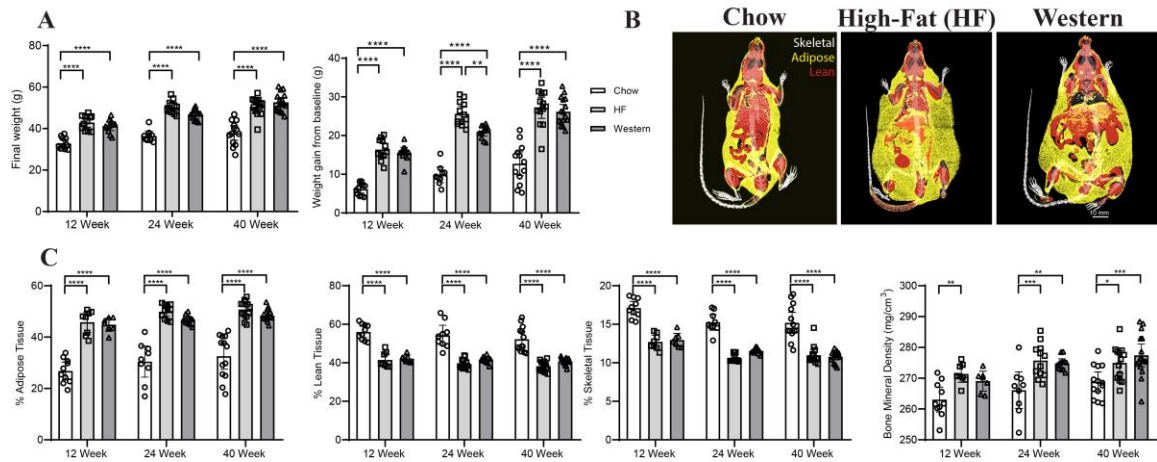


**Figure 3.1: Chronic consumption of high-fat and western diets increases adiposity and bone mineral density in C57BL/6N mice.**

(A) At all timepoints, mice fed the high-fat and western diets showed significant increases in overall weight and in weight-gain from baseline compared to age-matched chow fed controls. (B) Representative reconstructed micro-CT images of mice following 40-weeks of experimental diets. Isotropic surface-rendering of skeletal tissue (indicated in white) is overlaid with a mid-coronal slice where lean tissue is indicated in red and adipose tissue is indicated in yellow. (C) Quantitative micro-CT analysis of whole-body composition showed a significant increase in adiposity and significant decreases in both percentage of lean and skeletal and in mice fed the high-fat and western diet mice compared to age-matched chow fed controls at all time points. A significant increase was also seen in bone mineral density in mice following consumption of the high-fat and western diets at the 24- and 40-week timepoints.  $n=9-16$  mice per timepoint, per diet. Data are displayed as mean  $\pm$  95% CI; data points for each mouse are graphed within each group. \* $P<0.05$ , \*\* $P<0.01$ , \*\*\* $P<0.001$ , \*\*\*\* $P<0.0001$  by 2-way ANOVA.



### 3.5.2 Behavioral indicators of axial discomfort

We first investigated whether mice fed the high-fat or western diet showed behavioral indicators of stretch-induced axial discomfort using three complimentary assays established as indicators of discogenic back pain in a mouse model of degeneration<sup>40</sup>: behavior during tail suspension, changes in spontaneous activity after tail suspension, and tolerance to axial stretching in the grip force assay. In the tail suspension test, no significant differences were observed between diet groups at any time point investigated (**Figure 3.2A**). Similarly, changes in spontaneously activity induced by the tail suspension assay (locomotion pre versus post tail suspension) were not altered between experimental diet groups and age-matched chow fed controls (**Figure 3.2B**). Grip force during axial stretch was reduced in mice fed the high-fat diet compared to age-matched chow fed controls at 12- and 40-weeks and in mice fed the western diet at all time points compared to control (**Figure 3.2C**), suggesting decrease tolerance to axial stretch.

### 3.5.3 Behavioral indicators of mechanical and cold sensitivity

Mechanical and cold sensitivity were assessed in the hind paw using the Von Frey assay and by measuring the response of mice to the evaporative cooling of acetone, respectively. Mice fed the western diet showed a significant increase in mechanical sensitivity at the 24- and 40-week time points compared to age-matched chow fed controls, while mice fed a high-fat diet showed a significant increase in sensitivity only at the 24-week timepoint compared to controls (**Figure 3.3A**). In contrast, no significant difference was observed in sensitivity to cold between mice in either experimental diet group compared to age-matched chow fed controls at any time point (**Figure 3.3B**).

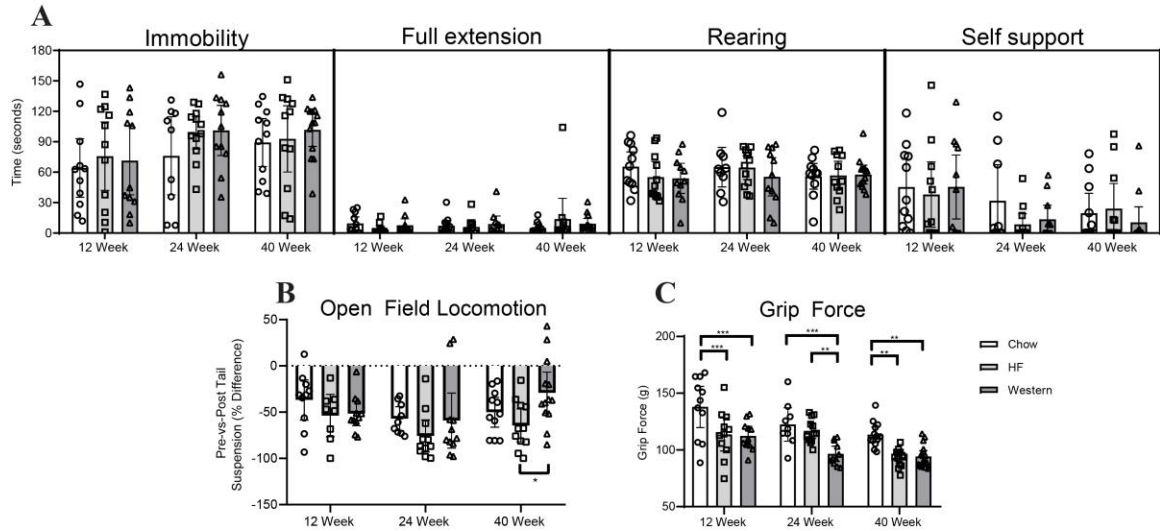


**Figure 3.2: Obesity induced by the high-fat and western diets reduces grip strength but does not alter behavior in tail suspension.**

(A) During tail suspension, the duration of time spent by mice immobile, in full extension, rearing or self-supported was quantified. No significant differences were detected between diet groups at any of the time points assessed. (B) Stretch-evoked discomfort was assessed using the open field assay, in which the total distance covered in 5 min immediately before (pre) and after (post) the 3 min tail suspension assay was quantified. Obesity induced by the high-fat and western diets did not alter behavior of mice in open field compared to age-matched chow fed controls at any of the time points assessed. However, a significant difference was seen between mice fed a high-fat and western diet at the 40-week timepoint. (C) Grip force during axial stretch was reduced in obese mice. Mice fed the high-fat diet showed a significant decrease in grip force at the 12- and 40-week time points compared to age-matched chow fed controls. Mice fed the western diet showed a significant decrease in grip force compared to age-matched chow-fed controls at all time points.  $n=9-16$  animals per timepoint, per diet. Data are plotted mean  $\pm$  95% CI; data points for each mouse are graphed within each group. \* $P<0.05$ , \*\* $P<0.01$ , \*\*\* $P<0.001$  by 2-way ANOVA.

### 3.5.4 Spontaneous locomotion

Behavior and locomotion in open field was assessed for all mice over a 2 h period. Mice fed the western diet showed a significant decrease in total distance travelled following 12 and 24 weeks compared to age-matched chow fed controls. Mice fed the high-fat diet showed a significant reduction in locomotion following 24-weeks compared to age-matched controls (**Figure 3.3C**). The number of rearing events was also significantly decreased in mice fed the high-fat and western diets at the 40-week time point compared to age-matched chow fed controls (**Figure 3.3C**).

### 3.5.5 Assessment of IVD degeneration

The effects of the high-fat and western diets on IVD health were assessed using both histopathological evaluation and molecular analysis (**Figure 3.4**). On average, no overt differences were detected in the histological appearance of lumbar IVDs between mice fed either the high-fat or western diet for 12- and 24-weeks compared to age-matched chow fed controls (**Figure 3.4A**). Accordingly, histopathological scoring using the modified Boos system showed no significant differences in degeneration between the groups. However, when data was analyzed by individual spinal level, mice fed the western diet showed significantly lower scores than their high-fat or chow fed counterparts at the L6S1 spinal level at the 12-week timepoint (**Figure 3.4B**). Following 40 weeks on the experimental diets, an accumulation of hypertrophic cells surrounded by a glycosaminoglycan-rich pericellular matrix was consistently detected in the inner annulus fibrosus of mice fed both the high-fat and western diets, but not in age-matched chow fed control mice (**Figure 3.4A** – black arrows). Despite this observation, histopathological

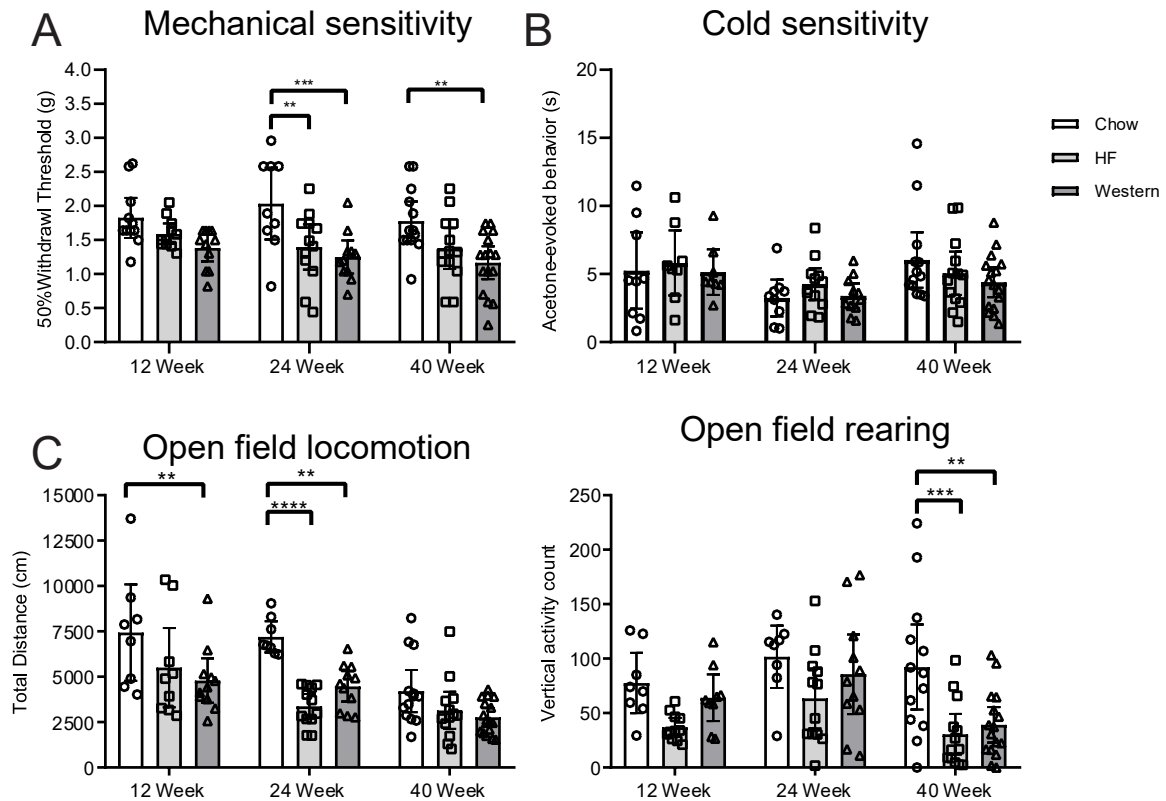


**Figure 3.3: Obesity induced by a high-fat and western diet increases sensitivity to mechanical stimulation and alters spontaneous locomotion.**

(A) Mechanical Sensitivity of the hind paw was assessed by manual application of Von Frey filaments using the Chaplin up-down method. Mice fed the western diet showed a significant decrease in withdrawal threshold at the 24- and 40-week time points compared to age-matched chow fed controls, indicative of increased mechanical sensitivity. Mice fed a high-fat diet showed a significant decrease in withdrawal threshold at the 24-week timepoint compared to control. (B) Sensitivity to cold was assessed by measuring the time spent in behavior evoked by evaporative cooling of acetone (flicking, stamping or licking of ventral surface of the paw) during the first 40s following application of acetone to the ventral surface of the hind paw. No significant differences were seen between the diet groups at any timepoint. (C) Spontaneous locomotor activity was recorded over three 2 hr sessions and averaged. Mice fed the western diet showed a significant decrease in the total distance travelled at the 12- and 24-week timepoint compared to age-matched chow fed controls, while mice fed the high-fat diet showed a decrease at the 24-week timepoint. The number of rearing events was significantly decreased in mice fed the high-fat and western diets compared to controls at the 40-week timepoint.  $n=9-16$  animals per timepoint, per diet. Data are plotted mean  $\pm$  95% CI; data points for each mouse are graphed within each group. \* $P<0.05$ , \*\* $P<0.01$ , \*\*\* $P<0.001$ , \*\*\*\* $P<0.0001$  by 2-way ANOVA.

scoring revealed no significant degeneration in the diet groups compared to chow fed controls at the 40-week time point (**Figure 3.4B**). Histopathological analysis was paired with qPCR to quantify expression of markers of inflammation, neural ingrowth, and matrix degrading enzymes in thoracic IVDs to further investigate molecular changes associated with diet-induced obesity. Mice fed the high-fat or western diets showed no significant differences in the expression of the genes investigated at the 12-week timepoint compared to age-matched chow fed controls (**Figure 3.4C**). Mice fed the high-fat diet showed no significant differences in gene expression compared to chow fed controls at the 24-week timepoint for any of the genes investigated. At the 40-week timepoint, mice fed the high-fat diet showed increased expression of inflammatory mediators (*Il-6*, *Ptgs2*), neurotrophins (*Bdnf*), as well as matrix degrading enzymes (*Adamts5*) compared to age-matched chow fed controls (**Figure 3.4C**). Mice fed the western diet showed increased expression of the inflammatory mediators *Il-1b* and *Ptgs2* compared to chow fed controls at 24 weeks; however, no significant differences in gene expression were detected at the 40-week timepoint (**Figure 3.4C**).

### 3.5.6 Assessment of degenerative changes in the knee

Since diet-induced obesity leads to other arthropathies, such as knee OA<sup>23</sup>, we investigated degenerative changes to the knee joint as a potential contributor to the pain-related behavioral outcomes we assessed. We focused this analysis on the 24- and 40-week timepoints where changes in behavioral measures were most consistently identified. No overt histological differences were detected in the knee joints of mice fed either the high-fat or western diet for 24 weeks compared to age-matched chow fed controls (**Figure**

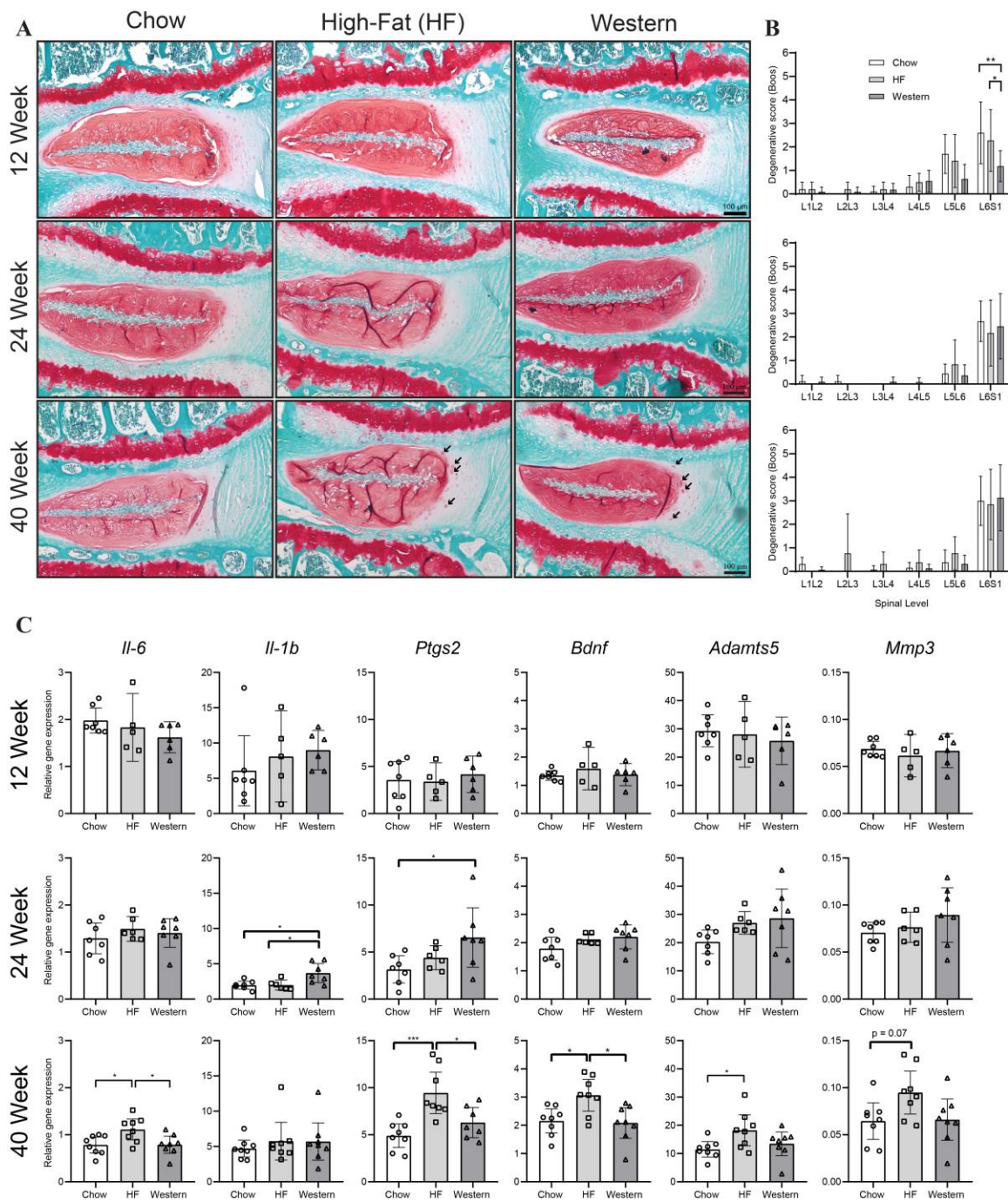


**Figure 3.4: Effect of diet-induced obesity on the intervertebral disc.**

(A) Representative histological sections of the L6/S1 spinal level of the lumbar spine stained with safranin-o/fast green from mice fed control chow, high-fat, or western diet for 12, 24, or 40 weeks. The accumulation of hypertrophic cells was detected within the inner annulus fibrosus of mice fed the high-fat and western diets for 40 weeks (highlighted by black arrows). (B) Evaluation of the grade of histopathological IVD degeneration using the modified Boos scoring system showed no significant differences between mice fed the control chow, high-fat or western diets at the 24- and 40-week timepoints. At the 12-week timepoint, mice fed the western diet showed a significant decrease in the degenerative score compared to mice fed chow and high-fat diets. n=9-16 animals per timepoint, per diet. Data are analyzed by Kruskal-Wallis test. (C) SYBR-based qPCR of intact thoracic intervertebral discs showed no significant difference between mice fed a chow, high-fat or western diet at the 12-week timepoint for any genes investigated. At the 24-week timepoint, significant increases in *Il-1b* and *Ptgs2* expression were seen in mice fed the western diet compared to control. By 40-weeks, significant increases in *Il-6*, *Ptgs2*, *Bdnf* and *Adamts5* expression were seen in mice fed the high-fat diet compared to control. n=5-8 animals per diet/per timepoint. Analyzed by one-way ANOVA. All data are plotted mean  $\pm$  95% CI; data points for each mouse are graphed within each group. \*P<0.05, \*\*\*P<0.001.

**3.5A**). Histopathological scoring using the OARSI system supported these observations (**Figure 3.5B**). At the 40-week timepoint, mice fed the western diet showed decreased proteoglycan staining in the medial femoral condyle (MFC) compared to age-matched controls (**Figure 3.5A**), resulting in significantly higher OARSI scores (**Figure 3.5B**) indicating early signs of osteoarthritis. However, no significant differences were seen in the other compartments of the knee joint or in the cumulative OARSI scores for the whole joint. In addition to histopathological analysis, cartilage thickness was measured by histomorphometry. Although no significant differences in cartilage thickness were detected in mice following 24 weeks on the experimental diets, mice fed the high-fat diet for 40 weeks showed a significant decrease in cartilage thickness specific to the lateral femoral condyle compared to age-matched chow fed controls (**Figure 3.5C**). Histomorphometry was similarly used to measure the relative surface area of trabecular bone between the articular cartilage and growth plate. Mice fed the western diet for 40 weeks showed a significant increase in subchondral trabecular bone compared to age-matched chow fed controls specifically in the medial tibial plateau (**Figure 3.5D**), suggesting sclerosis of the subchondral bone.

### 3.5.7 Analysis of sensory neuroplasticity within the lumbar spinal cord

To assess neuroplastic changes associated with neuroinflammation and chronic pain, lumbar spinal cords from mice at the 40-week time point were assessed for markers of astrocytes (glial fibrillary acidic protein, GFAP), microglia (ionized calcium-binding adapter molecule 1, IBA-1), and nociceptive innervation (calcitonin gene-related peptide, CGRP; **Figure 3.6A**). Although multiple mice in both the high-fat and western diet groups showed increased GFAP and IBA-1 staining in the upper and lower lumbar spinal cord



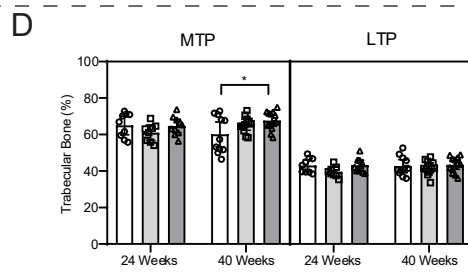
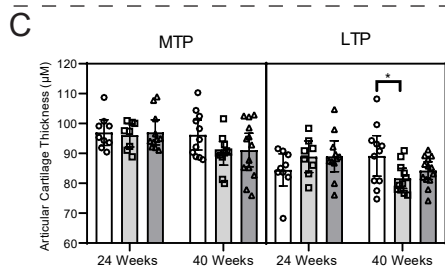
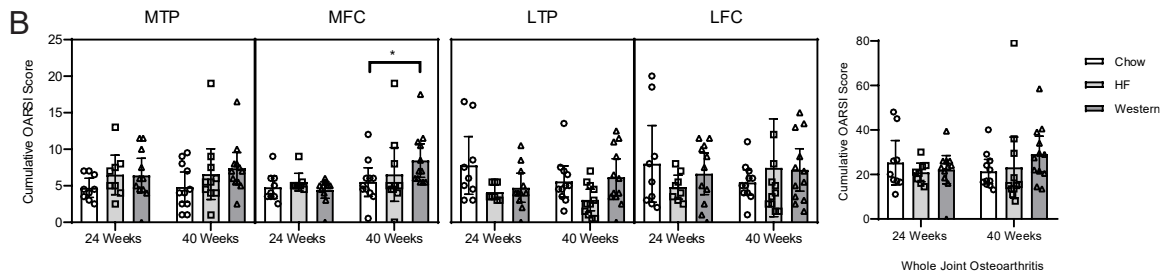
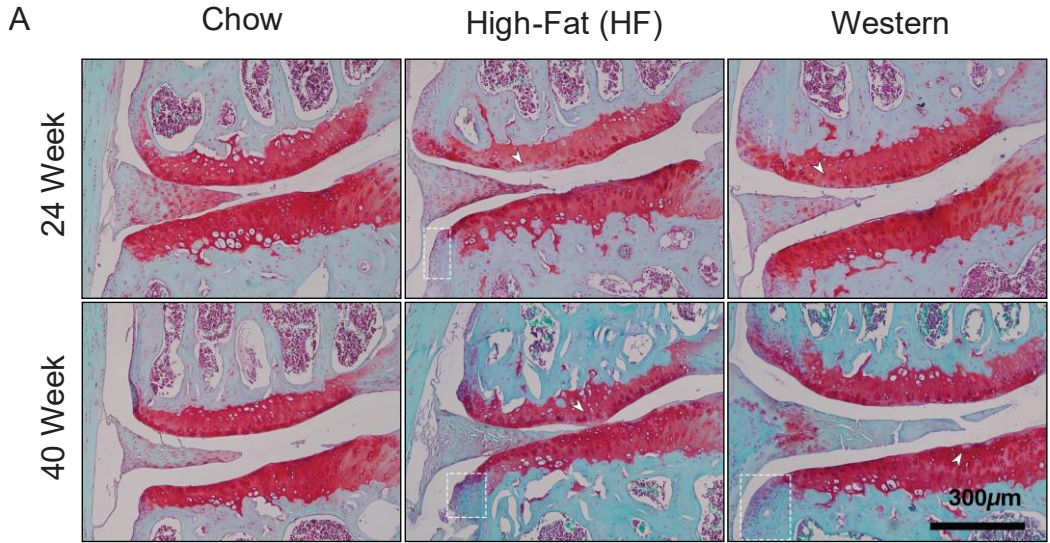


**Figure 3.5: Effect of diet-induced obesity on the knee joint.**

(A) Representative histological coronal sections of the medial knee compartment stained with safranin-o/fast green from mice fed either control chow, high-fat, or western diet for 24- or 40- weeks. Images are oriented with the medial femoral condyle (MFC) located superiorly, and the medial tibial plateau (MTP) inferiorly. White arrows indicate cartilage damage, presenting as loss of proteoglycan staining and focal fibrillation of the cartilage, and white boxes indicate osteophyte formation. (B) Histopathological grading of the knee joints using the murine Osteoarthritis Research Society International (OARSI) scale corresponding to MTP, MFC, lateral tibial plateau (LTP), and lateral femoral condyle (LFC), combined to generate the summed score for the whole joint. Mice fed the western diet for 40-weeks showed a significant increase in the degenerative score in the MFC compared to those fed the control chow. However, no difference was seen in the whole joint score between any of the groups at either timepoint. (C) Average articular cartilage thickness. After 40 weeks on the high fat diet, mice presented with decreased articular cartilage thickness on the LTP. No other differences were seen in any other joint compartment. Data analyzed by Kruskal-Wallis test. (D) Percent trabecular bone in the medial and lateral subchondral compartments of the tibia. Mice enrolled on the western diet for 40 weeks exhibited significantly more trabecular bone in the medial compartment for the tibia. n=9-16 animals per diet/per timepoint. Analyzed by one-way ANOVA. All data are plotted mean  $\pm$  95% CI, \*P<0.05.

compared to the average values for chow fed controls, quantification of fluorescent intensity within the dorsal horn showed no significant difference between diet conditions for any of the proteins investigated (**Figure 3.6B**).

### 3.5.8 Circulating inflammatory factors

Luminex xMAP multiplex assays were used to quantify a panel of 32 cytokines, chemokines, and growth factors in the serum of experimental mice. Mice fed a western diet showed increased levels of interleukin (IL)-1 $\beta$ , IL-6, IL-10, and tumor necrosis factor alpha (TNF $\alpha$ ) at the 12- and 40-week timepoints in their serum, however, no significant differences were seen when compared to chow fed control due to variability between animals (**Table 3.1**). Despite this variability, at the 40-week timepoint a significant increase in circulating monocyte chemoattractant protein 1 (MCP-1) was observed in mice fed a western diet compared to chow-fed control (**Table 3.1**). Animals fed a western diet showed for 24-weeks also showed significantly lower levels of circulating eotaxin and IL-1 $\alpha$  compared to chow fed controls, but no other differences in any of the other cytokines investigated (**Table 3.5, Supplementary Table 3**).

### 3.5.9 Linear regression analysis

To directly examine associations in the context of the observed variability within each experimental group in our study, linear regression modeling was conducted to determine whether diet, adiposity or age were predictors of behavioral, histological, or systemic outcomes (**Table 3.2**). Bivariate modelling demonstrated that both adiposity and age are independent predictors of multiple indicators of pain including stretch-induced axial discomfort (grip force), mechanical sensitivity (Von Frey assay) and spontaneous

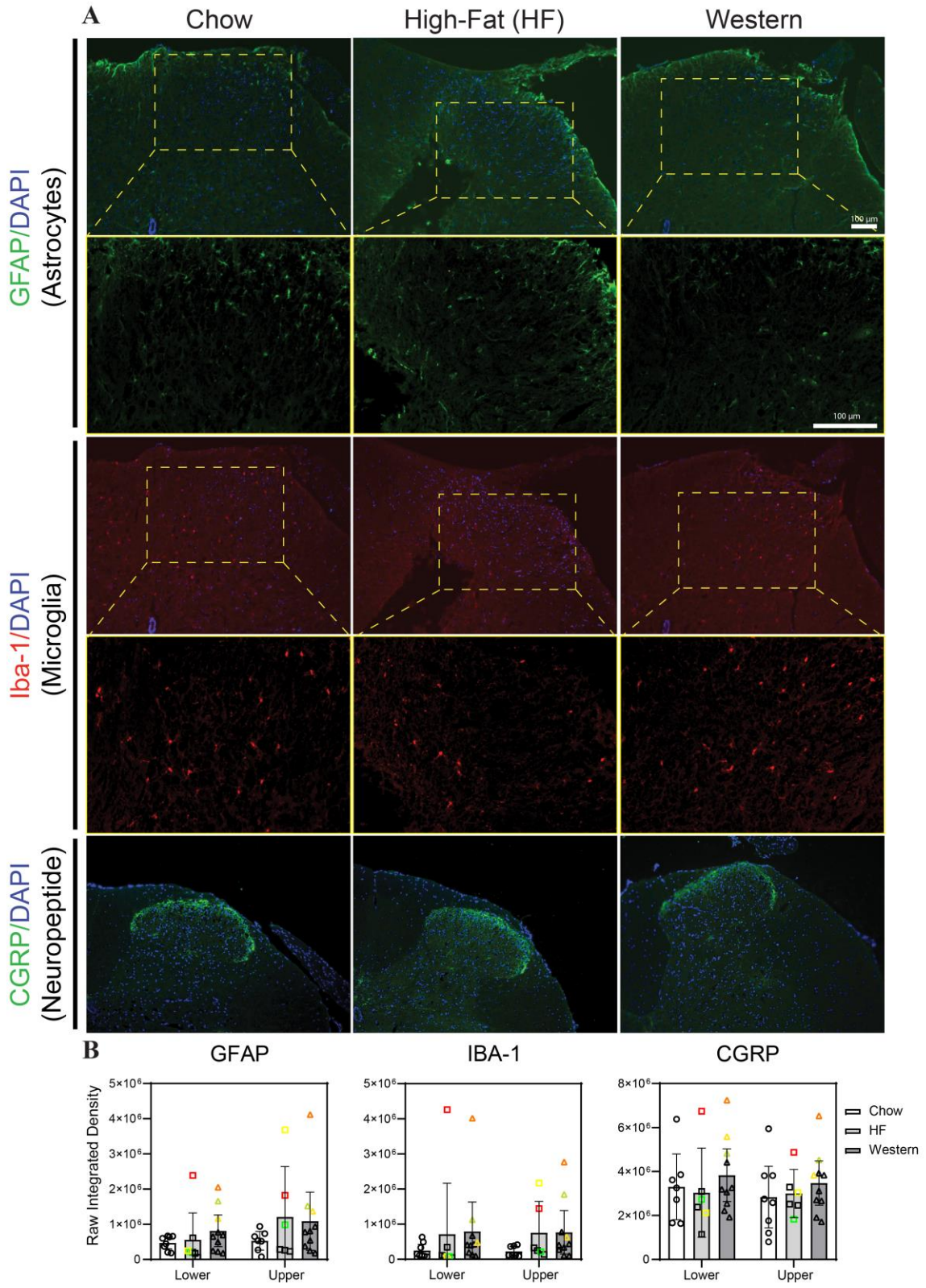


**Figure 3.6: Effect of diet-induced obesity on neuroplastic changes within the lumbar spinal cord.**

(A) Representative images showing transverse sections of the dorsal horn of the lumbar spinal cord used for immunohistochemical analysis of neuroplastic changes associated with chronic pain. Tissues were isolated from mice following 40 weeks of experimental diet. Slides were stained for glial fibrillary acidic protein (GFAP), ionized calcium-binding adapter molecule 1 (IBA1) and calcitonin gene-related peptide (CGRP). Yellow boxes indicate the region of interest for high magnification images (second row) for GFAP and IBA-1 (B) The fluorescence intensity averaged across the region of interest (lamellae 1-4 of the dorsal horn) of the upper (L1-L2) and lower (L3-L6) lumbar spinal cords. Mice fed a high-fat or western diet for 40-weeks showed no significant differences in immunoreactivity for any of the proteins investigated.  $n = 6-8$  animals/group. Individual data points of the same colour indicates the same animal. Data are plotted mean  $\pm$  95% CI.

**Table 3.1: Multiplex analysis of cytokines, chemokines and growth factors in serum.**

Analyte	12 Week				24 Week				40 Week			
	Chow	HF	Western	p-value	Chow	HF	Western	p-value	Chow	HF	Western	p-value
	n=6	n=6	n=6		n=5	n=6	n=6		n=5	n=6	n=6	
Mean (SD)	Mean (SD)	Mean (SD)	Mean (SD)	Mean (SD)	Mean (SD)	Mean (SD)	Mean (SD)	Mean (SD)	Mean (SD)	Mean (SD)	Mean (SD)	
IL-1B	13.9 (17.5)	32.3 (58.6)	39.4 (43.8)	0.54	22.5 (26.9)	15.3 (15.7)	41.1 (89.3)	0.72	2.0 (1.8)	2.0 (1.4)	6.4 (6.7)	0.16
IL-6	17.2 (14.3)	20.9 (28.1)	47.6 (67.0)	0.43	25.7 (31.9)	28.7 (35.0)	13.6 (12.2)	0.63	2.7 (3.8)	4.1 (1.9)	20.0 (30.2)	0.24
IL-10	45.8 (51.4)	56.6 (85.1)	153 (261.2)	0.47	19.0 (24.1)	17.2 (18.7)	15.1 (18.7)	0.95	0.5 (1.0)	0.4 (0.9)	2.1 (2.9)	0.25
IP-10	129.4 (53.8)	122.0 (32.4)	139.5 (38.7)	0.78	90.9 (53.2)	105.9 (43.8)	63.6 (49.5)	0.34	106 (14.3)	113.7 (24.2)	144.7 (67.9)	0.32
KC	453.4 (323.3)	690.2 (843.0)	856.0 (1324)	0.75	527.2 (363.1)	452.0 (230.1)	240.7 (108.5)	0.17	191.1 (85.0)	355.3 (223.4)	258.8 (139.5)	0.28
MCP-1	53.7 (58.7)	51.6 (46.4)	78.3 (65.6)	0.68	54.3 (23.8)	68.1 (42.3)	165.2 (259.5)	0.45	<b>13.6</b> <b>(9.6)</b>	<b>63.8</b> <b>(39.1)</b>	<b>135.3</b> <b>(93.7) *#</b>	<b>0.02*</b>
TNF $\alpha$	28.4 (31.4)	37.8 (54.2)	41.9 (35.0)	0.85	23.9 (23.6)	16.0 (22.7)	53.4 (96.2)	0.54	1.0 (1.9)	2.2 (4.1)	3.0 (5.1)	0.63
VEGF	2.2 (1.87)	6.8 (14.2)	13.1 (27.8)	0.59	2.9 (4.2)	1.5 (2.5)	1.9 (2.1)	0.73	5.4 (8.4)	2.1 (3.1)	1.0 (0.5)	0.33

Values are displayed in pg/mL and analyzed by one-way ANOVA. \* indicates significantly different from chow diet. # is significantly different from HF diet by Tukey's post-hoc test. P<0.05 is significant

whether diet, adiposity or age were predictors of behavioral, histological, or systemic outcomes (**Table 3.2**). Bivariate modelling demonstrated that both adiposity and age are independent predictors of multiple indicators of pain including stretch-induced axial discomfort (grip force), mechanical sensitivity (Von Frey assay) and spontaneous locomotion (open field). Despite their association with behavioral alterations, neither adiposity nor age were associated with measures of joint degeneration or levels of most circulating factors assessed (**Table 3.2**). Exceptions to this were TNF $\alpha$  and MCP-1, which were associated with age (bivariate), and the western diet (multivariate), respectively (**Table 3.2**). When diet, adiposity and age were accounted for, age was found to be the most robust predictor of all outcomes measured (**Table 3.2**). Aside from age, the multivariate model also showed that diet and adiposity are covariates for grip force and rearing in open field, respectively (**Table 3.2**). To determine if histopathological scores for joint damage were independently associated with behavioral indicators of pain, bivariate and multivariate regression modeling was completed. In this study, no significant association was detected between histopathological scores for IVD degeneration and pain-related behaviors. A weak but significant association was detected between histopathological scores for knee OA and grip force, but not for any of the other behavioral metrics assessed (**Table 3.6, Supplementary Table 4**).

### 3.6 Discussion

Obesity is one of the largest modifiable risk factors for the development of both IVD degeneration and associated LBP<sup>35,36</sup>, yet the biological mechanisms underlying this association are currently unknown. With the prevalence of obesity on the rise<sup>1</sup>, it is necessary to address this problem and identify underlying pathogenic mechanisms. The

**Table 3.2: Impact of diet-induced obesity and age on behavioral, molecular, and histological changes.**

Parameter	Bivariate (r)		Multivariate ( $\beta, r^2$ )				
	% Adipose	Timepoint	Diet ( $\beta$ )		% Adipose ( $\beta$ )	Timepoint ( $\beta$ )	Whole model ( $r^2$ )
			Experimental (Obesogenic)	Western			
<b>Behavioral</b>							
Grip Force	-0.41***	-0.45***	-21.96**	-6.23	0.4	-0.841**	0.45***
Mechanical Sensitivity (Von Frey)	-0.42***	-0.21*	-0.35	-0.14	-0.0007	-0.006	0.26***
Cold sensitivity (Acetone)	0.04	0.01	-	-	-	-	0.08
<u>Tail Suspension</u>							
Rearing	0.01	0.11	-	-	-	-	0.02
Immobility	0.18	0.19	-	-	-	-	0.05
Self-support	-0.22*	-0.30**	1.73	-0.46	-0.71	-0.74*	0.10*
Stretch	0.06	0.10	-	-	-	-	0.07
<u>Open Field</u>							
Locomotion	-0.49***	-0.35***	-1226	-59.3	-92.7	-93.5***	0.33***
Rearing	-0.52***	-0.40***	-0.88	-7.41	-2.87*	-2.059***	0.39***
<b>Histopathology</b>							
IVD degeneration (average Boos)	0.065	0.04	-	-	-	-	0.03
Knee OA (Cumulative OARSI)	0.07	0.08	-	-	-	-	0.05
<b>Neuroinflammation</b>							
<u>Lower spinal cord</u>							
GFAP	0.23	-	-	-	-	-	0.30
IBA-1	0.23	-	-	-	-	-	0.06
CGRP	0.024	-	-	-	-	-	0.18
<u>Upper spinal cord</u>							
GFAP	0.21	-	-	-	-	-	0.08
IBA-1	0.33	-	-	-	-	-	0.12
CGRP	0.31	-	-	-	-	-	0.18
<b>Systemic factors</b>							
IL-1B	0.04	0.21	-	-	-	-	0.12
IL-6	0.06	0.22	-	-	-	-	0.09
IL-10	0.03	0.21	-	-	-	-	0.14
IP-10	0.03	0.07	-	-	-	-	0.001
KC	0.002	0.25	-	-	-	-	0.08
MCP-1	0.23	0.04	-	-	-	-	0.18
TNF $\alpha$	0.03	0.30*	-	-	-	-	0.16
VEGF	0.01	0.12	-	-	-	-	0.06

*Note:* Experimental/ Obesogenic diets include the high-fat and western diet



current study was designed to investigate the longitudinal effects of diet-induced obesity on inflammation, IVD degeneration and pain using the mouse as a preclinical model. We show that obesity induced by both a high-fat and high-fat/high-sugar western diet led to behavioral indicators of pain in as little as 12-weeks, preceding gross structural changes to the IVD and knee joints. Following 40 weeks, changes in cellular morphology within the inner AF of the IVD were detected in mice fed both obesogenic diets compared to chow-fed controls; however, these changes were not associated with increased histopathological degeneration. Chronic consumption of the high-fat diet was associated with increased expression of *Il-6*, *Ptgs2*, *Bdnf*, *Adamts-5*, and *Mmp-3* within the IVD and a decrease in articular cartilage thickness within the lateral tibial plateau. In contrast, chronic consumption of the western diet was associated with increased expression of *Il-1b* and *Ptgs2* within the IVD, histopathological features of early OA, subchondral bone sclerosis, and increased serum MCP-1 levels. These findings highlight the complex interplay between diet, adiposity, pain, inflammation, and joint health.

Rodent models have proven useful to study IVD and joint biology since they allow insight into biological processes that regulate tissue homeostasis and degeneration. Numerous models have been described in which IVD degeneration is induced through genetic manipulation, surgical disruption, chemical injection or aberrant mechanical loading<sup>46</sup>. Although these studies contribute to understanding the cellular and molecular basis of IVD degeneration, few investigate the association with pain<sup>47</sup>. Given the discordance between structural IVD degeneration and pain development in humans<sup>10,48,49</sup>, and pre-clinical models<sup>50</sup>, it is important to investigate both pain and structural IVD degeneration and their relation to one another. Although pain cannot be directly measured in animals, several

indirect, quantitative behavioral assays have been developed to evaluate pain-like behaviors for a variety of different pain states<sup>51,52</sup>. Many of these behavioral metrics are not specific to back pain and are used to assess joint, inflammatory, and neuropathic pain<sup>53,54</sup>. Stretch-induced axial discomfort has however been established as a reliable measure of axial low back pain<sup>40</sup>. In the current study, mice fed obesogenic diets showed significant impairments in grip force at all timepoints compared to control mice, suggesting axial discomfort. In contrast, no significant difference was detected in the tail suspension assay between mice fed obesogenic diets and controls. This potentially contradictory data may be influenced by the nature of the tail suspension assay, which was originally used to test depressive behavior in mice<sup>55</sup>. In addition to musculoskeletal pathologies, obesity is also associated with depression<sup>33</sup>. In fact, recent studies demonstrated that mice fed a high-fat diet for 8 weeks showed increased time immobile in tail suspension, interpreted as a characteristic of depression-like behavior<sup>56</sup>. This behavior is in contrast to both genetic and age-related mouse models of IVD degeneration and axial pain which show increased time rearing in tail suspension<sup>57,58</sup>. This confounding factor may impact the outcome of tail suspension in the diet-induced obesity model, and consequently the interpretation of our findings.

In addition to indicators of stretch-induced axial discomfort, obese mice also displayed mechanical but not thermal (cold) hypersensitivity of the hind-paw. These alterations are consistent with results seen in a model of surgically induced IVD degeneration, where intradiscal injection of PBS induced mechanical hypersensitivity in rats<sup>59</sup>. However, these results directly contrasted a genetic model of IVD degeneration, where SPARC-null mice show thermal but not mechanical hypersensitivity compared to WT control<sup>39</sup>. While the

mechanisms underlying these differences are unclear, mechanical sensitivity is common in both inflammatory and neuropathic pain models<sup>60</sup>, and different models of pain are likely to impact nociception through different pathogenic mechanisms<sup>61</sup>. Obesity also appeared to impact non-reflexive (spontaneous) pain behaviors including distanced travelled and rearing in open field. These measurements have been previously shown to be decreased in both inflammatory and neuropathic pain models<sup>62</sup>. Taken together, our findings indicate that mice fed a high-fat or western diet display pain-related behaviors starting at the 12-week timepoint and persisting until the 40-week timepoint.

Previous studies established that high-fat diet-induced obesity accelerates OA progression in mice<sup>23,26</sup>; however, pain-related behaviors were found to be independent of osteoarthritis severity<sup>23</sup>. As IVD degeneration has been associated with many of the pain-related behaviors reported for OA<sup>38</sup>, we characterized both IVD degeneration and OA-associated knee degeneration in our experimental mice to account for both as factors contributing to pain. Histopathological scoring of lumbar IVDs did not reveal significant degeneration caused by the high-fat or western diet at any timepoint. However, mice fed both obesogenic diets showed a consistent accumulation of hypertrophic-like cells in the inner annulus fibrosus at 40 weeks, suggesting early degenerative change. Moreover, increased expression of inflammatory mediators (*Il-1b*, *Il-6*, *Ptgs2*), matrix degrading enzymes (*Adamts5*) and neurotrophins (*Bdnf*) were detected in mice fed the high-fat and western diets. These inflammatory cytokines are known drivers of IVD pathogenesis associated with ECM degeneration and expression of neurogenic factors such as NGF and BDNF that can contribute to pain<sup>63</sup>. Similarly, significant histopathological degeneration in the knee was only detected at the 40-week timepoint in mice fed the western diet. Linear regression

modeling indicates that the behavioral indicators of pain assessed are independent of joint degeneration, except for the grip force assay for which knee OA was a significant predictor of impairment. Together these findings indicate that diet-induced obesity may potentially accelerate the progression of structural IVD degeneration and knee OA at the later timepoints; however, these changes are mild and are likely independent of most pain-related behaviors.

Findings from the current study suggesting that pain-related behaviors precede molecular and structural alterations in joint tissues raise questions related to the source of the pain observed. These findings are however consistent with the hypothesis that pain is multifactorial. Obesity is considered a state of chronic inflammation associated with increases in several circulating inflammatory cytokines such as TNF $\alpha$  and IL-6 in humans<sup>64</sup>. Inflammation has been shown to contribute to peripheral and central sensitization and may lead to hyperexcitability of the nervous system and chronic pain<sup>65</sup>. Consistent with these findings, we demonstrate that consumption of the western diet led to increased levels of circulating MCP-1 in mice, a pro-algesic mediator that can increase primary afferent neuron activity<sup>66,67</sup>. Obesity may also impact central pain processing; in mice consumption of a high-fat diet increases the activation of microglia<sup>68</sup> while exposure of cultured astrocytes to saturated fatty acids induces cytokine release and astrocyte inflammation<sup>69</sup>. These neuroplastic changes can contribute to central sensitization through multiple mechanisms, including increased release of inflammatory factors contributing to modulation of synaptic activity<sup>65</sup>. Although the averaged values of GFAP and IBA-1 expression in the spinal cord were not significantly different between diet groups in our study, multiple mice in both the high-fat and western diet groups showed increased

activation of both microglia and astrocytes at the 40-week timepoint. These alterations to the nociceptive pathways at either the peripheral or central level may contribute to the pain response seen. While not assessed, obesogenic diets also lead to painful diabetic neuropathy, or nerve damage, which may also contribute to the pain phenotype observed<sup>70</sup>. Given the diverse impacts of obesity, it could be postulated that obesity-related pain may arise either from hyperexcitability or damage to nociceptive pathways in conjunction with tissue damage, and these contributions may differ between animals and over time. A limitation of this study is the utility of behavioral tests used to assess pain in our model. While they serve as indicators of pain in other models, many assays used in the current study also have been used to test muscle strength<sup>71</sup> and psychiatric disorders<sup>55</sup> which may be impacted by obesity<sup>33,72</sup>. To further explore whether these behavioral responses are due to pain, future studies may wish to pharmacologically inhibit nociceptive pathways to confirm that behavioral differences are due to pain.

Although the average weight gain was similar between the two obesogenic diets evaluated in this study, important differences in outcomes were detected. Mice fed the western diet showed a more consistent pain response compared to control at all timepoints than mice fed the high-fat diet. Furthermore, at the 40-week timepoint knee osteoarthritis and increases in systemic inflammation were only seen in mice fed the western diet. These findings highlight the importance of dietary composition in the study of obesity. In the context of OA, dietary fatty acid and carbohydrate composition can significantly impact joint health<sup>24,73</sup>. Diets high in saturated fatty acids or  $\omega$ -6 polyunsaturated fatty acids (PUFAs) induce more severe metabolic dysregulation and OA progression than diets enriched with  $\omega$ -3 PUFAs<sup>24</sup>. Aside from fat, diets high in sucrose can also accelerate OA

progression independent of weight gain<sup>73</sup>. These findings may explain our results, as the composition of the western diet is higher in both saturated fats and sucrose than the high-fat diet. Dietary composition has also been shown to impact IVD health. Diets rich in advanced glycation end-products (AGE) precursors accelerate IVD degeneration in mice in parallel with insulin resistance<sup>74</sup>.

A confounding factor in the interpretation of our findings was the substantial variability for many of the outcomes investigated, including substantial differences in weight gain between mice on both obesogenic diets. Despite controlling for genetics using an inbred strain, susceptibility to diet-induced obesity can be affected by social stress, microbiome composition and epigenetic mechanisms<sup>75-77</sup>. Accounting for this variability, previous studies in mice demonstrated that cartilage damage induced by a high-fat diet is proportional to adiposity<sup>23</sup>. In the current study, adiposity did not predict histopathological measures of joint degeneration; however, adiposity and age were significant predictors of behavioral indicators of pain. Highlighting the complexity of these models, increased adiposity was also not directly associated with increased circulating cytokine levels in our study. In humans, obese individuals can be classified as metabolically healthy (metabolically healthy obese (MHO)). MHO individuals are at less risk for developing obesity-related complications than metabolically abnormal obese individuals, including OA<sup>78</sup>. The mechanisms underlying MHO are not well understood, however, genetic, epigenetic and environmental factors are thought to play a role<sup>79,80</sup>. As adiposity does not directly correlate with systemic or neuroinflammation in the current model, it is important to investigate all aspects of metabolic syndrome (i.e. circulating lipids, glucose,

cytokines/adipokines, blood pressure) on both the musculoskeletal and nervous system in future models to determine their contribution to disease progression.

Taken together, this study highlights the complexity of the relationship between obesity, IVD degeneration and pain. Mice fed a high-fat or western diet showed pain-related behaviors that preceded structural joint degeneration in both the IVD and knee. The chronology of these findings may be of clinical importance, as pain may affect the progression of radiographic joint degeneration. While not directly investigated in IVD degeneration, knee pain has shown to be a predictor of accelerated radiographic OA through inflammation and reduced mobility<sup>81</sup>, which is also seen in IVD degeneration<sup>82</sup>. This raises the intriguing possibility that back pain may be both a consequence of structural IVD degeneration in the current model, and a contributor to it.

## 3.7 Supplementary Figures

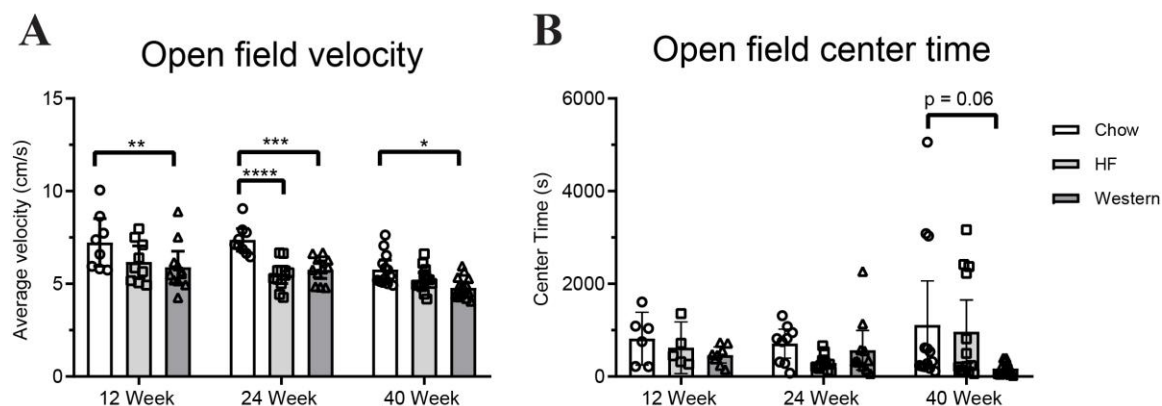


**Figure 3.7, Supplementary Figure 1: Spontaneous locomotion (Continued).**

Spontaneous Locomotion activity was recorded over three 2 hr sessions and averaged. (A) Mice fed the western diet showed a significant decrease in the average movement velocity at all timepoints compared to age-matched chow fed controls, while mice fed the high-fat diet showed a decrease at the 24-week timepoint. (B) The amount of time spent in the anxiety-inducing center area of the open field enclosure was decreased in mice fed the high-fat and western diets compared to controls but not significant at any timepoint.  $n=9-16$  animals per timepoint, per diet. Data are plotted mean  $\pm$  95% CI; data points for each mouse are graphed within each group. \* $P<0.05$ , \*\* $P<0.01$ , \*\*\* $P<0.001$ , \*\*\*\* $P<0.0001$  by one-way ANOVA.



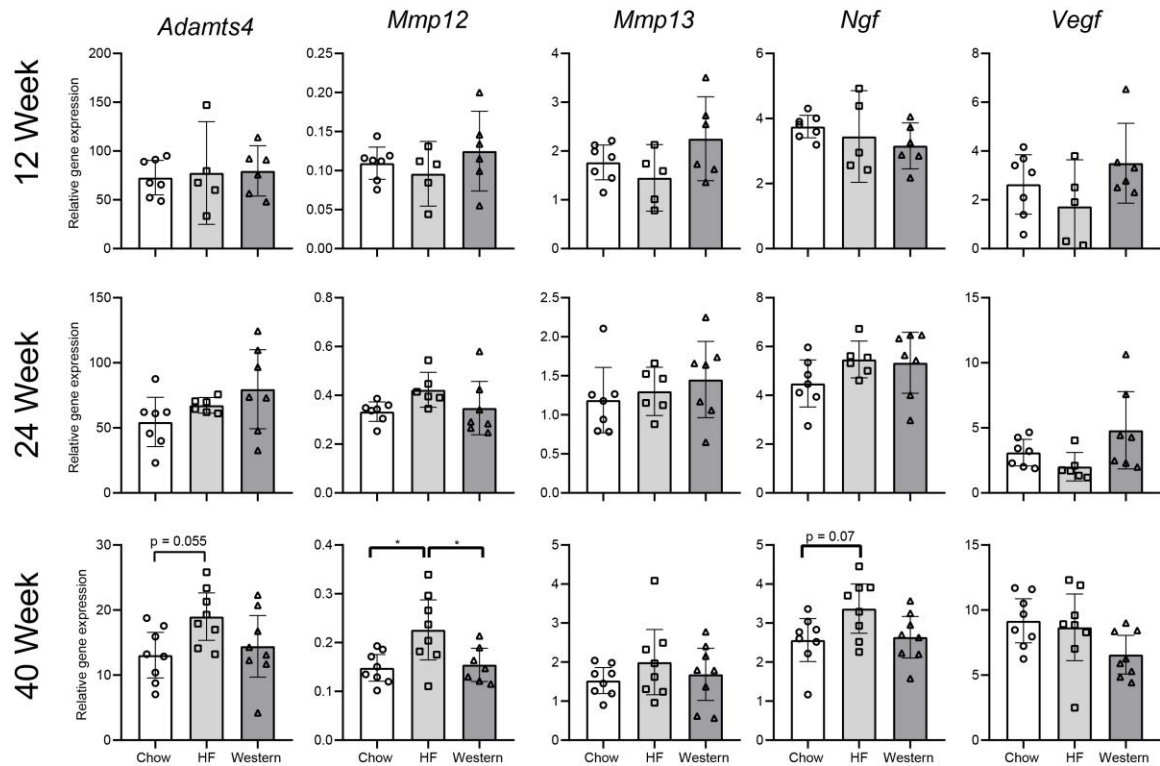


**Figure 3.8, Supplementary Figure 2: SYBR-based qPCR of thoracic IVDs (continued).**

SYBR-based qPCR of intact thoracic intervertebral discs showed no significant difference between mice fed a chow, high-fat or western diet at the 12-week and 24-week timepoint for any genes investigated. At 40-weeks a significant increase was seen in *Mmp12* expression in mice fed a high-fat diet compared to chow control. n=5-8 animals per diet/per timepoint. Analyzed by one-way ANOVA. All data are plotted mean ± 95% CI; data points for each mouse are graphed within each group. \*P<0.05, \*\*\*P<0.001.

**Table 3.3, Supplementary Table 1: Experimental diet compositions.**

	Control diet		Obesogenic diets			
	Chow		High fat		Western	
Product #	Envigo 2018		Envigo TD.06414		Envigo TD.10885	
Content	g	kcal%	% by weight	kcal%	% by weight	kcal%
Protein	19.2	20	23.5	18.3	17.3	14.8
Carbohydrate	67.3	70	27.3	21.4	47.5	40.6
Fat	4.3	10	34.3	60.3	23.2	44.6
kcal/g		3.85		5.1		4.7
Ingredient	g/kg		g/kg		g/kg	
Casein	N/A		265		195	
L-Cystine	N/A		4		3	
Corn starch	N/A		0		55.46	
Maltodextrin	N/A		160		60	
Sucrose	N/A		90		340	
Cellulose	N/A		65.5		50	
Soybean oil	N/A		30		20	
Anhydrous Milkfat	N/A		0		61	
Cholesterol	N/A				1.5	
Lard	N/A		310		0	
Vitamin Mix	N/A		21		19	
Mineral Mix	N/A		48		43	
Dicalcium phosphate	N/A		3.4		0	
Choline bitartrate	N/A		3.0		3.0	
SFA (% of fat)	N/A		34.8		58.3	
MUFA (% of fat)	N/A		39.1		28.2	
PUFA (% of fat)	N/A		22.5		8.9	
$\omega$ 6: $\omega$ 3 ratio	N/A		13.0		7.2	

**Table 3.4, Supplementary Table 2: Real-time qPCR primer sequences.**

<b>NCBI Gene Name</b>	<b>Primer Sequence 5' → 3'</b>
<i>Il6</i> Fwd	TCTCTGCAAGAGACTTCCATCCAGT
<i>Il6</i> Rev	AGTAGGGAAGGCCGTGGTTGTCA
<i>Il1b</i> Fwd	CCCTGCAGCTGGAGAGTGTGGA
<i>Il1b</i> Rev	TGTGCTCTGCTTGTGAGGTGCTG
<i>Ptgs2</i> Fwd	GGCGCAGTTTATGTTGTCTGT
<i>Ptgs2</i> Rev	CAAGACAGATCATAAGCGAGGA
<i>Bdnf</i> Fwd	TCATACTTCGGTTGCATGAAGG
<i>Bdnf</i> Rev	GACCTCTCGAACCTGCC
<i>Adamts5</i> Fwd	GGAGCGAGGCCATTTACAAC
<i>Adamts5</i> Rev	GCGTAGACAAGGTAGCCCCTTT
<i>Mmp3</i> Fwd	TTGTCCCGTTTCCATCTCTCTC
<i>Mmp3</i> Rev	TTGGTGATGTCTCAGGTTCCAG
<i>Adamts4</i> Fwd	GAGGAGGAGATCGTGTTTCCAG
<i>Adamts4</i> Rev	CAAACCCTCTACCTGCACCC
<i>Mmp12</i> Fwd	GCTTACCCCAAGCTGATTTCC
<i>Mmp12</i> Rev	ATGTTTTGGTGACACGACGGA
<i>Mmp13</i> Fwd	CTTCTTCTTGTTGAGCTGGAATC
<i>Mmp13</i> Rev	CTCTGTGGACCTCACTGTAGACT
<i>Ngf</i> Fwd	TGATCGGCGTACAGGCAGA
<i>Ngf</i> Rev	GCTGAAGTTTAGTCCAGTGGG
<i>Vegf</i> Fwd	CACTGGACCCTGGCTTTACT
<i>Vegf</i> Rev	GCAGTAGCTTCGCTGGTAGA
Annealing Temperature: 60°C	

**Table 3.5, Supplementary Table 3: Multiplex analysis of cytokines, chemokines and growth factors in serum (continued).**

Analyte	12 Week				24 Week				40 Week			
	Chow	HF	Western	p-value	Chow	HF	Western	p-value	Chow	HF	Western	p-value
	n=6	n=6	n=6		n=5	n=6	n=6		n=5	n=6	n=6	
Mean (SD)	Mean (SD)	Mean (SD)	Mean (SD)	Mean (SD)	Mean (SD)	Mean (SD)	Mean (SD)	Mean (SD)	Mean (SD)	Mean (SD)	Mean (SD)	
Ectaxin	2219 (3826)	2657 (3647)	3069 (3747)	0.93	823.7 (223.3)	711.4 (342.9)	306.2 (316.9)*#	0.03*	777.5 (279.9)	818.8 (169.6)	722.2 (198.3)	0.74
G-CSF	339.4 (308.8)	435.6 (342.7)	442.2 (416)	0.86	333.9 (297)	449.6 (348.3)	195.3 (139.3)	0.31	116.6 (95.7)	140.7 (88.5)	206.7 (226)	0.60
GM-CSF	78.9 (101.8)	58.6 (83.3)	67.4 (132.6)	0.98	79.4 (92.0)	55.8 (78.9)	61.8 (64.6)	0.88	33.2 (44.4)	21.1 (55.6)	59.0 (102.8)	0.66
IFN $\gamma$	25.4 (36.6)	52.0 (113.5)	89.7 (192.0)	0.70	74.1 (142.8)	11.7 (22.0)	16.6 (18.2)	0.38	13.4 (18.0)	57.4 (118.2)	20.8 (41.4)	0.58
IL-1A	389.8 (152.8)	347.7 (90.7)	248.5 (221.2)	0.33	423.4 (253.8)	149 (79.4)	109.4 (47.5)*#	0.01**	329.6 (182)	399.7 (153.6)	514.6 (631.4)	0.74
IL-2	109.3 (167.2)	159.3 (325.4)	164.7 (334.9)	0.93	111.8 (105.0)	51.5 (75.6)	51.3 (75.3)	0.43	56.6 (92.5)	19.6 (38.5)	41.2 (57.0)	0.60
IL-3	7.9 (8.8)	9.4 (10.7)	13.9 (23.6)	0.79	3.9 (4.2)	5.9 (6.5)	4.8 (7.1)	0.87	0 (0)	0.3 (0.6)	1.3 (3.0)	0.49
IL-4	2.5 (3.0)	8.2 (16.7)	7.9 (7.8)	0.59	2.9 (4.7)	3.0 (3.3)	3.5 (5.2)	0.97	0.1 (0.1)	0.1 (0.2)	5.9 (11.0)	0.25
IL-5	19.4 (16.9)	37.3 (44.9)	23.4 (17.5)	0.56	27.1 (33.2)	33.7 (37.9)	22.2 (14.3)	0.80	6.5 (3.6)	6.4 (5.9)	15.1 (15.2)	0.26
IL-7	24.6 (27.0)	30.2 (33.1)	260.7 (600.9)	0.43	97.6 (177.8)	32.4 (48.9)	5.0 (9.2)	0.32	1.5 (2.2)	5.1 (9.7)	104.0 (241.2)	0.41
IL-9	143.7 (145.9)	139.7 (151.3)	378.0 (724.7)	0.57	235.6 (318.7)	48.5 (36.6)	105.8 (139.1)	0.29	243.6 (334.6)	82.6 (88.5)	128.9 (112.0)	0.42
IL-12 (p40)	36.9 (48.8)	18.3 (22.2)	35.6 (43.9)	0.68	10.4 (14.6)	13.0 (15.1)	6.5 (9.5)	0.69	0 (0)	122.9 (291.5)	0 (0)	0.40
IL-12 (p70)	40.4 (45.8)	62.7 (108.2)	241 (310.2)	0.17	28.2 (30.6)	70.8 (129.8)	62.4 (88.3)	0.75	0 (0)	15.6 (38.2)	281.2 (657.5)	0.42
IL-13	137.6 (141.2)	133.5 (147.7)	210.2 (383.2)	0.84	231.7 (356.4)	80.3 (74.3)	87.0 (111)	0.43	62.9 (65.5)	55.9 (32.4)	107.3 (146)	0.62
IL-15	324.0 (357.3)	316.1 (357.3)	239.3 (294.7)	0.89	1231 (2454)	269.5 (473.2)	58.6 (69)	0.34	3.0 (6.8)	140.4 (203.1)	983.7 (2191)	0.42
IL-17	8.7 (8.1)	6.0 (9.4)	6.3 (9.7)	0.86	4.8 (3.5)	4.9 (5.4)	3.8 (5.3)	0.92	3.0 (1.9)	2.8 (3.4)	11.9 (22.8)	0.46
LIF	4.8 (5.2)	5.5 (6.1)	5.1 (5.7)	0.97	4.0 (6.7)	4.3 (5.3)	0.3 (0.4)	0.31	0 (0)	1.8 (3.5)	11.1 (25.3)	0.44
LIX	6937 (4608)	8908 (5462)	6397 (3134)	0.61	9955 (8707)	5235 (5285)	4320 (4376)	0.31	9699 (1509)	10211 (1959)	7224 (4547)	0.24
M-CSF	35.3 (38.7)	25.8 (31.7)	24.1 (27.3)	0.82	19.1 (25.3)	23.0 (23.7)	15.5 (17.0)	0.84	0.6 (1.1)	28.4 (44.7)	0.9 (0.8)	0.16
MIG	474.0 (417.7)	345.3 (353.3)	345.7 (344.2)	0.79	287.6 (193.5)	368.3 (436.5)	130.2 (82.1)	0.37	85.2 (36.7)	142.1 (110.6)	114.3 (58.0)	0.49
MIP-1A	249.6 (373)	333 (539.3)	587.6 (1032)	0.69	417.8 (401)	178.9 (207.3)	191.2 (150.7)	0.28	261.4 (302.7)	109.2 (133.0)	257.8 (146.2)	0.58
MIP-1B	126.5 (161.5)	104.7 (126.1)	144.1 (204.2)	0.92	217.2 (328.9)	97.1 (124.6)	123.7 (130.1)	0.62	88.3 (116.3)	100.7 (155.2)	210.6 (286.9)	0.55
MIP-2	236.8 (113.5)	195.8 (93.1)	256.3 (123.7)	0.64	127.4 (21.6)	149.8 (62.6)	111 (47.7)	0.40	168.8 (21.4)	198.9 (69.6)	161.7 (15.0)	0.33
RANTES	49.6 (44.4)	76.7 (57.5)	96.0 (73.9)	0.42	53.6 (69.5)	59.1 (57.2)	58.9 (30.2)	0.98	25.13 (22.17)	36.77 (44.93)	52.65 (46.62)	0.54

Values are displayed in pg/mL and analyzed by one-way ANOVA. \* indicates significantly different from chow diet. # is significantly different from HF diet by Tukey's post-hoc test. P<0.05 is significant

**Table 3.6, Supplementary Table 4: Association between behavioral indicators of pain and histological joint damage.**

Parameter	Bivariate (r)		Multivariate ( $\beta$ , $r^2$ )		
	IVD degeneration	Knee OA	IVD degeneration ( $\beta$ )	Knee OA ( $\beta$ )	Whole model ( $r^2$ )
<b>Behavioral</b>					
Von Frey	0.002	0.206	-	-	0.053
Grip Force	-0.015	<b>-0.254*</b>	-6.513	<b>-0.371*</b>	<b>0.102*</b>
Acetone	0.135	0.038	-	-	0.021
<b>Tail suspension</b>					
Rearing	0.089	0.042	-	-	0.004
Self-Support	0.012	0.047	-	-	0.009
Immobility	0.063	0.061	-	-	0.017
Stretch	0.019	0.001	-	-	0.003
<b>Open Field</b>					
Distance travelled	0.090	0.109	-	-	0.022
Rest time	0.140	0.025	-	-	0.048
Rearing	0.106	0.015	-	-	0.019

### 3.8 References

1. Blüher M. Obesity: global epidemiology and pathogenesis. *Nat Rev Endocrinol*. 2019. doi:10.1038/s41574-019-0176-8
2. De Gonzalez AB, Hartge P, Cerhan JR, et al. Body-mass index and mortality among 1.46 million white adults. *N Engl J Med*. 2010. doi:10.1056/NEJMoa1000367
3. Taylor VH, Forhan M, Vigod SN, McIntyre RS, Morrison KM. The impact of obesity on quality of life. *Best Pract Res Clin Endocrinol Metab*. 2013. doi:10.1016/j.beem.2013.04.004
4. Samartzis D, Karppinen J, Cheung JP, Lotz J. Disk degeneration and low back pain: are they fat-related conditions? *Glob Spine J*. 2013;3(3):133-144. doi:10.1055/s-0033-1350054
5. Shiri R, Karppinen J, Leino-Arjas P, Solovieva S, Viikari-Juntura E. The association between obesity and low back pain: a meta-analysis. *Am J Epidemiol*. 2010;171(2):135-154. doi:10.1093/aje/kwp356
6. Global Burden of Disease Study C. Global, regional, and national incidence, prevalence, and years lived with disability for 301 acute and chronic diseases and injuries in 188 countries, 1990-2013: a systematic analysis for the Global Burden of Disease Study 2013. *Lancet*. 2015;386(9995):743-800. doi:10.1016/S0140-6736(15)60692-4
7. Roelofs PDDM, Deyo RA, Koes BW, Scholten RJPM, Van Tulder MW. Nonsteroidal anti-inflammatory drugs for low back pain: An updated cochrane review. *Spine (Phila Pa 1976)*. 2008. doi:10.1097/BRS.0b013e31817e69d3
8. DePalma MJ, Ketchum JM, Saullo T. What is the source of chronic low back pain and does age play a role? *Pain Med*. 2011;12(2):224-233. doi:10.1111/j.1526-4637.2010.01045.x
9. Schwarzer AC, Aprill CN, Derby R, Fortin J, Kine G, Bogduk N. The relative contributions of the disc and zygapophyseal joint in chronic low back pain. *Spine (Phila Pa 1976)*. 1994;19(7):801-806. doi:10.1097/00007632-199404000-00013
10. Modic MT, Ross JS. Lumbar degenerative disk disease. *Radiology*. 2007;245(1):43-61. doi:10.1148/radiol.2451051706
11. Rodriguez-Martinez NG, Perez-Orribo L, Kalb S, et al. The role of obesity in the biomechanics and radiological changes of the spine: an in vitro study. *J Neurosurgery-Spine*. 2016;24(4):615-623. doi:10.3171/2015.7.Spine141306
12. Chan SC, Ferguson SJ, Gantenbein-Ritter B. The effects of dynamic loading on the intervertebral disc. *Eur Spine J*. 2011;20(11):1796-1812. doi:10.1007/s00586-

011-1827-1

13. Kerr GJ, Veras MA, Kim MK, Seguin CA. Decoding the intervertebral disc: Unravelling the complexities of cell phenotypes and pathways associated with degeneration and mechanotransduction. *Semin Cell Dev Biol.* 2017;62:94-103. doi:10.1016/j.semcdb.2016.05.008
14. Liuke M, Solovieva S, Lamminen A, et al. Disc degeneration of the lumbar spine in relation to overweight. *Int J Obes.* 2005;29(8):903-908. doi:10.1038/sj.ijo.0802974
15. DM U, I K, K T, et al. Obesity is associated with reduced disc height in the lumbar spine but not at the lumbosacral junction. *Spine (Phila Pa 1976).* 2014;39(16):E962-6. doi:10.1097/BRS.0000000000000411.
16. Sturmer T, Gunther KP, Brenner H. Obesity, overweight and patterns of osteoarthritis: the Ulm Osteoarthritis Study. *J Clin Epidemiol.* 2000;53(3):307-313. doi:10.1016/s0895-4356(99)00162-6
17. Rustenburg CME, Emanuel KS, Peeters M, Lems WF, Vergroesen P-PA, Smit TH. Osteoarthritis and intervertebral disc degeneration: Quite different, quite similar. *JOR Spine.* 2018. doi:10.1002/jsp2.1033
18. Dahaghin S, Bierma-Zeinstra SM, Koes BW, Hazes JM, Pols HA. Do metabolic factors add to the effect of overweight on hand osteoarthritis? The Rotterdam Study. *Ann Rheum Dis.* 2007;66(7):916-920. doi:10.1136/ard.2005.045724
19. Sellam J, Berenbaum F. Is osteoarthritis a metabolic disease? *Jt Bone Spine.* 2013;80(6):568-573. doi:10.1016/j.jbspin.2013.09.007
20. Dario AB, Ferreira ML, Refshauge KM, Lima TS, Ordonana JR, Ferreira PH. The relationship between obesity, low back pain, and lumbar disc degeneration when genetics and the environment are considered: a systematic review of twin studies. *Spine J.* 2015;15(5):1106-1117. doi:10.1016/j.spinee.2015.02.001
21. Nguyen NT, Magno CP, Lane KT, Hinojosa MW, Lane JS. Association of hypertension, diabetes, dyslipidemia, and metabolic syndrome with obesity: findings from the National Health and Nutrition Examination Survey, 1999 to 2004. *J Am Coll Surg.* 2008;207(6):928-934. doi:10.1016/j.jamcollsurg.2008.08.022
22. Zhuo Q, Yang W, Chen J, Wang Y. Metabolic syndrome meets osteoarthritis. *Nat Rev Rheumatol.* 2012;8(12):729-737. doi:10.1038/nrrheum.2012.135
23. Griffin TM, Fermor B, Huebner JL, et al. Diet-induced obesity differentially regulates behavioral, biomechanical, and molecular risk factors for osteoarthritis in mice. *Arthritis Res Ther.* 2010;12(4):R130. doi:10.1186/ar3068

24. Wu CL, Jain D, McNeill JN, et al. Dietary fatty acid content regulates Wound repair and the pathogenesis of osteoarthritis following joint injury. *Ann Rheum Dis*. 2015. doi:10.1136/annrheumdis-2014-205601
25. Griffin TM, Huebner JL, Kraus VB, Yan Z, Guilak F. Induction of osteoarthritis and metabolic inflammation by a very high-fat diet in mice: effects of short-term exercise. *Arthritis Rheum*. 2012;64(2):443-453. doi:10.1002/art.33332
26. Datta P, Zhang Y, Parousis A, et al. High-fat diet-induced acceleration of osteoarthritis is associated with a distinct and sustained plasma metabolite signature. *Sci Rep*. 2017;7(1):8205. doi:10.1038/s41598-017-07963-6
27. Collins KH, Paul HA, Reimer RA, Seerattan RA, Hart DA, Herzog W. Relationship between inflammation, the gut microbiota, and metabolic osteoarthritis development: studies in a rat model. *Osteoarthr Cartil*. 2015;23(11):1989-1998. doi:10.1016/j.joca.2015.03.014
28. Das UN. Is obesity an inflammatory condition? *Nutrition*. 2001;17(11-12):953-966. doi:10.1016/s0899-9007(01)00672-4
29. Griffin TM, Huebner JL, Kraus VB, Guilak F. Extreme obesity due to impaired leptin signaling in mice does not cause knee osteoarthritis. *Arthritis Rheum*. 2009;60(10):2935-2944. doi:10.1002/art.24854
30. Miao D, Zhang L. Leptin modulates the expression of catabolic genes in rat nucleus pulposus cells through the mitogen-activated protein kinase and Janus kinase 2/signal transducer and activator of transcription 3 pathways. *Mol Med Rep*. 2015;12(2):1761-1768. doi:10.3892/mmr.2015.3646
31. Liu C, Yang H, Gao F, et al. Resistin Promotes Intervertebral Disc Degeneration by Upregulation of ADAMTS-5 Through p38 MAPK Signaling Pathway. *Spine (Phila Pa 1976)*. 2016;41(18):1414-1420. doi:10.1097/BRS.0000000000001556
32. Kutlu S, Canpolat S, Sandal S, Ozcan M, Sarsilmaz M, Kelestimur H. Effects of central and peripheral administration of leptin on pain threshold in rats and mice. *Neuroendocrinol Lett*. 2003.
33. Wright LJ, Schur E, Noonan C, Ahumada S, Buchwald D, Afari N. Chronic pain, overweight, and obesity: findings from a community-based twin registry. *J Pain*. 2010;11(7):628-635. doi:10.1016/j.jpain.2009.10.004
34. Okifuji A, Hare BD. The association between chronic pain and obesity. *J Pain Res*. 2015;8:399-408. doi:10.2147/JPR.S55598
35. Teraguchi M, Yoshimura N, Hashizume H, et al. Metabolic Syndrome Components Are Associated with Intervertebral Disc Degeneration: The Wakayama Spine Study. *PLoS One*. 2016;11(2):e0147565. doi:10.1371/journal.pone.0147565



36. Jakoi AM, Pannu G, D'Oro A, et al. The Clinical Correlations between Diabetes, Cigarette Smoking and Obesity on Intervertebral Degenerative Disc Disease of the Lumbar Spine. *Asian Spine J.* 2017;11(3):337-347. doi:10.4184/asj.2017.11.3.337
37. Smith BW, Miller RJ, Wilund KR, O'Brien Jr. WD, Erdman Jr. JW. Effects of Tomato and Soy Germ on Lipid Bioaccumulation and Atherosclerosis in ApoE<sup>-/-</sup> Mice. *J Food Sci.* 2015;80(8):H1918-25. doi:10.1111/1750-3841.12968
38. Millecamps M, Tajerian M, Naso L, Sage EH, Stone LS. Lumbar intervertebral disc degeneration associated with axial and radiating low back pain in ageing SPARC-null mice. *Pain.* 2012;153(6):1167-1179. doi:10.1016/j.pain.2012.01.027
39. Miyagi M, Millecamps M, Danco AT, Ohtori S, Takahashi K, Stone LS. ISSLS Prize winner: Increased innervation and sensory nervous system plasticity in a mouse model of low back pain due to intervertebral disc degeneration. *Spine (Phila Pa 1976).* 2014;39(17):1345-1354. doi:10.1097/BRS.0000000000000334
40. Millecamps M, Czerminski JT, Mathieu AP, Stone LS. Behavioral signs of axial low back pain and motor impairment correlate with the severity of intervertebral disc degeneration in a mouse model. *Spine J.* 2015;15(12):2524-2537. doi:10.1016/j.spinee.2015.08.055
41. Chaplan SR, Bach FW, Pogrel JW, Chung JM, Yaksh TL. Quantitative assessment of tactile allodynia in the rat paw. *J Neurosci Methods.* 1994. doi:10.1016/0165-0270(94)90144-9
42. Beaucage KL, Pollmann SI, Sims SM, Dixon SJ, Holdsworth DW. Quantitative in vivo micro-computed tomography for assessment of age-dependent changes in murine whole-body composition. *Bone Reports.* 2016. doi:10.1016/j.bonr.2016.04.002
43. McCann MR, Patel P, Pest MA, et al. Repeated exposure to high-frequency low-amplitude vibration induces degeneration of murine intervertebral discs and knee joints. *Arthritis Rheumatol.* 2015;67(8):2164-2175. doi:10.1002/art.39154
44. Rutges JP, Duit RA, Kummer JA, et al. A validated new histological classification for intervertebral disc degeneration. *Osteoarthr Cartil.* 2013;21(12):2039-2047. doi:10.1016/j.joca.2013.10.001
45. Glasson SS, Chambers MG, Van Den Berg WB, Little CB. The OARSI histopathology initiative - recommendations for histological assessments of osteoarthritis in the mouse. *Osteoarthr Cartil.* 2010;18 Suppl 3:S17-23. doi:10.1016/j.joca.2010.05.025
46. Jin L, Balian G, Li XJ. Animal models for disc degeneration-an update. *Histol Histopathol.* 2018. doi:10.14670/HH-11-910
47. Mosley GE, Evashwick-Rogler TW, Lai A, Iatridis JC. Looking beyond the

- intervertebral disc: The need for behavioral assays in models of discogenic pain. *Ann N Y Acad Sci.* 2017. doi:10.1111/nyas.13429
48. Boden SD, Davis DO, Dina TS, Patronas NJ, Wiesel SW. Abnormal magnetic-resonance scans of the lumbar spine in asymptomatic subjects. A prospective investigation. *J Bone Jt Surg Am.* 1990;72(3):403-408. <http://www.ncbi.nlm.nih.gov/pubmed/2312537>.
  49. Jensen MC, Brant-Zawadzki MN, Obuchowski N, Modic MT, Malkasian D, Ross JS. Magnetic resonance imaging of the lumbar spine in people without back pain. *N Engl J Med.* 1994;331(2):69-73. doi:10.1056/NEJM199407143310201
  50. Masuda K, Aota Y, Muehleman C, et al. A novel rabbit model of mild, reproducible disc degeneration by an annulus needle puncture: Correlation between the degree of disc injury and radiological and histological appearances of disc degeneration. *Spine (Phila Pa 1976).* 2005. doi:10.1097/01.brs.0000148152.04401.20
  51. Deuis JR, Dvorakova LS, Vetter I. Methods used to evaluate pain behaviors in rodents. *Front Mol Neurosci.* 2017. doi:10.3389/fnmol.2017.00284
  52. Mogil JS. Animal models of pain: Progress and challenges. *Nat Rev Neurosci.* 2009. doi:10.1038/nrn2606
  53. Piel MJ, Kroin JS, van Wijnen AJ, Kc R, Im HJ. Pain assessment in animal models of osteoarthritis. *Gene.* 2014;537(2):184-188. doi:10.1016/j.gene.2013.11.091
  54. Burma NE, Leduc-Pessah H, Fan CY, Trang T. Animal models of chronic pain: Advances and challenges for clinical translation. *J Neurosci Res.* 2017. doi:10.1002/jnr.23768
  55. Steru L, Chermat R, Thierry B, Simon P. The tail suspension test: A new method for screening antidepressants in mice. *Psychopharmacology (Berl).* 1985. doi:10.1007/BF00428203
  56. Vagena E, Ryu JK, Baeza-Raja B, et al. A high-fat diet promotes depression-like behavior in mice by suppressing hypothalamic PKA signaling. *Transl Psychiatry.* 2019. doi:10.1038/s41398-019-0470-1
  57. Millicamps I, Tajerian M, Sage EH, Stone LS. Behavioral signs of chronic back pain in the SPARC-null mouse. *Spine (Phila Pa 1976).* 2011. doi:10.1097/BRS.0b013e3181cd9d75
  58. Vincent K, Mohanty S, Pinelli R, et al. Aging of mouse intervertebral disc and association with back pain. *Bone.* 2019. doi:10.1016/j.bone.2019.03.037
  59. Lai A, Moon A, Purmessur D, et al. Annular puncture with tumor necrosis factor-alpha injection enhances painful behavior with disc degeneration in vivo. *Spine J.*

2016. doi:10.1016/j.spinee.2015.11.019
60. Campbell JN, Meyer RA. Mechanisms of Neuropathic Pain. *Neuron*. 2006. doi:10.1016/j.neuron.2006.09.021
  61. Xu Q, Yaksh TL. A brief comparison of the pathophysiology of inflammatory versus neuropathic pain. *Curr Opin Anaesthesiol*. 2011. doi:10.1097/ACO.0b013e32834871df
  62. Cho H, Jang Y, Lee B, et al. Voluntary movements as a possible non-reflexive pain assay. *Mol Pain*. 2013. doi:10.1186/1744-8069-9-25
  63. Risbud M V, Shapiro IM. Role of cytokines in intervertebral disc degeneration: pain and disc content. *Nat Rev Rheumatol*. 2014;10(1):44-56. doi:10.1038/nrrheum.2013.160
  64. Bastard JP, Maachi M, Lagathu C, et al. Recent advances in the relationship between obesity, inflammation, and insulin resistance. *Eur Cytokine Netw*. 2006.
  65. Gangadharan V, Kuner R. Pain hypersensitivity mechanisms at a glance. *Dis Model Mech*. 2013;6(4):889-895. doi:10.1242/dmm.011502
  66. Richards N, Batty T, Dilley A. CCL2 has similar excitatory effects to TNF- $\alpha$  in a subgroup of inflamed C-fiber axons. *J Neurophysiol*. 2011. doi:10.1152/jn.00183.2011
  67. Jung H, Toth PT, White FA, Miller RJ. Monocyte chemoattractant protein-1 functions as a neuromodulator in dorsal root ganglia neurons. *J Neurochem*. 2008. doi:10.1111/j.1471-4159.2007.04969.x
  68. Lee SH, Wu YS, Shi XQ, Zhang J. Characteristics of spinal microglia in aged and obese mice: Potential contributions to impaired sensory behavior. *Immun Ageing*. 2015. doi:10.1186/s12979-015-0049-5
  69. Gupta S, Knight AG, Gupta S, Keller JN, Bruce-Keller AJ. Saturated long-chain fatty acids activate inflammatory signaling in astrocytes. *J Neurochem*. 2012. doi:10.1111/j.1471-4159.2012.07660.x
  70. Obrosova IG, Ilnytska O, Lyzogubov V V., et al. High-fat diet-induced neuropathy of pre-diabetes and obesity: Effects of “healthy” diet and aldose reductase inhibition. *Diabetes*. 2007. doi:10.2337/db06-1176
  71. Smith JP, Hicks PS, Ortiz LR, Martinez MJ, Mandler RN. Quantitative measurement of muscle strength in the mouse. *J Neurosci Methods*. 1995. doi:10.1016/0165-0270(95)00049-6
  72. Tam CS, Power JE, Markovic TP, et al. The effects of high-fat feeding on physical function and skeletal muscle extracellular matrix. *Nutr Diabetes*. 2015.

doi:10.1038/nutd.2015.39

73. Donovan EL, Lopes EBP, Batushansky A, Kinter M, Griffin TM. Independent effects of dietary fat and sucrose content on chondrocyte metabolism and osteoarthritis pathology in mice. *DMM Dis Model Mech*. 2018. doi:10.1242/dmm.034827
74. Illien-Junger S, Lu Y, Qureshi SA, et al. Chronic ingestion of advanced glycation end products induces degenerative spinal changes and hypertrophy in aging pre-diabetic mice. *PLoS One*. 2015;10(2):e0116625. doi:10.1371/journal.pone.0116625
75. Davis CD. The gut microbiome and its role in obesity. *Nutr Today*. 2016. doi:10.1097/NT.0000000000000167
76. Koza RA, Nikonova L, Hogan J, et al. Changes in gene expression foreshadow diet-induced obesity in genetically identical mice. *PLoS Genet*. 2006. doi:10.1371/journal.pgen.0020081
77. Bartolomucci A, Cabassi A, Govoni P, et al. Metabolic consequences and vulnerability to diet-induced obesity in male mice under chronic social stress. *PLoS One*. 2009. doi:10.1371/journal.pone.0004331
78. Lee S, Kim TN, Kim SH, et al. Obesity, metabolic abnormality, and knee osteoarthritis: A cross-sectional study in Korean women. *Mod Rheumatol*. 2015. doi:10.3109/14397595.2014.939393
79. Wang F, Liu H, Blanton WP, Belkina A, Lebrasseur NK, Denis G V. Brd2 disruption in mice causes severe obesity without Type 2 diabetes. *Biochem J*. 2010. doi:10.1042/BJ20090928
80. Iacobini C, Pugliese G, Blasetti Fantauzzi C, Federici M, Menini S. Metabolically healthy versus metabolically unhealthy obesity. *Metabolism*. 2019. doi:10.1016/j.metabol.2018.11.009
81. Wang Y, Teichtahl AJ, Abram F, et al. Knee pain as a predictor of structural progression over 4 years: data from the Osteoarthritis Initiative, a prospective cohort study. *Arthritis Res Ther*. 2018. doi:10.1186/s13075-018-1751-4
82. Urquhart DM, Berry P, Wluka AE, et al. 2011 Young Investigator Award winner: Increased fat mass is associated with high levels of low back pain intensity and disability. *Spine (Phila Pa 1976)*. 2011;36(16):1320-1325. doi:10.1097/BRS.0b013e3181f9fb66

## Chapter 4

### **Role of PPAR $\delta$ in the regulation of joint degeneration: context-specific roles in obesity and aging**

Chapter 4 is authored by Kerr, G.J., To, B., Margalik, D., Stone, L.S., Beier, F., and Séguin, C.A., and is entitled Role of PPAR $\delta$  in the regulation of joint degeneration: context-specific roles in obesity and aging. This study is currently unpublished but is in preparation for submission.

## 4 Role of PPAR $\delta$ in the regulation of joint degeneration: context-specific roles in obesity and aging

### 4.1 Co-authorship Statement

G.J. Kerr performed most of the experiments, contributed to study design and wrote the manuscript. B. To bred, genotyped, fed, and weighed the mice for the diet study (**Figure 4.1**). Additionally, B. To conducted the whole-body composition analysis (**Figure 4.1C-D**) and generated the reconstructed micro-CT image (**Figure 4.1E**). D. Margalik assisted with histology and scoring of the lumbar spine (**Figure 4.4**). B. To conducted all histological and histomorphometry analysis on the knee joints and G. J. Kerr assisted with histopathological scoring (**Figure 4.6**). Manuscript was written by G.J. Kerr with suggestions from Dr. C.A. Séguin.

## 4.2 Chapter Summary

**Introduction:** Despite being a major cause of disability worldwide, clinical treatment of intervertebral disc (IVD) degeneration and associated back pain is limited to symptomatic relief. While epidemiological studies have highlighted obesity as a major risk factor for the development of IVD degeneration and back pain, the biological mechanisms underlying this association are unknown. A potential mediator of obesity-associated IVD degeneration is the nuclear receptor peroxisome proliferator-activated receptor delta (PPAR $\delta$ ), as its ligands are dysregulated in obesity and its deletion has previously been shown to play a protective role in articular cartilage in the context of osteoarthritis.

**Methods:** *Ex vivo*, intact mouse IVD explants were treated with a synthetic agonist of PPAR $\delta$  (GW501516) and gene expression and glycosaminoglycan breakdown in the IVD were evaluated. *In vivo*, the role of PPAR $\delta$  was assessed in an age- and obesity-induced models of IVD degeneration using male and female *Col2-Cre;Ppard<sup>fl/fl</sup>* conditional knockout mice (*Ppard* KO). Following 50 weeks of experimental diet, mice were assessed for histological and molecular indicators of joint degeneration and behavioral indicators of pain.

**Results:** PPAR $\delta$  is expressed in the NP and AF and responds to PPAR $\delta$  agonism by increased expression of downstream target genes, indicating PPAR $\delta$  is functionally active in the IVD. Following 50 weeks of western diet, male mice showed indicators of IVD degeneration - changes not detected in female mice - and osteoarthritis induction in both sexes. *Ppard* KO mice showed protection from age-associated IVD degeneration but not from obesity-associated IVD degeneration or knee osteoarthritis. Pain-related behaviors were detected more consistently in female than male mice, despite a lack of

histopathological IVD degeneration. Bivariate and multivariate regression modeling indicates that sex and diet are robust predictors of many behavioral, histopathological, and molecular changes observed, while loss of PPAR $\delta$  is only a predictor of knee OA when sex and diet are accounted for. Regression analysis also reveals that alterations in pain-related behavior are independent of structural IVD degeneration.

**Conclusion:** While PPAR $\delta$  deletion may protect from age-associated IVD degeneration, it does not protect against obesity-associated IVD degeneration but may influence the pain associated with joint damage. This data demonstrates the complex, and context-dependent role of PPAR $\delta$  in the IVD and the need to evaluate multiple models of IVD degeneration for potential of clinical translation of novel therapeutic targets.

### 4.3 Introduction

Low back pain (LBP) is the single largest cause of disability worldwide, with a lifetime prevalence over 84% in Canada<sup>1,2</sup>. Despite efforts to improve the clinical management of LBP, treatments are limited to symptomatic relief without treating the underlying cause of the pain<sup>3</sup>. While several tissues appear to be involved in LBP, including the paraspinal muscles, ligaments, and facet joints<sup>4-6</sup>, degeneration of the fibrocartilaginous intervertebral disc (IVD) is believed to be the major contributor to pain in approximately 40% of cases<sup>4</sup>.

IVD degeneration has traditionally been considered a condition of “wear and tear”; however, this paradigm has shifted in recent years with the realization that IVD degeneration is an active process starting at the cellular level, ultimately leading to structural and functional failure<sup>7,8</sup>. Although the etiology of IVD degeneration remains



unclear, it appears to be multifactorial, as epidemiological studies have highlighted several modifiable and non-modifiable risk factors<sup>7-10</sup>. Of these, obesity is a major modifiable risk factor for the development of IVD degeneration and LBP. Obesity — defined as a body mass index (BMI) over 30 — substantially increases the risk of developing several metabolic, cardiovascular, neurological and musculoskeletal diseases<sup>11</sup>. In the spine, increased body weight is associated with indices of lumbar disc degeneration including disc space narrowing and decreased lumbar disc signal intensity detected by MRI<sup>12,13</sup>. Increased fat mass is also associated with increased LBP intensity and associated disability<sup>14</sup>. With the prevalence of obesity nearly tripling over the last 30 years<sup>11</sup>, it poses a large public health concern.

Despite the clinical associations between obesity, IVD degeneration, and LBP, the biological mechanisms underlying this association remain elusive. While increased mechanical load is thought to underlie in part these associations<sup>15</sup>, systemic factors including the chronic low-grade inflammation associated with obesity are also likely involved<sup>16</sup>. Metabolic and inflammatory abnormalities associated with obesity contribute to the development of osteoarthritis (OA)<sup>17</sup>, a degenerative musculoskeletal disease with many similarities to IVD degeneration<sup>18</sup>. Obesity is associated with chronic metabolic disorders including hypertension, diabetes mellitus and dyslipidemia, collectively known as metabolic syndrome<sup>19</sup>. In the context of OA, it is postulated that each component of metabolic syndrome may independently contribute to disease progression, as comprehensively reviewed by Zhuo et al.<sup>20</sup>. Specifically, alterations in the release of systemic factors (inflammatory cytokines, adipokines), nutrient exchange, advanced glycation end-products (AGEs) levels and glucose/lipid metabolism are believed to be

major contributors to OA progression<sup>17,20</sup>. Studies from multiple groups have demonstrated that obesity induced by a high-fat diet accelerates the progression of both age- and surgically-induced knee OA using mouse and rat models<sup>21–25</sup>, accompanied by behavioral indicators of pain<sup>21</sup>.

While not fully explored in the context of musculoskeletal diseases, the peroxisome-proliferator activated receptor (PPAR) family are current therapeutic targets for the management of metabolic syndrome<sup>26</sup>. The PPAR family of nuclear receptors consists of three isoforms (alpha, delta, gamma), that are activated by circulating fatty acid ligands<sup>26</sup>, and play distinct roles in energy balance and lipid/ glucose metabolism<sup>27</sup>. The two most studied isoforms, PPAR $\alpha$  and PPAR $\gamma$ , are highly expressed in the liver and adipose, respectively, and agonists of these receptors are being used clinically for obesity-associated conditions including dyslipidemia and type II diabetes mellitus<sup>26,28,29</sup>. Studies investigating the role of PPAR $\gamma$  in cartilaginous tissues demonstrated that cartilage-specific deletion of PPAR $\gamma$  leads to spontaneous OA development in mice<sup>30</sup>. In contrast to PPAR $\alpha$  and PPAR $\gamma$ , PPAR $\delta$  has broad expression patterns and affects glucose and lipid metabolism, cell differentiation, proliferation, apoptosis and immune regulation<sup>31</sup>. Using transgenic mouse models, studies have shown PPAR $\delta$  agonism improves insulin resistance, fat burning, and muscle endurance<sup>32–34</sup>; however, PPAR $\delta$  agonism has also been shown to induce catabolic processes within articular cartilage and chondrocytes<sup>35,36</sup>, suggesting tissue-specific or context dependent functions of PPAR $\delta$ . In explant and cell culture models, PPAR $\delta$  agonism leads to aggrecan and glycosaminoglycan degradation in cartilage through increased expression of *Mmp-3* and *Adamts-5*<sup>35,36</sup>, matrix remodelling enzymes implicated

in both OA and IVD degeneration<sup>37,38</sup>. Moreover, mice with deletion of PPAR $\delta$  in articular cartilage are protected from cartilage damage in a post-traumatic model of OA<sup>35</sup>.

Given that its ligands are dysregulated in obesity and the potential role it plays in articular cartilage, the present study aimed to investigate the role of PPAR $\delta$  in the IVD. We first investigated the effects of PPAR $\delta$  activation using an *ex vivo* organ culture system and validated that PPAR $\delta$  was functionally active within the IVD. We then examine the role of PPAR $\delta$  in the IVD *in vivo* using *Col2-Cre;Ppard<sup>fl/fl</sup>* mice to delete PPAR $\delta$  within the NP and inner AF. We used this mouse model to examine the role of PPAR $\delta$  in both age-associated and obesity-associated IVD degeneration and pain, using both male and female mice to specifically investigate sex as a variable.

## 4.4 Methods

### 4.4.1 Mice and Ex Vivo organ culture

Ten-week-old, C57BL/6N mice (Charles River: Wilmington, MA, USA) were used to isolate lumbar and thoracic spinal segments. Following removal of surrounding ligaments and musculature, IVDs were isolated from the vertebral columns using a stereoscope. Intact IVDs were used in *ex vivo* culture experiments. NP and AF tissue were further microdissected (as reported previously<sup>39</sup>) for gene expression analysis. For *ex vivo* organ culture, isolated IVDs (NP, AF, CEP) were equilibrated in organ culture media (DMEM low glucose (1g/L), 1% FBS, 1 % penicillin/streptomycin) overnight at 2% O<sub>2</sub>. On the following day, explants were treated with PPAR $\delta$  agonist GW501516 (Cedar Lane Labs: Burlington, ON, CAN) at concentrations of 0.01, 0.1, or 1  $\mu$ M in organ culture media for

4 or 7 days (6-7 IVDs per treatment) at 2% O<sub>2</sub>. Media was changed every 48 hours and DMSO-treated explants served as vehicle controls.

PPAR $\delta$ -KO mice were generated by breeding mice carrying the *Ppard* gene flanked by loxP sites (*Ppard*<sup>fl/fl</sup>; B6.129S4-Ppard<sup>tm1Rev</sup>/J, The Jackson Laboratories)<sup>40</sup> to mice carrying Cre recombinase under control of the type II collagen promoter (*Col2-Cre*)<sup>41</sup>, and genotyping was performed as previously reported<sup>41</sup>. Mice without cre-recombinase were used as controls (*Ppard*<sup>fl/fl</sup>; *Col2-Cre*<sup>-</sup> hereinafter referred to as WT) and cre-positive mice used as knockouts (*Ppard*<sup>fl/fl</sup>; *Col2-Cre*<sup>+</sup> hereinafter referred to as *Ppard* KO).

To determine the role of PPAR $\delta$  in the IVD, male and female mice were aged to 14 (n=9-13 per sex) or 25-months (n=4 male) of age and spinal tissues were harvested for histological and molecular analysis. To determine the role of PPAR $\delta$  in obesity-induced joint degeneration, (**Supplementary Figure 4.1**) mice were fed standard chow (Envigo 2018) until 10-weeks of age, when they were randomized into one of two diet groups (n = 9-13 mice per diet/ per genotype/ per sex;): standard chow (18% kcal fat, 58% kcal carbohydrate) or a high-fat, high-sugar western diet (45% kcal fat, 41% kcal carbohydrate; Envigo TD.10885) (**Supplementary Table 3.1**). Mice remained on the experimental diets until sacrifice at 60 weeks-of-age (50 weeks on diet). Mice were housed in standard cages and maintained on a 12 hr light/dark cycle, with food and water were consumed *ad libitum*; food consumption and body weight were measured weekly. All aspects of the study were conducted in accordance with the policies and guidelines set forth by the Canadian Council on Animal Care and were approved by the Animal Use Subcommittee of the University of Western Ontario (protocol 2017-154; **Appendix B**).

#### 4.4.2 Dimethylmethylene blue assay

The dimethylmethylene blue dye binding assay was performed on digested tissue explants and media collected from IVD explant cultures. Following 4 days in culture, explants were digested for 3 days in papain digest (125 µg/mL; Millepore Sigma Canada: Oakville, ON, CAN) at 60°C. The dimethylmethylene blue dye binding assay was performed as previously described<sup>42</sup>, and absorbance values were measured at a wavelength of 595 nm, with a reference wavelength of 655 nm on the Tecan Safire plate reader. GAG concentration in the media and tissue content were calculated based on a chondroitin sulfate standard curve, and GAG release into the media was normalized to the total GAG in each sample following papain digest.

#### 4.4.3 Histological analysis

For *ex vivo* organ cultures, one lumbar IVD from each treatment group was fixed overnight in 4% PFA, decalcified for 24h in TBD-2 (Thermo Fisher Canada: Mississauga, ON, CAN) and paraffin embedded. For the *in vivo* experiments, intact lumbar spine segments (L1-S1) and knees were isolated, fixed, decalcified and paraffin embedded, as previously described<sup>43</sup>. IVD explants and lumbar spines were sectioned sagittally, and knees were sectioned coronally at a thickness of 5 µm using a microtome (Leica Microsystems: Wetzlar, DEU) and stained using 0.1% Safranin-O/0.05% Fast Green or 0.04% Toluidine Blue, using methods previously described<sup>43,44</sup>.

To evaluate IVD degeneration, spine sections were scored by 2 independent scorers using the modified Boos system<sup>45</sup>. Knee joint health was assessed using the murine Osteoarthritis

Research Society International (OARSI) histopathological scale<sup>46</sup>. Articular surfaces of the medial femoral condyle (MFC), medial tibial plateau (MTP), lateral femoral condyle (LFC) and lateral tibial plateau (LTP), were scored by two blinded observers and averaged. For each joint surface, scores from 10 serial sections spanning 500  $\mu$ M of the joint were summed to represent OARSI score for each quadrant. Total scores from each of the four quadrants were then added together to generate whole joint OARSI score.

#### 4.4.4 Gene expression analysis

Intact IVDs were placed in TRIzol reagent (Thermo Fisher Canada: Mississauga, ON, CAN) (n=5-6 thoracic/lumbar IVDs per *ex vivo* treatment group; 4-5 thoracic IVDs per mouse from 5-8 mice per diet/per timepoint) and homogenized using a PRO250 tissue homogenizer (PRO Scientific: Oxford, CT, USA). To assess tissue-specific differences in gene expression, NP and AF tissue were further microdissected (as reported previously<sup>39</sup>) from WT mice and placed in in TRIzol reagent (Thermo Fisher Canada: Mississauga, ON, CAN) and homogenized manually using a pestle or using a PRO250 tissue homogenizer (PRO Scientific: Oxford, CT, USA) for NP and AF samples, respectively. RNA was extracted according to manufacturer's instructions and quantified using a NanoDrop 2000 spectrophotometer (Thermo Fisher Canada: Mississauga, ON, CAN). For the *ex vivo* and *in vivo* studies 0.5  $\mu$ g RNA was reverse transcribed into complementary DNA (cDNA) (iScript; Bio-Rad Laboratories (Canada): Mississauga, ON, CAN), while 0.15  $\mu$ g RNA was reverse transcribed for the NP/AF comparison due to sample size limitations. Gene expression was assessed by real-time PCR using a Bio-Rad CFX384 instrument. PCR analyses were run

in triplicate using 120 ng of cDNA per reaction and 310 nM forward and reverse primers with 2x SsoFast EvaGreen Supermix (Bio-Rad Laboratories (Canada): Mississauga, ON, CAN) using optimized PCR parameters and primers at an annealing temperature of 60°C (**Supplementary Table 4.1**). Primers were designed and validated to have efficiency values between 90 and 120%. For the *ex vivo* study and NP/AF comparison, transcript levels were calculated using  $\Delta\Delta C_t$ , with data normalized for input based on Ribosomal protein S29 (*Rps29*) and expressed relative to DMSO treated controls or AF samples, respectively. For the *in vivo* studies, transcript levels were calculated relative to a 6-point standard curve made from pooled cDNA generated from murine IVD explants treated with lipopolysaccharide for 4 days (50 mg/mL; Thermo Fisher Canada: Mississauga, ON, CAN).

#### 4.4.5 Micro-computed tomography (Micro-CT)

At sacrifice, mice in the diet study were immediately imaged by micro-CT (Locus Ultra, GE Healthcare Biosciences). Whole-body scans were acquired using 1000 projection images obtained over a single 16 s rotation (80 kv, 55 mA tube current, 16 ms exposure). A calibrating phantom composed of air, water and cortical bone-mimicking epoxy (SB3; Gammex, Middleton WI, USA) was scanned together with each of the animals. Data were reconstructed into 3D volumes with an isotropic voxel spacing of 154  $\mu\text{m}$  and scaled into Hounsfield units (HU). Using MicroView software (GE Healthcare Biosciences) three signal-intensity thresholds (-200, -30, and 190 HU) were used to classify each voxel as adipose, lean, or skeletal tissue, respectively. Custom software was used to calculate tissue

masses from assumed densities of 0.95 (adipose), 1.05 (lean), and 1.92 (skeletal) g/cm<sup>3</sup>. Volumetric measures were averaged over voxel volume<sup>47</sup>.

#### 4.4.6 Behavioral measures of pain

In the week prior to endpoint, mice in the diet study were assessed for behavioral indicators of pain. All mice were moved from conventional housing to the neurobehavioral testing facility two weeks prior to testing and habituated to all behavioral tests one week prior to data collection. On data collection days, animals were habituated to the testing room for 1 h before test start. To avoid confounding variables associated with the diurnal cycle, all behavioral testing was completed between 8 and 11 AM.

##### 4.4.6.1 Stretch-induced axial discomfort

Stretch-induced axial discomfort was measured using the grip force assay, as described previously<sup>48-50</sup>. For the grip force assay mice grabbed onto a metal bar attached to a grip force meter, and gently pulled back by their tails to exert axial stretch. Tolerance was assessed by measuring the grip strength (Grip Force Meter, Stoelting Co., Wood Dale, IL), in grams, for each mouse at the point of release.

##### 4.4.6.2 Hind limb sensitivity to cold and mechanical stimuli

Hind paw sensitivity to cold was assessed by measuring the time spent in behavior evoked by evaporative cooling of acetone (flicking, stamping or licking of ventral surface of the paw) during the first 40 s following application of 50  $\mu$ L acetone to the ventral surface of the hind paw. Mechanical sensitivity of the hindlimb was measured through application of



calibrated Von Frey filaments (Stoetling Co., Wood Dale, IL) to the plantar surface of the hind paw for 3 s or withdrawal. 50% withdrawal threshold was calculated using the Chaplan up-down method<sup>51</sup>, with a starting stimulus intensity of 1.4 g.

#### 4.4.6.3 Spontaneous activity

Spontaneous locomotor activity was assessed using open field activity monitors (AccuScan Instruments, Omnitech Electronic, Columbus, OH). Mice were placed into individual boxes and their activity was monitored over 30 min.

#### 4.4.6.4 Rotarod

Locomotor capacity was assessed with rotarod (30 mm diameter; Omnitech Electronics Inc: Columbus, OH, USA) that accelerated (0-30 rpm) for the first 60s and maintained at a maximal speed for an additional 240s. The experimental endpoint occurred when the animal fell from the rotating rod, detected by an infrared sensor. Animals that fell off once within the first 30 s were placed back onto the rod, and video recordings were used to confirm latency times.

#### 4.4.7 Pharmacological manipulation of pain

To assess whether behaviors indicative of stretch-induced axial discomfort (grip force) and mechanical sensitivity (Von Frey) were caused by pain, assays were repeated on all mice following administration of a weak opioid (Tramadol hydrochloride, 50 mg/kg, intraperitoneal (i.p.); Medisca: Richmond, BC, CAN). Testing was conducted 20 min and 45 min after tramadol injection for the Von Frey and grip force assay, respectively.

#### 4.4.7.1 Tail flick test

To assess the anti-nociceptive effects of tramadol, the latency of tail flick response was measured prior to injection, 20 min and 60 min after injection. Tail flick latency is the amount of time between applying heat to the tip of the tail through submersion in a hot water bath (set to 52°C), and voluntary tail withdrawal. The cutoff time was 12 s to prevent tissue injury and the antinociceptive response to tramadol was expressed as a percentage of the maximal possible effect (%MPE), as previously reported<sup>52</sup>.

#### 4.4.7.2 Spontaneous locomotion

To assess whether tramadol had a sedative effect, spontaneous activity in open field was measured over 10 min, 35 min after tramadol injection.

#### 4.4.8 Statistical analysis

For all assays except histopathological scoring of the joints, groups of male and female mice were compared between the different diet groups and genotypes by two-way ANOVA with Tukey's multiple comparisons test. For histopathological scores, within each timepoint mice were compared between the different diet groups by non-parametric Mann-Whitney U test.  $P < 0.05$  was considered significant. Statistical analysis was conducted using GraphPad Prism 8 (Graphpad Software: San Diego, CA, USA).

To assess the effect of sex, genotype, and diet on behavioral, molecular, and histological changes, bivariate and multivariate linear regression models were used to identify which variables remained independently associated with all other outcomes. Bivariate and

multivariate modelling was conducted using STATA 16 (StataCorp LLC: College Station, TX, USA).

## 4.5 Results

### 4.5.1 IVD cells express PPAR $\delta$ and respond to pharmacological activation

To determine whether PPAR $\delta$  was expressed and functional, intact IVD explants from 10-week-old WT mice were treated with increasing concentrations of the synthetic PPAR $\delta$  agonist GW501516 for 4 or 7 days (**Figure 4.1A**). After both 4 (**Figure 4.1B**) and 7 days (**Figure 4.1C**) of treatment, expression of known downstream PPAR $\delta$  effector genes including Pyruvate Dehydrogenase Kinase 4 (*Pdk4*) and Angiotensin-Like 4 (*Angptl4*) were significantly increased with agonist treatment. To assess the relative expression of PPAR $\delta$  in distinct IVD compartments, expression of *Ppard* was assessed NP and AF tissues isolated by microdissection from 10-week-old WT mice. NP cells showed significantly lower expression of *Ppard* than AF cells (**Figure 4.1D**). Genes involved in metabolism and oxidative stress altered by PPAR $\delta$  agonism in chondrocytes were also evaluated<sup>36</sup>. No significant difference in the expression levels of ATP-binding cassette transporter (*Abca1*), carnitine palmitoyltransferase 1A (*Cpt1a*), Glutathione S-transferase A4 (*Gsta4*), or Insulin Induced Gene 1 (*Insig1*) were detected in the IVD following agonist treatment (**Figure 4.11, Supplementary Figure 2**). After 7 days, treatment with 0.01  $\mu$ M GW501516 significantly upregulated the expression of Thioredoxin-interacting protein (*Txnip*) in IVD explants (**Figure 4.11, Supplementary Figure 2B**).

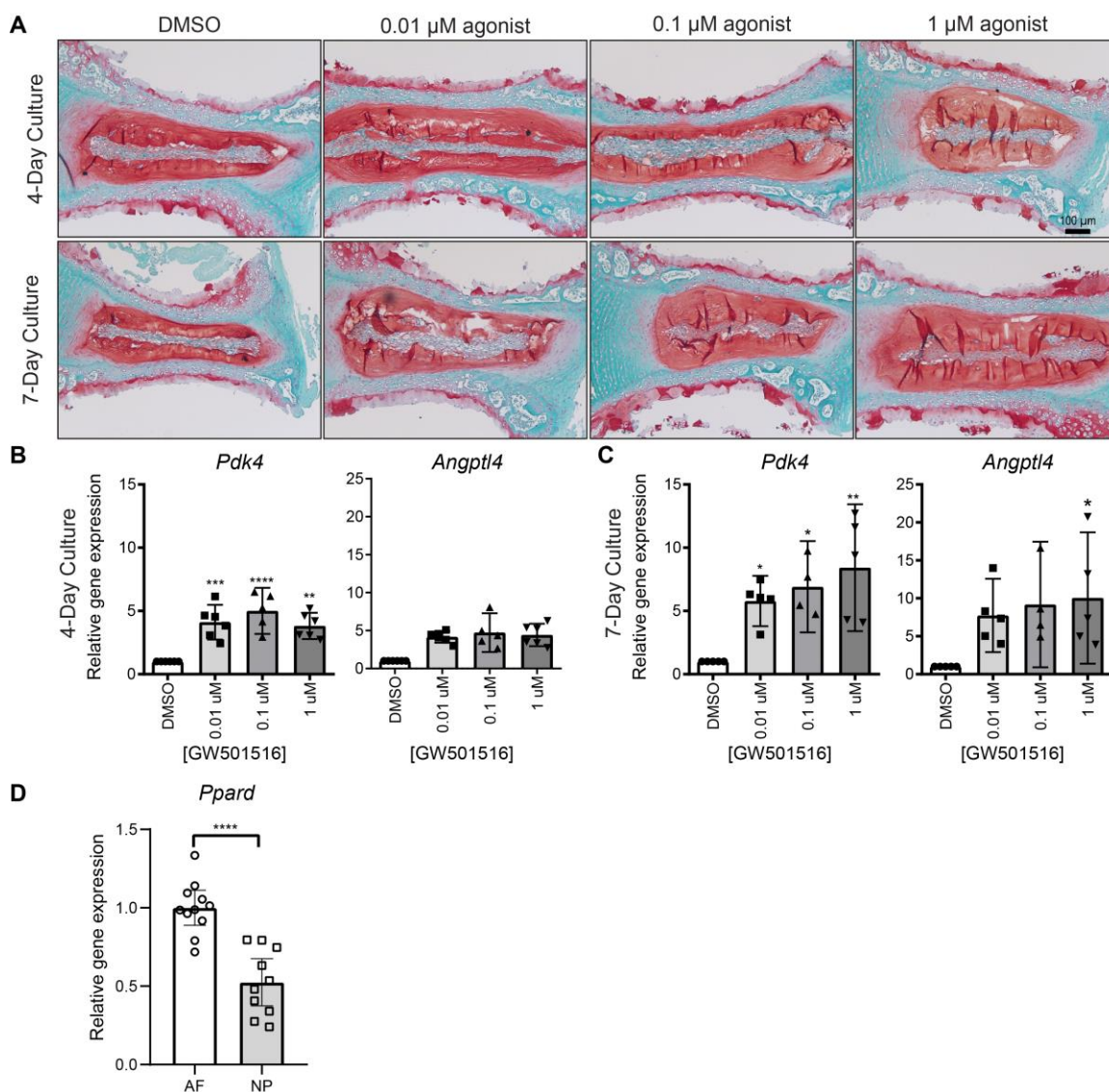


**Figure 4.1: PPAR $\delta$  is expressed in the IVD and responds to pharmacological agonism.**

(A) Representative histological sections of IVD explants cultured for 4 or 7 days in media supplemented with DMSO (vehicle control) or the PPAR $\delta$ -specific agonist GW501516 (0.01  $\mu\text{M}$ , 0.1  $\mu\text{M}$ , or 1  $\mu\text{M}$ ) stained with Safranin-O/Fast Green. (B & C) SYBR-based real-time qPCR analysis of IVD explants treated with GW501516 for 4 or 7 days show significant increases in the expression of known PPAR $\delta$  targets *Pdk4* and *Angptl4* (n=5-6 biological replicates). (D) SYBR-based real-time qPCR analysis of *Ppard* expression in NP and AF tissues isolated by microdissection. The expression of *Ppard* in the AF is significantly higher than expression in the NP (n=10-11). Data are presented as mean  $\pm$  95% CI. \*P<0.05, \*\*P<0.01, \*\*\*P<0.001, \*\*\*\*P<0.0001 by One-way ANOVA with Tukey's test compared to DMSO control for organ culture and by Welch's t-test for comparison of AF and NP tissue samples.

#### 4.5.2 Effect of PPAR $\delta$ activation on proteoglycan levels in the IVD

To determine the effects of PPAR $\delta$  activation on glycosaminoglycan (GAG) levels within intact IVDs, explants were treated with a vehicle control (DMSO), 0.01  $\mu$ M, 0.1  $\mu$ M, or 1  $\mu$ M GW501516 for 4 days (**Figure 4.12, Supplemental Figure 3**). While no gross morphological changes were observed, an apparent loss of proteoglycan staining was observed in explants cultured in the presence of 1  $\mu$ M GW501516 compared to DMSO control (**Figure 4.12, Supplementary Figure 3A**). To confirm these observations, levels of GAG were quantified in both the tissue explants and culture media using the dimethylmethylene blue dye binding (DMMB) assay. PPAR $\delta$  agonism was associated with a slight but not statistically significant increase in the release of GAG into the media (**Figure 4.12, Supplementary Figure 3B**). SYBR-based qPCR analysis was used to assess the expression of extracellular matrix genes and genes involved in matrix degradation. No significant differences were seen in the expression of matrix degrading enzymes (**Figure 4.12, Supplementary Figure 3C**) or extracellular matrix components (**Figure 4.12, Supplementary Figure 3D**).

#### 4.5.3 Deletion of PPAR $\delta$ may protect against age associated IVD degeneration

We next assessed the effect of PPAR $\delta$  deletion on age associated IVD degeneration. A conditional knockout mouse was generated using the Col2-Cre that our lab has demonstrated is expressed throughout the nucleus pulposus, inner two thirds of the AF and cartilage endplate, in addition to in addition to cartilaginous tissues, similar to other Col2-

Cre transgenic mouse lines<sup>53,54</sup>. WT and *Ppard* KO mice were aged to either 14 or 25 months-of-age and IVD health was assessed through histological analysis. At the 14-month timepoint, no discernable differences were detected in IVD health between WT and *Ppard* KO mice (**Figure 4.2A**). Accordingly, histopathological scoring showed no difference between WT and *Ppard* KO mice at any individual spinal level or in the average histopathological score in both male and female mice (**Figure 4.2B**). At the 25-month timepoint, male WT mice demonstrated advanced IVD degeneration, including a loss of proteoglycan content in the NP, accumulation of fibrotic matrix in the NP, and the loss of a distinct boundary between the NP and AF. In contrast, *Ppard* KO mice show more consistent maintenance of overall IVD structure and preservation of the NP cellularity and proteoglycan content (**Figure 4.2C**). While histopathological scoring indicated that *Ppard* KO animals had less degeneration on average than WT mice, the differences were not significant (**Figure 4.2D**).

#### 4.5.4 Wild-type and *Ppard* KO mice gain weight on the western diet

To investigate whether PPAR $\delta$  would play a similar role in obesity-induced IVD degeneration, at 10 weeks of age male and female WT and *Ppard* KO mice were randomized into groups fed either a high-fat/high-sugar western diet or chow control for 50 weeks (**Figure 4.10, Supplemental Figure 1**). As expected, following 50 weeks on the experimental diet both male and female mice fed the western diet showed a significant increase in body mass (**Figure 4.3A**) and weight gain (**Figure 4.3B**) compared to sex and genotype-matched chow fed controls. Analysis of whole-body composition by micro-CT demonstrated that for both WT and *Ppard* KO, male and female mice fed the western diet

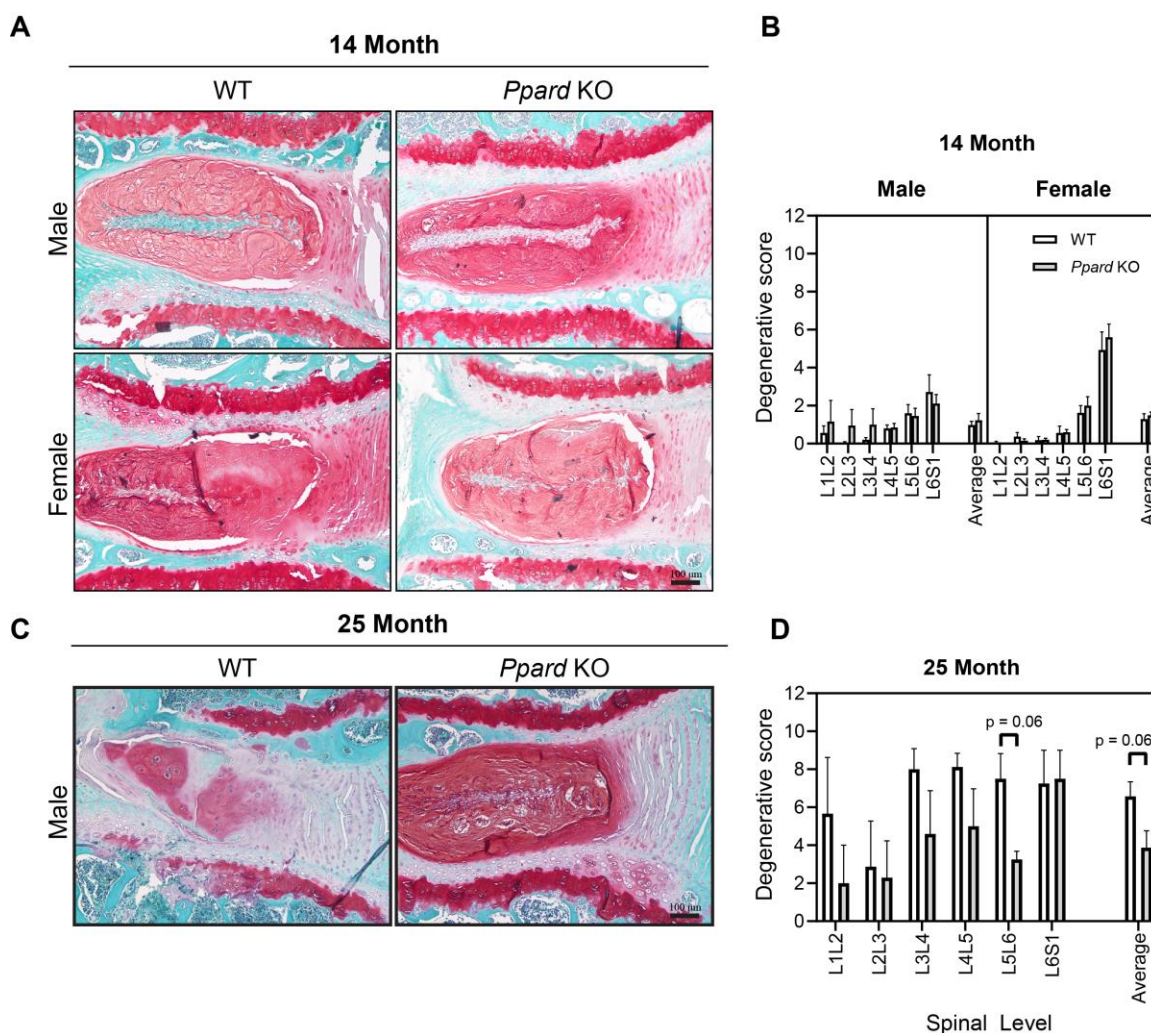


**Figure 4.2: Loss of *Ppard* alters age associated IVD degeneration.**

Representative images of mid-sagittal sections of lumbar IVDs stained with Safranin-O/Fast Green from 14-month old or 25-month-old wild-type (WT) and PPAR $\delta$  knockout (*Ppard* KO) mice paired with evaluation of the grade of histopathological degeneration using the modified Boos scoring system. (A) At 14 months-of-age, no differences in was detected in the histological appearance of IVD tissues between WT and PPAR $\delta$  KO mice. (B) At the 14-month timepoint, no differences in histopathological scores of IVD degeneration were seen between genotypes at either individual lumbar spinal levels or in the average degeneration score calculated for all lumbar IVDs. (C) At 25 months-of-age, male *Ppard* KO mice lacked histopathological signs of advanced IVD degeneration seen in WT mice, including a loss of proteoglycan content and accumulation of fibrotic matrix in the NP and the loss of a distinct boundary between the NP and AF. (D) At the 25-month timepoint, male *Ppard* KO mice showed lower degenerative scores at individual lumbar levels compared to WT; however, these changes did not result in significant differences in histopathological scores. Data are plotted mean  $\pm$  SEM and analyzed by Mann-Whitney U-test (n=9-13 for 14-month timepoint; n=3-5 for 25-month timepoint). \*P<0.05, \*\*\*P<0.001.

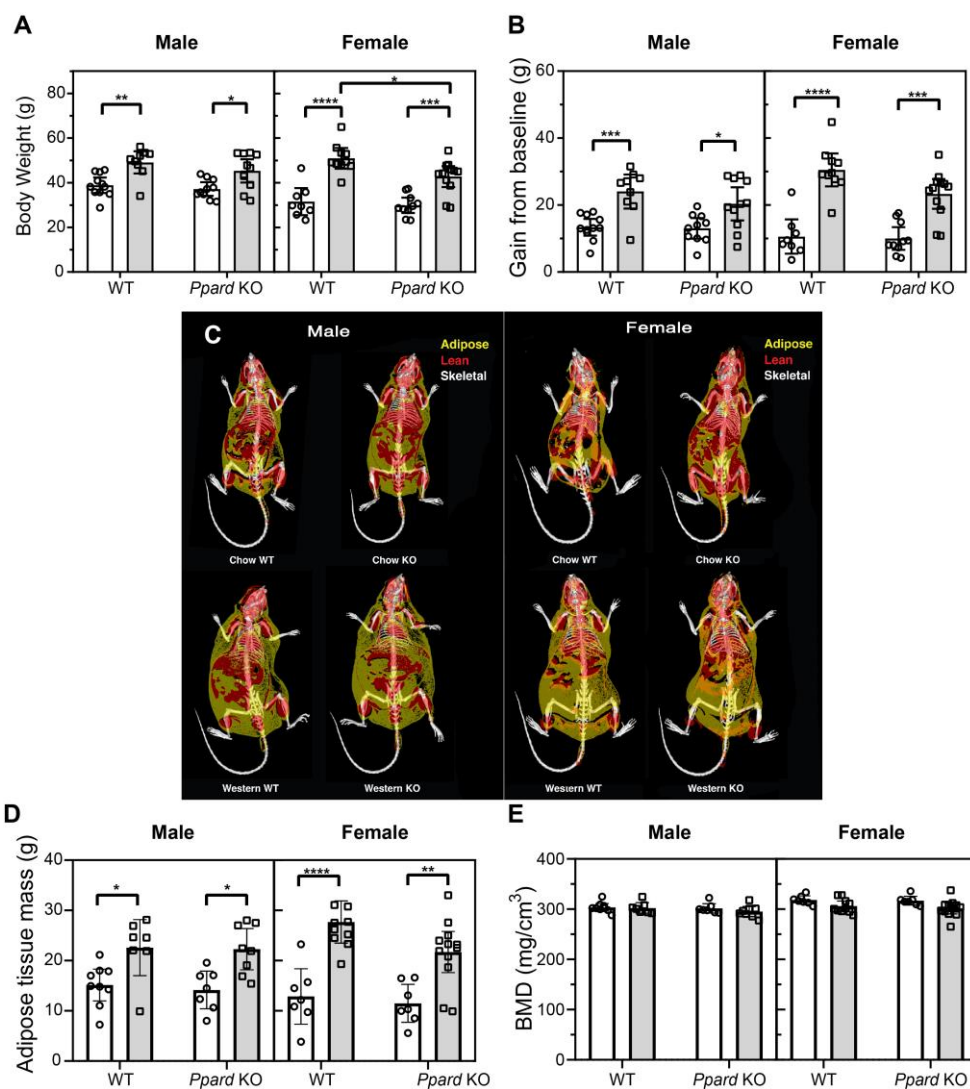


### Figure 4.3: Weight and adiposity.

(A) Following 50 weeks on the western diet, WT and *Ppard* KO mice showed a significant increase in body weight compared to chow-fed control. (B) Mice fed the western diet showed increased weight gain from baseline compared to chow-fed controls, regardless of sex or genotype. (C) Representative reconstructed micro-CT images of mice following 50-weeks of experimental diets. Isotropic surface-rendering of skeletal tissue (indicated in white) is overlaid with a mid-coronal slice where lean tissue is indicated in red and adipose tissue is indicated in yellow. Micro-CT based analysis of whole-body composition demonstrated a significant increase in (D) adipose tissue mass in all groups of mice fed the western diet compared to chow-fed controls; however, no differences were detected in (E) bone mineral density (BMD).  $n=9-13$  animals per genotype, sex, and diet. Data are plotted as mean  $\pm$  95% CI. \* $P<0.05$ , \*\* $P<0.01$ , \*\*\* $P<0.001$ , \*\*\*\* $P<0.0001$  by 2-way ANOVA with Tukey's test.



showed an increase in adipose tissue compared to chow controls (**Figure 4.3D**). No significant difference was seen in bone mineral density between diet groups in either WT or *Ppard* KO mice (**Figure 4.3E**).

#### 4.5.5 Deletion of PPAR $\delta$ does not protect against obesity related IVD degeneration

The effects of the western diet on IVD health was assessed through histopathological evaluation (**Figure 4.4**) and molecular analysis (**Figure 4.5**). In males, mice fed the western diet showed indicators of IVD degeneration not evident in chow control in both genotypes (**Figure 4.4A**). Histopathological changes included abnormal matrix deposition within the NP and a loss of clear demarcation between the NP and AF. Although no overt differences were detected between WT and *Ppard* KO mice, the western diet induced more consistent degeneration in male *Ppard* KO mice than in WT mice. Accordingly, histopathological scoring using the modified Boos scoring system showed significant increases in degeneration in the L6S1 spinal level of male *Ppard* KO mice fed a western diet compared to their chow-fed controls, but not in WT mice (**Figure 4.4B**). In females, no overt differences were detected in the histological appearance of the lumbar IVDs between the diet groups or genotypes (**Figure 4.4C**). As such, histopathological scoring did not show any differences in degeneration of lumbar IVDs between diet groups in female WT or *Ppard* KO mice (**Figure 4.4D**).

To further investigate the role of PPAR $\delta$  and changes associated with diet-induced obesity, SYBR-based qPCR was used to quantify the expression of extracellular matrix components (**Figure 4.5A**), matrix degrading enzymes (**Figure 4.5B**), and markers of inflammation and neural in-growth (**Figure 4.5C**) in thoracic IVDs. Despite no changes in IVD

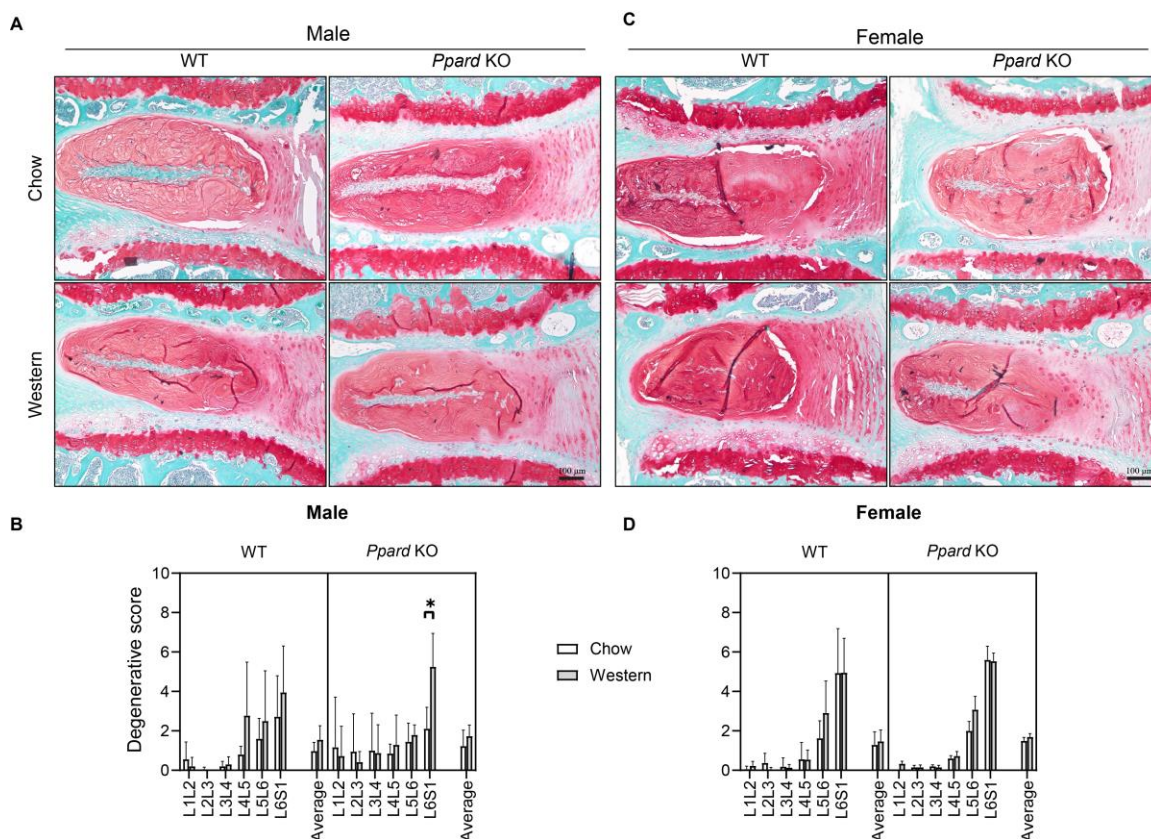


**Figure 4.4: Effect of diet-induced obesity and PPAR $\delta$  deletion on IVD health.**

Representative mid-sagittal sections of lumbar IVDs stained with Safranin-O/Fast Green from male (A) and female (C) wild-type (WT) and PPAR $\delta$  knockout (*Ppard* KO) mice fed either a chow control or western diet for 50 weeks. Male mice fed a western diet showed a loss of the demarcation between the NP and AF compared to chow control. This was observed in both WT and *Ppard* KO male mice, to a greater extent in *Ppard* KO animals. In female mice, no observable differences were seen between diet group or genotype. Evaluation of the grade of histopathological IVD degeneration using the modified Boos scoring system showed that (C) male *Ppard* KO mice fed a western diet showed significantly greater degeneration than their chow-fed controls at the L6/S1 spinal level. (D) No significant differences in histopathological scoring were seen between diets in female mice. n=9-13 mice per sex, genotype, and diet. Data is presented as mean  $\pm$  95% CI. \* $P$ <0.05 by Mann-Whitney U test.

histopathology, at 14 months-of-age male *Ppard* KO mice demonstrated increased expression of *Acan*, *Mmp3*, *Mmp13*, and *Il-1b* compared to WT mice (chow diet controls). Following 50 weeks of western diet, male WT mice showed a significant increase in the expression of *Acan* and *Il-1b* compared to chow fed controls, while male *Ppard* KO mice showed a significant increase in *Il-1b* expression compared to chow fed controls (**Figure 4.5A & 4.5C**). Male *Ppard* KO mice in the western diet group also showed a significant increase in *Il-1b* expression compared to male WT mice in the western diet group (**Figure 4.5C**). Similar patterns of gene expression were not detected in female mice. No differences in IVD gene expression were detected between female WT and *Ppard* KO mice. In female mice, changes associated with western-diet induced obesity were limited to down-regulation of *Colla1* expression in WT mice compared to chow fed controls (**Figure 4.5A**).

#### 4.5.6 Deletion of PPAR $\delta$ does not protect against obesity-related knee OA

Diet-induced obesity contributes to other arthropathies, such as knee OA<sup>29</sup>. Moreover, loss of *Ppard* protects from surgically induced posttraumatic OA<sup>35</sup>. We therefore examined the role of PPAR $\delta$  in obesity-induced OA. In male mice, chronic consumption of the western diet in both WT and *Ppard* KO mice led to increased erosion of the articular cartilage and osteophyte formation at the joint margins compared to sex-matched chow fed controls (**Figure 4.6A**). This corresponded to a significant increase in histopathological scores (**Figure 4.6B**). A similar trend was observed in female mice (**Figure 4.6C**). While female WT mice had more degeneration on average when fed the western diet compared to chow fed controls, this difference was not significant. Consumption of the western diet induced

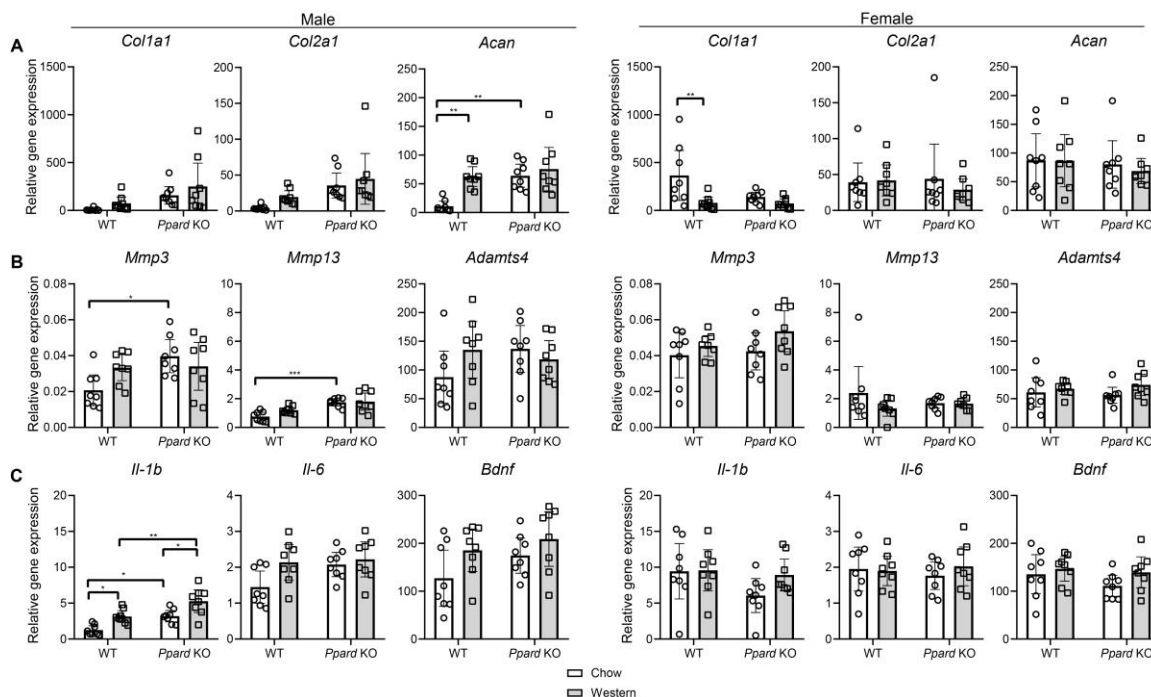


**Figure 4.5: Effect of diet-induced obesity and PPAR $\delta$  KO on IVD gene expression.**

SYBR-based qPCR analysis was conducted to assess the expression of (A) extracellular matrix genes, (B) matrix remodeling genes, and (C) proinflammatory and neurotrophic factors in IVDs of wild-type (WT) and PPAR $\delta$  knockout (*Ppard* KO) mice fed either a chow control or western diet for 50 weeks. Male *Ppard* KO mice showed increased expression of *Acan*, *Mmp3*, *Mmp13*, and *Il-1b* compared with WT mice. No significant differences were detected in female *Ppard* KO mice compared to WT controls. WT male mice fed the western diet showed significantly increased expression of *Acan* and *Il-1b*, while male *Ppard* KO mice fed a western diet only showed significant increases in *Il-1b* compared to genotype-matched chow-fed controls. Female WT mice fed the western diet showed significant decreases in *Colla1* expression compared to chow-fed controls. n=8 animals per sex, genotype, and diet. Data are plotted mean  $\pm$  95% CI. \* $P$ <0.05, \*\* $P$ <0.01, \*\*\* $P$ <0.001 by 2-way ANOVA with Tukey's test.

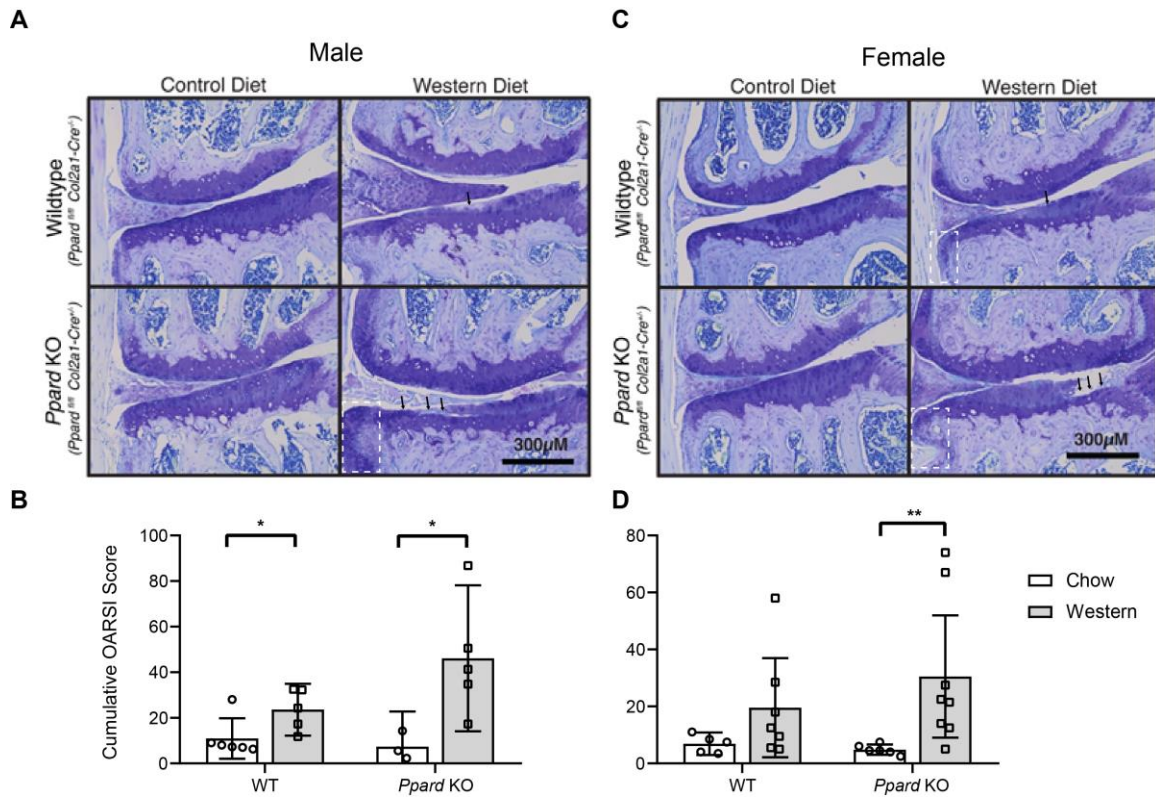


**Figure 4.6: Effect of diet-induced obesity and PPAR $\delta$  deletion on knee joint health.**

(A & C) Representative coronal sections of the medial knee compartment stained with toluidine blue male and female wild-type (WT) and PPAR $\delta$  knockout (*Ppard* KO) mice fed either a chow control or western diet for 50 weeks. Images are oriented with the medial femoral condyle (MFC) located superiorly, and the medial tibial plateau (MTP) inferiorly. Western diet-induced obesity was associated with indicators of osteoarthritis in all groups of mice assessed compared to chow-fed controls, marked by erosion of articular cartilage (arrows) and osteophyte formation (outlined in white dashed box). (B & D) Quantification of joint degeneration using the murine OARSI histopathological scoring system showed significant increases in joint degeneration in mice fed the western diet compared to chow fed controls for male WT and *Ppard* KO mice as well as female *Ppard* KO mice. n=4-8 animals per sex, genotype, and diet. Data are plotted mean  $\pm$  95% CI. \* $P$ <0.05, \*\* $P$ <0.01 by 2-way ANOVA with Tukey's test.

a significant increase in histopathological scores in female *Ppard* KO mice compared to chow fed controls (**Figure 4.6D**).

#### 4.5.7 Behavioral indicators of stretch-induced axial discomfort

To investigate the association between obesity, back pain, and the potential role of PPAR $\delta$ , we first investigated whether mice fed the western diet showed behavioral indicators of stretch-induced axial discomfort. Decreased grip force during axial stretch has been previously established as an indicator of discogenic back pain in a mouse model of IVD degeneration<sup>38</sup>. Loss of PPAR $\delta$  did not alter grip force in either male or female mice (**Figure 4.7A**). In male WT and *Ppard* KO, mice fed the western diet showed slight decreases in grip force during axial stretch, but these differences were not statistically different from chow fed control. In female WT and *Ppard* KO, mice fed the western diet showed a significant reduction grip force during axial stretch, indicative of axial discomfort (**Figure 4.7A**). To determine whether these behaviors were due to pain, the grip force assay was repeated on all mice following administration of a dose of the weak opioid tramadol (50 mg/kg I.P.). For all mice, the anti-nociceptive properties of the drug at this dosage were confirmed with the tail-flick assay (**Figure 4.13, Supplementary Figure 4**) and potential sedative effects of the drug were evaluated by measuring voluntary open field locomotion (**Figure 4.14, Supplementary Figure 5**). In male mice, tramadol treatment did not significantly alter grip force in any group (**Figure 4.7B**). In WT and *Ppard* KO female mice, tramadol treatment did not significantly affect grip force, however, the baseline significant difference associated with western diet-induced obesity in *Ppard* KO mice was no longer evident (**Figure 4.7C**).

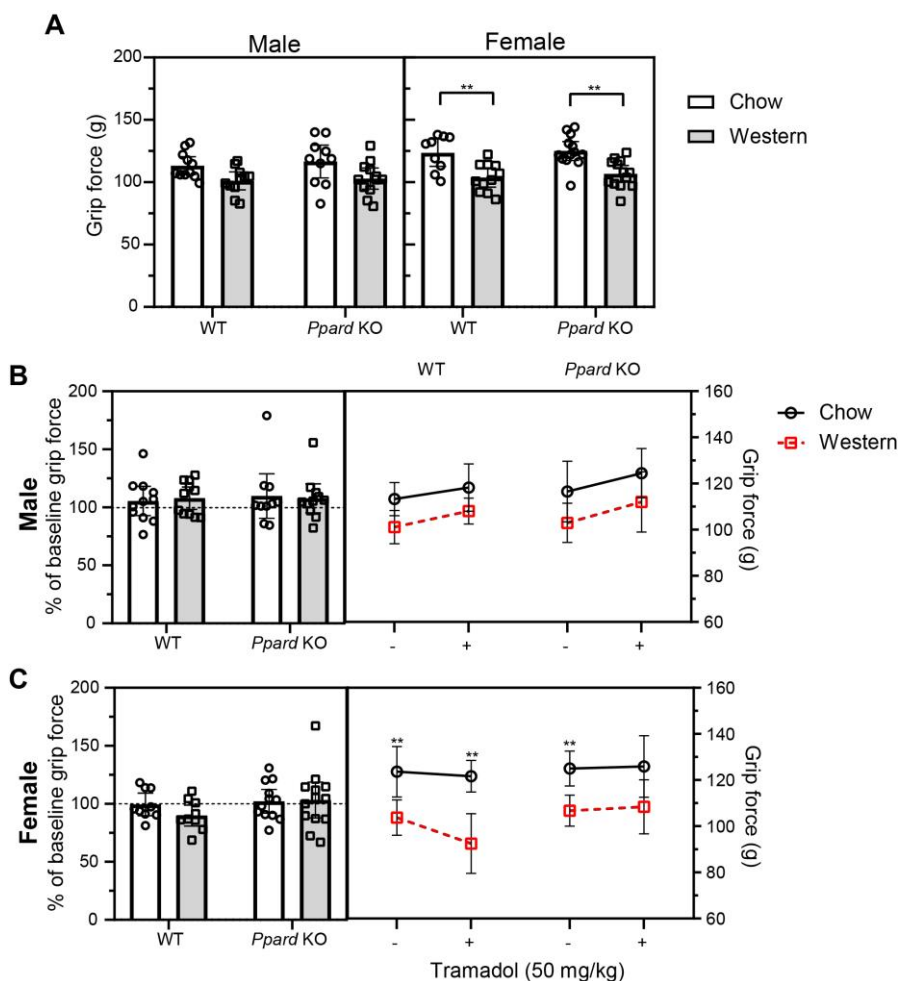


### Figure 4.7: Diet-induced obesity reduces grip strength in female mice.

(A) Stretch-induced axial discomfort was assessed in all groups of chow (control) and western diet fed mice. Loss of PPAR $\delta$  did not alter grip force in either male or female mice. Female wild-type (WT) and PPAR $\delta$  knockout (*Ppard* KO) mice fed the western diet showed reduced resistive grip force during axial stretch compared to chow-fed controls. To determine whether this was associated with pain, the grip force assay was repeated on all mice after receiving a dose of the weak opioid tramadol (50 mg/kg I.P.). (B) In male mice, tramadol did not significantly affect grip force in any group. (C) In female WT mice, tramadol did not significantly alter grip force in mice on both diets and did not prevent the significant difference associated with western diet-induced obesity. In female *Ppard* KO mice, tramadol did not significantly improve grip force in either diet group; however, the significant difference associated with western diet-induced obesity was no longer evident. Graphs on the left show the percent of baseline, which represents the grip force following tramadol treatment normalized to the pre-treatment (baseline) values for each animal. Graphs on the right show the average grip force (g) for mice in each group in the absence and following administration of tramadol.  $n=9-13$  mice per sex, genotype, and diet. Data are plotted mean  $\pm$  95% CI. \*\* $P<0.01$  between diets in each treatment group; † indicates significant ( $P<0.05$ ) tramadol-induced differences in grip force for mice fed the chow (black) or western (red) diet by 2-way ANOVA with Tukey's test.

#### 4.5.8 Behavioral indicators of cold and mechanical sensitivity

Cold sensitivity was assessed by measuring the response to evaporative cooling of acetone on the hind-paw. Cold sensitivity was not affected by loss of PPAR $\delta$  or by western diet-induced obesity in either male or female mice (**Figure 4.8A**). Mechanical sensitivity was then measured in the hind paw using the Von Frey assay. Loss of PPAR $\delta$  did not alter mechanical sensitivity in either male or female mice (**Figure 4.8A**). In males and female, WT mice fed the western diet showed a significant decrease in tolerance to mechanical stimulation compared to sex-matched chow fed controls. In both male and female *Ppard* KO mice, no difference in mechanical sensitivity was seen in mice fed the western diet compared to chow fed controls (**Figure 4.8B**). To assess whether these behavioral differences to mechanical stimulation were due to pain, the Von Frey assay was repeated on all mice following administration of a dose of the weak opioid tramadol (50 mg/kg I.P.). In male (**Figure 4.8C**) and female (**Figure 4.8D**) mice, tramadol significantly decreased mechanical sensitivity (increased withdrawal threshold) and prevented the baseline differences detected in mechanical sensitivity caused by western diet-induced obesity.

#### 4.5.9 Behavioral indicators of physical function and spontaneous locomotion

Locomotor capacity was first assessed using an accelerating rotarod assay where the outcome measure was time to fall. Loss of PPAR $\delta$  did not alter locomotor capacity in the rotarod assay in either male or female mice (**Figure 4.9A**). Moreover, western diet-induced obesity did not affect performance of male mice in the rotarod assay; no significant difference was seen in time to fall in either WT or *Ppard* KO mice compared to chow fed controls (**Figure 4.9A**). In females however, western diet-induced obesity was associated



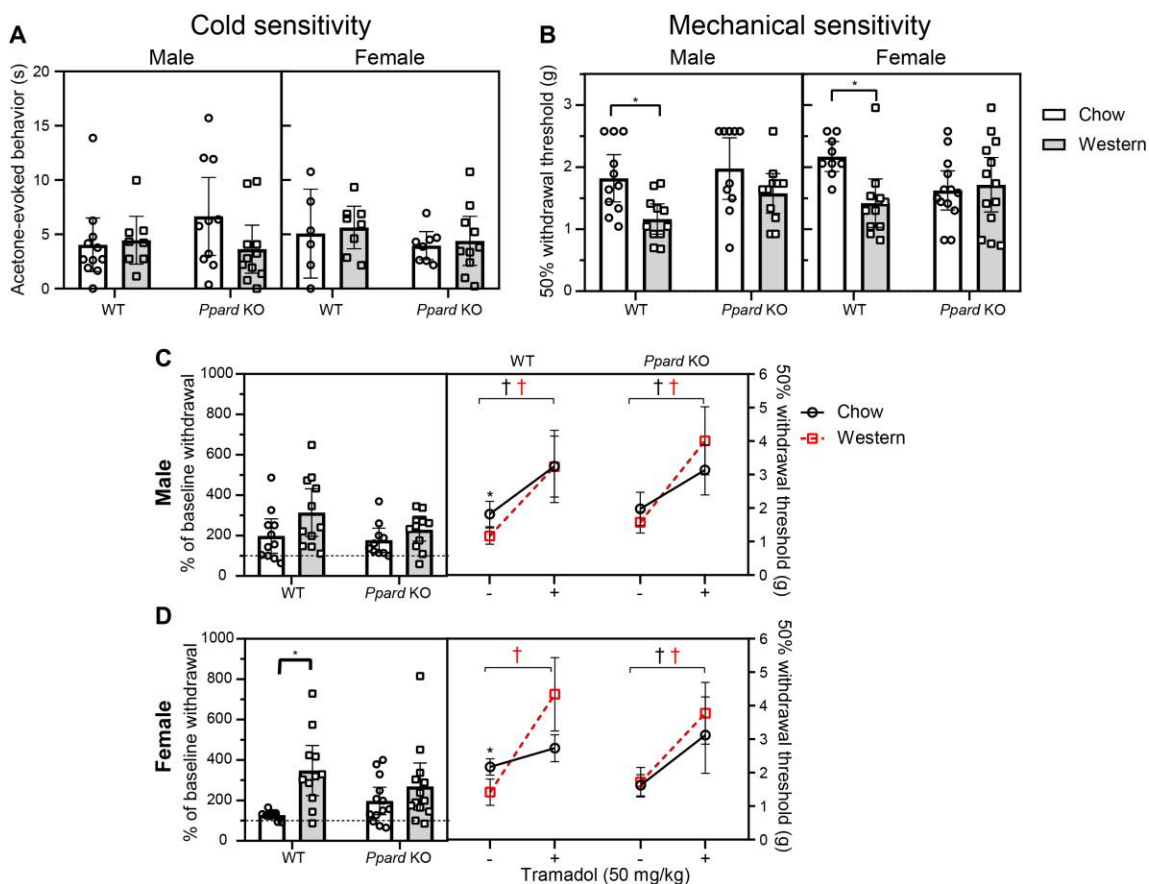


**Figure 4.8: Diet-induced obesity increases sensitivity to mechanical stimuli in wild-type mice.**

(A) Sensitivity to cold was assessed by measuring the time spent in behavior evoked by evaporative cooling of acetone following application to the ventral surface of the hind paw. No differences were detected between any of the groups. (B) Mechanical sensitivity of the hind paw was assessed by manual application of Von Frey Filaments using the Chaplin up-down method. Male and female wild-type (WT) mice fed the western diet showed increased mechanical sensitivity compared to chow-fed controls, indicated by a decreased tactile response threshold. Mechanical hypersensitivity was not detected following consumption of the western diet in PPAR $\delta$  knockout (*Ppard* KO) mice. To determine whether mechanical sensitivity was associated with pain, the assay was repeated on all mice after receiving a dose of the weak opioid tramadol (50 mg/kg I.P.). In (C) male and (D) female mice, administration of tramadol significantly decreased mechanical sensitivity; withdrawal thresholds in mice fed the western diet were not different from those of chow-fed controls. Graphs on the left show the percent of baseline, which represents the withdrawal thresholds following tramadol treatment normalized to the pre-treatment (baseline) values for each animal. Graphs on the right show the average grip force (g) for mice in each group in the absence and following administration of tramadol.  $n=9-13$  animals per sex, genotype, and diet. Data are plotted mean  $\pm$  95% CI. \* $P<0.05$  between diets in each treatment group; † indicates significant ( $P<0.05$ ) tramadol-induced differences in withdrawal threshold for mice fed the chow (black) or western (red) diet by 2-way ANOVA with Tukey's test.

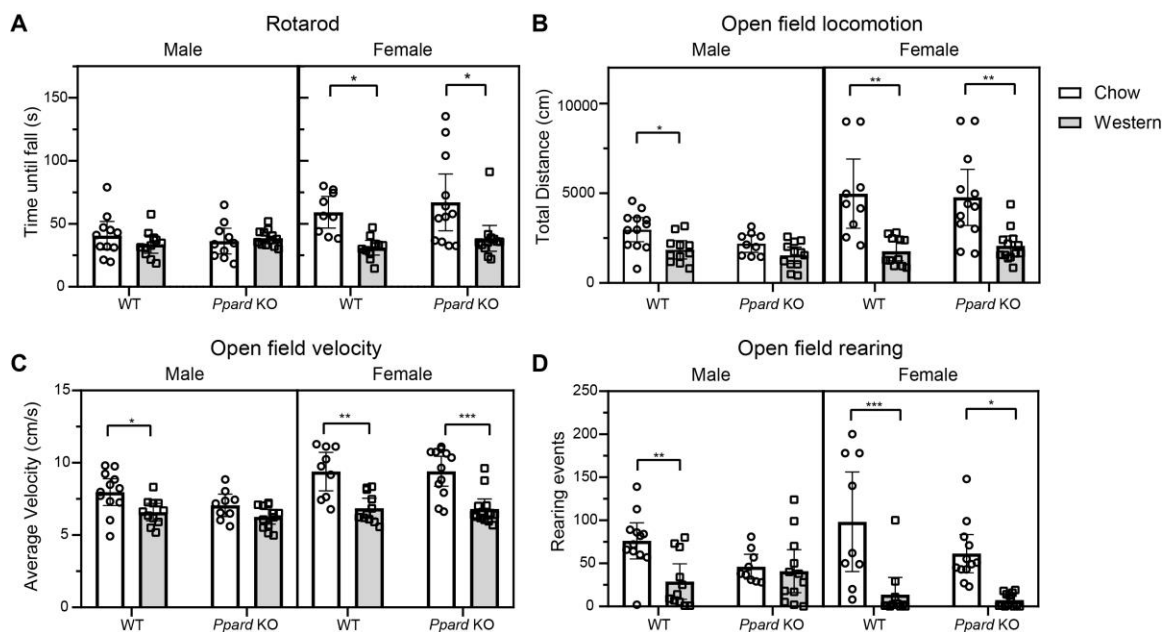


**Figure 4.9: Diet-induced obesity affects physical function and locomotion.**

(A) Locomotor capacity was assessed using an accelerating rotarod assay. No significant differences were seen in male mice between diet groups or genotypes. In female mice, obesity induced by the western diet was associated with decreased motor function in both wild-type (WT) and PPAR $\delta$  knockout (*Ppard* KO) mice compared to chow-fed controls. (B-D) Spontaneous activity was measured over 30 min in open field. No differences in spontaneous activity were observed between WT and *Ppard* KO mice. Compared to chow-fed controls, WT male mice fed the western diet showed reduction in distance and velocity of locomotion as well as vertical activity (rearing); changes not observed in *Ppard* KO mice. Compared to chow-fed controls, female WT and *Ppard* KO mice fed the western diet showed reduction in distance and velocity of locomotion as well as vertical activity (rearing). n=9-13 animals per sex, genotype, and diet. Data are plotted mean  $\pm$  95% CI. \* $P$ <0.05, \*\* $P$ <0.01, \*\*\* $P$ <0.001 by 2-way ANOVA with Tukey's test.

with a significantly decreased time to fall compared to chow fed controls, for both WT and *Ppard* KO mice (**Figure 4.9A**).

Spontaneous locomotion in open field was also assessed for all mice over a 30 min period. Loss of PPAR $\delta$  did not alter total locomotion, velocity of movement or rearing in either male or female mice (**Figure 4.9B-D**). Male WT mice fed the western diet showed a significant decrease in total distance travelled (**Figure 4.9B**), average velocity (**Figure 4.9C**), and the number of rearing events (**Figure 4.9D**) compared to sex-matched chow fed controls. However, these differences were not observed in male *Ppard* KO mice. In females, both WT and *Ppard* KO mice fed the western diet showed significant decreases in the total distance travelled, average velocity, and the number of rearing events compared to sex-matched chow fed controls (**Figure 4.9B-D**). These data suggest that diet-induced obesity impairs physical function in female, and to a lesser degree, in male mice.

#### 4.5.10 Statistical modeling

To account for the large amount of variability within the data and outcome measures assessed in the diet study, linear regression modeling was conducted to assess whether sex, genotype or diet were predictors of the behavioral, histological, and molecular differences observed (**Table 4.1**). Bivariate modeling demonstrated that the western diet alone was a significant predictor of all behavioral alterations except for cold sensitivity, as well as histopathological degeneration of the knee and alterations in extracellular matrix gene expression in the IVD (**Table 4.1**). Sex was found to be an independent predictor of rotarod performance, spontaneous locomotion, histopathological changes to the IVD, and expression of inflammatory and matrix degrading enzymes (*Mmp3*, *Mmp13*, *Adamts4*, *Il-1b*, *Bdnf*). When sex, genotype and diet were adjusted for using multivariate analysis,

**Table 4.1: Impact of sex, genotype, and diet on behavioral, molecular and histological changes.**

Parameter	Bivariate (r)			Multivariate ( $\beta$ , $r^2$ )			
	Sex	Genotype	Diet	Sex ( $\beta$ )	Genotype ( $\beta$ )	Diet ( $\beta$ )	Whole Model ( $r^2$ )
<b>Behavioral</b>							
Von Frey	0.03	0.10	<b>-0.28**</b>	0.03	0.13	<b>-0.35**</b>	<b>0.09*</b>
Grip force	0.09	0.17	<b>-0.57***</b>	2.35	5.36 (p=0.057)	<b>-18.44***</b>	<b>0.36***</b>
Acetone	0.02	0.017	0.10	-	-	-	0.01
Rotarod	<b>0.22*</b>	0.152	<b>-0.33**</b>	<b>10.22*</b>	6.93	<b>-15.47***</b>	<b>0.18***</b>
<b>Open field</b>							
Total Distance	<b>-0.31**</b>	-0.04	<b>-0.52***</b>	<b>1150.18***</b>	-154.69	<b>-1935.68***</b>	<b>0.37***</b>
Rearing	-0.09	-0.19	<b>-0.51***</b>	-6.39	-15.85 (p=0.06)	<b>-45.92***</b>	<b>0.30***</b>
Velocity	<b>0.29**</b>	0.12	<b>-0.48***</b>	<b>1.70***</b>	-0.71	<b>-2.74***</b>	<b>0.34***</b>
<b>Histopathology</b>							
L6S1 Boos	<b>0.323**</b>	0.17	0.21 (p=0.056)	<b>1.67**</b>	0.82	<b>1.08*</b>	<b>0.17**</b>
Average Boos	0.05	0.19	0.18	-	-	-	0.07
Cumulative OARSI score	-0.22	0.28	<b>0.53***</b>	<b>-9.97*</b>	<b>9.83*</b>	<b>19.53***</b>	<b>0.40***</b>
<b>Gene expression</b>							
<i>Col1a1</i>	0.09	0.11	0.06	-	-	-	0.02
<i>Col2a1</i>	0.08	0.23	<b>0.27*</b>	3.51	13.39	<b>16.12*</b>	<b>0.13*</b>
<i>Acan</i>	0.22	0.18	<b>0.34**</b>	16.09	13.09	<b>27.00**</b>	<b>0.19**</b>
<i>Mmp3</i>	<b>0.89***</b>	0.08	0.12	<b>62.14***</b>	1.60	6.03	<b>0.81***</b>
<i>Mmp13</i>	<b>-0.84***</b>	0.14	0.06	<b>-1.38***</b>	<b>0.31**</b>	0.15	<b>0.75***</b>
<i>Adams4</i>	<b>-0.85***</b>	0.03	0.03	<b>-118.19***</b>	3.75	8.29	<b>0.72***</b>
<i>Il-1b</i>	<b>0.65***</b>	0.11	0.16	<b>4.44***</b>	0.49	0.99	<b>0.45***</b>
<i>Il-6</i>	0.13	0.07	0.17	-	-	-	0.06
<i>Bdnf</i>	<b>-0.42***</b>	0.03	0.23	<b>-48.38***</b>	0.07	<b>27.11*</b>	<b>0.23**</b>

similar trends were seen for all the outcomes measured, with sex and diet being covariates for many behavioral and histological outcomes. Focusing on histological outcomes, sex, diet, and genotype were all significant predictors of histopathological knee OA, while sex and diet were significant predictors of IVD degeneration (**Table 4.1**). In addition to looking at the association between sex, diet, and genotype on behavioral outcomes, we wanted to determine whether histopathological joint damage was predictive of pain-related behavior, independent of sex, diet, and genotype. To do so we constructed another bivariate and multivariate linear regression model (**Table 4.3, Supplementary Table 2**), and this analysis indicated that knee OA was associated with alterations to grip force and differences in spontaneous locomotion; however, IVD degeneration was not significantly associated with any of these behavioral outcomes.

## 4.6 Discussion

Previous research suggests that the nuclear receptor PPAR $\delta$  plays a catabolic role in articular cartilage, and that genetic deletion protects against both post-traumatic and age-associated OA<sup>35,55</sup>. Our study represents the first examination of the role of PPAR $\delta$  in the IVD and the role of PPAR $\delta$  in an obesity-induced model of IVD degeneration and osteoarthritis. The present study shows that PPAR $\delta$  is expressed and functionally active in the IVD. We evaluated the effect of PPAR $\delta$  inactivation on age- and obesity-associated IVD degeneration *in vivo* using *Col2-Cre;Ppard<sup>f/f</sup>* mice to delete PPAR $\delta$  within the NP and inner AF. With age, *Ppard* KO mice showed considerably less IVD degeneration than WT controls, yet in a western diet-induced obesity model, *Ppard* KO mice showed a higher proportion of moderate-severe IVD degeneration compared to WT animals. Moreover, loss of PPAR $\delta$  in joint tissues appeared to modulate behavioral indicators of pain and physical

function. Taken together, these findings illustrate a complex, and likely context-dependent role of PPAR $\delta$  in the IVD and articular cartilage.

A member of the nuclear receptor superfamily, PPAR $\delta$  acts as a transcription factor whose ligands are fatty acids and their metabolites, ultimately altering transcription of downstream target genes<sup>33,56</sup>. Previous studies have highlighted common downstream targets of PPAR $\delta$  in chondrocytes as well as other tissues including *Pdk4* and *Angptl4*<sup>36,57</sup>, which we showed were induced in IVD explants treated with the PPAR $\delta$  agonist GW501516. These findings indicate that PPAR $\delta$  is functionally active in the IVD. In articular cartilage explants, PPAR $\delta$  agonism induces proteoglycan degradation, mediated through upregulation of matrix degrading enzymes including *Mmp3* and *Adamts5*<sup>35</sup>. Although, IVD explants treated with the PPAR $\delta$  agonist showed a loss of safranin-O staining within the NP, no significant differences were seen in the expression of any matrix degrading enzymes investigated. These findings may be impacted by the use of intact IVDs in organ culture and potential differential effects of PPAR $\delta$  agonism in its distinct tissue types. Anatomically, the IVD is a heterogeneous structure composed of three distinct, yet interdependent tissues: the gelatinous nucleus pulposus (NP), the fibrocartilaginous annulus fibrosus (AF), and cartilage endplates. In adults, the major cell type of the NP are chondrocyte-like NP cells, which secrete a matrix very similar to that of articular cartilage, in contrast to AF cells which are phenotypically more similar to fibroblasts<sup>58</sup>. Gene expression analysis in the current study demonstrated that *Ppard* expression is significantly higher in the AF than in the NP, highlighting the need to evaluate the effect of PPAR $\delta$  activation in each tissue type independently.

Previous work by our group demonstrated that deletion of PPAR $\delta$  in articular cartilage protects against both surgically-induced<sup>35</sup>, and age-associated knee OA<sup>55</sup>. Consistent with these findings, deletion of PPAR $\delta$  within the IVD appears to protect from age associated IVD degeneration, largely within the NP. In our current study, analysis of whole IVD gene expression at 14 months-of-age (a timepoint not associated with histopathological change) showed increased expression of aggrecan as well as genes involved in matrix degradation (*Mmp3*, *Mmp13*) and inflammation (*Il-1b*) in male *Ppard* KO mice. While these results suggest early degenerative changes, inhibitors of IL-1 $\beta$  signaling and matrix metalloproteinases significantly impact the effects of these proteins<sup>59,60</sup>, and their expression levels were not quantified and may counteract this increased expression. Further studies are however required to examine the underlying mechanisms behind this protective effect, specifically focused on characterizing molecular changes within IVD sub-compartments in *Ppard* KO mice over time.

Given the protective effect of PPAR $\delta$  deletion in age-associated IVD degeneration, we wanted to determine whether this phenotype would be recapitulated in a model of diet-induced obesity. Since PPAR $\delta$  ligands are dysregulated in obesity<sup>33</sup> we postulated that its deletion would protect against both obesity-induced IVD degeneration and osteoarthritis. In contrast to our hypothesis, our findings demonstrated that western diet-induced obesity accelerated IVD degeneration in male *Ppard* KO mice. Moreover, a greater proportion of male *Ppard* KO mice fed the western diet showed severe degeneration than did male WT mice fed the western diet, although these differences were not significant. Like in the IVD, western diet-induced obesity accelerated OA progression in both WT and *Ppard* KO mice. Although histopathological scores of OA severity were not different between *Ppard* KO

and WT mice on the western diet, statistical modeling identified genotype as a significant predictor of knee joint damage when sex and diet were accounted for. Taken together, these findings underscore a context dependent role for PPAR $\delta$  in joint degeneration.

While the exact role of PPAR $\delta$  is not known in the IVD, PPAR $\delta$  activation regulates the transcription of many genes involved with lipid metabolism in chondrocytes, including enzymes associated with fatty acid oxidation<sup>35,36</sup>. These studies postulated that in a post-traumatic model of OA, PPAR $\delta$ -mediated cartilage degeneration may result from increased production of reactive oxygen species (ROS) as a consequence of increased fatty acid oxidation<sup>35</sup>. While this increase in ROS production may be detrimental to cartilage or the IVD under physiological conditions, PPAR $\delta$ -mediated lipid catabolism may be essential in pathological conditions such as obesity. Studies investigating the role of diet-induced obesity determined that free fatty acids induce lipotoxicity in chondrocytes leading to cell death<sup>61</sup>. As a major regulator of lipid metabolism, PPAR $\delta$  may directly contribute to the prevention of lipotoxicity. Supporting this, studies in human skeletal muscle cells demonstrated that PPAR $\delta$  activation prevents lipotoxicity, through reductions in fatty-acid induced inflammation and endoplasmic reticulum stress<sup>62</sup>. In addition to the direct effects of PPAR $\delta$  deletion, alterations in PPAR $\alpha$  and PPAR $\gamma$  signaling should also be considered, as share common ligands with PPAR $\delta$  and therefore may contribute to obesity-induced changes in joint tissues<sup>63</sup>. Together, these putative mechanisms may contribute to the context-specific role demonstrated for PPAR $\delta$  in joint degeneration.

Although there are many similarities in the initiation and progression of IVD degeneration and OA (as reviewed in<sup>18</sup>), our data highlights important differences. Consistent with our previous study in wild-type mice<sup>64</sup>, animals fed a western diet often showed moderate to



severe knee OA compared to chow control, while alterations to the IVD were subtle and histopathological degeneration was localized to a single spinal level (L6-S1). In the knee, metabolic alterations associated with obesity are postulated to be the major contributor to joint degeneration. Supporting this, leptin deficient mice become obese yet do not develop knee OA, suggesting that systemic factors may play a key role in obesity-induced OA<sup>65</sup>. In the IVD, the relative contributions of mechanical and metabolic factors to obesity-induced degeneration remain unknown. While speculative, the data from the current study suggests that biomechanical factors may play a more substantial role in obesity-associated IVD degeneration. In this study, obesity-induced histopathological IVD degeneration was localized to the lowest lumbar spinal level (L6-S1). In humans, accelerated IVD degeneration at the lumbosacral joint (L5S1) is attributed to increased mechanical loading at this site<sup>66</sup>. If systemic factors were the major contributor to obesity-associated IVD degeneration in our model, we would expect to see a more homogenous pattern of IVD degeneration at multiple spinal levels; observations not seen in the current study. However, the analysis of IVD degeneration was limited to a single timepoint in the current study and it may be that generalized IVD degeneration may follow a more chronic exposure to the obesogenic diet. It should also be noted that in addition to altered mechanical loading, the size and geometry of IVDs differ based on spinal levels<sup>67</sup>, which may impact the diffusion of nutrients and systemic molecules into the IVD thereby impacting levels of systemic metabolic effectors. Future studies should explore the relative contributions of mechanical and metabolic factors in the development of obesity-induced IVD degeneration and back pain.

Despite the utility of using rodent models to study IVD biology, few studies also assess the clinical problem associated with IVD degeneration - pain<sup>68</sup>. In humans and animals, there is often a discord between radiographic IVD degeneration and pain<sup>69,70</sup>. For example, two animals may have equally degenerative IVDs, yet have different pain-related behaviors<sup>70</sup>. Although pain cannot be directly measured in animals, several indirect, quantitative behavioral assays have been developed to evaluate pain-like behaviors for distinct pain states<sup>71,72</sup>. While many behavioral metrics are non-specific and are used to assess OA pain<sup>73</sup>, stretch-induced axial discomfort is a validated measure of axial low back pain<sup>50</sup>. In the current model, western diet induced obesity was associated with stretch-induced axial discomfort in female mice fed the western diet, measured using the modified grip force assay. To determine whether these differences were truly a measure of pain, mice were treated with Tramadol, a centrally acting opioid analgesic previously shown to improve grip strength and mechanical hypersensitivity in other pain models<sup>74-76</sup>. However, in the current study, obesity-associated differences in grip force were not altered by tramadol. Since grip force is also used to assess muscle strength<sup>77</sup>, and neuromuscular deficits have been suggested as an initiating factor in obesity-induced OA<sup>21</sup>, we postulate that obesity-induced neuromuscular deficits may contribute to the behavioral differences observed and should be further explored in the context of IVD degeneration and back pain.

Obesity induced by the western diet in WT mice was also associated with mechanical, but not thermal hypersensitivity of the hind paw; findings that were consistent with previous work from our group<sup>64</sup>. Mechanical sensitivity was inhibited by tramadol, indicating that these behavioral differences were likely as a result of pain. Interestingly, *Ppard* KO mice did not show obesity-induced mechanical sensitivity, despite having increased prevalence

of IVD degeneration and knee OA. While the mechanisms underlying this phenotype in *Ppard* KO mice are not understood, previous work done by our group has demonstrated that subcutaneous injection of a PPAR $\delta$  antagonist reduced pain-related behaviors in a surgically-induced model of OA, despite not improving structural joint degeneration<sup>78</sup>. Together, these findings demonstrate that western diet-induced obesity induces pain related behavior in mice, and intriguingly, that loss of PPAR $\delta$  in joint tissues may modulate this outcome.

Our study also demonstrated that obesity-induced pain behaviors were more consistent in female compared to male mice. These findings are supported by both clinical and basic research, which show that the prevalence of chronic pain is higher in females than males<sup>79</sup>. While several underlying mechanisms have been suggested, including cognitive and sociocultural differences, differences in gonadal sex hormones also play a biological role in pain<sup>79</sup>. Several studies establish the pro-nociceptive role of estrogen that is mediated through its receptors, estrogen receptor  $\alpha$  (ER $\alpha$ ) and estrogen receptor  $\beta$  (ER $\beta$ )<sup>80</sup>. In normal mice and in a model of inflammatory pain, global deletion of ER $\alpha$  or ER $\beta$  eliminated underlying sex differences seen in mechanical sensitivity<sup>80</sup>. In addition to the sexual dimorphism observed in pain-related behaviors, sex differences were also seen in the progression of structural IVD degeneration induced by the western diet. Male mice fed the western diet showed accelerated IVD degeneration compared to chow controls; a result not observed in female mice. While the underlying mechanism are currently unknown, previous studies have illustrated that female mice fed a high-fat diet have an increased capacity for adipocyte enlargement, resulting in reduced adipose tissue inflammation, fat deposition in non-adipose tissues, and better insulin sensitivity compared to male mice<sup>81</sup>.

These sex-dependent metabolic phenotypes may modulate the systemic effects of obesity and thereby alter the progression of structural IVD degeneration. Furthermore, sex may also impact PPAR $\delta$  signaling. Estrogen receptors (ER $\alpha$ , ER $\beta$ ) can inhibit PPAR $\alpha$  and PPAR $\gamma$  signaling through competitive binding of hormone response elements and reduced availability of coactivators<sup>82,83</sup>. Although not examined to date, a similar interaction may exist between estrogen receptors and PPAR $\delta$ , potentially impacting the results of this study.

Taken together, this study highlights the complex, and context-dependent role of PPAR $\delta$  within the IVD and joint tissues. Our analysis demonstrates that deletion of PPAR $\delta$  in cartilaginous tissues plays a protective role in age-associated IVD degeneration yet does not protect against obesity-associated IVD degeneration or osteoarthritis. These findings underscore potential differences in the pathogenesis of joint degeneration and associated pain based on the underlying cause. As many promising basic science discoveries fail to enter clinical use<sup>84</sup>, these differences should be further explored in the context of IVD degeneration and applied to clinical trials and basic research.

## 4.7 Supplementary Figures

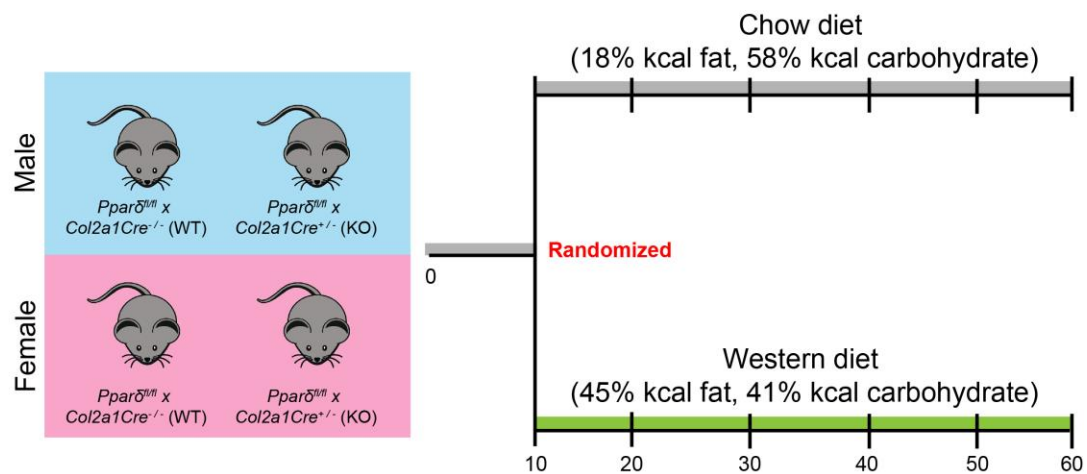


**Figure 4.10, Supplementary Figure 1: Schematic overview of PPAR $\delta$  diet study design.**

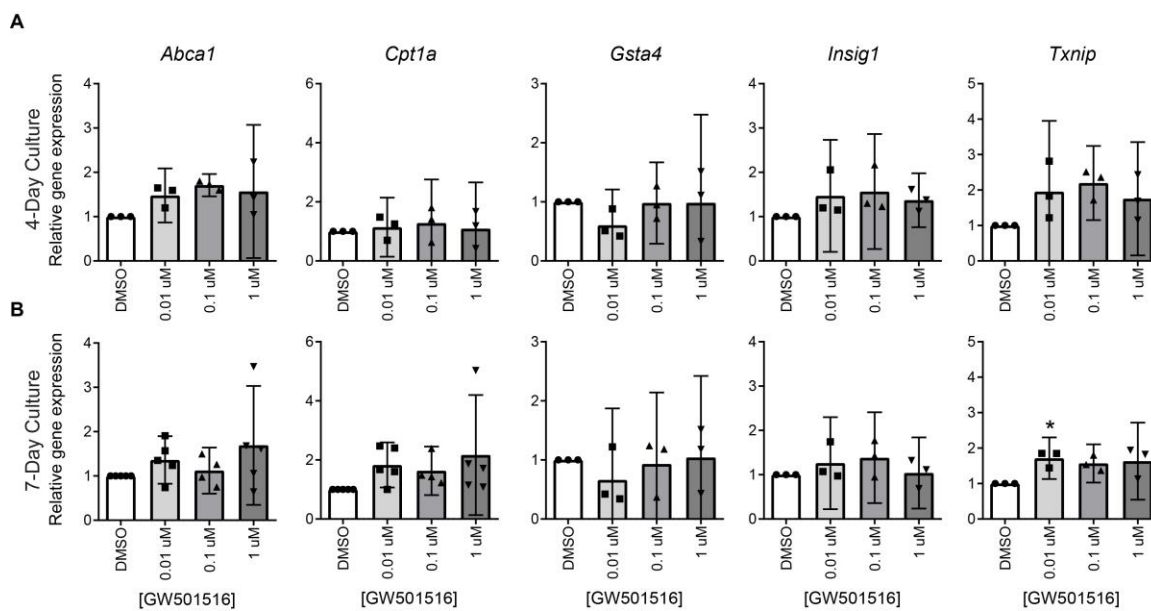


**Figure 4.11, Supplementary Figure 2: Effect of PPAR $\delta$  activation on metabolic gene expression in IVD explant cultures.**

SYBR-based real-time qPCR analysis of gene expression in IVD explants incubated for (A) 4 days or (B) 7 days with increasing concentrations of the PPAR $\delta$  agonist GW501516. Expression of *Abca1*, *Cpt1a*, *Gsta4*, and *Insig1* were not altered by PPAR $\delta$  agonist treatment at either time point. After 7 days of treatment, a significant increase in the expression of *Txnip* was induced by 0.01  $\mu\text{M}$  agonist treatment. Values are represented as the mean  $\pm$  SEM. (n= 3-5 independent trials). \* $P$ <0.05 compared to DMSO control by one-way ANOVA with Tukey's test.

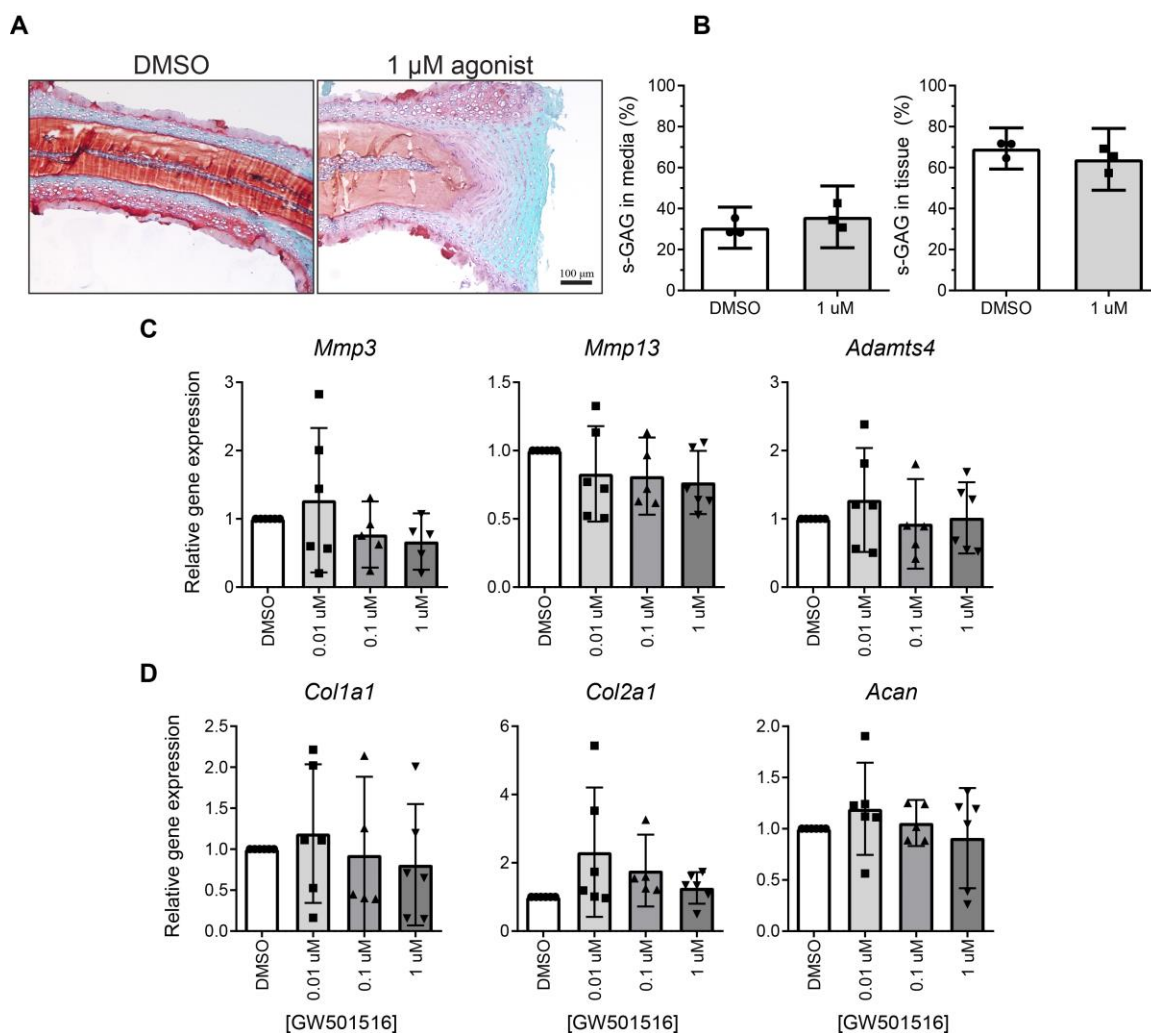


**Figure 4.12, Supplementary Figure 3: Effect of PPAR $\delta$  agonism on extracellular matrix in IVD explant cultures.**

(A) Representative sections of IVD explants treated for 4 days with DMSO or 1  $\mu$ M PPAR $\delta$  agonist GW501516 stained with Safranin-O/Fast Green. Explants treated with GW501516 show less intense safranin-o staining within the NP, suggesting proteoglycan loss. (B) The amount of sulfated glycosaminoglycan (s-GAG) released into the media and remaining within IVD explants was quantified using the dimethylmethylene blue assay. Data is presented as mean  $\pm$  95% CI (n= 3 independent trials, P < 0.05 versus DMSO). SYBR-based qPCR analysis of (C) matrix remodeling genes and (D) extracellular matrix genes in IVD explants after 4 days incubation with GW501516 or vehicle control (DMSO). No significant difference in gene expression was detected for any of the genes investigated. Expression was normalized to the expression of the house-keeping gene *Rps29* and expressed relative to DMSO control. Data is presented as mean  $\pm$  95% CI (n= 5-6 independent trials, P < 0.05 versus DMSO).

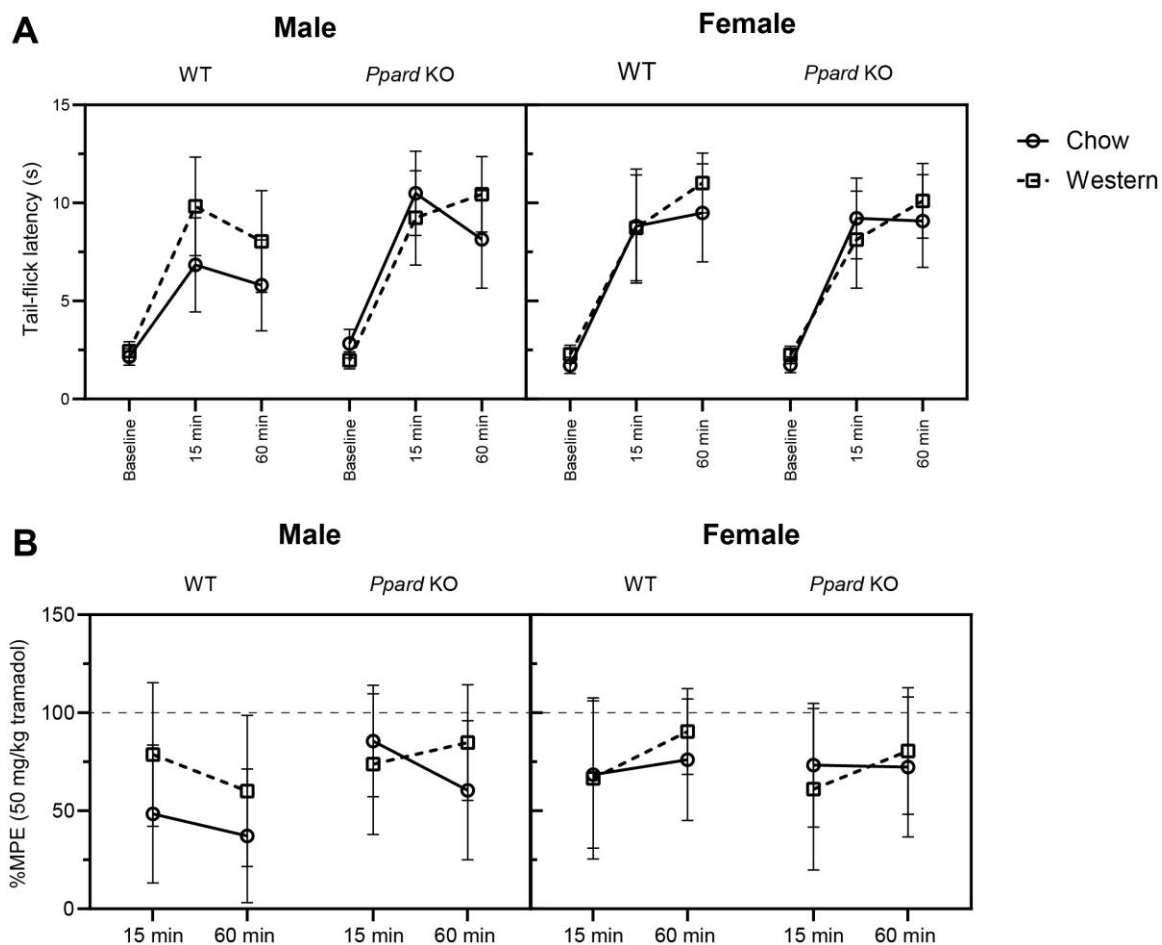


**Figure 4.13, Supplementary Figure 4: Tail Flick assay.**

To determine the anti-nociceptive response of tramadol, the latency of the tail flick response was assessed prior to (baseline) and after IP injection of tramadol (50 mg/kg). (A) The tail flick response was elicited by applying radiant heat to the tip of the tail and the withdrawal time recorded. A cutoff time of 12 seconds was used to avoid tissue injury. (B) The response to thermal stimulation was plotted as the percentage of maximal possible effect (%MPE) which is calculated as  $[(T_1 - T_0)/(T_2 - T_0)] \times 100$ .  $T_0$  and  $T_1$  were the tail flick latency times before and after administration of tramadol and  $T_2$  is the cutoff time. No significant differences were seen between any condition.  $n=9-13$  animals per sex, genotype, and diet. Data are plotted mean  $\pm$  95% CI.



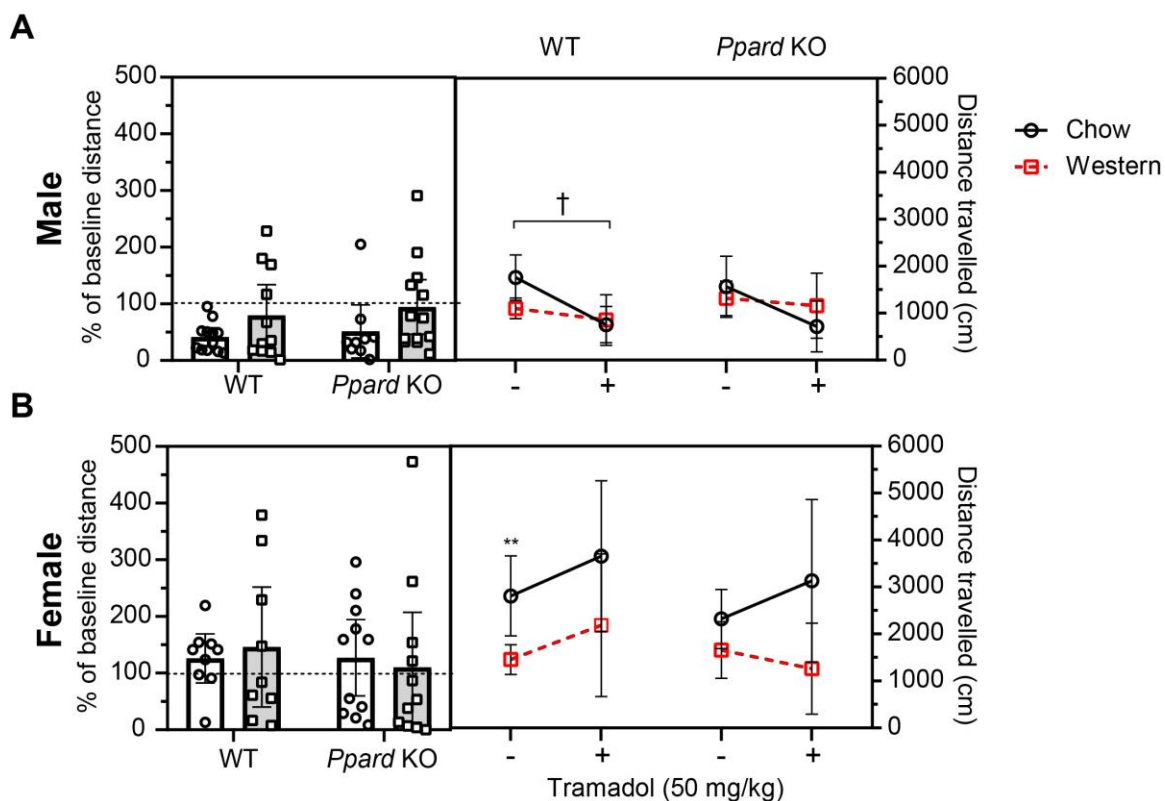


**Figure 4.14, Supplementary Figure 5: Tramadol induced a slight sedative effect in male mice.**

Spontaneous locomotion was measured over 10 min to assess the sedative effects of tramadol. (A) In male mice, tramadol (50 mg/kg I.P.) had a slight sedative effect leading to reduced spontaneous movement in both diet conditions, a change detected to a greater extent in chow-fed mice compared to mice fed the western diet. (B) In female mice, average spontaneous locomotion increased with the addition of tramadol. Graphs on the left show the percent of baseline, which represents the distance travelled following tramadol treatment normalized to the pre-treatment (baseline) values for each animal. Graphs on the right show the distance travelled for mice in each group in the absence and following administration of tramadol.  $n=9-13$  animals per sex, genotype, and diet. Data are plotted mean  $\pm$  95% CI. \*\* $P<0.01$  between diets in each treatment group; † indicates significant ( $P<0.05$ ) tramadol-induced differences in distance travelled for mice fed the chow (black) or western (red) diet by 2-way ANOVA with Tukey's test.

**Table 4.2, Supplementary Table 1: Realtime qPCR primer sequences**

	<b>Primer Sequence 5' → 3'</b>
<i>Pdk4 Fwd</i>	CCGCTTAGTGAACACTCCTTC
<i>Pdk4 Rev</i>	TGACCAGCGTGTCTACAAACT
<i>Angptl4 Fwd</i>	CATCCTGGGACGAGATGAACT
<i>Anptl4 Rev</i>	TGACAAGCGTTACCACAGGC
<i>Cidea Fwd</i>	TGGAAAAGGGACAGAAATGG
<i>Cidea Rev</i>	TCTCGTACATCGTGGCTTTG
<i>Ppard Fwd</i>	TCCATCGTCAACAAAGACGGG
<i>Ppard Rev</i>	ACTTGGGCTCAATGATGTCAC
<i>Coll1a1 Fwd</i>	CTGGCGGTTTCAGGTCCAAT
<i>Coll1a1 Rev</i>	TCCAGGCAATCCAGGAGC
<i>Col2a1 Fwd</i>	GCACATCTGGTTTGGAGAGACC
<i>Col2a1 Rev</i>	TAGCGGTGTTGGGAGCCA
<i>Acan Fwd</i>	CTGGGATCTACCGCTGTGAAG
<i>Acan Rev</i>	GTGTGGAAATAGCTCTGTAGTGGAA
<i>Mmp3 Fwd</i>	TTGTCCCGTTTCCATCTCTCTC
<i>Mmp3 Rev</i>	TTGGTGATGTCTCAGGTTCCAG
<i>Mmp13 Fwd</i>	CTTCTTCTTGTTGAGCTGGAACTC
<i>Mmp13 Rev</i>	CTCTGTGGACCTCACTGTAGACT
<i>Adamts4 Fwd</i>	GAGGAGGAGATCGTGTTTCCAG
<i>Adamts4 Rev</i>	CAAACCCTCTACCTGCACCC
<i>Il-1b Fwd</i>	CCCTGCAGCTGGAGAGTGTGGA
<i>Il-1b Rev</i>	TGTGCTCTGCTTGTGAGGTGCTG
<i>Il6 Fwd</i>	TCTCTGCAAGAGACTTCCATCCAGT
<i>Il6 Rev</i>	AGTAGGGAAGGCCGTGGTTGTCA
<i>Bdnf Fwd</i>	TCATACTTCGGTTGCATGAAGG
<i>Bdnf Rev</i>	GACCTCTCGAACCTGCCC
<i>Adamts5 Fwd</i>	GGAGCGAGGCCATTTACAAC
<i>Adamts5 Rev</i>	GCGTAGACAAGGTAGCCCACTTT
<i>Abca1 Fwd</i>	GCTACCCACCCTACGAACAA
<i>Abca1 Rev</i>	GGAGTTGGATAACGGAAGCA
<i>Cpt1a Fwd</i>	TCAATCGGACCCTAGACACC
<i>Cpt1a Rev</i>	TGGTAGGAGAGCAGCACCTT
<i>Gsta4 Fwd</i>	GCTGGAGTGGAGTTTGAGGA
<i>Gsta4 Rev</i>	TGTGTCAGCATCATCCCATC
<i>Insig1 Fwd</i>	GACGAGGTGATAGCCACCAT
<i>Insig1 Rev</i>	TGGCCATTCTCTCTTGAAC
<i>Txnip Fwd</i>	GGTCTCAGCAGTGCAAACAG
<i>Txnip Rev</i>	AGCTCGAAGCCGAACTTGTA

**Table 4.3, Supplementary Table 2. Association between behavioral indicators of pain and histological joint damage.**

Parameter	Bivariate (r)		Multivariate ( $\beta$ , $r^2$ )		
	IVD degeneration	Knee OA	IVD degeneration ( $\beta$ )	Knee OA ( $\beta$ )	Whole model
<b>Behavioral</b>					
Von Frey	0.08	0.25	-	-	0.07
Grip Force	-0.16	<b>-0.56***</b>	-0.64	<b>-0.45***</b>	<b>0.32***</b>
Acetone	0.06	0.01	-	-	0.002
Rotarod	0.10	0.20	-	-	0.04
<b>Open field</b>					
Total Distance	-0.13	<b>-0.41**</b>	-403.8	<b>-44.0**</b>	<b>0.19*</b>
Rearing	0.12	<b>0.33*</b>	-	-	0.13
Velocity	0.09	<b>-0.49***</b>	0.06	<b>-0.08***</b>	<b>0.24**</b>

## 4.8 References

1. Global Burden of Disease Study C. Global, regional, and national incidence, prevalence, and years lived with disability for 301 acute and chronic diseases and injuries in 188 countries, 1990-2013: a systematic analysis for the Global Burden of Disease Study 2013. *Lancet*. 2015;386(9995):743-800. doi:10.1016/S0140-6736(15)60692-4
2. Cassidy JD, Carroll LJ, Côté P. The Saskatchewan health and back pain survey: The prevalence of low back pain and related disability in Saskatchewan adults. *Spine (Phila Pa 1976)*. 1998. doi:10.1097/00007632-199809010-00012
3. Roelofs PDDM, Deyo RA, Koes BW, Scholten RJPM, Van Tulder MW. Nonsteroidal anti-inflammatory drugs for low back pain: An updated cochrane review. *Spine (Phila Pa 1976)*. 2008. doi:10.1097/BRS.0b013e31817e69d3
4. DePalma MJ, Ketchum JM, Saullo T. What is the source of chronic low back pain and does age play a role? *Pain Med*. 2011;12(2):224-233. doi:10.1111/j.1526-4637.2010.01045.x
5. Schwarzer AC, Aprill CN, Derby R, Fortin J, Kine G, Bogduk N. The relative contributions of the disc and zygapophyseal joint in chronic low back pain. *Spine (Phila Pa 1976)*. 1994;19(7):801-806. doi:10.1097/00007632-199404000-00013
6. Modic MT, Ross JS. Lumbar degenerative disk disease. *Radiology*. 2007;245(1):43-61. doi:10.1148/radiol.2451051706
7. Adams M, Roughley PJ. What is intervertebral disc degeneration, and what causes it? *Spine (Phila Pa 1976)*. 2006. doi:10.1097/01.brs.0000231761.73859.2c
8. Zhao CQ, Wang LM, Jiang LS, Dai LY. The cell biology of intervertebral disc aging and degeneration. *Ageing Res Rev*. 2007;6(3):247-261. doi:10.1016/j.arr.2007.08.001
9. Battie MC, Videman T, Parent E. Lumbar disc degeneration: epidemiology and genetic influences. *Spine (Phila Pa 1976)*. 2004;29(23):2679-2690. <http://www.ncbi.nlm.nih.gov/pubmed/15564917>.
10. Kelsey JL, Githens PB, White 3rd AA, et al. An epidemiologic study of lifting and twisting on the job and risk for acute prolapsed lumbar intervertebral disc. *J Orthop Res*. 1984;2(1):61-66. doi:10.1002/jor.1100020110
11. Blüher M. Obesity: global epidemiology and pathogenesis. *Nat Rev Endocrinol*. 2019. doi:10.1038/s41574-019-0176-8
12. DM U, I K, K T, et al. Obesity is associated with reduced disc height in the lumbar spine but not at the lumbosacral junction. *Spine (Phila Pa 1976)*. 2014;39(16):E962-6. doi:10.1097/BRS.0000000000000411.

13. Liuke M, Solovieva S, Lamminen A, et al. Disc degeneration of the lumbar spine in relation to overweight. *Int J Obes*. 2005;29(8):903-908. doi:10.1038/sj.ijo.0802974
14. Hussain SM, Urquhart DM, Wang Y, et al. Fat mass and fat distribution are associated with low back pain intensity and disability: Results from a cohort study. *Arthritis Res Ther*. 2017. doi:10.1186/s13075-017-1242-z
15. Dario AB, Ferreira ML, Refshauge KM, Lima TS, Ordonana JR, Ferreira PH. The relationship between obesity, low back pain, and lumbar disc degeneration when genetics and the environment are considered: a systematic review of twin studies. *Spine J*. 2015;15(5):1106-1117. doi:10.1016/j.spinee.2015.02.001
16. Ruiz-Fernández C, Francisco V, Pino J, et al. Molecular relationships among obesity, inflammation and intervertebral disc degeneration: Are adipokines the common link? *Int J Mol Sci*. 2019. doi:10.3390/ijms20082030
17. Sellam J, Berenbaum F. Is osteoarthritis a metabolic disease? *Jt Bone Spine*. 2013;80(6):568-573. doi:10.1016/j.jbspin.2013.09.007
18. Rustenburg CME, Emanuel KS, Peeters M, Lems WF, Vergroesen P-PA, Smit TH. Osteoarthritis and intervertebral disc degeneration: Quite different, quite similar. *JOR Spine*. 2018. doi:10.1002/jsp2.1033
19. Nguyen NT, Magno CP, Lane KT, Hinojosa MW, Lane JS. Association of hypertension, diabetes, dyslipidemia, and metabolic syndrome with obesity: findings from the National Health and Nutrition Examination Survey, 1999 to 2004. *J Am Coll Surg*. 2008;207(6):928-934. doi:10.1016/j.jamcollsurg.2008.08.022
20. Zhuo Q, Yang W, Chen J, Wang Y. Metabolic syndrome meets osteoarthritis. *Nat Rev Rheumatol*. 2012;8(12):729-737. doi:10.1038/nrrheum.2012.135
21. Griffin TM, Fermor B, Huebner JL, et al. Diet-induced obesity differentially regulates behavioral, biomechanical, and molecular risk factors for osteoarthritis in mice. *Arthritis Res Ther*. 2010;12(4):R130. doi:10.1186/ar3068
22. Wu CL, Jain D, McNeill JN, et al. Dietary fatty acid content regulates Wound repair and the pathogenesis of osteoarthritis following joint injury. *Ann Rheum Dis*. 2015. doi:10.1136/annrheumdis-2014-205601
23. Griffin TM, Huebner JL, Kraus VB, Yan Z, Guilak F. Induction of osteoarthritis and metabolic inflammation by a very high-fat diet in mice: effects of short-term exercise. *Arthritis Rheum*. 2012;64(2):443-453. doi:10.1002/art.33332
24. Datta P, Zhang Y, Parousis A, et al. High-fat diet-induced acceleration of osteoarthritis is associated with a distinct and sustained plasma metabolite signature. *Sci Rep*. 2017;7(1):8205. doi:10.1038/s41598-017-07963-6

25. Collins KH, Paul HA, Reimer RA, Seerattan RA, Hart DA, Herzog W. Relationship between inflammation, the gut microbiota, and metabolic osteoarthritis development: studies in a rat model. *Osteoarthr Cartil.* 2015;23(11):1989-1998. doi:10.1016/j.joca.2015.03.014
26. Botta M, Audano M, Sahebkar A, Sirtori CR, Mitro N, Ruscica M. PPAR agonists and metabolic syndrome: An established role? *Int J Mol Sci.* 2018. doi:10.3390/ijms19041197
27. Tyagi S, Gupta P, Saini A, Kaushal C, Sharma S. The peroxisome proliferator-activated receptor: A family of nuclear receptors role in various diseases. *J Adv Pharm Technol Res.* 2011. doi:10.4103/2231-4040.90879
28. Steiner G, Hamsten A, Hosking J, et al. Effect of fenofibrate on progression of coronary-artery disease in type 2 diabetes: The Diabetes Atherosclerosis Intervention Study, a randomised study. *Lancet.* 2001. doi:10.1016/S0140-6736(00)04209-4
29. Mooradian AD, Chehade J, Thurman JE. The role of thiazolidinediones in the treatment of patients with type 2 diabetes mellitus. *Treat Endocrinol.* 2002. doi:10.2165/00024677-200201010-00002
30. Vasheghani F, Monemdjou R, Fahmi H, et al. Adult cartilage-specific peroxisome proliferator-activated receptor gamma knockout mice exhibit the spontaneous osteoarthritis phenotype. *Am J Pathol.* 2013. doi:10.1016/j.ajpath.2012.12.012
31. Narkar VA, Downes M, Yu RT, et al. AMPK and PPARdelta agonists are exercise mimetics. *Cell.* 2008;134(3):405-415. doi:10.1016/j.cell.2008.06.051
32. Fan W, Waizenegger W, Lin CS, et al. PPAR $\delta$  Promotes Running Endurance by Preserving Glucose. *Cell Metab.* 2017. doi:10.1016/j.cmet.2017.04.006
33. Evans RM, Barish GD, Wang YX. PPARs and the complex journey to obesity. *Nat Med.* 2004. doi:10.1038/nm1025
34. Lee CH, Olson P, Hevener A, et al. PPAR $\delta$  regulates glucose metabolism and insulin sensitivity. *Proc Natl Acad Sci U S A.* 2006. doi:10.1073/pnas.0511253103
35. Ratneswaran A, LeBlanc EA, Walser E, et al. Peroxisome proliferator-activated receptor delta promotes the progression of posttraumatic osteoarthritis in a mouse model. *Arthritis Rheumatol.* 2015;67(2):454-464. doi:10.1002/art.38915
36. Ratneswaran A, Sun MM, Dupuis H, Sawyez C, Borradaile N, Beier F. Nuclear receptors regulate lipid metabolism and oxidative stress markers in chondrocytes. *J Mol Med.* 2017;95(4):431-444. doi:10.1007/s00109-016-1501-5
37. Risbud M V, Shapiro IM. Role of cytokines in intervertebral disc degeneration: pain and disc content. *Nat Rev Rheumatol.* 2014;10(1):44-56.

doi:10.1038/nrrheum.2013.160

38. DANCEVIC CM, McCulloch DR. Current and emerging therapeutic strategies for preventing inflammation and aggrecanase-mediated cartilage destruction in arthritis. *Arthritis Res Ther.* 2014. doi:10.1186/s13075-014-0429-9
39. Veras MA, McCann MR, Tenn NA, Séguin CA. Transcriptional profiling of the murine intervertebral disc and age-associated changes in the nucleus pulposus. *Connect Tissue Res.* 2020. doi:10.1080/03008207.2019.1665034
40. Barak Y, Liao D, He W, et al. Effects of peroxisome proliferator-activated receptor  $\delta$  on placentation, adiposity, and colorectal cancer. *Proc Natl Acad Sci U S A.* 2002. doi:10.1073/pnas.012610299
41. Terpstra L, Prud'Homme J, Arabian A, et al. Reduced chondrocyte proliferation and chondrodysplasia in mice lacking the integrin-linked kinase in chondrocytes. *J Cell Biol.* 2003. doi:10.1083/jcb.200302066
42. Stanton H, Golub SB, Rogerson FM, Last K, Little CB, Fosang AJ. Investigating ADAMTS-mediated aggrecanolysis in mouse cartilage. *Nat Protoc.* 2011. doi:10.1038/nprot.2010.179
43. McCann MR, Patel P, Pest MA, et al. Repeated exposure to high-frequency low-amplitude vibration induces degeneration of murine intervertebral discs and knee joints. *Arthritis Rheumatol.* 2015;67(8):2164-2175. doi:10.1002/art.39154
44. Pest MA, Russell BA, Zhang YW, Jeong JW, Beier F. Disturbed cartilage and joint homeostasis resulting from a loss of mitogen-inducible gene 6 in a mouse model of joint dysfunction. *Arthritis Rheumatol.* 2014;66(10):2816-2827. doi:10.1002/art.38758
45. Rutges JP, Duit RA, Kummer JA, et al. A validated new histological classification for intervertebral disc degeneration. *Osteoarthr Cartil.* 2013;21(12):2039-2047. doi:10.1016/j.joca.2013.10.001
46. Glasson SS, Chambers MG, Van Den Berg WB, Little CB. The OARSI histopathology initiative - recommendations for histological assessments of osteoarthritis in the mouse. *Osteoarthr Cartil.* 2010;18 Suppl 3:S17-23. doi:10.1016/j.joca.2010.05.025
47. Beaucage KL, Pollmann SI, Sims SM, Dixon SJ, Holdsworth DW. Quantitative in vivo micro-computed tomography for assessment of age-dependent changes in murine whole-body composition. *Bone Reports.* 2016. doi:10.1016/j.bonr.2016.04.002
48. Millecamps M, Tajerian M, Naso L, Sage EH, Stone LS. Lumbar intervertebral disc degeneration associated with axial and radiating low back pain in ageing SPARC-null mice. *Pain.* 2012;153(6):1167-1179. doi:10.1016/j.pain.2012.01.027

49. Miyagi M, Millecamps M, Danco AT, Ohtori S, Takahashi K, Stone LS. ISSLS Prize winner: Increased innervation and sensory nervous system plasticity in a mouse model of low back pain due to intervertebral disc degeneration. *Spine (Phila Pa 1976)*. 2014;39(17):1345-1354. doi:10.1097/BRS.0000000000000334
50. Millecamps M, Czerminski JT, Mathieu AP, Stone LS. Behavioral signs of axial low back pain and motor impairment correlate with the severity of intervertebral disc degeneration in a mouse model. *Spine J*. 2015;15(12):2524-2537. doi:10.1016/j.spinee.2015.08.055
51. Chaplan SR, Bach FW, Pogrel JW, Chung JM, Yaksh TL. Quantitative assessment of tactile allodynia in the rat paw. *J Neurosci Methods*. 1994. doi:10.1016/0165-0270(94)90144-9
52. Dai X, Brunson CD, Rockhold RW, Loh HH, Ho IK, Ma T. Gender differences in the antinociceptive effect of tramadol, alone or in combination with gabapentin, in mice. *J Biomed Sci*. 2008. doi:10.1007/s11373-008-9252-0
53. Wei J, Tower RJ, Tian T, et al. Spatial distribution of type II collagen gene expression in the mouse intervertebral disc. *JOR Spine*. 2019;2(4). doi:https://doi.org/10.1002/jsp2.1070
54. Jin H, Shen J, Wang B, Wang M, Shu B, Chen D. TGF- $\beta$  signaling plays an essential role in the growth and maintenance of intervertebral disc tissue. *FEBS Lett*. 2011. doi:10.1016/j.febslet.2011.03.034
55. Ratneswaran A, To B, Kerr G., Benipal S, Beier F. PPARdelta inactivation protects against joint damage in age associated osteoarthritis. Prep.
56. Rastinejad F, Huang P, Chandra V, Khorasanizadeh S. Understanding nuclear receptor form and function using structural biology. *J Mol Endocrinol*. 2013. doi:10.1530/JME-13-0173
57. Fang L, Zhang M, Li Y, Liu Y, Cui Q, Wang N. PPARgene: A Database of Experimentally Verified and Computationally Predicted PPAR Target Genes. *PPAR Res*. 2016. doi:10.1155/2016/6042162
58. Pattappa G, Li Z, Peroglio M, Wismer N, Alini M, Grad S. Diversity of intervertebral disc cells: Phenotype and function. *J Anat*. 2012. doi:10.1111/j.1469-7580.2012.01521.x
59. Brew K, Nagase H. The tissue inhibitors of metalloproteinases (TIMPs): An ancient family with structural and functional diversity. *Biochim Biophys Acta - Mol Cell Res*. 2010. doi:10.1016/j.bbamcr.2010.01.003
60. Boraschi D, Tagliabue A. The interleukin-1 receptor family. *Semin Immunol*. 2013. doi:10.1016/j.smim.2013.10.023



61. Lee SW, Rho JH, Lee SY, et al. Dietary fat-associated osteoarthritic chondrocytes gain resistance to lipotoxicity through PKCK2/STAMP2/FSP27. *Bone Res.* 2018. doi:10.1038/s41413-018-0020-0
62. Klingler C, Zhao X, Adhikary T, et al. Lysophosphatidylcholines activate PPAR $\delta$  and protect human skeletal muscle cells from lipotoxicity. *Biochim Biophys Acta - Mol Cell Biol Lipids.* 2016. doi:10.1016/j.bbalip.2016.09.020
63. Mandrup S, Bugge A. Molecular mechanisms and genome-wide aspects of PPAR subtype specific transactivation. *PPAR Res.* 2010. doi:10.1155/2010/169506
64. Kerr GJ, To B, White I, et al. Diet-induced obesity leads to behavioral indicators of pain preceding structural joint degeneration in wild-type mice. *Prep.*
65. Griffin TM, Huebner JL, Kraus VB, Guilak F. Extreme obesity due to impaired leptin signaling in mice does not cause knee osteoarthritis. *Arthritis Rheum.* 2009;60(10):2935-2944. doi:10.1002/art.24854
66. Siemionow K, An H, Masuda K, Andersson G, Cs-Szabo G. The effects of age, sex, ethnicity, and spinal level on the rate of intervertebral disc degeneration: A review of 1712 intervertebral discs. *Spine (Phila Pa 1976).* 2011. doi:10.1097/BRS.0b013e3181f2a177
67. Zhong W, Driscoll SJ, Wu M, et al. In vivo morphological features of human lumbar discs. *Med (United States).* 2014. doi:10.1097/MD.0000000000000333
68. Mosley GE, Evashwick-Rogler TW, Lai A, Iatridis JC. Looking beyond the intervertebral disc: The need for behavioral assays in models of discogenic pain. *Ann N Y Acad Sci.* 2017. doi:10.1111/nyas.13429
69. Boden SD, Davis DO, Dina TS, Patronas NJ, Wiesel SW. Abnormal magnetic-resonance scans of the lumbar spine in asymptomatic subjects. A prospective investigation. *J Bone Jt Surg - Ser A.* 1990. doi:10.2106/00004623-199072030-00013
70. Masuda K, Aota Y, Muehleman C, et al. A novel rabbit model of mild, reproducible disc degeneration by an annulus needle puncture: Correlation between the degree of disc injury and radiological and histological appearances of disc degeneration. *Spine (Phila Pa 1976).* 2005. doi:10.1097/01.brs.0000148152.04401.20
71. Deuis JR, Dvorakova LS, Vetter I. Methods used to evaluate pain behaviors in rodents. *Front Mol Neurosci.* 2017. doi:10.3389/fnmol.2017.00284
72. Mogil JS. Animal models of pain: Progress and challenges. *Nat Rev Neurosci.* 2009. doi:10.1038/nrn2606
73. Piel MJ, Kroin JS, van Wijnen AJ, Kc R, Im HJ. Pain assessment in animal models

- of osteoarthritis. *Gene*. 2014;537(2):184-188. doi:10.1016/j.gene.2013.11.091
74. Raffa RB, Friderichs E, Reimann W, Shank RP, Codd EE, Vaught JL. Opioid and nonopioid components independently contribute to the mechanism of action of tramadol, an “atypical” opioid analgesic. *J Pharmacol Exp Ther*. 1992.
  75. Montilla-García Á, Tejada M, Perazzoli G, et al. Grip strength in mice with joint inflammation: A rheumatology function test sensitive to pain and analgesia. *Neuropharmacology*. 2017. doi:10.1016/j.neuropharm.2017.07.029
  76. Kaneko K, Umehara M, Homan T, Okamoto K, Oka M, Oyama T. The analgesic effect of tramadol in animal models of neuropathic pain and fibromyalgia. *Neurosci Lett*. 2014. doi:10.1016/j.neulet.2014.01.007
  77. Bonetto A, Andersson DC, Waning DL. Assessment of muscle mass and strength in mice. *Bonekey Rep*. 2015. doi:10.1038/bonekey.2015.101
  78. Ratneswaran A. Effects of pharmacological administration of PPARdelta inhibitors on post-traumatic osteoarthritis. 2016.
  79. Rosen S, Ham B, Mogil JS. Sex differences in neuroimmunity and pain. *J Neurosci Res*. 2017. doi:10.1002/jnr.23831
  80. Li L, Fan X, Warner M, Xu XJ, Gustafsson JÅ, Wiesenfeld-Hallin Z. Ablation of estrogen receptor  $\alpha$  or  $\beta$  eliminates sex differences in mechanical pain threshold in normal and inflamed mice. *Pain*. 2009. doi:10.1016/j.pain.2009.01.005
  81. Medrikova D, Jilkova ZM, Bardova K, Janovska P, Rossmeisl M, Kopecky J. Sex differences during the course of diet-induced obesity in mice: Adipose tissue expandability and glycemic control. *Int J Obes*. 2012. doi:10.1038/ijo.2011.87
  82. Yoon M. PPAR in obesity: Sex difference and estrogen involvement. *PPAR Res*. 2010. doi:10.1155/2010/584296
  83. Bonofiglio D, Gabriele S, Aquila S, et al. Estrogen receptor  $\alpha$  binds to peroxisome proliferator-activated receptor response element and negatively interferes with peroxisome proliferator-activated receptor  $\gamma$  signaling in breast cancer cells. *Clin Cancer Res*. 2005. doi:10.1158/1078-0432.CCR-04-2453
  84. Contopoulos-Ioannidis DG, Ntzani EE, Ioannidis JPA. Translation of highly promising basic science research into clinical applications. *Am J Med*. 2003. doi:10.1016/S0002-9343(03)00013-5

## Chapter 5

### 5 General Discussion

#### 5.1 Overview

The overall objective of my thesis was to assess how mechanical loading and obesity impact intervertebral (IVD) physiology. Despite being established risk factors for the development of both IVD degeneration and related back pain, the biological mechanisms by which these factors contribute to disease initiation and progression remain elusive. To address this, we utilized mouse models to understand the biological impact of both mechanical loading and obesity on the IVD. In order to contextualize our findings within systemic changes to musculoskeletal health, we also investigated the impact of these risk factors on the knee joint, as there are similarities between the IVD degeneration and knee osteoarthritis (OA) in terms of both risk factors and pathological processes<sup>1</sup>.

We first investigated the impact of mechanical loading, specifically whole-body vibration (WBV) on IVD health in **Chapter 2**. This study built upon previous research from our lab which demonstrated that whole-body vibration (WBV) induces IVD degeneration and knee osteoarthritis (OA) in as little as 4 weeks in a mouse model, using vibrational parameters that model those used clinically<sup>2,3</sup>. Previous studies were however limited to the analysis of only young, male mice of a single outbred stock (CD1) and do not accurately recapitulate the diverse human population currently using WBV platforms. To determine whether these findings would be consistent in another mouse model, I exposed inbred C57BL/6 mice to the same vibrational parameters as the previous studies<sup>2,3</sup> for either 4 or 8 weeks. Analysis of these results revealed that the same vibrational parameters previously shown to induce histopathological IVD degeneration and knee OA in CD1 mice did not affect joint health

in C57BL/6 mice. Furthermore, molecular changes seen at the transcriptional level in the IVD were not observed in the C57BL/6 mice. From this initial study, we concluded that C57BL/6 mice were resistant to WBV-induced joint degeneration, at least at the specific vibrational parameters used.

Next, I investigated the impact of diet-induced obesity on IVD degeneration and associated pain in **Chapter 3**. Despite the established clinical association between obesity, IVD degeneration and low back pain<sup>4,5</sup>, there have been no studies to directly investigate the impact of diet-induced obesity on IVD degeneration and pain. To address this, I characterized the longitudinal impact of diet-induced obesity on pain-related behavior and structural IVD degeneration in a mouse model. In this study, male wild-type C57BL/6N mice were randomized into one of three diet groups (chow control, high-fat, or a high-fat/high-sugar western diet) and fed the experimental diets for 12, 24, 40 or weeks. At endpoint, all mice were assessed for behavioral indicators of pain as well as histological IVD degeneration. We demonstrated that diet-induced obesity led to pain-related behaviors in as little as 12 weeks, with behavioral differences persisting until the 40-week timepoint. Histopathological analysis showed that diet-induced obesity did not affect IVD health until the 40-week timepoint, where early degenerative changes were observed. At the molecular level, mice fed the western diet showed increased expression of *Il-1b* and *Ptgs2* in the IVD at the 24-week timepoint, while mice fed a high-fat diet showed increased expression of *Il-6*, *Ptgs2*, *Bdnf*, and *Adamt5* at the 40-week timepoint. Since behavioral indicators of pain preceded structural and molecular alterations to the IVD, we then investigated other potential mechanisms to explain the pain phenotype observed. We quantified markers of neuroinflammation and systemic inflammation, as they have been previously shown to

impact pain sensitivity<sup>6,7</sup>. While no significant differences were found in the levels of most markers investigated, mice fed the high-fat and western diet tended to show elevated levels of inflammatory cytokines and neuroinflammation, which could impact the pain phenotype seen.

Lastly, we investigated the role of peroxisome proliferator-activated receptor delta (PPAR $\delta$ ) in the IVD and its role in age- and diet-associated IVD degeneration in **Chapter 4**. Since previous studies have demonstrate that PPAR $\delta$  activation has a deleterious role in other cartilaginous joints<sup>8</sup>, we sought to determine its role in the IVD. Intact IVDs were isolated and treated in organ culture with the synthetic PPAR $\delta$  agonist GW501516. Gene expression analysis showed upregulation of known PPAR $\delta$  target genes (*Pdk4* and *Angptl4*)<sup>9</sup>, indicating that PPAR $\delta$  was functional and responsive in IVD tissues. Similar to articular cartilage<sup>8</sup>, PPAR $\delta$  agonism appeared to decrease proteoglycan staining in the NP; however, no differences were seen in the expression of matrix degrading enzymes. PPAR $\delta$  expression was then measured in different compartments of the IVD, demonstrating a 2-fold greater expression of *Ppard* in the AF compared to the NP. To assess the role of PPAR $\delta$  in the IVD, we characterized mice with cartilage-specific deletion of PPAR $\delta$  in age-associated IVD degeneration. At 14 months-of-age loss of *Ppard* did not alter the gross histological features of the IVD; however, gene expression analysis showed an upregulation of matrix metalloproteinases (*Mmp3*, *Mmp13*) and *Il-1b* which are typically associated with accelerated degeneration<sup>10,11</sup>. At 25 months-of-age, male *Ppard KO* mice appeared to be protected from age-associated degeneration observed in WT mice; however, differences in histopathological scores were not significant.

Given that PPAR $\delta$  ligands are dysregulated in obesity<sup>12</sup>, and the potential protective role of PPAR $\delta$  inactivation in age-associated IVD degeneration, we then investigated the effects of PPAR $\delta$  inactivation in a model of western diet-induced obesity. After 50 weeks on the western diet, male *Ppard* KO mice showed significantly greater IVD degeneration than chow-fed controls. Moreover, a greater proportion of *Ppard* KO mice on the western diet showed moderate-severe IVD degeneration than WT mice on the western diet, although average histopathological scores were not significantly different between the two groups. These findings suggest that, contrary to our hypothesis, loss of *Ppard* may accelerate obesity-induced IVD degeneration. Of note, neither PPAR $\delta$  inactivation nor western diet-induced obesity impacted IVD degeneration in female mice, indicating important sex-specific effects. To determine whether IVD degeneration was associated with pain, we carried out a series of behavioral assays and demonstrated that western diet induces pain related behavior in both male and female mice, with a more consistent response seen in females. Interestingly, despite significant increases in joint degeneration, male *Ppard* KO mice fed the western diet did not show pain-related behaviors when compared to chow-fed control. While these findings need to be further explored, they suggest that PPAR $\delta$  may contribute to painful joint degeneration.

## 5.2 Contributions and significance of findings

Back pain is an extremely prevalent, debilitating condition that has a significant impact at both on the individual and societal level<sup>13-15</sup>. The aim of this thesis was to answer several key questions surrounding the role of two environmental risk factors associated with IVD degeneration and associated pain using the mouse as a preclinical model. Our studies highlight several consistent findings which are important considerations in future clinical

and pre-clinical research. First, our studies underscore that the relationship between environmental risk factors (e.g. mechanical loading, obesity), IVD degeneration, and back pain is complex. While these risk factors may drive IVD degeneration and pain in certain circumstances, their effects on IVD health is influenced by interactions with non-modifiable risk factors such as age, genetic background, and sex (i.e. effects of WBV on CD-1 *versus* C57BL/6 mice, obesity-induced IVD degeneration in male *versus* female mice). Second, although clinical or histological features of IVD degeneration may be similar at endpoint, disease pathogenesis may be driven by entirely different mechanism based on the degeneration-inducing catalyst (i.e. PPAR $\delta$  regulates age but not obesity-induced IVD degeneration). Lastly, our studies highlight the importance of taking an integrated approach (assessing both musculoskeletal and nervous tissues) when investigating the relationship of these risk factors with joint degeneration and pain. Mechanical loading and obesity impact other tissues including articular joints, connective tissue, and the nervous system, which may interact with, and contribute to both structural IVD degeneration and pain (**Figure 5.1**). Aside from these general themes, each chapter independently contributes important findings illustrating the role of mechanical loading and obesity in the initiation and progression of IVD degeneration and associated pain.

In **Chapter 2**, we present work in which we show that C57BL/6 mice are resistant to WBV-induced joint damage using vibrational parameters that have been shown to induce joint damage in CD1 mice, and model those used clinically. While this data was negative, it highlights the need for more comprehensive evaluations of the direct impact of WBV on joint health in the human population. Vibrational parameters such as duration, frequency,

and acceleration, along with the direct load experienced by the joints may determine whether WBV therapy is therapeutic or detrimental.

**Chapters 3 & 4** present novel data characterizing the impact of diet-induced obesity on IVD degeneration and pain over time in a mouse model. Despite being one of the largest modifiable risk factors for the development of IVD degeneration and back pain<sup>4,5</sup>, no studies have directly assessed whether diet-induced obesity accelerates IVD degeneration, back pain, or investigated biological mediators underlying this association. Our studies show that diet-induced obesity leads to behavioral indicators of pain starting at the 12-week timepoint, yet histological indicators of IVD degeneration are not seen until the 40-week timepoint, increasing in severity following 50 weeks. The chronology of these findings raises the possibility that IVD degeneration may not be the primary causative factor in some cases of obesity-associated LBP. While speculative, it could be postulated that systemic inflammation caused by obesity directly alters the neural excitability, leading to a pain response in absence of overt joint tissue damage. This systemic inflammation, coupled with inactivity because of pain, may accelerate the IVD degeneration in this model. Aside from obesity-related inflammation, dyslipidemia, hyperglycemia, and hypertension may also impact musculoskeletal and nervous tissues and contribute to the findings observed (**Figure 5.1**). While the etiology remains elusive, our findings demonstrate that diet-induced obesity contributes to both structural IVD degeneration and pain in a mouse model. These findings lay the groundwork for future studies investigating potential biological mechanisms underlying these associations.



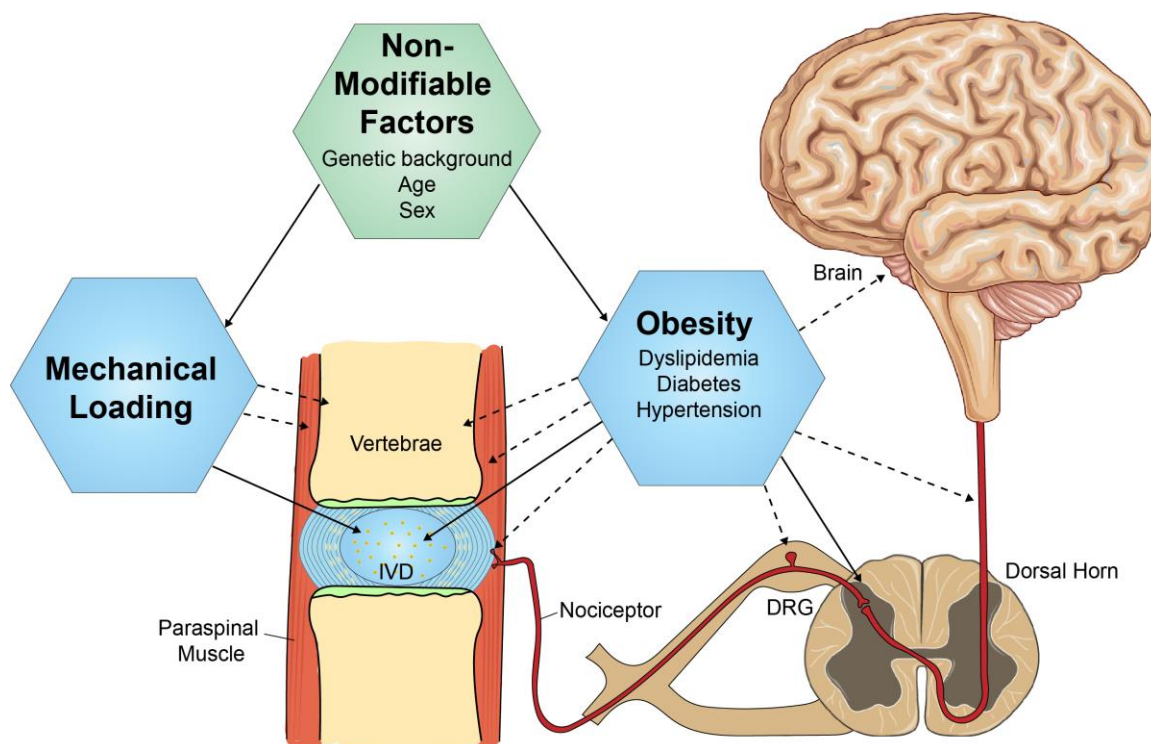


**Figure 5.1: Schematic illustrating the proposed contributions of mechanical loading and obesity to IVD degeneration and associated pain.**

This thesis highlights the complex interaction between environmental risk factors (i.e. mechanical loading and obesity) and non-modifiable factors (i.e. age, genetic background, sex) on IVD degeneration and associated pain. In addition to affecting the IVD directly, these factors can also impact other tissues (i.e. other joints, muscles, bone, nervous tissues) which may contribute to both structural IVD degeneration and associated pain. Solid lines indicate direct assessments made in this thesis, and dashed lines indicate potential contributions to IVD degeneration and pain not directly investigated in this thesis.

In **Chapter 4**, we investigate the nuclear receptor PPAR $\delta$  as a potential mediator of age- and obesity-associated IVD degeneration. Our findings demonstrated that similar its role in articular cartilage, deletion of PPAR $\delta$  may protect against age-associated IVD degeneration<sup>16</sup>. However, deletion of PPAR $\delta$  did not protect from obesity-induced IVD degeneration or knee OA. In fact, on the western diet a higher proportion of *Ppard* KO mice showed moderate/severe IVD degeneration than did WT mice. These findings indicate that PPAR $\delta$  plays a context dependent role in the IVD (**Figure 5.2**) and highlight that the etiology of IVD degeneration is likely multifactorial and providing evidence that disc degeneration should be treated as a group of diseases with separate pathogenesis but a common radiological/histological endpoint. In addition to evaluating the impact of PPAR $\delta$  on the IVD health, this study also illustrates the importance of assessing the correlation between structural IVD degeneration and pain, and sex-related differences. Obesity induced by the western diet accelerated IVD degeneration in male mice but did not significantly impact IVD health in female mice. In contrast, female mice showed more consistent pain-related behaviors on the western diet than male mice, despite having no significant IVD degeneration.

### 5.3 Limitations of research

As with other MSK tissues, human IVD tissue is difficult to obtain, especially healthy tissues or those corresponding to the early stages of disease. As such, animal models are often used to understand the pathophysiology of IVD degeneration and associated back pain<sup>17</sup>. Rodents are the most frequently used small animal model based on their ease of use, low cost, and the ability to manipulate their genome<sup>17</sup>. Despite their widespread use, some limitations associated with the use of mouse models include the persistence of notochordal

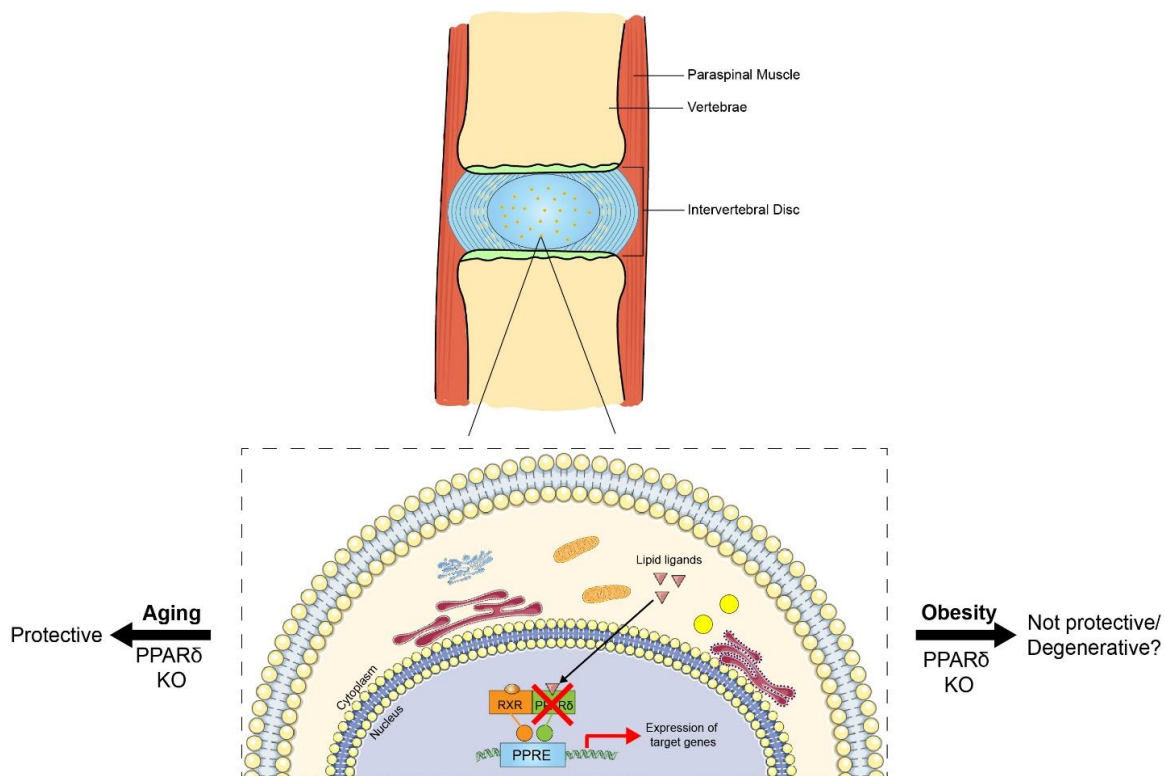


**Figure 5.2: Schematic overview of proposed context-dependent role of PPAR $\delta$  in the IVD.**

Our findings highlight the complexities of nuclear receptor signaling in the IVD and other cartilaginous tissues. While PPAR $\delta$  deletion was protective in a model of age-associated IVD degeneration, it did not appear to play a protective role in a model of obesity-related IVD degeneration. Furthermore, a higher proportion of *Ppard* KO mice showed more severe IVD degeneration on the western diet than WT mice, suggesting that in the context of obesity loss of PPAR $\delta$  may accelerate IVD degeneration.

cells in the NP into adulthood, and altered mechanical loading as reviewed recently<sup>18</sup>. Although there is an obvious size difference between human and mouse IVDs, and the limitations mentioned above need to be acknowledged, both species have similar geometry, biomechanics and IVD extracellular composition<sup>19-21</sup>.

In **Chapter 2**, we show that C57BL/6 mice are resistant to WBV-induced joint degeneration, in contrast to previous studies by our group demonstrating the deleterious effects of WBV in CD-1 mice<sup>3,22</sup>. However, these experiments were performed with only a single protocol of WBV and little is known regarding what parameters of WBV (i.e. frequency, amplitude, duration of exposure) may be beneficial or detrimental to joint health. Previous studies have reported that vibration magnitude is attenuated differently in different strains of mice<sup>23</sup>, and that the resonant frequency range also differs between strains of mice<sup>23</sup>, raising the question about what loads are being experienced by the joint tissues themselves. While mechanical loading is a key regulator of IVD cell homeostasis, cells can only respond to local mechanical forces, and can have differential responses dependent on both the cell type and loading parameters applied<sup>24-27</sup>. If the local mechanical load experienced by the joint tissues differed between CD1 and C57BL/6 mice, this could explain the differential response. Additional factors including baseline bone properties or differences in posture have also been shown to impact WBV transmission through the body and could be further explored to better understand the differences observed between the strains of mice<sup>28,29</sup>.

In **Chapter 3**, we establish the effect of diet-induced obesity on IVD degeneration and pain. Designed as a proof-of-concept, this study had several limitations. First, only male mice were used. Studies in humans have shown that females have a higher prevalence of

spinal disorders and chronic pain conditions than males<sup>30,31</sup>. Second, this study was limited to only a single formulation of the high-fat and western diets, limiting the generalizability of our results. While not investigated in the context of the IVD, recent studies examining the effects of diet-induced obesity on knee OA show that dietary composition is an important determinant of OA progression in obesity. Diets high in saturated fatty acids or  $\omega$ -6 polyunsaturated fatty acids (PUFAs) induce more severe metabolic dysregulation and OA progression than diets enriched with  $\omega$ -3 PUFAs<sup>32</sup>. Aside from fat, diets high in sucrose also accelerate OA progression independent of weight gain<sup>33</sup>. A third limitation is the use of behavioral assays to assess pain. While many of the behaviors examined are altered in experimental pain models, most can be impacted by additional biological and psychosocial factors<sup>34,35</sup>. In systemic conditions such as obesity, the impact of co-morbidities on behavioral outcomes should be considered. For example, grip force during axial stretch and tail suspension assays have been shown to measure of discogenic back pain<sup>36</sup>, but are also used to assess muscle strength and the effects of anti-depressants, respectively<sup>37,38</sup>. Moreover, other joints should also be assessed, as obesity has been shown to globally impact joint health which may contribute to the pain-related behavior observed<sup>39</sup>. Finally, it is becoming increasingly accepted that IVD degeneration is not just a disease of the IVD, but also the adjacent structures including the muscle, ligaments, vertebrae and facet joints<sup>1</sup>. Understanding the direct effects of obesity on these structures, and their relation to IVD degeneration and pain, is an important consideration for future studies.

In **Chapter 4**, we established the effect of PPAR $\delta$  deletion in the IVD using both age and obesity-induced models of degeneration. One limitation of this study was the Cre-driver used. Using fluorescent reporter mice, our group has shown that *Col2-Cre* targets the NP,

inner 2/3 of the AF, and the CEP. However, in addition to effecting recombination in the IVD, the *Col2-Cre* is also active in cartilaginous tissues of all joints as well as synovial fibroblasts and some osteoblasts<sup>40,41</sup>. Given that many of the behavioral indicators of pain would be impacted by degeneration associated changes in other joints<sup>42</sup>, use of the *Col2-Cre* impairs our ability to draw conclusions about the relative contribution of IVD changes and the precise role of PPAR $\delta$  to the pain-related phenotype observed. A second limitation common to all studies is the ability to assess tissue-specific changes within the IVD. In all three studies, gene expression analysis was conducted on intact IVDs. Given that the IVD is a heterogenous structure, composed of distinct tissues with diverse cellular phenotypes in each tissue<sup>43</sup>, the tissue-specific effects of each intervention were evaluated.

In **Chapter 4** we used an *ex vivo* IVD organ culture system to evaluate the effect of PPAR $\delta$  activation. Organ culture has been suggested as a physiologically relevant model in which cells remain in their endogenous microenvironment, while *in vitro* conditions are modulated<sup>17</sup>. One limitation of the organ culture system relates to the heterogeneity of the IVD<sup>43</sup> and the inability to differentiate the role of PPAR $\delta$  activation within each cell type (NP, AF, and CEP). Although monolayer culture would allow for cell type specific experimentation, expansion of primary NP and AF cells in monolayer culture has been shown to alter cellular processes and phenotype<sup>17</sup>.

## 5.4 Future Directions

The findings of this thesis can be further expanded on in several ways, some of which address the limitations detailed above. To better understand the effects of vibrational loading on the IVD it would be important to quantify the transmission of vibration within joint tissues *in vivo* during WBV. One potential method to quantify site-specific vibrational

amplitude in live mice is through non-invasive x-ray imaging of mice carrying zirconium dioxide fiducial marker beads embedded around the joint tissues (i.e. spine and knee joint) during WBV. Similar protocols have been previously used to assess the effects of cyclic loading on strain in the porcine anterior cruciate ligament<sup>44</sup>. This study would allow us to assess the effects of posture, soft tissue dampening and resonance effects on the transmission of vibration to specific anatomical locations (i.e. spine, knee). Site-specific findings could then be correlated to the biological effects of WBV characterized in each respective tissue. Future work can also follow up on putative biological pathways underlying this association using transcriptomics and proteomic approaches.

To further characterize the role of diet-induced obesity in IVD degeneration and associated pain, future studies should take a more integrated approach given the systemic effects of obesity on the body. In addition to investigating structural joint degeneration within the IVD, the effects of obesity should be directly assessed in surrounding spinal tissues including muscles, ligaments, and the facet joints to determine if their dysfunction contributes to IVD degeneration and/or axial pain. In the context of pain, the impact of obesity should be assessed longitudinally through a repeated measures design, where animals undergo behavioral testing prior to randomization and at regular intervals throughout the time course of the study (e.g. every 4 weeks). These findings would allow us to determine the point at which pain-related behaviors initiated and whether they persisted in each animal. These findings could then be correlated with non-invasive, *in vivo* assessments of joint degeneration such as T2-weighted MRI, which has been shown to detect degenerative changes in both the IVD and articular cartilage of the knee in rodent models<sup>45,46</sup>. Pathological changes within the peripheral and central nervous system should

be more thoroughly examined to determine potential mechanisms underlying the pain response associated with diet-induced obesity. Examples include quantification of markers of peripheral nerve injury (ATF3) in the dorsal root ganglia (DRG) and the production of immune and glial mediators (e.g. TNF $\alpha$ , IL-1 $\beta$ , BDNF) in the spinal cord<sup>47,48</sup>.

To more robustly characterize the cellular pathways responsible for the association between obesity and IVD degeneration, a systems biology approach using multiple -omics technologies (i.e. epigenomics, transcriptomics, proteomics, metabolomics) could be used to independently assess isolated NP and AF tissues in this model. To specifically address the heterogeneity of cell types within the IVD, single-cell RNA sequencing could also be used. Finally, future studies could also be designed to investigate potential biological pathways or dietary constituents that are associated with accelerated IVD degeneration and pain.

Characterization of the role of PPAR $\delta$  in age- and obesity-associated IVD degeneration was limited by the transgenic model used. To address the off-target effects associated with use of the *Col2-Cre*, future studies could be conducted using the *Noto-Cre* mouse strain, which our group has been shown to be specific for notochord-derived cells of the NP<sup>49</sup>. To address tissue specific-differences, AF-specific Cre-drivers such as *Gdf5-Cre* or *Scx-Cre* may also be used, although these are also associated with off-target effects in other MSK tissues<sup>50,51</sup>. In addition to using a systems biology approach (as detailed above) to assess the effects of PPAR $\delta$  agonism in the NP and AF, the interplay between different nuclear receptors should also be investigated. There is substantial overlap between nuclear receptor signaling<sup>52</sup>, and given the similarity between the ligands and DNA binding domains between the PPAR subtypes<sup>53</sup>, the consequence of deleting PPAR $\delta$  on PPAR $\alpha$  and PPAR $\gamma$



signaling should be investigated. To do so, chromatin immunoprecipitation with subsequent DNA sequencing (ChIP seq) could interrogate alternate binding of PPAR $\alpha$  and PPAR $\gamma$  when PPAR $\delta$  is no longer present.

Taken together, the results of this thesis highlight the complex nature of mechanical loading and obesity on IVD health. Furthermore, these studies highlight the importance of assessing for pain in conjunction with structural IVD degeneration as they are not always mutually exclusive. Importantly, for effective clinical translation, potential therapeutic targets should be evaluated in multiple different preclinical models of IVD degeneration that consider factors such as genetics, sex, and age.

## 5.5 References

1. Rustenburg CME, Emanuel KS, Peeters M, Lems WF, Vergroesen P-PA, Smit TH. Osteoarthritis and intervertebral disc degeneration: Quite different, quite similar. *JOR Spine*. 2018. doi:10.1002/jsp2.1033
2. McCann MR, Veras MA, Yeung C, et al. Whole-body vibration of mice induces progressive degeneration of intervertebral discs associated with increased expression of Il-1 $\beta$  and multiple matrix degrading enzymes. *Osteoarthr Cartil*. 2017. doi:10.1016/j.joca.2017.01.004
3. McCann MR, Patel P, Pest MA, et al. Repeated exposure to high-frequency low-amplitude vibration induces degeneration of murine intervertebral discs and knee joints. *Arthritis Rheumatol*. 2015;67(8):2164-2175. doi:10.1002/art.39154
4. Teraguchi M, Yoshimura N, Hashizume H, et al. Metabolic Syndrome Components Are Associated with Intervertebral Disc Degeneration: The Wakayama Spine Study. *PLoS One*. 2016;11(2):e0147565. doi:10.1371/journal.pone.0147565
5. Jakoi AM, Pannu G, D'Oro A, et al. The Clinical Correlations between Diabetes, Cigarette Smoking and Obesity on Intervertebral Degenerative Disc Disease of the Lumbar Spine. *Asian Spine J*. 2017;11(3):337-347. doi:10.4184/asj.2017.11.3.337
6. Gangadharan V, Kuner R. Pain hypersensitivity mechanisms at a glance. *Dis Model Mech*. 2013;6(4):889-895. doi:10.1242/dmm.011502
7. Bastard JP, Maachi M, Lagathu C, et al. Recent advances in the relationship between obesity, inflammation, and insulin resistance. *Eur Cytokine Netw*. 2006.
8. Ratneswaran A, LeBlanc EA, Walser E, et al. Peroxisome proliferator-activated receptor delta promotes the progression of posttraumatic osteoarthritis in a mouse model. *Arthritis Rheumatol*. 2015;67(2):454-464. doi:10.1002/art.38915
9. Fang L, Zhang M, Li Y, Liu Y, Cui Q, Wang N. PPARgene: A Database of Experimentally Verified and Computationally Predicted PPAR Target Genes. *PPAR Res*. 2016. doi:10.1155/2016/6042162
10. Abe Y, Akeda K, An HS, et al. Proinflammatory cytokines stimulate the expression of nerve growth factor by human intervertebral disc cells. *Spine (Phila Pa 1976)*. 2007. doi:10.1097/01.brs.0000257556.90850.53
11. Le Maitre CL, Freemont AJ, Hoyland JA. The role of interleukin-1 in the pathogenesis of human intervertebral disc degeneration. *Arthritis Res Ther*. 2005. doi:10.1186/ar1732
12. Botta M, Audano M, Sahebkar A, Sirtori CR, Mitro N, Ruscica M. PPAR agonists and metabolic syndrome: An established role? *Int J Mol Sci*. 2018.

doi:10.3390/ijms19041197

13. Snelgrove S, Lioffi C. An interpretative phenomenological analysis of living with chronic low back pain. *Br J Health Psychol.* 2009. doi:10.1348/135910709X402612
14. MacNeela P, Doyle C, O’Gorman D, Ruane N, McGuire BE. Experiences of chronic low back pain: a meta-ethnography of qualitative research. *Health Psychol Rev.* 2015. doi:10.1080/17437199.2013.840951
15. Katz JN. Lumbar disc disorders and low-back pain: Socioeconomic factors and consequences. In: *Journal of Bone and Joint Surgery - Series A.* ; 2006. doi:10.2106/JBJS.E.01273
16. Ratneswaran A, To B, Kerr G., Benipal S, Beier F. PPARdelta inactivation protects against joint damage in age associated osteoarthritis. *Prep.*
17. Alini M, Eisenstein SM, Ito K, et al. Are animal models useful for studying human disc disorders/degeneration? *Eur Spine J.* 2008;17(1):2-19. doi:10.1007/s00586-007-0414-y
18. Daly C, Ghosh P, Jenkin G, Oehme D, Goldschlager T. A Review of Animal Models of Intervertebral Disc Degeneration: Pathophysiology, Regeneration, and Translation to the Clinic. *Biomed Res Int.* 2016. doi:10.1155/2016/5952165
19. Beckstein JC, Sen S, Schaer TP, Vresilovic EJ, Elliott DM. Comparison of animal discs used in disc research to human lumbar disc: Axial compression mechanics and glycosaminoglycan content. *Spine (Phila Pa 1976).* 2008. doi:10.1097/BRS.0b013e318166e001
20. Showalter BL, Beckstein JC, Martin JT, et al. Comparison of animal discs used in disc research to human lumbar disc: Torsion mechanics and collagen content. *Spine (Phila Pa 1976).* 2012. doi:10.1097/BRS.0b013e31824d911c
21. O’Connell GD, Vresilovic EJ, Elliott DM. Comparison of animals used in disc research to human lumbar disc geometry. *Spine (Phila Pa 1976).* 2007. doi:10.1097/01.brs.0000253961.40910.c1
22. McCann MR, Veras MA, Yeung C, et al. Whole-body vibration of mice induces progressive degeneration of intervertebral discs associated with increased expression of Il-1beta and multiple matrix degrading enzymes. *Osteoarthr Cartil.* 2017;25(5):779-789. doi:10.1016/j.joca.2017.01.004
23. Rabey KN, Li Y, Norton JN, Reynolds RP, Schmitt D. Vibrating Frequency Thresholds in Mice and Rats: Implications for the Effects of Vibrations on Animal Health. *Ann Biomed Eng.* 2015;43(8):1957-1964. doi:10.1007/s10439-014-1226-y
24. Chan SC, Ferguson SJ, Gantenbein-Ritter B. The effects of dynamic loading on

- the intervertebral disc. *Eur Spine J.* 2011;20(11):1796-1812. doi:10.1007/s00586-011-1827-1
25. Setton LA, Chen J. Mechanobiology of the intervertebral disc and relevance to disc degeneration. *J Bone Jt Surg Am.* 2006;88 Suppl 2:52-57. doi:10.2106/JBJS.F.00001
  26. Hsieh AH, Twomey JD. Cellular mechanobiology of the intervertebral disc: new directions and approaches. *J Biomech.* 2010;43(1):137-145. doi:10.1016/j.jbiomech.2009.09.019
  27. Neidlinger-Wilke C, Galbusera F, Pratsinis H, et al. Mechanical loading of the intervertebral disc: from the macroscopic to the cellular level. *Eur Spine J.* 2014;23 Suppl 3:S333-43. doi:10.1007/s00586-013-2855-9
  28. Tankisheva E, Jonkers I, Boonen S, et al. Transmission of whole-body vibration and its effect on muscle activation. *J Strength Cond Res.* 2013. doi:10.1519/JSC.0b013e31827f1225
  29. Judex S, Donahue LR, Rubin C. Genetic predisposition to low bone mass is paralleled by an enhanced sensitivity to signals anabolic to the skeleton. *FASEB J.* 2002;16(10):1280-1282. doi:10.1096/fj.01-0913fje
  30. Andersson GBJ. Epidemiological features of chronic low-back pain. *Lancet.* 1999. doi:10.1016/S0140-6736(99)01312-4
  31. Rosen S, Ham B, Mogil JS. Sex differences in neuroimmunity and pain. *J Neurosci Res.* 2017. doi:10.1002/jnr.23831
  32. Wu CL, Jain D, McNeill JN, et al. Dietary fatty acid content regulates Wound repair and the pathogenesis of osteoarthritis following joint injury. *Ann Rheum Dis.* 2015. doi:10.1136/annrheumdis-2014-205601
  33. Donovan EL, Lopes EBP, Batushansky A, Kinter M, Griffin TM. Independent effects of dietary fat and sucrose content on chondrocyte metabolism and osteoarthritis pathology in mice. *DMM Dis Model Mech.* 2018. doi:10.1242/dmm.034827
  34. Mogil JS. Animal models of pain: Progress and challenges. *Nat Rev Neurosci.* 2009. doi:10.1038/nrn2606
  35. Cobos E, Portillo-Salido E. "Bedside-to-Bench" Behavioral Outcomes in Animal Models of Pain: Beyond the Evaluation of Reflexes. *Curr Neuropharmacol.* 2013. doi:10.2174/1570159x113119990041
  36. Millecamps M, Czerminski JT, Mathieu AP, Stone LS. Behavioral signs of axial low back pain and motor impairment correlate with the severity of intervertebral disc degeneration in a mouse model. *Spine J.* 2015;15(12):2524-2537.


doi:10.1016/j.spinee.2015.08.055


37. Bonetto A, Andersson DC, Waning DL. Assessment of muscle mass and strength in mice. *Bonekey Rep.* 2015. doi:10.1038/bonekey.2015.101
38. Steru L, Chermat R, Thierry B, Simon P. The tail suspension test: A new method for screening antidepressants in mice. *Psychopharmacology (Berl).* 1985. doi:10.1007/BF00428203
39. Griffin TM, Fermor B, Huebner JL, et al. Diet-induced obesity differentially regulates behavioral, biomechanical, and molecular risk factors for osteoarthritis in mice. *Arthritis Res Ther.* 2010;12(4):R130. doi:10.1186/ar3068
40. Pest MA, Beier F. Developmental biology: Is there such a thing as a cartilage-specific knockout mouse? *Nat Rev Rheumatol.* 2014. doi:10.1038/nrrheum.2014.168
41. Fosang AJ, Golub SB, East CJ, Rogerson FM. Abundant LacZ activity in the absence of Cre expression in the normal and inflamed synovium of adult Col2a1-Cre; ROSA26RLacZ reporter mice. *Osteoarthr Cartil.* 2013. doi:10.1016/j.joca.2012.11.013
42. Burma NE, Leduc-Pessah H, Fan CY, Trang T. Animal models of chronic pain: Advances and challenges for clinical translation. *J Neurosci Res.* 2017. doi:10.1002/jnr.23768
43. Pattappa G, Li Z, Peroglio M, Wismer N, Alini M, Grad S. Diversity of intervertebral disc cells: Phenotype and function. *J Anat.* 2012. doi:10.1111/j.1469-7580.2012.01521.x
44. Blokker AM, Getgood A, Nguyen D, Holdsworth DW, Burkhart TA. Insertion of Small Diameter Radiopaque Tracking Beads into the Anterior Cruciate Ligament Results in Repeatable Strain Measurement Without Affecting the Material Properties. *Ann Biomed Eng.* 2020. doi:10.1007/s10439-020-02511-2
45. Bedore J, Sha W, McCann MR, Liu S, Leask A, Séguin CA. Impaired intervertebral disc development and premature disc degeneration in mice with notochord-specific deletion of CCN2. *Arthritis Rheum.* 2013. doi:10.1002/art.38075
46. Huang GS, Lee HS, Chou MC, et al. Quantitative MR T2 measurement of articular cartilage to assess the treatment effect of intra-articular hyaluronic acid injection on experimental osteoarthritis induced by ACLX. *Osteoarthr Cartil.* 2010. doi:10.1016/j.joca.2009.08.014
47. Ji RR, Nackley A, Huh Y, Terrando N, Maixner W. Neuroinflammation and central sensitization in chronic and widespread pain. *Anesthesiology.* 2018. doi:10.1097/ALN.0000000000002130

48. Tsujino H, Kondo E, Fukuoka T, et al. Activating transcription factor 3 (ATF3) induction by axotomy in sensory and motoneurons: A novel neuronal marker of nerve injury. *Mol Cell Neurosci*. 2000. doi:10.1006/mcne.1999.0814
49. McCann MR, Tamplin OJ, Rossant J, Seguin CA. Tracing notochord-derived cells using a Noto-cre mouse: implications for intervertebral disc development. *Dis Model Mech*. 2012;5(1):73-82. doi:10.1242/dmm.008128
50. Mundy C, Yasuda T, Kinumatsu T, et al. Synovial joint formation requires local Ext1 expression and heparan sulfate production in developing mouse embryo limbs and spine. *Dev Biol*. 2011. doi:10.1016/j.ydbio.2010.12.022
51. Yoshimoto Y, Takimoto A, Watanabe H, Hiraki Y, Kondoh G, Shukunami C. Scleraxis is required for maturation of tissue domains for proper integration of the musculoskeletal system. *Sci Rep*. 2017. doi:10.1038/srep45010
52. De Bosscher K, Desmet SJ, Clarisse D, Estebanez-Perpina E, Brunsveld L. Nuclear receptor crosstalk — defining the mechanisms for therapeutic innovation. *Nat Rev Endocrinol*. 2020. doi:https://doi.org/10.1038/s41574-020-0349-5
53. Tyagi S, Gupta P, Saini A, Kaushal C, Sharma S. The peroxisome proliferator-activated receptor: A family of nuclear receptors role in various diseases. *J Adv Pharm Technol Res*. 2011. doi:10.4103/2231-4040.90879


# Appendices

## APPENDIX A: PERMISSION TO REUSE MATERIAL





[Home](#)
[Help](#)
[Email Support](#)
[Sign In](#)
[Create Account](#)



**C57BL/6 mice are resistant to joint degeneration induced by whole-body vibration**

**Author:** Kerr, M.R.; McCann, J.K.; Branch, A.; Ratneswaran, M.A.; Pest, D.W.; Holdsworth, F.; Beier, S.J.; Dixon, C.A.; Séguin

**Publication:** Osteoarthritis and Cartilage

**Publisher:** Elsevier

**Date:** March 2017

© 2016 Osteoarthritis Research Society International. Published by Elsevier Ltd.

Please note that, as the author of this Elsevier article, you retain the right to include it in a thesis or dissertation, provided it is not published commercially. Permission is not required, but please ensure that you reference the journal as the original source. For more information on this and on your other retained rights, please visit: <https://www.elsevier.com/about/our-business/policies/copyright#Author-rights>

BACK
CLOSE WINDOW

© 2020 Copyright - All Rights Reserved | Copyright Clearance Center, Inc. | [Privacy statement](#) | [Terms and Conditions](#)  
 Comments? We would like to hear from you. E-mail us at [customercare@copyright.com](mailto:customercare@copyright.com)

## APPENDIX B: ANIMAL PROTOCOL NOTICE OF APPROVAL



**AUP Number: 2017-154**

**PI Name: Seguin, Cheryle**

**AUP Title: Mouse Models to Characterize Intervertebral Disc Development and Disc Disease**

**Approval Date: 11/01/2017**

**Official Notice of Animal Care Committee (ACC) Approval:**

Your new Animal Use Protocol (AUP) 2017-154:1: entitled " Mouse Models to Characterize Intervertebral Disc Development and Disc Disease " has been APPROVED by the Animal Care Committee of the University Council on Animal Care. This approval, although valid for up to four years, is subject to annual Protocol Renewal.

Prior to commencing animal work, please review your AUP with your research team to ensure full understanding by everyone listed within this AUP.

As per your declaration within this approved AUP, you are obligated to ensure that:

- 1) Animals used in this research project will be cared for in alignment with:
  - a) Western's Senate MAPPs 7.12, 7.10, and 7.15  
[http://www.uwo.ca/univsec/policies\\_procedures/research.html](http://www.uwo.ca/univsec/policies_procedures/research.html)
  - b) University Council on Animal Care Policies and related Animal Care Committee procedures  
[http://uwo.ca/research/services/animalethics/animal\\_care\\_and\\_use\\_policies.htm](http://uwo.ca/research/services/animalethics/animal_care_and_use_policies.htm)
- 2) As per UCAC's Animal Use Protocols Policy,
  - a) this AUP accurately represents intended animal use;
  - b) external approvals associated with this AUP, including permits and scientific/departmental peer approvals, are complete and accurate;
  - c) any divergence from this AUP will not be undertaken until the related Protocol Modification is approved by the ACC; and
  - d) AUP form submissions - Annual Protocol Renewals and Full AUP Renewals - will be submitted and attended to within timeframes outlined by the ACC.
  - e) [http://uwo.ca/research/services/animalethics/animal\\_use\\_protocols.html](http://uwo.ca/research/services/animalethics/animal_use_protocols.html)
- 3) As per MAPP 7.10 all individuals listed within this AUP as having any hands-on animal contact will
  - a) be made familiar with and have direct access to this AUP;
  - b) complete all required CCAC mandatory training ([training@uwo.ca](mailto:training@uwo.ca)); and
  - c) be overseen by me to ensure appropriate care and use of animals.
- 4) As per MAPP 7.15,
  - a) Practice will align with approved AUP elements;
  - b) Unrestricted access to all animal areas will be given to ACVS Veterinarians and ACC Leaders;
  - c) UCAC policies and related ACC procedures will be followed, including but not limited to:
    - i) Research Animal Procurement
    - ii) Animal Care and Use Records
    - iii) Sick Animal Response
    - iv) Continuing Care Visits
- 5) As per institutional OH&S policies, all individuals listed within this AUP who will be using or potentially exposed to hazardous materials will have completed in advance the appropriate institutional OH&S training, facility-level training, and reviewed related (M)SDS Sheets.  
<http://www.uwo.ca/hr/learning/required/index.html>

Submitted by: Copeman, Laura  
on behalf of the Animal Care Committee  
University Council on Animal Care



## CURRICULUM VITAE

**Geoffrey Kerr**

---

### Post-secondary Education and Degrees

---

- 2015-Present*      **PhD in Physiology and Pharmacology (Collaborative Program in Musculoskeletal Health)**  
 The University of Western Ontario (London, Ontario)  
 Schulich School of Medicine & Dentistry, Bone & Joint Institute  
 Supervisor: Dr. Cheryle Séguin, PhD
- 2011-2015*      **Bachelor of Medical Science (BMSc. 2015)**  
**Honors Double Major in Physiology & Pharmacology**  
 The University of Western Ontario (London, Ontario)  
 Schulich School of Medicine & Dentistry

---

### Publications

---

- 2017*      **Geoffrey J. Kerr**, Matthew R. McCann, Jennifer K. Branch, Michael A. Pest, Anusha Ratneswaran, David W. Holdsworth, Frank Beier, S. Jeffrey Dixon, and Cheryle A. Séguin. C57BL/6 mice are resistant to whole-body vibration-induced joint degeneration. *Osteoarthritis and Cartilage*. 2017 Mar; 25(3):421-425.
- 2017*      **Geoffrey J. Kerr\***, Matthew A. Veras\* (co-first author), Min Kyu Mark Kim, Cheryle A. Séguin. Decoding the intervertebral disc: unravelling the complexities and cell phenotypes and pathways associated with degeneration and mechanotransduction. *Semin Cell Dev Biol*. 2017 Feb; 62:94-103.

---

### Fellowships and Awards

---

- 2019*      Mogenson Trust Award (Hari and Gudrun Sharma Award)
- 2019*      Canadian Institute of Health Research National Poster Competition, Silver Medal
- 2019*      Canadian Institute of Health Research Travel Award
- 2019*      SixSense Case Competition – First Place
- 2018*      Canadian Bone and Joint Young Investigators Forum – Top Scientific Abstract

2017	Canadian Connective Tissue Conference – Oral Presentation Award
2017	Natural Sciences and Engineering Research Council of Canada – Post-graduate scholarship
2017	Transdisciplinary Bone & Joint Training Award
2017	Ontario Graduate Scholarship (Declined)
2016	Physiology and Pharmacology Research Day – Poster Award
2016	Canadian Connective Tissue Conference – Poster Award
2015	Transdisciplinary Bone & Joint Training Award

---

### Teaching

---

2019-2020	PP 3000 – Physiology & Pharmacology Laboratory, UWO
2016-2019	Physiology 2130 – Introduction to Human Physiology, UWO
2015-2016	Physiology 3130Y – Physiology Laboratory, UWO

---

### Supervision

---

2019-2020	1-4 <sup>th</sup> Year Honors Student
2018-2019	1-4 <sup>th</sup> Year Honors Student
2017-2018	1-4 <sup>th</sup> Year Honors Student
2016-2017	1-4 <sup>th</sup> Year Honors Student

---

### Presentations at Scientific Meetings

---

#### Oral Presentations

2019	<b>Advances in Joint Health and Disease Symposium</b> “Investigating the relationship between diet-induced obesity, intervertebral disc degeneration and back pain.” (Toronto, Ontario)
2018	<b>Canadian Bone and Joint Conference: Young Investigators Forum</b> “Investigating the role of peroxisome proliferator-activated receptor delta in intervertebral disc health and degeneration.” (London, Ontario)
2017	<b>Canadian Connective Tissue Society Conference</b> “Male mice are more susceptible to whole-body vibration induced joint damage than age-matched female mice” (Montreal, Quebec)

#### Poster Presentations

2019	<b>Orthopedic Research Society – PSRS Spine Research Symposium</b> “Investigating the relationship between diet-induced obesity, intervertebral disc degeneration and back pain.” (Skytop, Pennsylvania, USA)
------	--

- 2019 **Canadian Institute of Health Research National Poster Presentation**  
“Investigating the relationship between diet-induced obesity, intervertebral disc degeneration and back pain.” (Winnipeg, Manitoba)
- 2019 **London Health Research Day**  
“Investigating the relationship between diet-induced obesity, intervertebral disc degeneration and back pain.” (London, Ontario)
- 2019 **Canadian Pain Society Scientific meeting**  
“Investigating the relationship between diet-induced obesity, intervertebral disc degeneration and back pain.” (Toronto, Ontario)
- 2019 **Gordon Research Conference in Cartilage Biology and Pathology**  
“Investigating the relationship between diet-induced obesity, intervertebral disc degeneration and back pain.” (Galveston, Texas, USA)
- 2019 **Gordon Research Seminars in Cartilage Biology and Pathology**  
“Investigating the relationship between diet-induced obesity, intervertebral disc degeneration and back pain.” (Galveston, Texas, USA)
- 2018 **Physiology & Pharmacology Research Day**  
“Investigating the role of peroxisome proliferator-activated receptor delta in intervertebral disc health and degeneration.” (London, Ontario)
- 2018 **Canadian Bone and Joint Conference**  
“Investigating the role of peroxisome proliferator-activated receptor delta in intervertebral disc health and degeneration.” (London, Ontario)
- 2017 **Physiology & Pharmacology Research Day**  
“Male mice are more susceptible to whole-body vibration induced joint damage than age-matched female mice.” (London, Ontario)
- 2017 **Gordon Research Conference Cartilage Biology and Pathology**  
“Male mice are more susceptible to whole-body vibration induced joint damage than age-matched female mice.” (Lucca, Italy)
- 2017 **Gordon Research Seminars Cartilage Biology and Pathology**  
“Male mice are more susceptible to whole-body vibration induced joint damage than age-matched female mice.” (Lucca, Italy)
- 2016 **Physiology & Pharmacology Research Day**  
“Genetic strain-specific differences in the effect of whole-body vibration on joint health.” (London, Ontario)
- 2016 **Canadian Connective Tissue Conference**  
“Genetic strain-specific differences in the effect of whole-body vibration on joint health.” (Hamilton, Ontario)
- 2016 **Canadian Bone and Joint Conference**  
“Genetic strain-specific differences in the effect of whole-body vibration on joint health.” (London, Ontario)
- 2016 **London health Research Day**

“Genetic strain-specific differences in the effect of whole-body vibration on joint health.” (London, Ontario)

2015

**Physiology & Pharmacology Research day**

“The effect of repeated exposure to whole-body vibration on intervertebral disc and joint health.” (London, Ontario)